Gluten replacement and starch reduction in producing gluten free bread

Yi Ren, MSc

Thesis submitted to the University of Nottingham for the degree of Doctor of Philosophy

Division of Food, Nutrition and Dietetics
School of Biosciences
University of Nottingham
Loughborough

LE12 5RD

September 2019

Abstract

The main target of the project is to investigate gluten replacement and starch replacement in gluten free products for the purpose of dealing with gluten intolerance, obesity, diabetes, and meeting the public requirement of healthy diets. The focus of the first part is on psyllium seed husk powder (PSY), whose main compound is heteroxylan. Both whole PSY and fractions (by temperature) were investigated. Fractions show distinct rheological properties, arabinose/xylose ratios and sidechain substitutions. Two hypotheses were proposed focusing on either chemical and molecular structural properties or hierarchical molecular conformations.

Cellulose, fibrillated cellulose (FC) and mixtures with PSY were then investigated. FC suspensions appear as flocculates which can be promoted by either high temperature or distance reduction between fibres. Unheated PSY-FC appears to be binary phase mixture and the rheological property is enhanced with the increase of fibrillation time. The heated mixtures form interpenetrating composites and the treatment on the cellulose surface by fibrillation does not alter the rheological property. However, further fibrillation, which causes significant loss of integrity of the cellulose fibres, enhances the rheological properties and a denser and clumped structure was observed. PSY interacts with cellulose and FC via, possibly, arabinan sidechains, molecular compatibility, or trapping by FC fibres.

PSY and methylcellulose (MC) were then applied in the production of gluten free bread based on rice flour. A comprehensive study of the influences of the addition levels of MC, PSY and water on dough rheological properties, proving behaviours, and bread qualities were performed and principal component analysis was applied to understand the correlations between different responses and to reduce the number of data dimensions. Additions of MC and PSY strengthen gluten free doughs but water dilutes the systems and softens the doughs. Dough extensibility is closely correlated with specific volume and can be a good predictor of bread quality. Extensibility can be increased by a coincident increase of hydrocolloid addition, especially MC, and water addition. Appropriate extensibility allows doughs to flow which facilities expansion during proving and generates larger loaves with a less dense crumb and softer texture. Other rheological responses are less significantly correlated to specific volume but sensitive to formulation variations and reflect dough structures and stability.

The starch replacement of gluten free bread by cellulose (FC0) and fibrillated cellulose (FC60) was then investigated. Similar to the effects previously reported for hydrocolloids, both FC0 and FC60 decrease pasting temperature due to water and volume competition with starch. Comparing the replacement by either FC0 and FC60, fibrillation increases the functionality of cellulose and enhances the composite structure. They significantly strengthen the doughs due to their high water binding ability and fibrous structure but reduce extensibility. They restrain the volume increase during proving and lead to lower specific volume of loaves with denser and harder crumb. However, the crumb structure is finer.

Additionally, the generalised Maxwell model was applied to study the dough rheology. The relaxation frequencies were estimated which are higher than the deformation rate

during proving. It suggests that gluten free doughs behave like viscoelastic fluid during proving.

In summary, gluten free bread with partial replacement of flour can be produced by incorporation of MC, PSY, cellulose and fibrillated cellulose. Deliberate consideration of the addition levels of MC and water would be required to improve bread quality while addition of PSY and flour replacements by cellulose and fibrillated cellulose are detrimental to loaf volume and, therefore, lead to denser and harder crumb. Water addition level needs to be adjusted in further work to improve the bread quality.

Acknowledgements

The present research was performed in the Division of Food, Nutrition and Dietetics at the Univerisity of Nottingham, funded by the University of Nottingham via Vice-Chancellor's Scholarship for Research Excellence (International) and PepsiCo International Limited.

First of all, I would like to express my sincere appreciation to my supervisor, Prof. Tim Foster, who kindly offered me this opportunity and various training and learning opportunities, for his continuous support and guidance, wealth of knowledge, patience, and encouragement. He helped to improve my research capability and finally complete this thesis.

I would also like to thank Dr Gleb Yakubov for his valuable discussions about the second chapter. I would like to thank Dr William MacNaughtan for his support and knowledge, especially in NMR. I would like to thank Dr Bettina Wolf and Dr Guy Channel for their suggestions on rheology, thank Dr Roger Ibbett for helping me with monosaccharide analysis using Dionex and thank Khatija Nawaz Husain for her technical help with confocal laser scanning microscopy.

I would like to extend my gratitude to Bruce Linter from PepsiCo for his advice.

I am grateful to all students, staff, and members in Food Sciences. Especially, I would like to thank Jade Phillips who did biochemical measurements with me and Sonia Holland for sharing information on covalent labelling of polysaccharides. I would like to thank technicians for providing training on the equipment. Many thanks to all for the friendship and wonderful environment.

Table of Contents

List of Figures

List of Tables

List of abbreviations and symbols

ATR FTIR	Attenuated total reflectance Fourier transform infrared spectroscopy
(Δ)BS	(Change of) backscattering
A/X ratio	Arabinose to xylose ratio
Ara	Arabinose
CNC	Cellulose nanocrystals
CPMAS NMR	Cross polar magic angle spinning Nuclear magnetic resonance
CPMG	Carr-Purcell-Meiboom-Gill
DMSO	Dimethyl sulfoxide
DP	Degree of polymerisation
DSC	Differential scanning calorimetry
FC	Fibrillated cellulose
FITC	Fluorescein isothiocyanate
G’	Storage (elastic) modulus
G’’	Loss (viscous) modulus
HPMC	Hydroxypropyl methylcellulose
LVE	Linear viscoelastic
MC	Methylcellulose
MFC	Microfibrillated cellulose
NFC	Nanofibrillated cellulose
PCA	Principal components analysis
PSY	Psyllium seed husk powder
RSD	Response surface design
RVA	Rapid visco analyser
TPA	Texture profile analysis
TTS	Time-temperature superposition
w/w %	Weight percentage
Xyl	Xylose
η^*	Complex viscosity
η_0^*	Zero shear viscosity
λ	Relaxation time
ω	Angular frequency

w_{rel}	Relaxation frequency

List of Manuscripts under preparation

Ren, Y., Yakubov, G., Linter, B. R., MacNaughtan, B. & Foster, T. J. Temperature fractionation, and physicochemical and rheological analysis of psyllium. Manuscript submitted for publication.

Ren, Y., Linter, B. R. & Foster, T. J. Cellulose fibrillation and interaction with psyllium heteroxylan. Manuscript submitted for publication.

Ren, Y., Linter, B. R. & Foster, T. J. Investigations of gluten free bread dough rheology, proving and baking performance and bread qualities by response surface design and principle component analysis. Manuscript in preparation.

Ren, Y., Linter, B. R. & Foster, T. J. Starch replacement of gluten free bread by cellulose and fibrillated cellulose. Manuscript submitted for publication.

List of presentations

Ren, Y. & Foster, T. J. Food intolerance and healthy diet - gluten-free bread with low calorie content and glycemic index. 2nd Annual Conference - Manufacturing Food Futures, 23-23 March 2016. Loughborough, UK (poster presentation).

Ren, Y. & Foster, T. J. Applications of Methyl Cellulose and Psyllium in Gluten Free Bread and Manufacturing Issues. Gluten Free Bakery Conference, 16-17 March 2017. Chipping Campden, UK (oral presentation).

Ren, Y. & Foster, T. J. Flour property comparison for gluten free bread production. 3rd Annual Conference - Manufacturing Food Futures, 30-31 March 2017. Birmingham, UK (oral and poster presentation).

Ren, Y. & Foster, T. J. The Influences of Methyl Cellulose and Psyllium and Their Applications in a Flour-Water System with Medium Water Content (ca. 55%). 19th Gums & Stabilisers for the Food Industry Conference, 27-30 June 2017. Berlin, Germany (oral presentation).

Ren, Y. & Foster, T. J. Texture-improving approaches for low moisture gluten free bakery products- hydrocolloids and modified starch. 4th Annual Conference - Manufacturing Food Futures, 26-27 March 2018. Sutton Bonington, UK (oral and poster presentation).

Ren, Y. & Foster, T. J. Rheological properties of gluten free bread doughs under small deformation tests and possible application of strain-rate frequency superposition. Annual European Rheology Conference, 17 20 April 2018. Sorrento, Italy (poster presentation).

Ren, Y. & Foster, T. J. Temperature fractionation, and physicochemical and rheological analysis of psyllium. 32nd EFFoST International Conference, 6-8 November 2018. Nantes, France (poster presentation).

Chapter 1.

Introduction

Wheat flour is widely consumed as a main ingredient in diets all over the world. However, many people around the world are intolerant to gluten which leads to coeliac disease and other gluten-triggered health problems. On the other hand, the population of overweight adults and children has continued to increase around the world and obesity has been become a global health challenge during the past three decades which lead to numerous health problems including type 2 diabetes. Therefore, it is beneficial and important to produce gluten-free products with low-calorie content and glycaemic index without losing the texture and quality for the purpose of dealing with gluten intolerance and diabetes and controlling the prevalence of obesity.

1.1. Gluten-intolerance and obesity

1.1.1. Gluten intolerance

Many people around the world are intolerant to gluten, which leads to coeliac disease and other gluten-triggered health problems (Catassi et al., 2012; Czaja-Bulsa, 2015). Coeliac disease, the most widely studied gluten-triggered disease, is an autoimmune genetically determined chronic inflammatory intestinal disorder (Fasano & Catassi, 2001; Schuppan, 2000). The disease is multifactorial in terms of both genetic (intrinsic) and environmental (extrinsic) factors, and, as a result, the clinical manifestation spectrum ranges widely and heterogeneously from asymptomatic to severe malabsorption with the characteristics ranging from the normal but invaded intestinal mucosa, villous atrophy, to the final formation of flattened villi on the small intestinal mucosa (Di Sabatino & Corazza, 2009; Schuppan, 2000; Wahab, Meijer, Goerres & Mulder, 2002). For coeliac patients, the toxic proteins in gluten are prolamins which are abundant in proline and glutamine (Holmes, Catassi & Fasano, 2009). It is reported that the prevalence of the coeliac disease in the world is approximately 1 in every 100 people

(Zandonadi, Botelho & Araujo, 2009). Besides, the amount of diagnosed coeliac patients is increasing as the development of diagnostic methods increase (Arendt, Renzetti & Bello, 2009; Unsworth & Brown, 1994). In addition to coeliac disease, gluten sensitivity is also an issue in public health. According to a new nomenclature proposed by Sapone et al. (2012), apart from coeliac disease, there are other gluten-related disorders, i.e. gluten ataxia, dermatitis herpetiformis, wheat allergy, and gluten sensitivity. Gluten ataxia and dermatitis herpetiformis are also autoimmune problems. Aziz et al. (2014) found that gluten sensitivity was reported by 13% of the population and the prevalence of diagnosed coeliac disease was 0.8% in Sheffield, UK.

1.1.2. Gluten free diet

A gluten-free diet is the only treatment to coeliac disease with the expected outcome that the absorbing surface area recovers and absorbs nutrients normally (Shepherd & Gibson, 2013). However, exclusion of certain foods could lead to an unbalanced diet and limited variety in food choices, and, therefore, be adverse to a healthy diet. The elimination of wheat from diet requires substitute foods including other grains, whole grains, milk, egg, and meat for the supplementation of energy, protein, fibres, and other micronutrients (Skypala & McKenzie, 2019). However, dietary analysis of children and adolescents shown unbalanced intakes of the three major nutrients with a low proportion of complex carbohydrate but high consumption of protein and lipid (Hopman, le Cessie, von Blomberg & Mearin, 2006; Mariani et al., 1998; Öhlund, Olsson, Hernell & Öhlund, 2010). The gluten free diet could be low in energy and protein when milk and eggs are also eliminated which are also commonly seen food allergens (Skypala & McKenzie, 2019) which might further increase the intake of lipid. Additionally, a gluten free diet

could fail to support the full recovery of gut microbiota and the use of prebiotics could be required (Marasco et al., 2016).

1.1.3. Obesity

On the other hand, the removal of gluten from the diet easily lead to a significant increase in body fat stores and weight gain in coeliac patients (Capristo et al., 2000; Hager et al., 2012). A study on teenagers undergoing gluten free diets also shows a higher incidence of overweight or obesity (Mariani et al., 1998). In addition, coeliac disease is found related to type-1 diabetes which is also an autoimmune disease, especially for children (Bao et al., 1999; Lorini et al., 1996; Maki, Hallstrom, Huupponen, Vesikari & Visakorpi, 1984).

The proportion of overweight adults and children has increased around the world and obesity has become a global health challenge during the past three decades (Ng et al., 2014). Obesity is a result of unbalanced energy intake and expenditure and the prevalence of obesity around the world is caused by consumption of energy-dense foods and reduced physical activity due to the changing of living styles (World Health Organization, 2018). According to the World Health Organization (2018), 'obesity is defined as abnormal or excessive fat accumulation that may impair health'. Obesity is related to type 2 diabetes, cardiovascular diseases, certain types of cancer, obstructive sleep apnea, osteoarthritis, and depression (Haslam & James, 2005; Luppino et al., 2010). It is suggested that the risk of becoming diabetic increases with the gaining of body weight over a certain threshold (Resnick, Valsania, Halter & Lin, 2000). According to an estimation of the prevalence of diabetes over the next two decades after 2010, the number of adult diabetes patients, with a 50% increase, will increase faster

than population growth (Shaw, Sicree & Zimmet, 2010). To prevent obesity and diabetes, a diet containing low calories and/or glycaemic index is recommended or even necessary (Ludwig, 2002). However, the intake of starch-rich food (e.g. white bread) will increase dietary glycaemic index and can increase the incidence of type-2 diabetes while the intakes of dietary fibres can lower the risk (Hodge, English, O'Dea & Giles, 2004). Hence, the replacement of starch with dietary fibre can be adopted in the control of the incidence of type-2 diabetes (Fellstone, 2011).

1.2. Bread and Gluten free bread

1.2.1. Gluten and wheat bread

Gluten is storage protein in wheat and other related species such as rye, barley, and oats (Biesiekierski, 2017; Shewry, Halford, Belton & Tatham, 2002). The existence of gluten contributes to elasticity, extensibility, resistance to stretch, mixing tolerance and gas holding abilities of bread dough and therefore influences bread appearance and crumb structure (Arendt et al., 2009; Wieser, 2007). The main functions of gluten in bread making are network formation and water binding (Bache & Donald, 1998; Cuq, Boutrot, Redl & Lullien-Pellerin, 2000; Day, Augustin, Batey & Wrigley, 2006; Fellstone, 2011). Gluten mainly consists of glutenins and gliadins (insoluble in water but different solubility in ethanol) with a ratio close to 1:1.1 in common bread wheat flour (Abdelaal, Hucl & Sosulski, 1995). They both contain high amounts of glutamine and proline (Wieser, 2007). Gliadins are mostly monomeric proteins with only intramolecular disulphide bonds. Glutenins consist of a backbone of high molecular weight subunits and branches of low molecular weight subunits with both intra- and intermolecular disulphide bonds forming a network. Gliadins interact with glutenins via non-covalent bonds including hydrogen bonds, ionic bonds and hydrophobic bonds. Glutenins

contribute to strength and elasticity of dough but gliadins influence dough viscosity and extensibility (Arendt et al., 2009; Belitz, 2009).

The formation of bread doughs requires hydration and mechanical energy input (kneading). Gluten has high water absorbability that 1 g of native gluten can absorb 2.5 to 3 g of water. Hydration allows the formation of hydrogen bonds in addition to disulphide bonds which further contribute to the viscoelastic property of doughs. The hydration level of gluten might influence the formation of particulate proteins and aggregates (Kontogiorgos, 2011). In addition, gluten competes for water with starch and other minor components such as arabinoxylan and β-glucan. On the other hand, mechanical mixing (kneading) breaks glutenin macromolecules into smaller units by scission of disulphide bonds which can partially recover (with adjacent molecules) during resting of the doughs, and, therefore, allow realignment of glutenins (Cauvain, 2015). Kneading also incorporates air as small gas cells which are nuclei for the further growth of gas cells during proving and baking. Over-kneading leads to shorter and thinker protein strands and a softer dough which is detrimental to the gas retention ability of doughs. The diagrams in Figure 1.1 represent dough structures before proving highlighting small gas cells nuclei, starch granules, and gluten matrix.

After hydration and kneading, the doughs are proved at an appropriate atmosphere to allow yeasts to grow and generate carbon dioxide for loaf rising (Figure 1.1d). Taking a macroscopic view, the gluten network allows gas cell expansion and stabilises cells during proving and forms films between them (Kokelaar, van Vliet & Prins, 1996). Dissolution of carbon dioxide, enzymatic degradation of starch and development of flavour are also happening during proving.

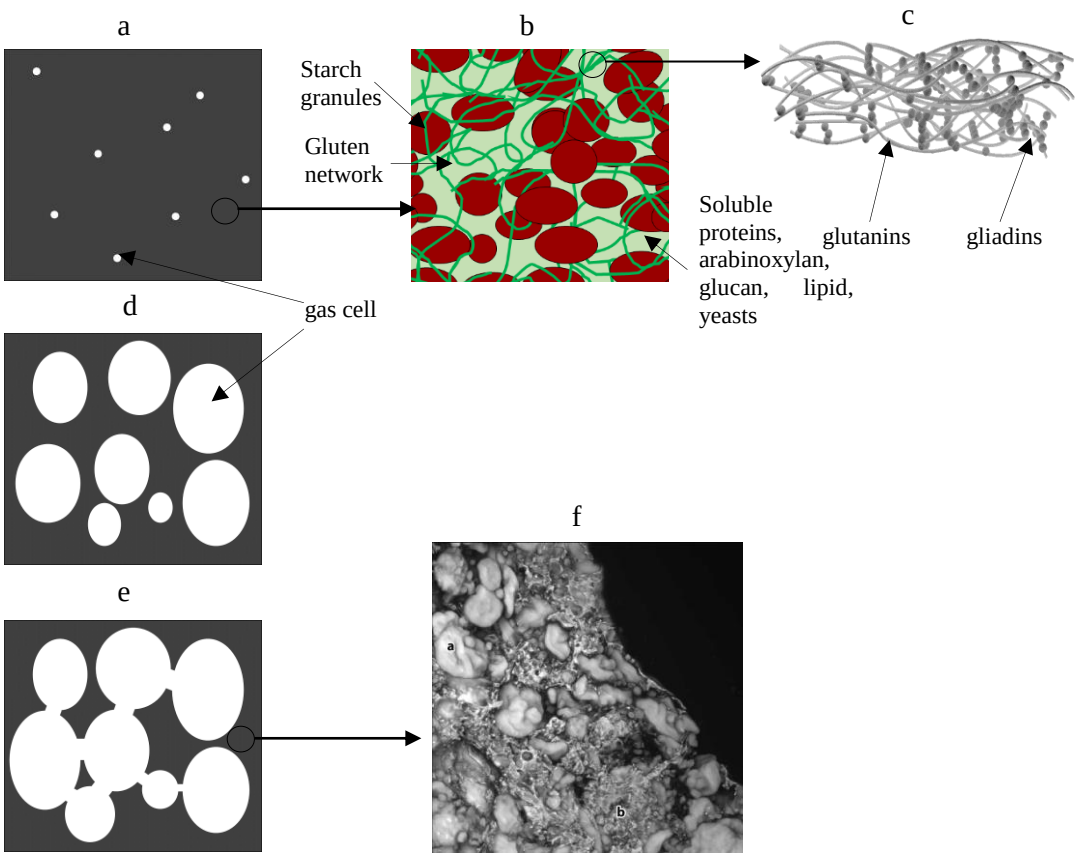

Figure 1.1. Schematic representations of wheat bread dough before proving highlighting small gas cells nuclei (a), starch granules and gluten matrix (b) and gluten structure (Miguel, Martins-Meyer, Figueiredo, Lobo & Dellamora-Ortiz, 2013) (c); wheat doughs during and after proving (d); and after baking (e) highlighting microstructure of bread crumb (Zannini, Jones, Renzetti & Arendt, 2012) (f).

The doughs experience dramatic changes during baking including yeast deactivation, further expansion of gas cells, gluten and other protein denaturation, starch gelatinisation, and structural changes from foam to sponge-like (Figure 1.1e). As one of the major changes, about 55 % of the oven rising is attributed to thermal gas expansion, approximately 35 % is due to the release of carbon dioxide from the matrix and only the remaining 10 % comes from yeast activity before being deactivated by high temperature (Cauvain, 2015). Baking is associated with dramatic water loss and redistribution. Gluten is denatured at high temperature and releases water which

participates in starch gelatinisation (Willhoft, 1971). Water also migrates toward either the surface or the thermal core of the loaves and the driving forces include temperature gradient, moisture gradient and partial water vapour pressure gradient among which the partial water vapour pressure gradient results in evaporation-condensation-diffusion of water which promotes heat transition from surface to the core of loaves and increases moisture content in the core (Lucas et al., 2015; Wagner, Lucas, Le Ray & Trystram, 2007). In wheat bread, the solid matrix of the crumbs consists of a bicontinuous phase of gelatinised starch and a gluten network which encloses the starch granules and fibre fragments (Figure 1.1f) (Arendt et al., 2009). Gluten also contributes to bread quality by binding water which prohibits staling. The gluten network slows down the movement of water; thus, gluten-free bread is more prone to staling (Hager et al., 2012).

1.2.2. Gluten-free bread

For the purpose of dealing with gluten intolerance and meeting the trend of "free from" food among consumers and markets, gluten free products, including gluten free bread, are becoming a new challenge and a favourite of both manufacturers and researchers. However, as a result of the absence of gluten, gluten-free bread tends to have inferior textural quality. The supply of gluten-free products in the market is small and with low-quality in terms of texture, colour, flavour and price (Fellstone, 2011). In addition, most gluten-free bread is made of high starch content ingredients, they mostly have higher staling rates and shorter shelf-life (Arendt et al., 2009). The removal of gluten in bread making generates a less stable and viscous liquid batter instead of bread dough and then results in products with crumbling texture, poor colour, and post-baking inferiorities (Gallagher, Gormley & Arendt, 2004; Torbica, Hadnadev & Dapcevic, 2010).

There are two basic criteria for gluten replacement, compatibility and availability (Fellstone, 2011). To produce gluten-free bread, other sources of proteins or carbohydrates can be used such as rice flour, corn flour, sorghum flour, chestnut flour, Chickpea flour, tiger nut flours, isolated starch, and whey protein etc. Rotsch (1954; cited in Gallagher et al., 2004) suggested that gluten-free bread can only be made by adding gel alternatives to gluten to retain gas. The polymers which contribute to the texture of bakery products include gas-retaining agents, setting agents and conventional dough ingredients such as softener, plasticisers and emulsifiers (Engleson, Lendon & Atwell, 2012).

Currently, a large number of formulations and methodologies have been developed for gluten-free bread manufacturing, which can be categorised as the application of alternative flour blends, enzyme treatments and sourdough applications, and other treatments, among which, the application of alternative flour blends is the main and basic method. An alternative flour blend is mostly a blend of one or more types of starch and/or starch-based flours and, in most cases, hydrocolloids. One of the early studies on rice bread was conducted by Nishita, Roberts, Bean and Kennedy (1976) who investigated the additions of different kinds of hydrocolloids, dough conditioners and lipids. They reported that hydroxypropyl methylcellulose (HPMC) and refined vegetable oils gave better loaves in the absence of dough conditioners and surfactants. Haque and Morris (1994) also investigated rice flour based bread with the addition of HPMC and isabgol (psyllium) under different water contents and proving temperatures and obtained higher aeration than most commercial wheat bread. Onyango, Unbehend and Lindhauer (2009) evaluated different cellulose derivatives and reported that the addition of methylcellulose (MC) formed softer crumb and a reduced staling rate compared to HPMC (firmness: hydroxypropylcellulose > microcrystalline cellulose >

HPMC > MC > Carboxymethylcellulose) in sorghum and cassava starch bread. Xanthan gum is another popular hydrocolloid appearing in many commercial gluten free flour blends. Its fibrous structure provides stability, consistency, and cohesiveness to doughs and final products. Zandonadi et al. (2009) produced gluten free bread with single addition of psyllium with good acceptance. Mariotti, Lucisano, Pagani and Ng (2009) also reported the promising utilisation of psyllium in gluten free bread by mixing it with other kinds of flours. Cappa, Lucisano and Mariotti (2013) evidenced a central role of psyllium in gluten free bread production because of its film forming ability; and anti-staling effect as it has high water binding ability. More interestingly, Haque and Morris (1994) found that the incorporation of gluten in rice flour did not give a comparable loaf at the same addition level as in soft wheat flour. Therefore, the logic of gluten free bread production should, to a certain extent, not fully rely on the knowledge of wheat bread production. In another word, it should be a comprehensive and integrated investigation aiming at structure and texture improvement instead of simply finding alternatives to gluten.

1.3. Starch and rice flour

1.3.1. Starch

1.3.1.1. Molecules and structures

Starch is energy storage polysaccharide produced by green plants via photosynthesis. It is synthesised and stored in chloroplasts by green leaves or in the amyloplasts of storage organs of plants e.g. seeds, fruits, roots, tubers, and stems. Starch largely exists in grains (e.g. rice, wheat, and corn), potatoes, cassava etc., which is one of the main energy and nutrient sources for humans and livestock. It is also used, sometimes modified, as a thickener, stabiliser, and emulsifier to modify the texture and structure of foods.

Starch is composed of amylose and amylopectin (Figure 1.2a). Amylose is a linear polysaccharide composed of α (1→4) linked D-glucopyranosyl units with molecular weight in the order of 10^5 to 10^6 Da. There might be a small amount of α (1→6) linked branches and phosphate groups whose influence on the solution behaviour of the molecules is insignificant (Buléon et al., 1998; Hoover, 2001). Amylopectin is α (1→4) linked glucan with 5 to 6% branched by α (1→6) glycosidic bonds with molecular weight of approximately 10^8 Da.

Amylopectin chains can be classified into A chains (outer chains which are branches to the inner chains), B chains (inner chains) and C chains (one per amylopectin molecule with one reducing end) (Peat, Whelan & Thomas, 1952). It can also be classified according to chain length such that short chains (S chain) consist of both A and B chains with degree of polymerisation (DP) between 14 to 18, and long chains (L chain) consisting of long B chains with DP of 45 to 55 or higher (Buléon et al., 1998). S chains form discrete clusters while L chains are backbones supporting the clusters of S chains (Buléon et al., 1998) (Figure 1.2c). It is widely accepted that amylopectin forms left-handed double helix (Figure 1.2b) with six glucose units per turn which compose the crystalline regions of starch granules.

The cluster model proposed by Robin, Mercier, Charbonniere and Guilbot (1974) and French (1972) is widely accepted describing the supermolecular structure of amylopectin. It is composed of alternating amorphous regions and crystalline regions. The amorphous regions contain (1→6) branching points. The lateral alignment of clusters forms the crystalline regions and, therefore, A chains (short chains) define the thickness of the crystalline region (Figure 1.2c) (Buléon et al., 1998).

Three types (A, B, and C types) of crystalline forms were found in starch giving distinct X-ray diffraction patterns where the double helices are packed in different ways (Figure 1.2g) (Imberty et al., 1991). Type A crystalline regions are denser than type B and type C contain both type A and type B. Type A (A starch) is widely found in cereals with bigger starch granules while type B (B starch) is usually found in cereals with higher amylose content, tubers, and banana. Whereas type C is found in peas and beans. Additionally, amylose form complexes (V-type) with fatty acids, iodine, alcohols or dimethylsulfoxide (DMSO), where amylose adopts left-handed single helical conformation with six, seven, or eight glucose per turn depending on the size of the inclusion (Pérez & Bertoft, 2010).

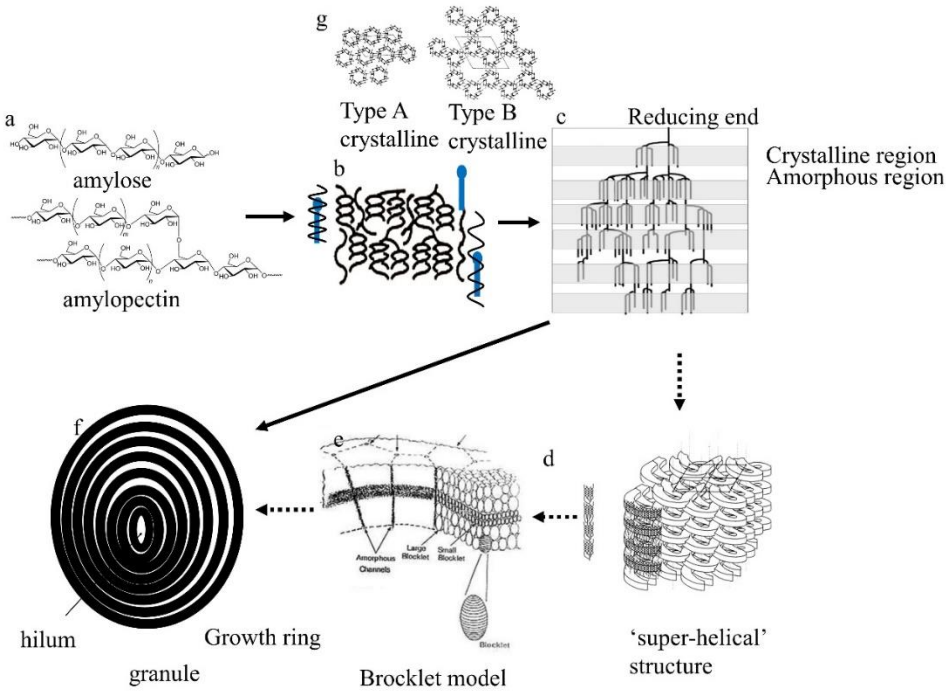

Figure 1.2. Schematic representation of amylose and amylopectin (a) and the hierarchical structural composition of starch granule modified from Buléon, Colonna, Planchot and Ball (1998) (b) (c),Oostergetel and van Bruggen (1993) (d),Gallant, Bouchet and Baldwin (1997) (e), and Imberty, Buléon, Tran and Péerez (1991) (g)

The amorphous and crystalline regions form growth rings of starch with a hilum. However, how the different structural levels constitute the starch granules are not fully illustrated (Pérez & Bertoft, 2010). Hence, dashed lines are used in Figure 1.2 representing possible constitutions of different structural levels. Oostergetel and van Bruggen (1993) proposed 'super-helical' arrangement of the semi-crystalline domains (Figure 1.2d) based on electron diffraction pattern of potato starch fragments. The super-helices are left handed with a diameter of 18nm. A brocklet concept (Figure 1.2e) was proposed by Gallant et al. (1997). Brocklets are in roughly ellipsoidal in shape composed of alternating lamellae of crystalline and amorphous amylopectin with diameters of 20 to 500 nm. The size of the brocklet varies within the different locations in starch granules and across botanical origins (Gallant et al., 1997). The radial channels of semi-crystalline or amorphous regions exist in granules which allow amylose to leach out during gelatinisation and increase sensitivity to enzymes (Gallant et al., 1997).

Starch granules vary in size and shape. Amaranth starch has the smallest granules (1 to 3 μm) while large starch granules are found in potato (5 to 100 μm). Wheat starch granules show bimodal distribution where large granules have a size of approximately 25 μm and small granules are smaller than 10 μm (Mason, 2009). In terms of granule shape, rice and corn starch granules are polyhedron shape; potato starch has oval granules; and wheat starch granules are either spherical or flat circular (Jackson, 2003).

1.3.1.2. Starch during cooking

Starch granules gelatinise at elevated temperatures with water addition during which irreversible structural transition occurs with disruption of granules and viscous slurries or pastes are generated. In the conventional analysis of pasting profiles, a rapid visco

analyser (RVA) is used to measure the viscosity of starch pastes in excess water during heating (gelatinisation) and cooling (retrogradation) with shearing. A typical profile is shown in Figure 1.3. Native starch granules are dispersed in water at low temperature (typically lower than 50 ºC) with low viscosity (number 1 in Figure 1.3). When temperature increases, starch granules significantly absorb water and swell which leads to a sharp increase in viscosity (number 2 in Figure 1.3). The onset temperature is marked as the pasting temperature. With a further increase of temperature, starch granules are finally closely packed giving a peak viscosity (number 3 in Figure 1.3). Amylose leaches out of granules during this process (Schirmer et al., 2015), and is soluble in a freshly prepared solution existing as random coils (Hayashi, Kinoshita & Miyake, 1981). Starch granules lose their integrity with shearing at high temperature (marked as breakdown ('4' in Figure 1.3)) which leads to a trough viscosity ('5' in Figure 1.3).

This irreversible structural transition of starch during heating is significantly influenced by moisture content. By analysing the differential scanning calorimetry (DSC) traces of potato starch, Donovan (1979) proposed that, with sufficient water, the amorphous regions absorb water and swell and the crystallites are pulled apart which is accompanied by unfolding and hydration of the helices at a lower temperature (66 ºC for potato starch); however, a limited amount of water leads to locally high water content, which allows a proportion of crystallites to lose their conformational order at the low temperature while the remaining crystallites melt at a higher temperature when water is uniformly redistributed.

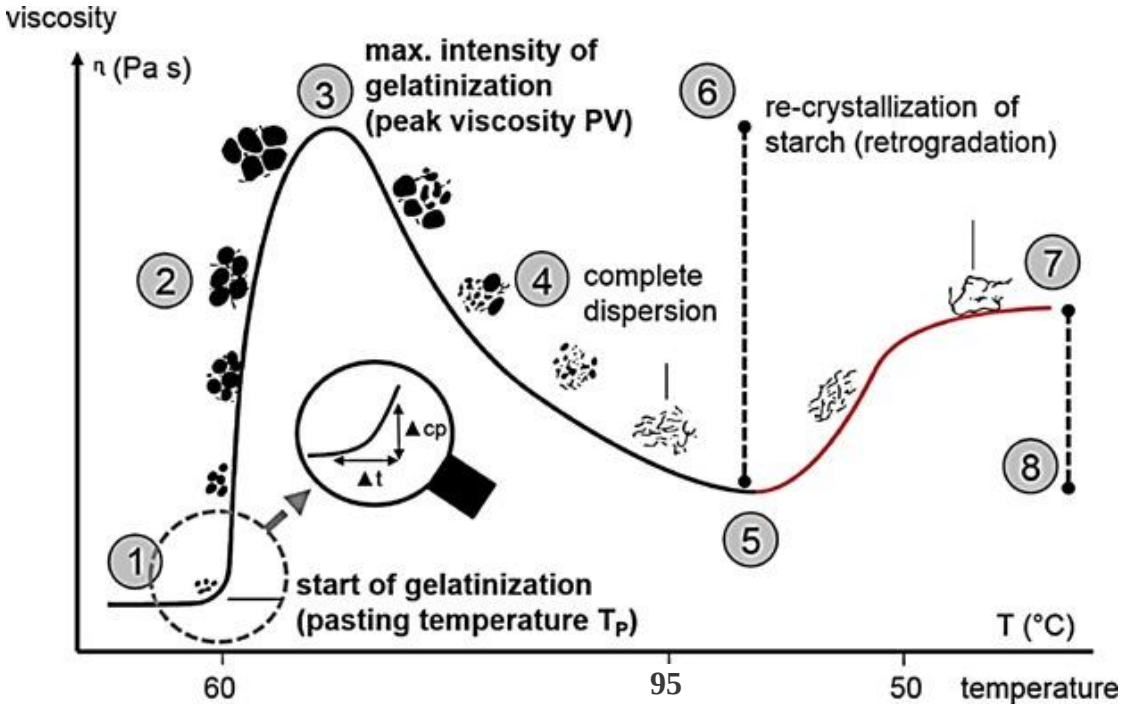

Figure 1.3. pasting profile and schematic representation of starch modified from Schirmer, Jekle and Becker (2015).

Water is insufficient in wheat doughs for full starch gelatinisation though starch absorbs water from denatured gluten. Under such condition together with low shearing (comparing to the experimental condition in RVA), wheat starch swells and gelatinises and forms an inhomogeneous network of swollen and interconnected starch granules with amylose accumulated in the centre due to phase separation of amylose and amylopectin (Hug-Iten, Handschin, Conde-Petit & Escher, 1999).

1.3.1.3. Starch retrogradation

Retrogradation describes the molecular association and ordering of starch chains in gelatinised starch pastes by mainly hydrogen bonds after cooling, resulting in the formation of an elastic gel (Hoover, 2001). Retrogradation contributes to an increase in viscosity during cooling in the pasting profile which is marked as setback (number 7

and 8 in Figure 1.3). During retrogradation, amylose, on a short time scale, forms double helices in the range of 40 to 70 glucose residues in the absence of inclusions (Jane & Robyt, 1984; Miles, Morris, Orford & Ring, 1985). It has been suggested that, on longer time scales, the amylose double helices form junction zones and contribute to the formation of a gel (Gidley, 1989; Gidley & Bociek, 1985). The amylopectin retrogradation is slower than amylose. The outermost short chains (DP of approx. 15 (Miles et al., 1985)) of amylopectin crystallise during storage (Ring et al., 1987). The crystallites formed during retrogradation are weaker than the crystalline regions in native starch (Sasaki, Yasui & Matsuki, 2000).

1.3.2. Rice flour

Rice flour is made from finely milled rice grains. It is widely used in gluten free bread production as one of the main ingredients because of its bland taste, white colour, low sodium content, easily digested carbohydrates, and hypoallergenic properties (Kadan, Robinson, Thibodeaux & Pepperman, 2001). The amylose content of rice flour varies in the range from 0 (waxy) to 30% depending on botanical origin. Amylose content significantly influences the behaviour of rice flour during gelatinisation and retrogradation. Amylose forms complexes with lipids which restricts the release of amylose from starch granules during gelatinisation and, as a result, reduces swelling power and solubility (Morrison, Tester, Snape, Law & Gidley, 1993; Tester & Morrison, 1990). In the pasting profiles, a high amylose content leads to higher pasting temperature, lower peak viscosity, and higher setback viscosity (Jane et al., 1999). Starch granules with high amylose content are more resistant to mechanical damage during milling (Han, Campanella, Mix & Hamaker, 2002).

Additionally, damaged starch also influences flour properties. Damaged starch decreases gelatinisation temperature (Morrison, Tester & Gidley, 1994), increases water absorbability of flour (Hatcher, Anderson, Desjardins, Edwards & Dexter, 2002), and increases susceptibility to enzyme digestion and hydrolysis (Dhital, Shrestha & Gidley, 2010). However, an excessive amount of damaged starch decreases swelling during cooking and increases solubility in cold water, as a result of degradation of amylopectin, which leads to inferior effects in e.g. noodle or bread productions (Tran et al., 2011).

Additionally, rice flour contains 2.5% lipid and 7% protein. Rice proteins tend to aggregate and form a denser structure after cooking (Hamaker & Bugusu, 2003; Schober, 2009). Therefore, rice proteins are expected to have fewer negative impacts on starch gel strength and uniformity (Schober, 2009) than the presence of lipid.

1.4. Hydrocolloids and dietary fibres

1.4.1. Methylcellulose

Hydrocolloids have a wide application in the food industry because of their functions to create structure, stablise the system, influence texture and sensory profiles (Foster, 2010). Methylcellulose (MC) is one of the most popular hydrocolloids in the formulation of gluten free bread (Masure, Fierens & Delcour, 2016). Cellulose molecules are linear chains of glucose linked by β (1→4) glycosidic bonds which strongly associate via extensive hydrogen bonds and are insoluble in water. MC is produced by etherification of cellulose with an intermediate substitution (degree of substitution between 1.4 and 2.0 usually) (Grover, 1993; Li et al., 2002). In the industrial production of cellulose ethers, for economical and technical convenience, cellulose is usually only activated, for example, in alkaline solutions instead of being

dissolved; therefore, the reaction firstly occurs in amorphous domains (Burchard, 2003). This heterogeneous substitution leads to a large variety of cellulose ethers (Burchard, 2003). Along the molecular chains of MC and other cellulose derivatives, the hydroxyl residues of native cellulose molecules are partially substituted (by methyl in the case of MC) (Figure 1.4) which make them water soluble and endow them with desired functionalities. The solubility is achieved by the steric repulsion between backbones caused by the substituting chemical groups (Burchard, 2003). However, due to the heterogeneous reaction during production, there are underivatised segments on the molecular chains which form bundles. The bundles lead to deviation of rheology behaviour in solution from solutions of entangled coils (Haque, Richardson, Morris, Gidley & Caswell, 1993b).

MC and other cellulose ethers are widely applied in various industries including foods, cosmetics, pharmaceuticals, and civil construction etc. One of the most favourable property is their thickening effect. The underivatised segments form bundles with dangling outer chains which significantly enlarge the hydrodynamic volume and, hence, increase their contribution to viscosity. The viscosity of solutions of MC and other cellulose ethers are significantly influenced by molecular weight, concentration, and temperature (below gelation temperature).

Thermoreversible gelation is another unique property of MC and other cellulose ethers. They form gels during heating and return to the liquid state upon cooling. As for the thermal gelation mechanism, an early study by Heymann (1935) proposed that dehydration is involved in the early step of gelation which leads to coagulation and the formation of a loose network with a strong tendency of syneresis. Haque and Morris (1993) later postulated, which is widely accepted, that methylcellulose gelation includes

molecular strand softening, separation of strand ends, and hydrophobic association due to the exposure of hydrophobic methyl substituents at a higher temperature and finally form a gel network. Hydroxypropyl groups significantly affect the property of cellulose ether which causes different properties between MC and HPMC. The Hydroxypropyl group is more polar due to its hydroxyl groups, which alter the hydrophobic effect (Haque et al., 1993b). Additionally, due to their larger size and higher internal flexibility, increased substitution by hydroxypropyl groups severely interferes with the molecular associations of the polymer chains (Haque et al., 1993b). Therefore, compared to MC, HPMC forms gels at a relatively higher temperature (50-55°C for MC, 58-90°C for HPMC depending on the degree of hydroxypropyl substitution) and the gel strength is softer. The gelation temperature also shows a negative response to increases in concentration or molecular weight (Funami et al., 2007).

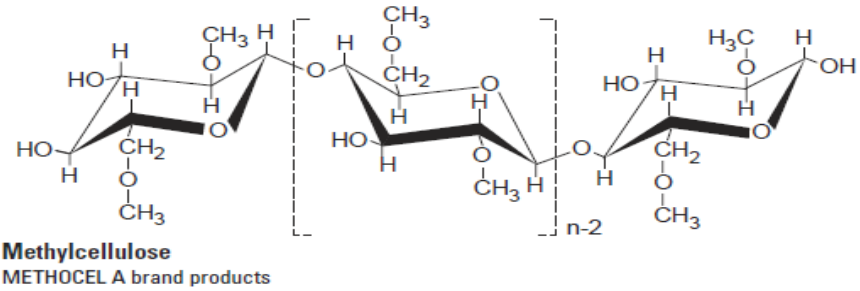

Figure 1.4. Molecule structure of Methylcellulose (The DOW Chemical Company, 2002)

1.4.2. Psyllium and heteroxylan

Plantago is a genus which includes about 200 species. There are two species whose name contain ‘psyllium’, i.e. *Plantago ovata* (Indian wheat, blond psyllium) and *Plantago psyllium* (sand plantain, French psyllium, dark psyllium). However, psyllium, also known as ispaghula or isabgol, commonly refers to *Plantago ovata*, which is

mainly cultivated in northern India. Psyllium has been being traditionally used in medical treatment in some countries and it is proven that psyllium has the ability to lower cholesterol levels, be used as laxative, and improves insulin sensitivity (Anderson et al., 2000; Madgulkar, Rao & Warrier, 2015; Song, Sawamura, Ikeda, Igawa & Yamori, 2000). The husk of psyllium seeds is used for commercial production of mucilage. It is widely used as binders in the landscape industry, pharmaceutical and drug delivery systems, and as thickeners in the food industry. It is commonly used in ice cream and gluten free bread as thickener and stabiliser.

The mucilage forming polysaccharides in psyllium husk are mainly composed of heteroxylans. The xylan backbone is composed of β-(1 → 4) linked D-xylose while the sidechains contain various motifs of arabinose and/or xylose which can be substituted on C3 or/and C2 positions of the backbone xylose sugars (Edwards, Chaplin, Blackwood & Dettmar, 2003; Fischer et al., 2004; Guo, Cui, Wangb & Young, 2008; Yu et al., 2017). Due to the large amount of arabinose, arabinoxylan is widely used in the literature referring to psyllium polysaccharides for comparability to cereal and hemicellulose arabinoxylans which usually have a simpler structures. Small amounts of galacturonic acid and rhamnose have also been identified (Fischer et al., 2004; Guo et al., 2008; Yu et al., 2017). However, it is under debate whether psyllium heteroxylan is substituted by these rhamnose and galacturonic acid which leads to a charged polymer; or the mucilage contains both neutral heteroxylan and polyuronide (Farahnaky, Askari, Majzoobi & Mesbahi, 2010; Fischer et al., 2004; Laidlaw & Percival, 1949).

Alkaline extraction or fractionation of psyllium husk mucilage has been widely applied with different alkaline concentrations (Guo et al., 2008; Haque, Richardson, Morris & Dea, 1993a; Marlett & Fischer, 2005; Yu et al., 2017). The alkaline fractionation is

usually combined with water fractionation at different temperatures (Guo et al., 2008; Yu et al., 2017). Fractions with different chemical and structural properties and/or rheological properties were obtained by different fractionation procedures. In addition to solvent quality, Van Craeyveld, Delcour and Courtin (2009) found that the extractability increases with a decrease in the concentration of psyllium husk and an increase in extraction temperature.

Psyllium heteroxylans, at least the majority of them, are insoluble in water, while they have high water absorbability and show 'weak gel' property (storage moduli higher than loss moduli and storage moduli is frequency dependent) (Haque et al., 1993a). However, detailed molecular structure and conformation, and mechanism of the gel property of psyllium heteroxylan have not been fully characterised.

1.5. Cellulose

Cellulose abundantly exists in the cell wall of plants as a structuring material. It usually accounts for 20 to 30% of parenchyma cell walls, by dry weight (Franz & Blaschek, 1990). It can also be secreted by some bacteria and algae. The material was firstly isolated and analysed by Payen (1838). The cellulose molecule is a β-glucan composed of (1→4) linked D-glucose with every second glucose residue rotated by 180°, which adopts a flat, 2-fold helical conformation (Huber, Iborra & Corma, 2006; Wyman et al., 2005). Cellulose is insoluble in water; instead, it forms crystallites which are stabilised by intramolecular hydrogen bonds between ring oxygen and O3-H; and O6 and O2-H of a neighbouring glucose; and intermolecular hydrogen bonds between O3 with O6-H and O2 with O6-H. The sheets with their more hydrophobic surfaces exposed are stacked together and stabilised by van der Waals forces (Figure 1.5a). In this way,

approximately 36 individual cellulose chains associate in parallel into larger units known as elementary fibrils or protofibrils with amorphous regions in between, which further pack into microfibrils with diameters ranging from 2 to 20 nm (Habibi, Lucia & Rojas, 2010; Pääkkö et al., 2007; Wyman et al., 2005). The amorphous regions lead to dislocations which lead to tilts and twists of the microfibrils (Habibi et al., 2010; Pääkkö et al., 2007; Wyman et al., 2005). The assembling process occurs in a rosette-shaped plasma membrane complex (Brown, 1996). The microfibrils are orientated as several layers around a lumen and further packed into macrofibrils with amorphous lignin and hemicellulose (Bledzki & Gassan, 1999) (Figure 1.5b).

Cellulose crystallites have four forms, i.e. I_α, I_β, II and III. Native cellulose secreted by bacteria and algae is mainly in Iα crystalline form and plant cell wall cellulose is mainly in I_β form. I_α and I_β crystallites are same in the fibre repeat distance with the value of 1.043 nm for the interior fibre repeats and 1.029 nm on the surface of the crystallites (Davidson, Newman & Ryan, 2004). They are mainly different in the relative displacement of the sheets in the chain direction with different hydrogen bond patterns where 2-OH and 6-OH groups have different orientations (Nishiyama et al., 2003) (Figure 1.6). The different hydrogen bond patterns are likely to be the reason that cellulose I_β is more stable than I_α. Cellulose I_α can convert to cellulose I_β by annealing.

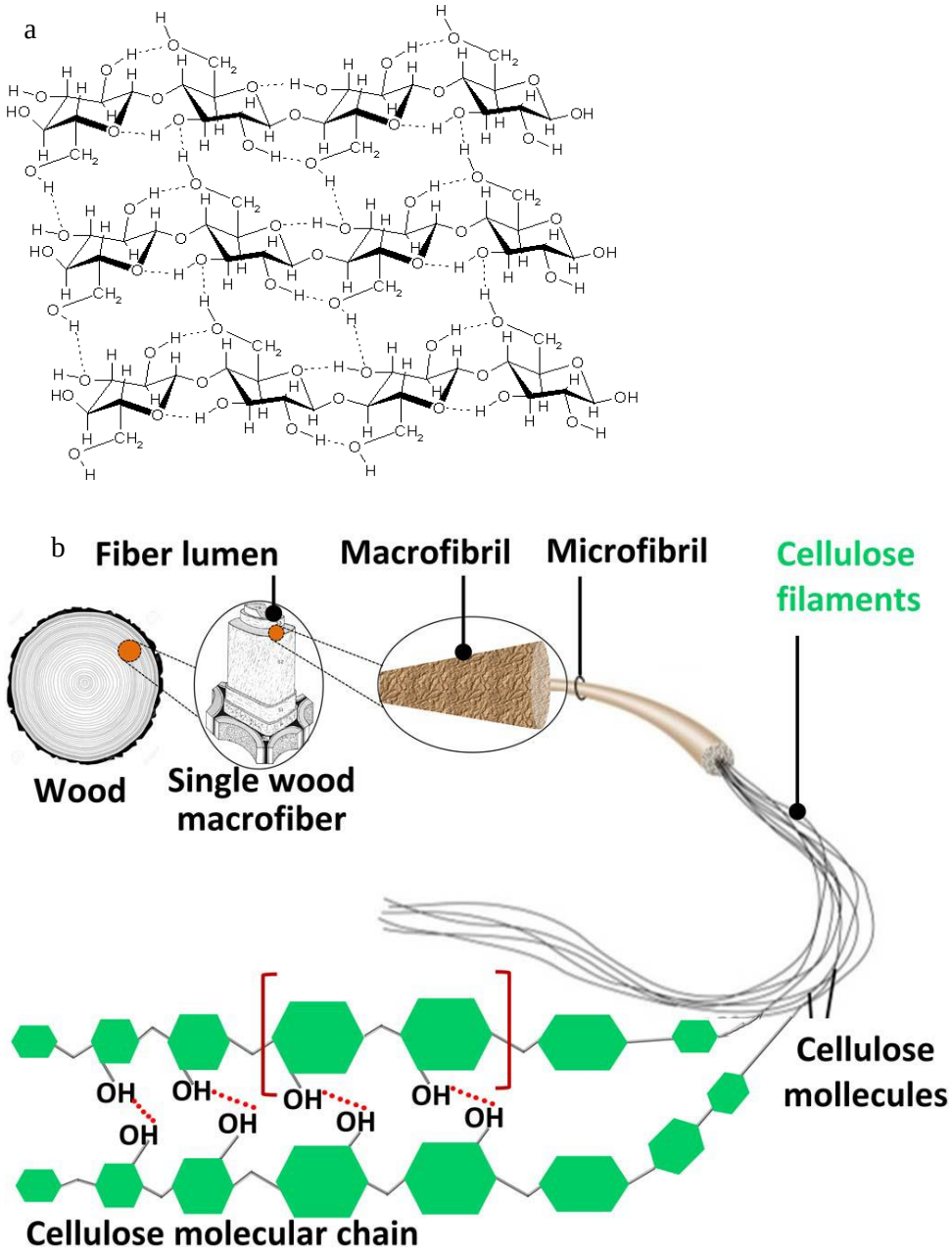

Figure 1.5. Schematic representation of structure of crystallite of native cellulose (https://www.doitpoms.ac.uk/tlplib/wood/structure_wood_pt1.php) (a) and the hierarchical structural composition of cellulose in wood (Hisseine, Omran & Tagnit-Hamou, 2018) (b).

Cellulose I recrystallises during mercerisation by alkaline treatment or regeneration which generates cellulose II, which is more thermodynamically stable. Being different from cellulose I, the molecules are arranged in an antiparallel manner in the cellulose II

crystalline form. Cellulose III_1 and cellulose III_2 are produced by mercerizing cellulose I or II respectively in ammonia or diamine treatment.

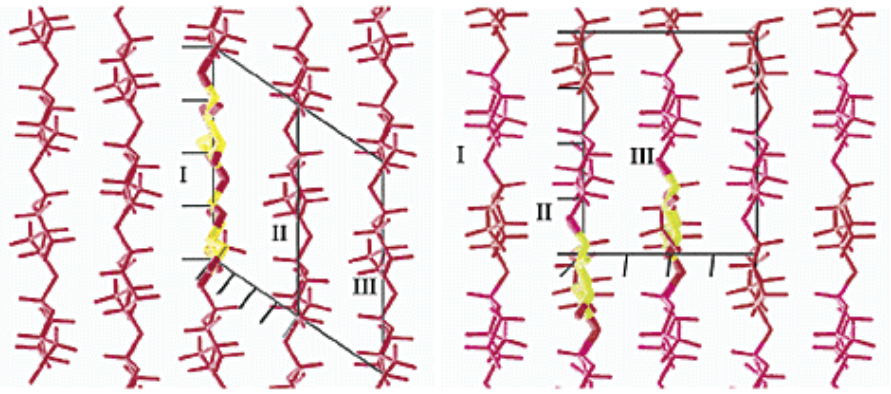

Figure 1.6. Projections of the I_α (left) and I_β (right) crystalline structures of cellulose in the direction perpendicular to the chain axis and in the plane of the hydrogen bonded sheets (middle) (Nishiyama, Sugiyama, Chanzy & Langan, 2003)

1.5.1. Nanocellulose

Nanocellulose refers to nano-structured cellulose. It is classified into three types, i.e. Microfibrillated cellulose (MFC), cellulose nanocrystals (CNC) (Figure 1.7), and bacterial cellulose. MFC is produced by mechanical treatment, such as high shearing, which leads to delamination of the high level cellulose structure and the generation of long fibrils. Therefore, MFC has very high aspect ratios which forms a highly entangled network of fibril aggregates with strong mechanical properties. CNC, also known as whiskers, is produced by chemical treatment, e.g. strong acidic treatment with sonication, which attacks the weak amorphous dislocations and produces crystalline rods. CNC, in contrast, has low aspect ratios, which is used in the preparation of high-performance nanocomposites, barrier films, and chiral materials etc. Bacterial cellulose is secreted by certain bacteria (mainly *Gluconacetobacter* strains).

1.5.2. Microfibrillated cellulose

Microfibrillated cellulose (MFC) is also referred to as cellulose microfibril, microfibrillar cellulose, or nanofibrillated cellulose (NFC). A MFC fibre is usually an aggregate of cellulose microfibrils (Svagan, Azizi Samir & Berglund, 2007). Cellulose microfibrillation was first introduced by Turbak, Snyder and Sandberg (1983a) and Herrick, Casebier, Hamilton and Sandberg (1983). They treated wood pulp by high pressure and shearing in a Gaulin homogenizer, which lead to physical unwinding of native cellulose fibres and generated highly entangled cellulose fibrils. The generated MFC has significantly increased surface area, high liquid retention ability, and high reactivity in enzymatic or chemical treatments (Herrick et al., 1983; Turbak et al., 1983a). In addition to homogenisers, another equipment widely used to produce MFC by generating high pressure and shearing is a microfluidiser, generating higher pressures up to 30000 psi (Siqueira, Bras & Dufresne, 2010). Therefore, MFC with thinner and more uniform dimensions can be produced (Lavoine et al., 2012). Refiners, cryocrushing, grinders, and extrusion were also used to produce MFC, which sometimes are combined with high pressure homogeniser and microfluidiser (Alemdar & Sain, 2008; Heiskanen, Harlin, Backfolk & Laitinen, 2014; Iwamoto, Nakagaito, Yano & Nogi, 2005; Wang & Sain, 2007). Although MFC is usually produced by fibrillating native cellulose (cellulose I), it has also been obtained by a cellulose regeneration process by electrospinning which generates cellulose II crystallites (Li & Xia, 2004; Walther, Timonen, Díez, Laukkanen & Ikkala, 2011).

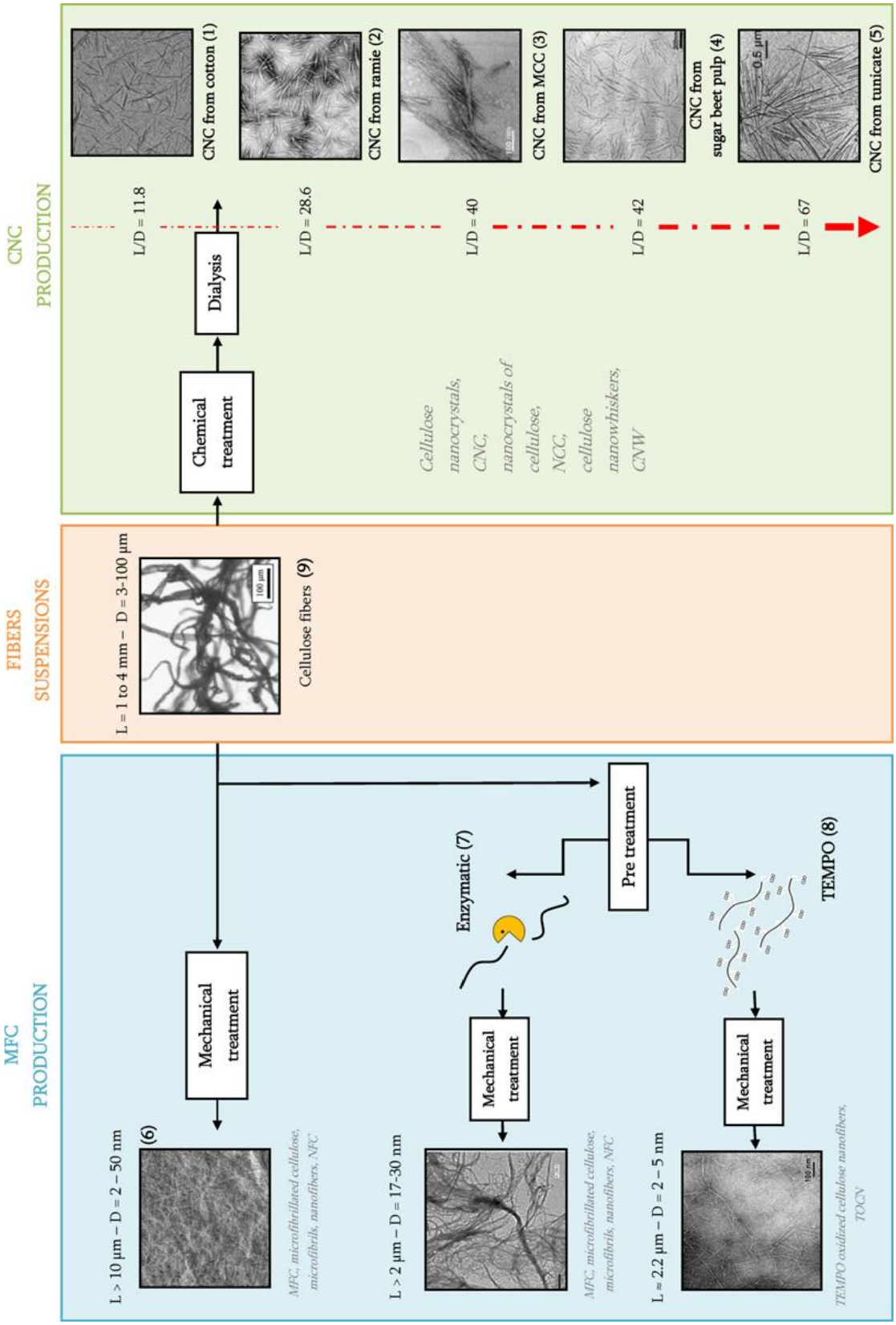

Figure 1.7. Summary of treatments to cellulose and classification of nanocellulose (Lavoine et al., 2012)

Pre-treatment is important to reduce the energy input during fibrillation. Firstly, purification by alkaline is widely applied to remove lignin, pectins and hemicelluloses (Siró & Plackett, 2010). Other pre-treatments include a reduction in hydrogen bonding; addition of a repulsive charge; and/or a decrease the degree of polymerisation or the amorphous linkages and the methods include enzymatic treatment, TEMPO mediated oxidation, and carboxymethylation and acetylation (Lavoine et al., 2012).

1.6. Objectives

The main project target was to produce gluten-free bread with high textural and nutritional qualities by gluten replacement and partial starch replacement with the purpose of dealing with gluten intolerance, obesity, and type-2 diabetes. The work was built on investigations on the formulation of alternative flour blends, the addition of hydrocolloids e.g. MC and psyllium, the characterisation of gluten free bread, and testing the application of low energy density cellulose as a starch replacer.

More specifically, the objectives were:

- To investigate the rheological behaviours and molecular structural properties of psyllium husk heteroxylan.
- To develop a quick cellulose fibrillation method and to investigate novel aqueous composites of (fibrillated) cellulose and psyllium husk mucilage.
- To investigate the roles of methylcellulose and psyllium in gluten free dough and bread properties based on comprehensive characterisation; and correlations of parameters by simultaneous application of response surface design (RSD) and principal components analysis (PCA).

- To investigate the starch/flour reduction of rice flour based gluten free bread by cellulose and fibrillated cellulose.

1.7. Thesis structure

Chapter 1 of this thesis provides a general introduction of the materials and literature relevant to the project. Based on the four detailed objectives, the project was composed of four sections and the results are presented in chapter 2, 3, 4, and 5. Each chapter contains a specific introduction and materials and methods section (Figure 1.8). In most cases these chapters formed significant input to manuscript submissions.

The work in Chapter 2 focused on psyllium husk which produces mucilage once hydrated. The mucilage was fractionated at different temperatures and the obtained fractions show unique rheological properties. Molecular compositions and structures were analysed and two hypotheses were proposed to interpret the observed molecular and rheological properties.

In Chapter 3, purified wood cellulose was fibrillated by a colloid mill. The method to concentrate the suspensions were studied. Cellulose and fibrillated cellulose were used to prepare mixtures with psyllium and psyllium fractions prepared in Chapter 2. It has been shown that psyllium heteroxylan interacts with cellulose and fibrillated cellulose.

The work in Chapter 4 investigated the influences of methylcellulose and psyllium on gluten free doughs and bread. The characterisation of dough properties, bread qualities, and proving and baking performance was maximised which generated a large number of parameters. Therefore, simultaneous application PCA and RSD was applied to reduce the dimension size and study the correlations between responses. This is the first attempt

to combining PCA with RSD to investigate the additions of hydrocolloids in gluten free bread and to generate a more comprehensive characterisation.

Starch replacement by cellulose and fibrillated cellulose are presented in chapter 5. The influences on dough rheology, proving and baking performance, and bread quality were investigated.

Chapter 6 attempts to bring the findings of this work to a series of conclusions, which in turn provide a number of recommendations for further studies.

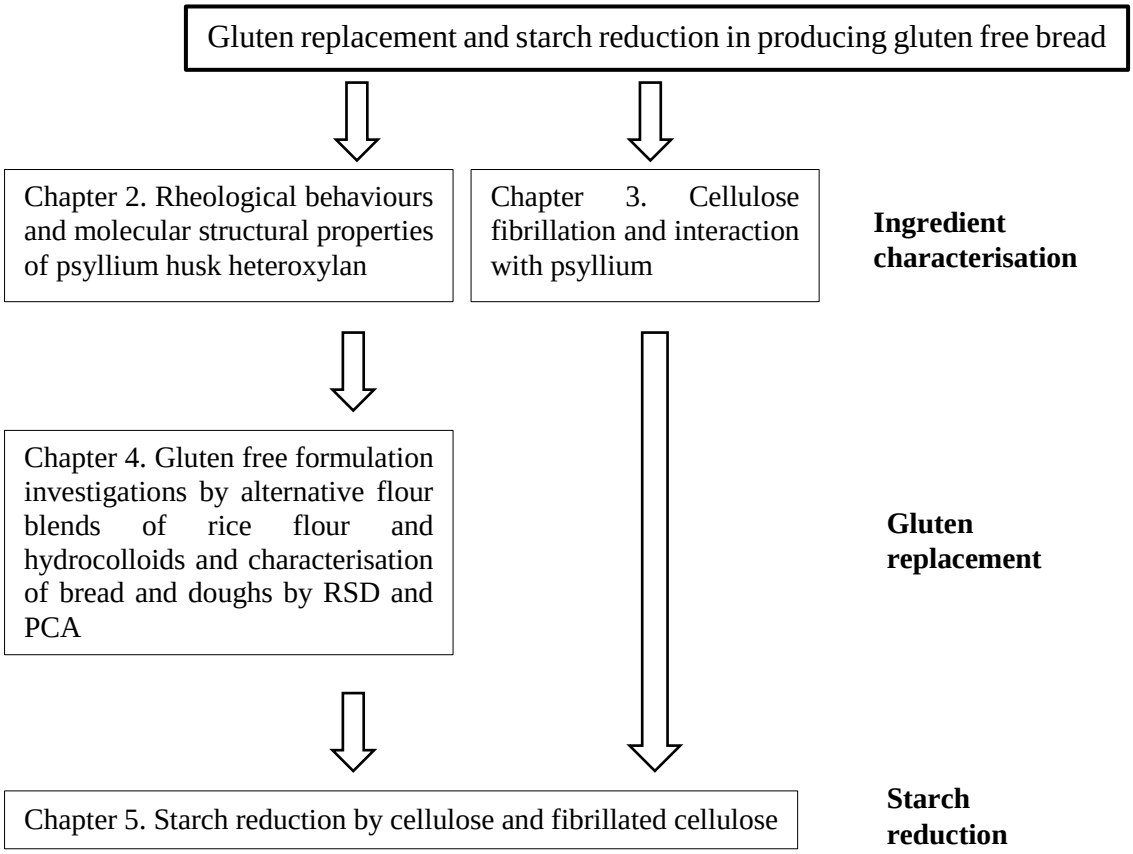

Figure 1.8. Thesis structure

Chapter 2.

Temperature fractionation, physicochemical and rheological analysis of psyllium husk heteroxylan

Highlights:

- Psyllium husk heteroxylan is fractionated by a straightforward method
- Fractions show distinct rheological properties
- Arabinose/xylose ratio can be estimated by 2nd-derivative FTIR and ^{13}C NMR spectra
- Composition and spatial arrangement of sidechains are influential
- Two hypotheses were proposed

Keywords:

Psyllium husk, Heteroxylan (arabinoxylan), Time-temperature superposition (TTS), Temperature fractionation, arabinose/xylose ratio, rheology

Abstract

Psyllium husk is a source of natural dietary fibre with marked water absorbability and gelling properties, which makes it an attractive functional ingredient for applications in the food industry, such as gluten free bread and breakfast cereals. The main functional component of psyllium husk is a complex branched heteroxylan. In this study, a straightforward sequential fractionation of hydrated psyllium seed husk powder (PSY) based on temperature-dependent behaviours was applied. The F20 (20°C fraction) showed the highest yield followed by F60, while 13.5% of the PSY is unextractable (residue).

The obtained fractions show unique rheological properties as analysed using small amplitude oscillatory shear rheometry and the time-temperature superposition (TTS) technique. The results indicate that: 1) only F20 was influenced by heat treatment, 2) high temperature fractions showed stronger gel properties, 3) a three-step softening/melting was observed, 4) F60 has longest relaxation time as shown in TTS master curves. The four fractions were also characterised using the monosaccharide analysis, FTIR, and ^{13}C NMR. The arabinose/xylose ratio is found to increase with the increase in fractionation temperature and FTIR and ^{13}C-NMR spectra supported that low temperature fraction is less branched. Two hypotheses were therefore proposed: The first one based on models by Haque et al. (1993a) and Yu et al. (2019) focusing on chemical and structural properties of the molecules. The second hypothesis highlights differences in hierarchical molecular conformations of polysaccharides which is proposed by Diener et al. (2019). Sidechain substitution, composition and length of sidechains are critical and significantly influence the properties of each fraction.

2.1. Introduction

The seed husk of psyllium, also known as ispaghula or isabgol, referring to *Plantago ovata* Forsk, is a source of natural dietary fibre, which has good water absorbability and shows gelling properties and can, therefore, be applied in food production as a novel functional ingredient. It has been being traditionally used in medical treatment in some countries and it is proven that psyllium has the ability to lower cholesterol levels, be used as laxative, and improve insulin sensitivity (Anderson et al., 2000; Madgulkar et al., 2015; Song et al., 2000). Psyllium is currently widely used in applications ranging from gluten free bread making to drug delivery thanks to its high water binding capacity, thickening effect and gel-forming ability (Cappa et al., 2013; Chavanpatil, Jain, Chaudhari, Shear & Vavia, 2006; Haque & Morris, 1994; Mancebo, San Miguel, Martínez & Gómez, 2015; Mariotti et al., 2009; Singh, 2007).

The functional part is the mucilage from the seed husk where the main polysaccharide is heteroxylan mainly composed of (1 → 4) linked β-D-xylose with sidechains on C-3 or C-2 positions containing arabinose and xylose in various motifs (Edwards et al., 2003; Fischer et al., 2004; Guo et al., 2008; Yu et al., 2017). Small amounts of galacturonic acid and rhamnose were also identified and other reports stated that the psyllium heteroxylan is slightly charged (Fischer et al., 2004; Guo, Cui, Wang, Goff & Smith, 2009; Guo et al., 2008; Yu et al., 2017). Laidlaw and Percival (1949) evidenced that extracts of psyllium seed husk contain both neutral arabinoxylan and polyuronide, however, Farahnaky et al. (2010) confirmed the presence of carboxylic groups on the psyllium molecules. However, Fischer et al. (2004) found that the main compound, arabinoxylan, is neutral but with trace amounts of other sugars. The conflicts in full agreement of structure often lie in different extraction methods adopted.

Most studies on the psyllium husk are based on defined extraction and sometimes fractionation methods. Farahnaky et al. (2010) mechanically extracted psyllium husk with water with a yield of 28.5%. However, alkaline extraction is more common. Guo et al. (2008) extracted and fractionated psyllium gums by hot water and alkaline solutions with yield up to 61.4% for an alkaline gel fraction and the molecules in different fractions showed different molecular structures and stability in terms of hydrodynamic radius. Marlett and Fischer (2005) and Fischer et al. (2004) used alkaline and acid solutions to extract and fraction psyllium husk (highest yield is 57.5% for alkaline extracted gel) and they also showed differences in the molecular composition and viscosity. More information about extractability of psyllium husk polysaccharide was recorded by Van Craeyveld et al. (2009) showing an extraction increase being more significant when the concentration of psyllium husk decreased rather than with an extraction temperature increase, showing effects on gel structure. They also observed a higher yield using an alkaline extraction method, where the charge state of uronic acid is affected.

Although psyllium husk polysaccharide has been extracted and fractionated by water and alkaline solutions and the fractions show differences in terms of molecular structure and rheological properties, they all show gel-like property when hydrated in water (Farahnaky et al., 2010; Guo et al., 2009; Haque et al., 1993a; Yu et al., 2017). An earlier study by Haque et al. (1993a) proposed a ‘weak gel’ property describing the rheological behaviour of the psyllium polysaccharide dispersion. Guo et al. (2009) investigated the structure and rheological properties of alkaline extracted psyllium gel and the subsequent influence of Ca^{2+}. They found that the addition of Ca^{2+} changed the gel microstructure from fibres to aggregates, increasing elastic modulus and critical

strain in a certain range of addition level, and increasing thermal stability. The influences of concentration, temperature, and pH on the gel properties of psyllium were investigated by Farahnaky et al. (2010). They found that freeze-dried psyllium gel adopts lath sheet-like structure, and higher concentration, heat treatment, and higher pH increased structure stability, generated ordered structure, and decreased pore size distribution, respectively. Efforts have also been made to modify the properties of psyllium husk polysaccharides by acid treatment and phosphorylation (Cheng, Blackford, Wang & Yu, 2009; Rao, Warrier, Gaikwad & Shevate, 2016). For the mechanism of the gel-like property, an early study attributed gelation to the association of unsubstituted (1 → 4) linked xylan backbones existing as continuous blocks (Sandhu, Hudson & Kennedy, 1981). Later Haque et al. (1993a) described the polysaccharides as being packed as strands, which then form a 'weak gel' with tenuous interactions. The latest work has focused on the stability and importance of hydrogen bonds between sidechains maintaining and influencing the gel structure and property (Yu et al., 2019).

Because psyllium husk is usually applied as dispersion in water, whose property is influenced by temperature and given that different structures have been observed in the whole psyllium suspension, this study extracted and fractionated suspension of psyllium seed husk powder (PSY) in water at different temperatures by a straight, simple, and sequential process which can be easily applied in industry to generate fractions with different properties (Lundin & Hermansson, 1995; Richardson, Clark, Russell, Aymard & Norton, 1999). Additionally, exploring the molecular structure and conformation and microstructure provided a better understanding of the mechanism of the gel-like rheological property. PSY polysaccharide is widely referred to arabinoxylan in the literature due to the high content of arabinose and comparability to other arabinoxylan

found in other cereal materials and hemicellulose. However, ‘heteroxylan’ is adopted in this work because of the complex sidechains.

2.2. Methods and materials

2.2.1. Materials

Psyllium husk powder (Vitacel®) was kindly donated by the JRS (J. Rettenmaier & Söhne Group, Rosenberg, Germany). Toluidine blue and methyl blue were purchased from Sigma–Aldrich (UK).

2.2.2. Temperature fractionation and sample preparation

PSY was extracted and fractionated in water at 20 °C, 40 °C, 60 °C, 80 °C, and 100 °C which are labelled F20, F40, F60, F80, and F100. The unextractable polysaccharides and other unidentified substances are termed residue. To fractionate PSY, 10 g of PSY were hydrated in 2000 ml of RO water for 2 hours with stirring and then homogenized by an Ultra-Turrax homogenizer (T25, Ika®-Werke, Germany) for 10 min. The suspension was then centrifuged (Beckman J2-21 centrifuge, rotor JA-10) at 17700 g and 20 °C for 60 minutes. The supernatant was collected and freeze-dried and labelled as F20. The gel and insoluble phases were redispersed to the volume of 2000 ml by high speed shearing for 1 minute using an Ultra turrax homogeniser followed by 2 hour stirring at 40 °C. The suspension was homogenised for 10 minutes again and centrifuged at 17700 g and 40 °C for 60 minutes. The supernatant was collected and freeze-dried and labelled as F40. The same procedure was performed on the remaining gel and solid part but at 60 °C, 80 °C and 100 °C. The supernatants of high temperature fractions were

concentrated by rotary evaporator with the temperature set at 60 °C before freeze drying. The residue was also freeze dried.

The yields of different temperature fractions are shown in Table 2.1; the highest yield is observed for F20 with F100 having the lowest yield. The yield of residue is slightly higher than that observed by Guo et al. (2008). They reported that some water-extractable heteroxylan is trapped within the husk walls and can be released only under alkaline conditions. Therefore, the conditions used in this study, i.e. 100 °C and high shearing, is not sufficient to fully extract PSY polysaccharide.

For rheological and other tests, a fresh suspension of PSY was prepared by dispersing PSY in RO water at room temperature and allowed to hydrate for 1 hour before tests. F20 was dispersed in water using an Ultra turrax and hydrated at room temperature for 30 minutes with stirring. The sample was degassed under vacuum and stirred for another 30 minutes. F40, F60, and F80 were prepared in a similar way and stirred at corresponding temperatures. Stock dispersions were prepared in the same way and stored at 4 °C.

2.2.3. Chemical and monosaccharide analysis

The protein content of PSY was converted with the factor of 6.25 from nitrogen content analysis by Nitrogen Analyser NA 2000 (Fisons Scientific Equipment, Loughborough, UK). Lipid content was obtained by extraction with a chloroform-methanol mixture (2:1). Moisture content was obtained by drying at 105 °C and ash content was measured using a muffle furnace at 550° for 6 hours.

Monosaccharide composition of whole PSY and fractions were analysed by hydrolysing 2 mg of samples in 66.7 µl 12M sulphuric acid for 1 hour at 37 °C followed by incubation at 99 °C for 2 hours after dilution to 1M sulphuric acid. The supernatants were diluted 100 times with 10mM NaOH. Analysis of monosaccharides was performed by high-performance anion exchange chromatography with pulsed amperometric detection (HPAEC-PAD) (Dionex, UK) with a CarboPac PA20 column. The mobile phase was 10mM NaOH with a flow rate of 0.5 ml min^{-1}. The data were calculated against arabinose, galactose, glucose, and xylose as standards.

2.2.4. ATR-FTIR measurements

FTIR spectra of whole PSY and freeze-dried fractions were collected by a Bruker Tensor 27 spectrometer (Germany) equipped with diamond attenuated total reflection (ATR) crystal in the range from 4000 to 550 cm^{-1}. The spectra were acquired averaging 128 scans with a resolution of 4 cm^{-1} against an empty background. Normalisation and baseline correction on whole spectra were performed by Opus 7.2.139.1294. Smoothing and 2nd derivatives of spectra over 1020 to 920 cm^{-1} were calculated by GraphPad Prism 7.04.

2.2.5. ^{13}C solid-state Nuclear Magnetic Resonance (^{13}C CPMAS NMR)

^{13}C CPMAS NMR spectra of dry samples were recorded on a Bruker AVANCE III 600 NMR spectrometer (Karlsruhe Germany) equipped with narrow bore magnet and 4-mm triple resonance probe. Samples were packed into 4mm rotors and spun at 10 kHz. Adamantane with an upfield peak (29.5 ppm) was tested as an external standard to

reference chemical shift scales. The Proton 90° pulse length was 3 μs followed by contact period with 83 kHz for field strength of the proton and spin locking field.

Peak fitting was performed on certain peaks by Lorentzian function as shown in equation (2.1) where y_0, x_c, w, and A indicate baseline, peak centre, peak width at half maximum, and area under the peak respectively. The areas were used to estimate A/X ratio.

$$y = y_0 + \frac{2A}{\pi}\frac{w}{4(x - x_c)^2 + w^2} \qquad (2.1)$$

2.2.6. Rheological properties

Oscillation tests were performed using an MRC 301 rheometer (Anton Paar, Austria), with parallel plate geometry including a sandblasted upper plate (PP50-SN11649, Anton Paar). The measuring gap was 1 mm. Extra sample was trimmed by a spatula and the edge of samples was covered by low viscosity mineral oil (Sigma, USA) to prevent drying of samples. The temperature was controlled by a Peltier system with the assistant of a water bath (R1, Grant, Shepreth). Amplitude sweeps, frequency sweeps, temperature sweeps, and time dependence tests were performed.

The freshly prepared suspension of PSY was tested at both 20 °C and 98 °C. The tests at 98 °C were performed by loading a sample at room temperature, increasing to 98 °C, and holding for 500 seconds before tests. Tests on heated and cooled samples were performed by loading samples at room temperature, increasing to 98 °C, holding for 10 minutes, cooling back to 20 °C, and holding for 120 seconds before tests. During temperature sweep tests, the temperature was increased from 20 °C to 98 °C, held for

10 minutes, and cooled back to 20 °C. The heating rate was 1 °C min^{-1}. Two cycles of heating and cooling were applied to PSY suspension with 2 hours holding at 20 °C in between.

For the fractions, freshly prepared samples were loaded onto the rheometer at 20 °C. F20 was first subjected to a frequency sweep test at 20 °C followed by temperature sweep test with the same temperature profile for the whole PSY sample as described above. A frequency sweep test was performed again after the end of the second heating and cooling circle followed by an amplitude sweep test. F40, F60, and F80 were also loaded at 20 °C but the temperature increased to 40 °C, 60 °C, and 80 °C individually and frequency sweep tests were performed at corresponding temperatures. The samples were cooled back to 20 °C and the same sequence of tests on F20 were performed. Samples rested for 120 to 500 seconds before tests and between two different tests. Amplitude sweep tests were performed at a frequency of 10 rad s^{-1} and frequency tests were performed with a strain of 0.2% which is in the linear viscoelastic (LVE) region. Strain and angular frequency applied in temperature sweep tests were 0.2% and 10 rad s^{-1} respectively.

To perform time-temperature superposition (TTS), the mechanical spectra of 4 fractions were obtained at different temperatures ranging from 20 °C to 80 °C. More specifically, the sample was loaded at 20 °C and the temperature changed in the range from 20 °C to 80 °C during which the sample was tested at each constant temperature. The tests at each temperature were repeated at least twice regardless of the temperature history ahead. The strain used at low temperatures was 0.2% but it was 2% at temperatures higher than 60 °C to reduce noise.

2.2.7. Fluorescent and optical microscopy

PSY was dispersed and hydrated in an aqueous solution of 0.1% toluidine blue for 1 hour. A drop of the dispersion was mounted onto the hot stage (THMS600, Linkam, Surrey, U.K.) and observed via bright field illumination with a Leitz Diaplan microscope (Germany). The sample was heated from 20 °C to 95 °C at 5 °C min^{-1} and a series of images were captured at different temperatures by a digital camera.

As for the acquisition of fluorescent images, PSY was dispersed in saturated methyl blue and hydrated for 1 hour. Half of the suspension was heated in a boiling water bath for 20 minutes followed by 1 hour cooling at room temperature. Then the heated and unheated samples were scanned using a fluorescent microscope (Evos FL, Waltham, US) equipped with a DAPI (357/44 - 447/60 nm) light cube. The heated PSY fractions (collected after DSC traces) were stained with saturated methyl blue and imaged by the fluorescent microscope.

2.3. Results

2.3.1. Properties of whole PSY suspensions

The moisture content, protein content, ash content, and lipid content of PSY were 7.23±0.03%, 3.40±0.03%, 2.89±0.01%, and 3.30±0.30%, respectively. The monosaccharide composition of PSY includes 22.68±0.51% arabinose, 3.32±0.12% galactose, 3.99±0.11% glucose, and 55.38±0.98% xylose with total sugar of 85.36%. The results of chemical and monosaccharide composition analysis can be seen to be similar to Guo et al. (2008). The major monosaccharide components in PSY are arabinose and xylose. However, the contents of protein and lipid are slightly higher, which possibly indicates contamination during husking and milling processing.

The rheological properties of PSY were measured by frequency sweep tests and temperature sweep tests (Figure 2.1). A freshly prepared PSY suspension shows gel-like property at room temperature as G' is higher than G'' (Figure 2.1a). The 'gel' melted during heating as both G' and G'' decreased whereas upon cooling a stronger 'gel' is formed, with G' being much greater than G''. Upon reheating and cooling this gel-like rheological property appears to be thermoreversible.

To understand the structure better, a frequency sweep test was performed on freshly prepared, heated (at 98 °C), and cooled PSY suspensions and mechanical spectra are shown in Figure 2.1b**.** Both freshly prepared and cooled PSY showed that G' were higher than G'' in the measurable frequency range and both moduli show dependence on frequency. The logarithmic values of complex viscosity (η*) decreased linearly with that of angular frequency (ω) with slopes of -0.67 and -0.86 for freshly prepared and cooled PSY respectively. The latter one is consistent with the results from Haque et al. (1993a) on alkaline extracted psyllium gel, in which they suggested a similarity with xanthan showing 'weak gel' network. As for the freshly prepared PSY, η* showed less dependence on ω, while G' and G'' were more frequency dependent. However, the thermal property of the melting of PSY was evaluated by DSC with the same temperature profile as the temperature sweep tests performed by rheometer (data not shown) and no thermal peaks were identified and the heat flow in the two cycles superimpose each other. This is in agreement with recent work by Yu et al. (2017) who describe PSY gels as 'physical gels'. Additionally, the T2 spectra of unheated and heated PSY 'gel' did not show any significant difference with a value of 977 ms for the dominant peak, which is assigned to water protons (data not shown). It suggested that heat treatment does not influence water mobility in PSY suspensions. Therefore, it is

implausible that the three dimensional network formation which occurs during conventional gelation can explain the significant rheological difference before and after heating.

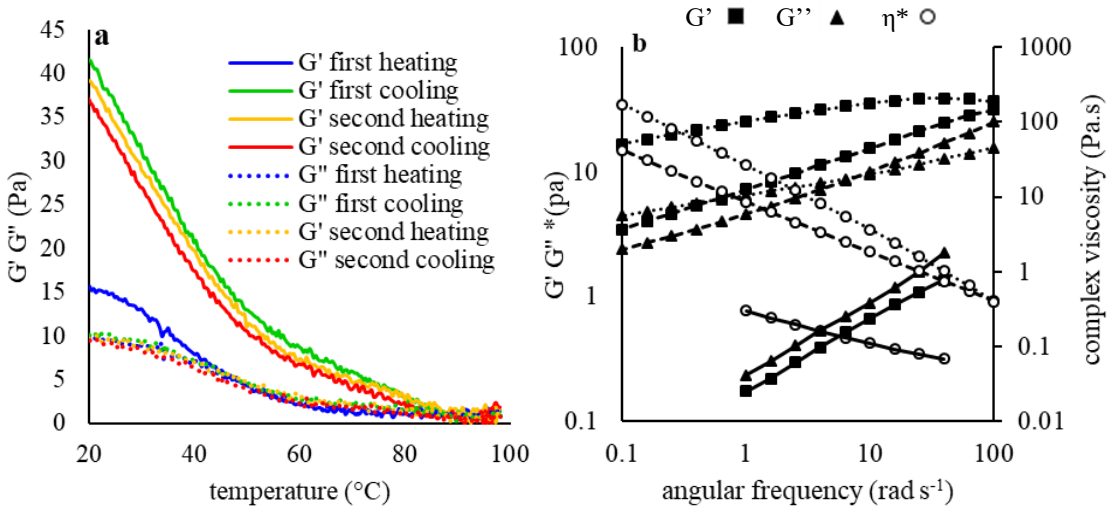

Figure 2.1. Storage and loss moduli (G' and G'') of 1.64% (w/w) PSY over temperature changes (**a**) with a heating rate of 1 °C min^{-1}, frequency of 10 rad s^{-1}, and 0.02% strain. Mechanical spectra (**b**) of 1.64% PSY at 20 °C before heating (– – –), at 98 °C (——), and after being heated at 20 °C (·····). Applied strain was 0.8% for tests at 20 °C and 2% for tests at 98 °C.

The mechanical spectrum of PSY at 98 °C (Figure 2.1b) shows G'' slightly higher than G' with pronounced frequency dependence. It suggests melting of structure. The spectrum was found to be similar to Haque et al. (1993a) who suggested that the melting has not been completed at, in their case, 91 °C, showing a residual gel-like character. Therefore, a possible interpretation of this data is that the weak interactions or bonds between molecules were disturbed by heating, therefore, the samples showed slightly more fluid like property. Guo et al. (2009) described this 'melting' as a continuous and long procedure rather than a sharp melting period, evidenced by no change in enthalpy when analysed by DSC. Indeed Guo et al. (2009) also found their heat up and cooling profiles to be superimposable, without full melting of their gel structures up to 85°C.

To visualise the effect of heating PSY dispersions, a hydrated PSY particle was focused on under a light microscope equipped with a hot stage. The images obtained are shown in Figure 2.2a. When PSY was hydrated, it swelled to form a gel phase surrounding an insoluble core (visible under polarised light, image not shown) which is thought to be the insoluble part of the husk. During heating from 25 °C to 95 °C, the gel phase gradually expanded and disappeared which did not recover after cooling back to room temperature. Only partial disappearance of this phase was observed and the remaining part was associated with the insoluble core which suggests that the gel phase contain different heteroxylan with different responses to temperature. Yu et al. (2017) identified three distinct mucilage layers of hydrated whole psyllium seed dominated by different arabinoxylans with different molecular conformation and rheological properties. To further visualise the PSY suspension, heated and unheated samples were stained by methyl blue and illuminated by fluorescent light (Figure 2.2b). The majority of PSY polysaccharides are not water soluble as clear hydrated particles are seen. Intact hydrated PSY particles are observed in the left image though slight fibrous structures exist between the particles. At the concentration of 1.64% (w/w), these particles can be closely packed. Therefore, the freshly prepared PSY suspension can be described as a concentrated suspension of gel particles. However, it can be seen that these 'gel particles' have large diameters (about 0.9 mm for the particle shown in Figure 2.2b left) close to the geometry gap (1 mm) in the rheological measurements. Therefore, the rheological properties of freshly prepared PSY suspension can be ascribed to the viscoelastic properties of the gel particles and physical contacts and frictions between these particles as defects which, at least partially, lead to lower frequency dependence of η^* and higher frequency dependence of G' compared to the heated suspensions. However, after heat treatment, a fibrous structure with cloudy areas dominate the microstructure, which

might play the role of junction zone formation and responsible for the thermoreversible gel like properties.

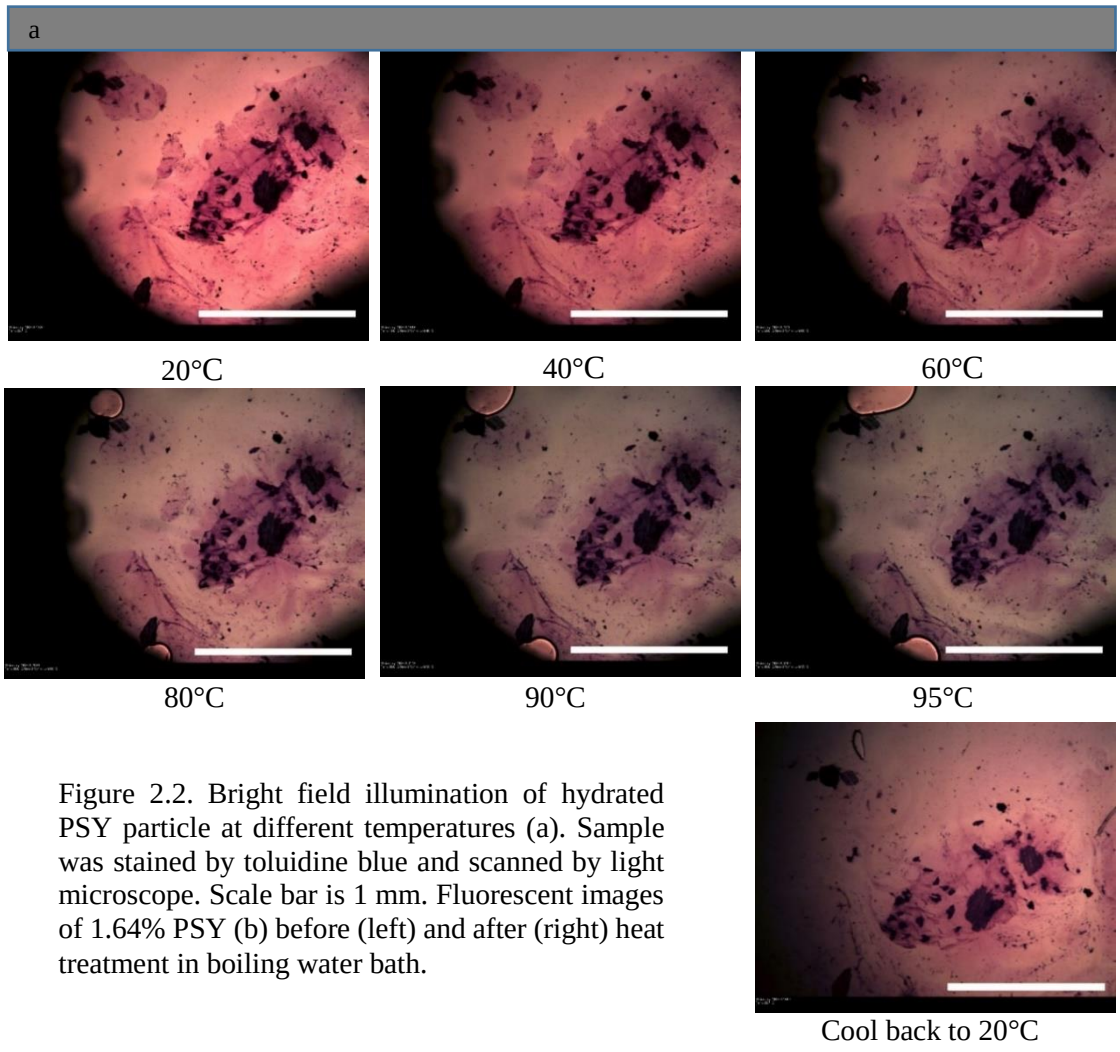

Figure 2.2. Bright field illumination of hydrated PSY particle at different temperatures (a). Sample was stained by toluidine blue and scanned by light microscope. Scale bar is 1 mm. Fluorescent images of 1.64% PSY (b) before (left) and after (right) heat treatment in boiling water bath.

Fractionation of PSY with water at different temperatures and alkaline were explored by Guo et al. (2008) and the fractions showed differences at the molecular level. Yu et al. (2017) discovered a formation of three layers of mucilage when the whole seeds were hydrated which can be extracted by cold water, warm water (65 °C), and alkaline. Based on the different rheological responses to temperature, the sequential fractionation of PSY at different temperatures has been explored.

Table 2.1. Yields and A/X ratios of PSY fractions

	Yield (%)	A/X ratio by		
		monosaccharide analysis	2^{nd}-derivative FTIR spectra peak 1/peak 2	^{13}C-NMR spectra $peak_{64}/peak_{66.3}$
F20	27.65	0.298±0.009	0.737	0.684
F40	19.05	0.305±0.006	0.884	0.919
F60	24.22	0.322±0.005	0.893	1.007
F80	8.96	0.363±0.010	1.63	1.497
F100	1.57	1.979±0.064	9.211	
residue	13.66	10.048±2.348		
	95.11 (total yield)	0.417±0.002 (whole PSY)	0.923 (whole PSY)	0.385 (whole PSY)

2.3.2. Rheological properties

The water suspension of PSY was fractionated at different temperatures and four fractions were characterised by small amplitude oscillatory shear tests. Strain amplitude sweep spectra of these four fractions are shown in Figure 2.3a. All four fractions have a similar length of LVE (linear viscoelastic) regions. Interestingly, they showed G'' peaks before structure breakdown (final sharp decrease at high strain) which were more pronounced in F40, F60, and F80. This phenomenon is usually observed in concentrated dispersions and cross-linked polymers due to a significantly large amount of deformation energy released. Therefore, F20 is significantly different from other fractions at either the molecular level or microstructure where there might be less or weaker molecular interactions or associations, or the molecular associates are less rigid.

Frequency sweep tests were performed on unheated and heated F20, F40, F60, and F80 at 20 °C. They were also tested at corresponding fractionating temperatures i.e. 20 °C, 40 °C, 60 °C and 80 °C, respectively. The mechanical spectra are shown in Figure 2.3b, c, d, and e. All fractions showed that G' is higher than G'' before and after heat treatment suggesting gel-like properties. However, only F20 show difference before and after heat treatment while others showed overlapping spectra. F80 showed slightly lower moduli after heat treatment, possibly, because of slight molecule degradation at high temperature. Interestingly, all fractions displayed G' slightly higher than G'' at their individual fractionating temperatures which indicates that the fractionation did not happen in a solution state, instead, fractions tend to be rheologically dispersable at their fractionating temperature. Their rheological properties and extractability might be concentration and time dependent. Comparing all fractions, high temperature fractions show higher moduli and less dependence on frequency (F60 and F80 were similar) suggesting that high temperature fractions have stronger gel properties. Similarly, as shown in Figure 2.6e, F20 and F40 did not withstand their own weights when placed upside down but F60 and F80 stayed on the bottom of the bottles.

The rheological responses were monitored during both heating and cooling, as shown in Figure 2.4. The storage moduli of F20 during the first heating was lower than cooling and the second heating and cooling cycle which was in agreement with mechanical spectra (Figure 2.3b, c, d, and e), that heat treatment only influences F20. Apart from first heating for F20, other G' traces of all other fractions almost superimposed although there is a slight decrease during the second heating/cooling cycle, especially F80 possibly due to syneresis or high temperature induced molecular degradation. Reversible rheological behaviour without hysteresis over temperature changes has also

been reported previously on both whole PSY extracts and fractionated samples (Guo et al., 2009; Haque et al., 1993a). It is also noticed that the G' decrease during heating and G' increase during cooling were separated into three parts during which G' changed at different rates with a certain linear relationship with temperature when plotted in linear/linear scales. The rate of G' change during low and high temperatures was greater than that during the intermediate temperature range, which was also highlighted by Haque et al. (1993a). They ascribed it to conformational transitions where coils are obtained at high temperature due to loss of conformational order. To further understand the difference between the four fractions, the data from the second heating were used to calculate the points where G' values changed decreasing rates as shown in Figure 2.4. The calculation was performed by defining upward and downward inflexions with 5% bandwidth. The second inflection points of F60 and F80 could not be calculated with these parameters though they are visually observable. The main discrepancy is that the first inflection points increased to a higher temperature in the order of F20 < F40 < F80 < F60 with 10°C difference. However, the positions of second infection points, which is likely due to loss of conformation order as suggested by Haque et al. (1993a), happen at similar temperature (65 to 70 °C) over four fractions with similar and low G' values. The G' values decrease to almost zero at the end of heating (>88°C) indicating a full melt of the structure. Weak interactions might exist which can only recovery slowly.

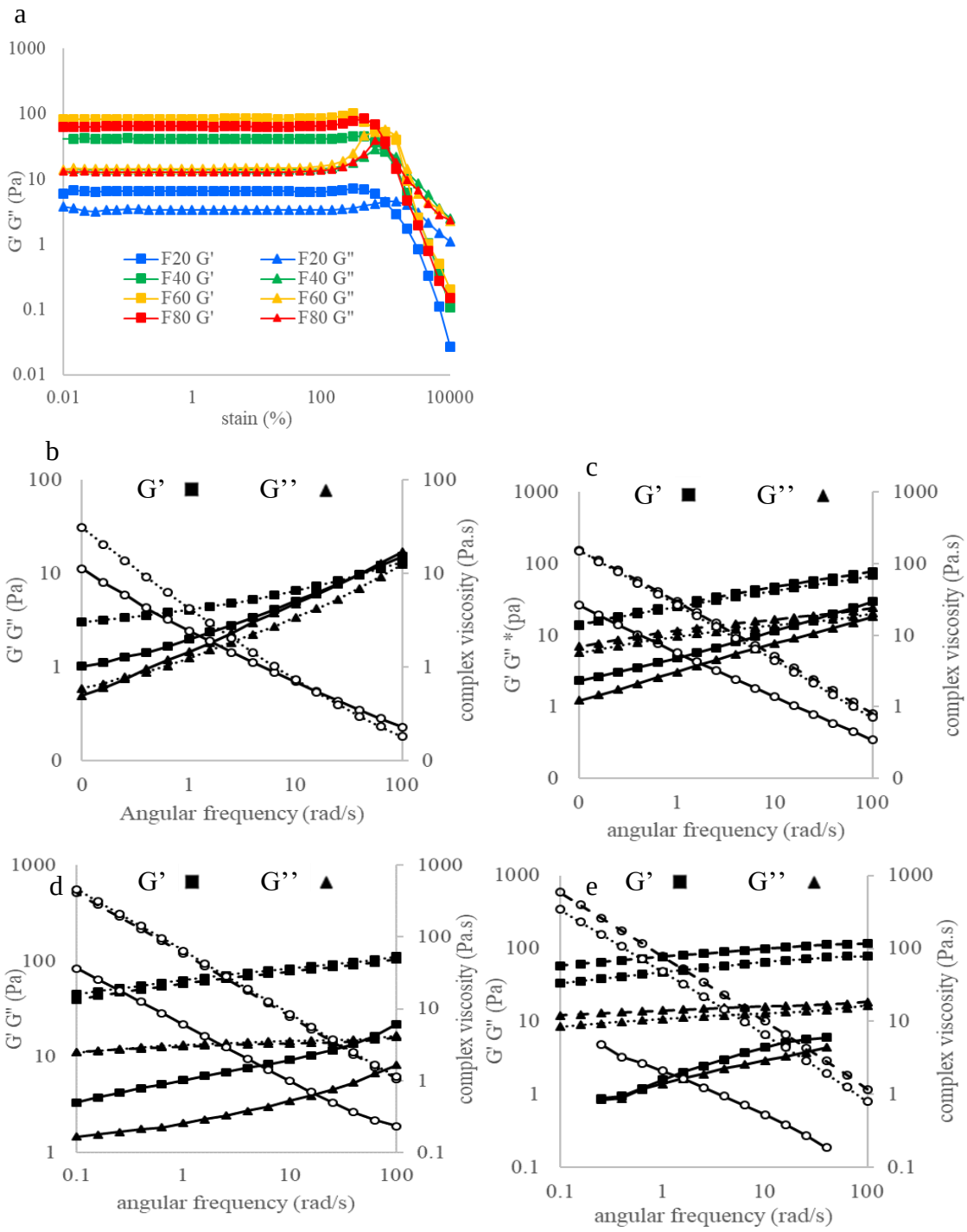

Figure 2.3. Strain amplitude sweep of 1.64% F20, F40, F60, and F80 at 20 °C (a). Mechanical spectra of 1.64% F20 (b), F40 (c), F60 (d), and F80 (e). To obtain mechanical spectra, samples were tested at their fractionating temperatures (20 °C, 40 °C, 60 °C, and 80 °C individually) (——). F40, F60, and F80 were also tested at 20 °C before (– – –) and after (·····) heat treatment at 98°C.

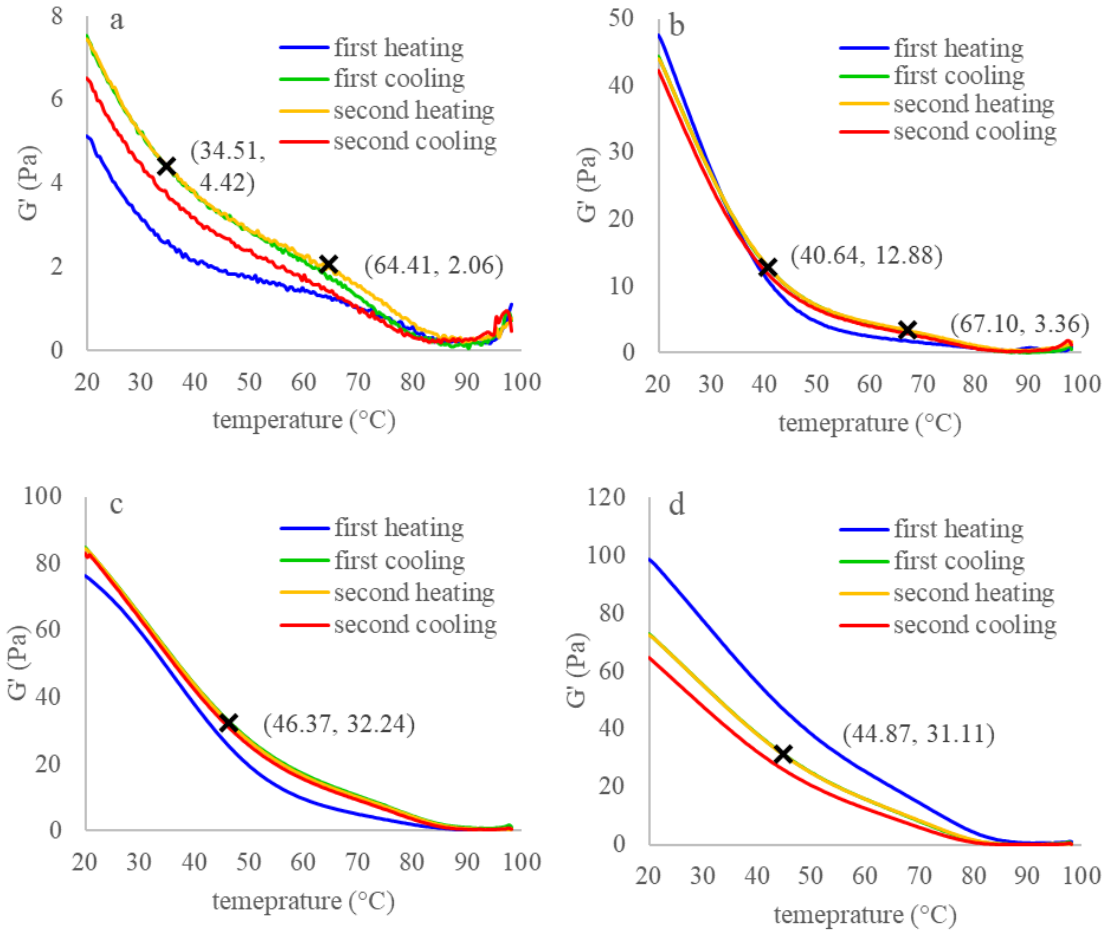

Figure 2.4. Storage moduli G' of 1.64% F20 (a), F40 (b), F60 (c), and F80 (d) over two cycles of heating and cooling. Changes of melting speeds are shown as a cross on the graphs which were calculated based on the second heating. Mathematical determination of the upward and downward inflection points were performed on linear/linear scales with bandwidth of 5%.

Table 2.2. Shifting factors (a) of angular frequency to obtain mater curves shown in Figure 2.5.

Measurement temperature °C	F20	F40	F60	F80
20	1	1	1	1
30	1.236E-01	7.159E-02	9.485E-02	8.387E-02
40	1.112E-02	4.655E-03	8.094E-03	6.299E-03
50	1.007E-03	3.329E-04	3.688E-04	2.426E-04
60	1.025E-04	2.553E-05	2.107E-05	1.549E-05
70	5.833E-06	1.183E-06	8.334E-07	5.527E-07
80	1.687E-07	3.086E-08	1.577E-08	8.665E-09

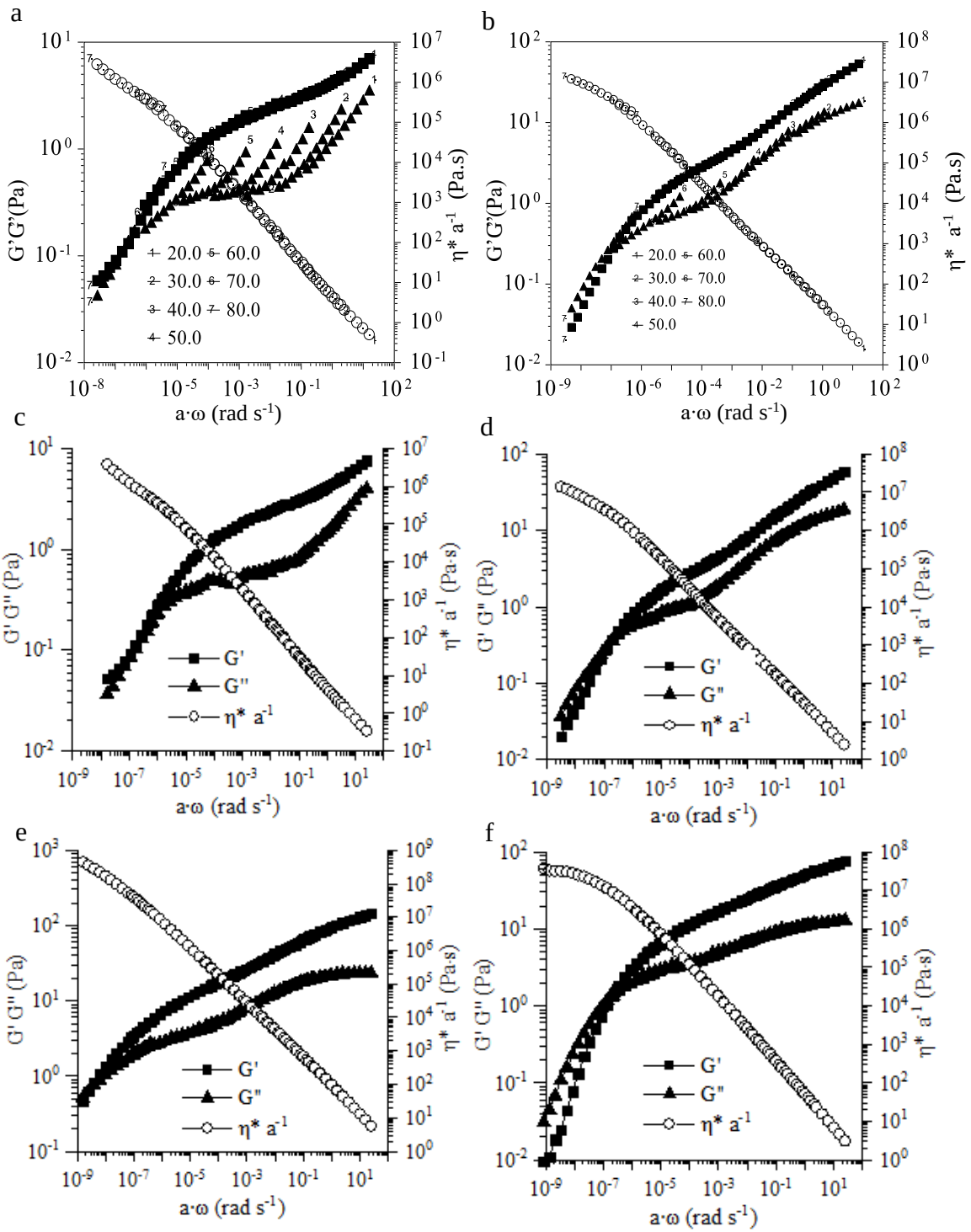

Figure 2.5. Time–temperature superposition of F20 (a) and F40 (b) after angular frequency shifted and master curves of F20 (c) and F40 (d) with G'' smoothed as well as master curves of F60 (e) and F80 (f) without smoothing required. The concentration was 1.64% and reference temperature is 20 °C. a is the shifting factor of angular frequency.

Similar to the suspension of whole PSY, no thermal peak was observed on DSC traces (data not shown). The assumption was therefore made that PSY and fractions are thermo-rheologically simple materials and an attempt was made to perform time-temperature superposition (TTS) to further study the gelling properties (Figure 2.5). Frequency sweep tests were performed at different temperatures between 20 to 80 °C. The mechanical spectra measured at the same temperature were obtained with high reproducibility regardless of the temperature history they experienced which further support the reversible rheological behaviour observed in temperature sweep tests. The mechanical spectra at different temperatures were shifted to obtain master curves and the shifting factors (a) are shown in Table 2.2. However, the loss moduli of F20 and F40 (Figure 2.5a and b) were less well fitted and must be smoothed to generate master curves. The lack of superposition is caused by immiscibility, multiphase, and semicrystalline formation with morphological changes (Nickerson, Paulson & Speers, 2004). Hence, molecular association or/and microstructural heterogeneity might exist in F20 and F40. As shown in Table 2.2, the shifting factors of high temperature fractions were lower which is reflected in master curves, as that high temperature fractions are slightly more shifted to the left. More evidently, F60 has lower relaxation frequency (G'-G'' crossover frequency), i.e. longer relaxation time, compared to other fractions, which suggests longer or more branched molecules which are able to flow in a range of slow motion. Another interesting point is that, except for F20, the complex viscosity (η^*) of all other three fractions showed a tendency to reach a plateau of zero shear viscosity (η_0^*) which indicates the possibility that these polysaccharides behave like entangled polymers in a solution state. More interestingly, Yu et al. (2019) addressed structure similarity between gel state and solution state. The value of η_0^* of F60 tends to be the highest which also suggest a higher molecular weight.

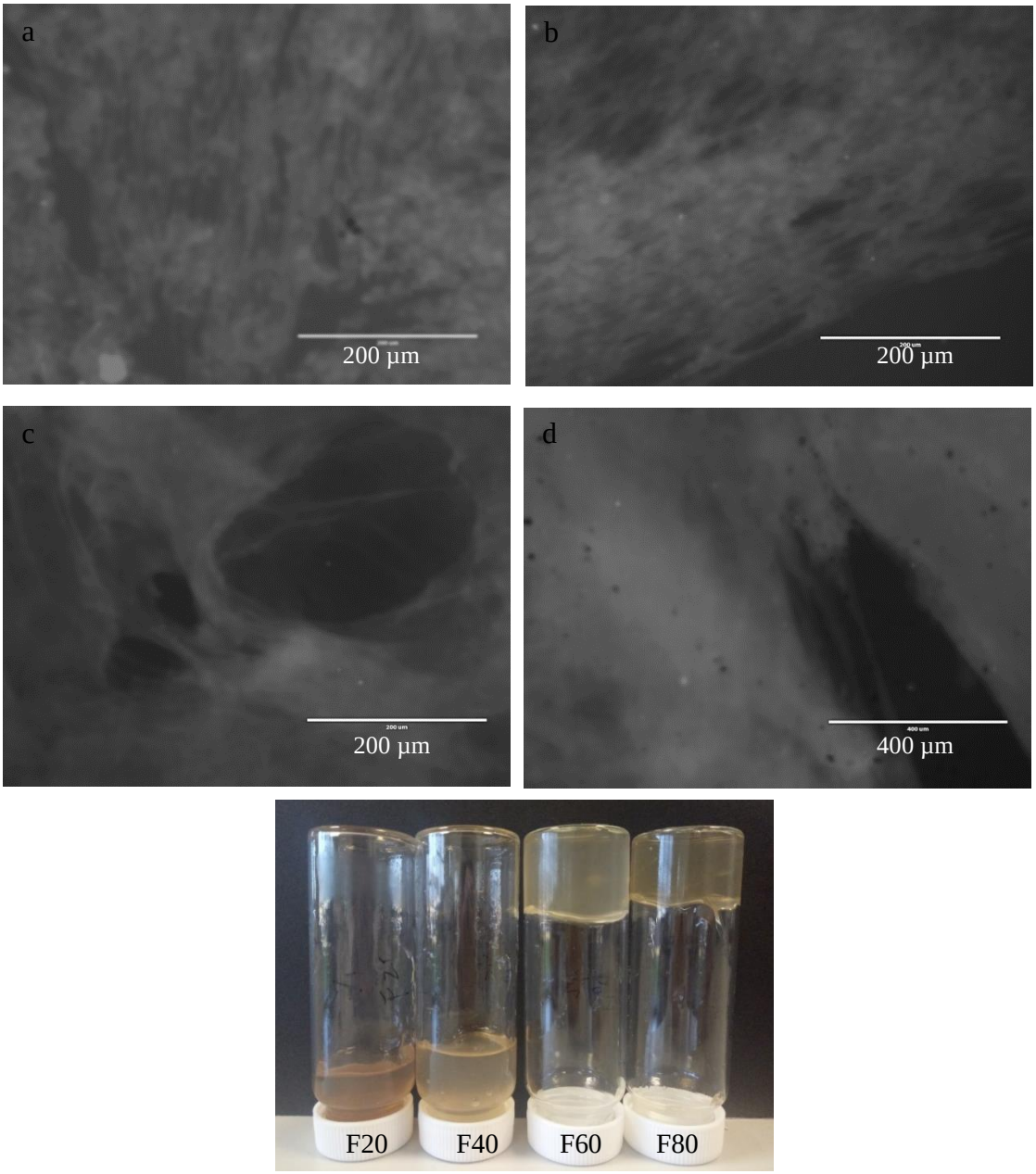

Figure 2.6. Fluorescent images of 1.64% heated F20 (a), F40 (b), F60 (c), F80 (d) stained with methyl blue emitted by DAPI light and four fractions palced upside down (e).

2.3.3. Microstructure of PSY fractions

Fluorescent images of heated PSY fractions are shown in Figure 2.6. F20 and F40 showed fibrous aggregates and more heterogeneous structures which are in agreement with the lack of fit of G'' to obtain master curves of these two fractions in the TTS

experiment. Nevertheless, the structures of F60 and F80 are much finer. These structural differences are also reflected from the decrease in turbidity from F20 to F80 (Figure 2.6e). The fibrous gel structure of PSY has been also reported by Haque et al. (1993a) and Guo et al. (2009) who investigated PSY extracted by 2.5 M NaOH and 0.5 M NaOH, respectively. Compared to the image of heated whole PSY suspension (Figure 2.2b), it can be speculated that the fibrous strands are mainly low temperature fractions while the cloudy parts are high temperature fractions. It worth mentioning that the heated PSY gel is quite flexible and stretchable which forms stable bubbles easily as observed during experiment operations (data not shown). Such structure, i.e. strands linked by cloudy areas as 'junction zones', might be the foundation of the weak gel property and flexibility.

2.3.4. Analysis of heteroxylan composition and structure

2.3.4.1. Monosaccharide analysis

Arabinose to xylose (A/X) ratio (Table 2.1) was first considered and calculated based on the results of monosaccharide analysis. The whole PSY sample showed an A/X ratio of 0.417 which is similar to the results from Van Craeyveld et al. (2009). A/X ratio increased in higher temperature fractions and F100 and residue show a ratio higher than 1. For most cereal arabinoxylans with simpler molecular structures, water solubility and extractability increase with higher A/X ratios since arabinose sidechains interfere the packing of xylan backbones (Andrewartha, Phillips & Stone, 1979; Izydorczyk, Macri & MacGregor, 1998; Mandalari et al., 2005; Zhang, Smith & Li, 2014). However, the data in Table 2.1 show that heteroxylan from PSY with higher A/X ratio is harder to be extracted by water and requires higher temperatures. Therefore, the extractability and fractionation of PSY heteroxylan must be influenced by other factors rather than

solubility which is decided by backbone packing. In fact, as described in section 3.2, each fraction is rheologically dispersable at their fractionating temperature. In addition, the A/X ratios of whole PSY and extractable fractions are generally lower than the heteroxylan or, more specifically, arabinoxylan from other cereals like wheat flour (0.5 – 0.8) (Cleemput, Roels, Van Oort, Grobet & Delcour, 1993; Izydorczyk, Biliaderis & Bushuk, 1991), wheat bran (0.5 - 1) (Aguedo, Fougnies, Dermience & Richel, 2014; Zhou et al., 2010), maize bran (Rose & Inglett, 2010), rye flour (1), rye bran (0.74) (Delcour, Vanhamel & De Geest, 1989), and non-waxy rice (0.7 – 1.2) (Lai, Lu, He & Chen, 2007). However, it has been evidenced that the heteroxylan from psyllium husk is highly branched (Fischer et al., 2004; Guo et al., 2008; Yu et al., 2017). Hence, there should be a larger amount of xylose units in sidechains, especially in low temperature fractions which show lower A/X ratio.

2.3.4.2. FTIR spectroscopy

Full FTIR spectra and 2nd derivative spectra of whole PSY and fractions are shown in Figure 2.7. The full spectra showed broad absorption peaks from approx. 3660 to 2990 cm^{-1} of O-H stretching vibrations and peaks of C-H stretching at 2924 and 2855 cm^{-1}. The peak of CO_2 absorption was seen at 2360 cm^{-1}. The peak at 1732 cm^{-1} was assigned to C=O stretching in carboxyl group of uronic acid (Marchessault & Liang, 1962). It can be seen that F20 showed a slightly higher peak of uronic acid which is in agreement with Guo et al. (2008) that the fractions with higher uronic acid content are cold water-extractable. The peak at 1146/1162 cm^{-1} was assigned to C-O-C vibration of glycosidic bonds. The typical peak profile of arabinoglucuronoxylan due to ring vibrations, C-OH stretching vibrations of side groups, and C-O-C glycosidic bond vibration were observed showing peaks at 1162/1152, 1037/1027 cm^{-1} (Kacurakova, Capek, Sasinkova,

Wellner & Ebringerova, 2000). Although the peaks at 1109 and 1070 cm^{-1} were not shown compared to the observation by Kacurakova et al. (2000), a shoulder at this range was seen. In addition, anomers of pyranose and furanose can be differentiated in the range of 900 to 800 cm^{-1} (Kacurakova et al., 2000; Mathlouthi & Koenig, 1987; Zhbankov, Andrianov & Marchewka, 1997). As shown in Figure 2.7a and the insert highlighting the range from 930 to 780 cm^{-1}, peaks were observed at 895 cm^{-1} assigned to β-linkage of pyranoses in all spectra with obvious shoulders at 866 cm^{-1} assigned to α-linkage of furanose in residue and F100. The shoulder was also shown in F40, F60, and F80 with similar intensity but less pronounced in F20. It has been evidenced that the PSY polysaccharide is constituted by β-xylose in pyranose form in the backbone and both α-arabinose in furanose form and β-xylose in sidechains substituting on C-3 or/and C-2 (Edwards et al., 2003; Fischer et al., 2004; Guo et al., 2008; Yu et al., 2017). Therefore, the observation suggests that residue and F100 are heavily substituted by arabinose followed by F40, F60, and F80 while F20 is less branched by arabinose.

Second-derivative spectra of arabinoxylan in the range from 1020 to 920 cm^{-1} reflect A/X ratio and substitution positions on xylan backbones (Robert, Marquis, Barron, Guillon & Saulnier, 2005). The second derivative spectra of whole PSY, F20, F40, F60, and F80 (Figure 2.7b) show two peaks at approximately 978 (peak 2) and 955 (peak 1) cm^{-1} and the height ratio of these two peaks was calculated and shown in Table 2.1. From F20 to F100, peak 1/peak 2 increased which is another evidence of the increase of A/X ratio (Robert et al., 2005). A peak appeared at 943 cm^{-1} in the spectra of F100 and residue suggest a possible increase of C-2 substitution (Robert et al., 2005).

2.3.4.3. ^{13}C solid-state NMR spectroscopy

Whole PSY and freeze-dried factions were subjected to CPMAS NMR spectroscopy analysis shown in Figure 2.8. Except for residue, all other samples show a similar peak at 104 ppm which is a merging for C1 of arabinose, xylose and other monosaccharide residues. Therefore, A/X ratio cannot be calculated by integrating this peak as described by Rondeau-Mouro, Ying, Ruellet and Saulnier (2011). However, some differences were noticed in the range from 95 to 68 ppm which are assigned to C2 to C4 of polysaccharides. Because that substitution by either neighbouring monosaccharide

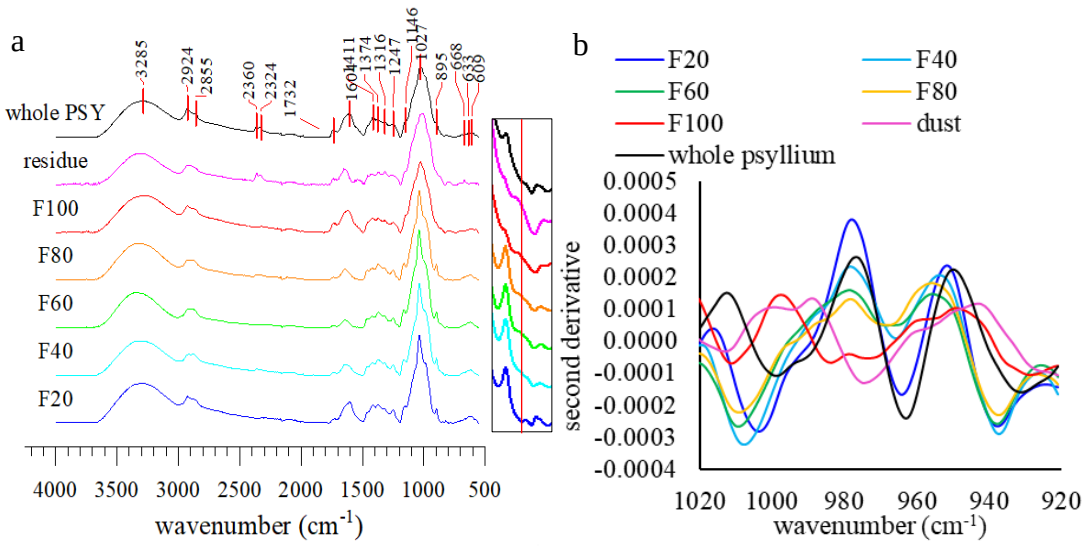

Figure 2.7. FTIR spectra of whole PSY and fractions (a) and 2nd derivative (multiplied by -1) of the region from 1020 to 920 cm^{-1} (b). The insert in a zoom in the shoulder at 866 cm^{-1} guided by a red line.

residue in the backbone or by sidechains leads to downfield shift, a detailed evaluation of this range can help to differentiate molecular conformation in terms of branching and glycosidic bonds. All spectra showed peaks or shoulder at 82 ppm assigned to substituted C2 and C3 while unsubstituted C2 and C3 contribute to peaks at 75 ppm with a shoulder at 76 ppm assigned to substituted C4. A discernible peak of unsubstituted C4 was at 70 ppm. The high temperature fractions revealed lower

intensity of unsubstituted C2 and C3 which indicates that high temperature fractions might be heavily branched on C2 and C3 of the xylan backbone. An obvious increase in peak intensity of unsubstituted C4 was noticed in lower temperature fractions. Arabinose units are only linked via 1→3 linkages (Fischer et al., 2004; Guo et al., 2008), therefore the difference is mainly attributed to linkages of xylose residue and there might be more unsubstituted C4 of xylose units in lower temperature fractions especially F20. There are therefore two possibilities: firstly that low temperature fractions have more branching xylose as monosaccharide substitutes or sidechains containing xylose units. These xylose units can be terminal xylose in sidechains. They can also be 1→3 linked xylose in the middle position of trisaccharides sidechains (Fischer et al., 2004). Therefore, the unsubstituted C4 could belong to either terminal xylose or xylose in the middle position of sidechains. Another possibility is that there are more 1→3 linkages in the xylan backbones of low temperature fractions (Guo et al., 2008; Haque et al., 1993a; Kennedy, Sandhu & Southgate, 1979; Sandhu et al., 1981). Haque et al. (1993a) and Sandhu et al. (1981) presumed alternating 1→3 and 1→4 linkage arrangement and 1→3 linkages in the backbone lead to conformational changes of the macromolecules.

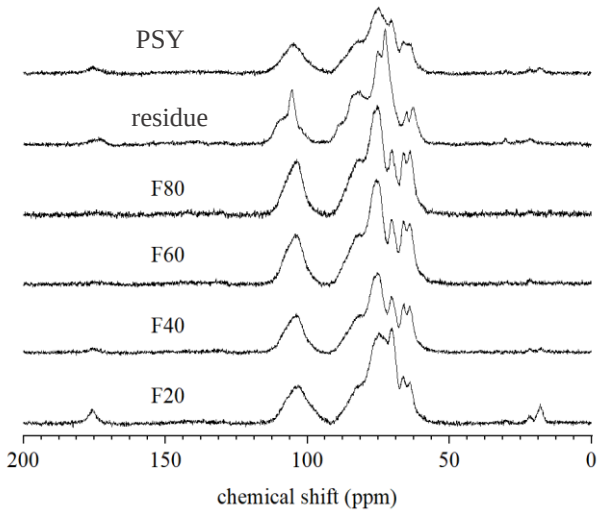

Figure 2.8. ^{13}C NMR spectra (divided by sum) of F20, F40, F60, F80, residue, and whole PSY.

Although C1 peaks were not separated, C5 of xylose (66 ppm) and arabinose (64.0 ppm) residue were clearly resolved on the spectra. Signals from C5 of arabinose and xylose were integrated and the ratio was calculated to estimate A/X ratio as shown in Table 2.1. The results were comparable to the ratios calculated from FTIR 2nd-derivative spectra but both are higher than the results of monosaccharide analysis. Correction must be applied as the calculation are based on the abundance of carbon atom but it further evidenced that high temperature fractions contain more arabinose units.

Residue was distinct from others with distinguishable C1 peaks at 109.4 ppm and 105.4 ppm. It also showed a signal at 88.4 ppm as a shoulder which is related to C4 of crystalline cellulose (Atalla & Vanderhart, 1984; Wickholm, Larsson & Iversen, 1998). The shoulder assigned to substituted C4 of xylan is absent compared to other fractions but residue showed a sharp peak at 72.6 ppm. It is difficult to assign this peak but, considering the high amount of arabinose in residue, it might be assigned to C2 of arabinose (Fischer et al., 2004; Palaniappan, Yuvaraj, Sonaimuthu & Antony, 2017). However, it might be related to C2/C5 of cellulose I_{α} (Kono et al., 2002). Therefore, the presence of arabinan and cellulose in crystalline form can be speculated.

The spectrum of whole PSY show three small peaks at 175, 22, and 18 ppm, which suggests the existence of small amounts of pectin and protein (Alba et al., 2018; Foster, Ablett, McCann & Gidley, 1996). These three peaks are also observed in the spectra of F20 and residue, therefore these pectin or/and protein are either cold water extractable or not extractable.

2.4. Discussion: Molecular conformation and gel forming mechanism

We have demonstrated that four PSY fractions show distinct rheological properties and microstructures. We also demonstrated that the composition and degree of substitution of their sidechains are different. Sidechains of polysaccharides have significant and complex impacts on the molecular conformation and behaviours in solutions. As mentioned in section 3.4.1, solubility can be increased and chain association can be interfered by higher degrees of substitution as exampled by cereal arabinoxylan and cellulose ethers. However, PSY heteroxylans are distinct from other cereal arabinoxylans as they are heavily substituted but with lower A/X ratios (xylose units in sidechains). PSY heteroxylans, at least the majority of them, are insoluble in water and show gel like property upon hydration. There is no direct evidence obtained in this project or in literature detailing the molecular structures or conformations of PSY heteroxylans. However, sidechain compositions and spatial arrangements are likely to play a critical role in diversifying the rheological properties of these macromolecules. We propose two hypotheses to understand the distinct rheological behaviours. One focuses on chemical and structural properties of the heteroxylan molecules, and the other one is based on hierarchical molecular conformations.

The conformation of dry arabinoxylan from rice endosperm cell wall is an extended, left-handed, three-fold helix (Yui, Imada, Shibuya & Ogawa, 1995). However, the conformation of soluble arabinoxylan from wheat in solution is proposed to be semi-flexible random coils (Dervilly-Pinel, Thibault & Saulnier, 2001). Haque et al. (1993a) proposed that PSY arabinoxylan adopts conformation of three-fold twisted ribbon based on work by Nieduszynski and Marchessault (1972), that hydrated xylan forms anti-parallel three-fold helical molecule chains with water columns forming hydrogen

bonds between neighbouring chains. The water molecules between xylan chains can be replaced by monosaccharide substitution on O-2 and/or O-3 (Haque et al., 1993a). It is highly possible that this model by Haque et al. (1993a) can describe the case of low temperature fraction which is possibly less substituted or substituted with mono-units of xylose. However, the existence of other factors, e.g. longer sidechains or 1→3 linkages in backbone etc., might disturb this molecular association. Therefore, the heteroxylan molecules in low temperature fractions partially associate and then form 'weak gel' with fibrous structure (Figure 2.6) characterised as ordered and rigid chains cross-linked by weak junction zones as suggested by Haque et al. (1993a). The molecular association is evidenced by rheological behaviours (amplitude sweep tests and TTS) as described in section 2.3.2.

On the other hand, as shown in Figure 2.6, the structure of high temperature fractions are finer which indicates that the extensive inter-chain association is restricted. As described earlier, the high temperature fractions are substituted to a higher degree than low temperature fractions, with higher A/X ratio. In addition, there are long sidechains composed of 2 or more arabinose or/and xylose (Yu et al., 2017) such as Ara-α-(1→3)-Xyl-β-(1→3)-Ara reported by (Fischer et al., 2004), which do not fit into the packing model of xylan. Hence, chain association in high temperature fractions is prohibited. Therefore, the gel structure is possibly maintained by hydrogen bonds between sidechains as advised by Yu et al. (2017, 2019) who suggested 'physical gel' to describe this structure. The strength, amount, and time/temperature-dependence formation of hydrogen bonds between sidechains could be dependent more on entropic favourability. Moreover, the high degree of sidechain substitution also increases chain rigidity

sterically which might contributes to the stronger gel property and longer relaxation time, as shown in Figure 2.3b, c, d, and e.

The PSY fractions show three-step G' decrease during heating with two sharp and one intermediate slower decrease (Figure 2.4). Haque et al. (1993a) assigned the differences to helical conformational transitions and loss of conformations transferring into coils. The initial sharp G' decrease is likely due to the temperature-dependent softening. The intermediate slower G' decrease and the decrease at higher temperature range might be assigned to conformational transitions of the helical molecules and the final transition into coils. The structural transition during heating and cooling of these heteroxylans are similar to xanthan which also undergoes helix-coil transition during heating (Norton, Goodall, Frangou, Morris & Rees, 1984). This three step softening and melting process is reversible as shown by its reversible rheological behaviour (Figure 2.4). The low temperature fractions finish the initial temperature-dependent softening at a slightly lower temperature but the high temperature fractions complete this process at a higher temperature. However, the conformational transitions and loss of ordered molecular conformation occur at similar temperature ranges for all four fractions which suggest similarities in their molecular structures and conformations. In addition, the initial heat treatment only increased the moduli of F20 (Figure 2.3 and 2.4) suggesting that the heat treatment influences its molecular association which is, then, reversible during following heating-cooling cycles.

Another hypothesis could be made to describe the structures and conformations of PSY heteroxylan based on Diener et al. (2019)'s hierarchical structure model for polysaccharides based on carrageenan that the primary linear structure forms single helices as secondary structure which further forms supercoiled helices (tertiary structure)

and the quaternary structure includes intermolecular supercoiling. Being different from carrageenan, PSY heteroxylans are heavily substituted by complex sidechains. Sidechains can be critical in determining the backbone conformation which is the case of 5-fold helical xanthan (Foster, 1992). The properties of sidechains can contribute significantly to the properties of polysaccharide which was well exampled by Abbaszadeh et al. (2015) that xanthan, which is acetylated and pyruvylated to different degrees, varies on shear rheology moduli and conformational transition temperature. PSY heteroxylan, especially the low temperature fraction, could also form tertiary and quaternary supercoiling as molecular associations. However, ^{13}C NMR spectra show that high temperature fraction is highly substituted on both C2 and C3 by, possibly, long sidechains, which influence spatial arrangement and increase chain rigidity, which is shown as G' and G'' overshot in amplitude sweep tests and longer relaxation time reflected by TTS master curves. The increased rigidity is likely to interfere with the further formation of compact tertiary and quaternary structure in high temperature fractions. Based on Diener et al. (2019)'s model, the three-step G' decrease during heating and G' increase during cooling reflect initial temperature-dependent softening and stepwise melting and recovery of the hierarchical structure. F20 is the only fraction to show a more gel-like property after heat treatment, which indicates conformational difference caused by temperature changes. Other higher temperature fractions and F20 in the following heating and cooling cycles show reversible conformational transitions.

The possibility must be taken into consideration that the sidechain substitution of PSY heteorxylans could be complicated. Each fraction could contain different molecules with different rheological properties. Classification of these heteroxylans and a specific and purifying fractionation or extraction process might be problematic. In addition,

blockiness is widely found in nature that, for example, blocky distribution of sidechains influences the sidechain-dominated properties of polysaccharides, such as de-esterified pectin and cellulose (Ström et al., 2007; Sullo, Wang, Koschella, Heinze & Foster, 2013). Blocky distribution of motifs with certain molecular, conformational or rheological characteristics could also exist in PSY heteroxylans which lead to further complexity.

2.5. Conclusion

It has been noticed that hydrated whole PSY shows a gel-like property which melts during heating while forming a stronger gel during cooling where a combined fibrous and cloudy structure was observed. It then melts and recovers reversibly during following heating and cooling. A simple sequential fractionation of PSY heteroxylans was performed. The fractions are rheological dispersible instead of being soluble at their corresponding fractionating temperatures. High temperature fractions show stronger gel like property. The four fractions show reversible three step softening and melting process during heating. F60 is distinct from other fractions as 1) the first sharp G' decrease stopped at a higher temperature even than F80 (Figure 2.4), 2) it showed lower relaxation frequency which is longer relaxation time (Figure 2.5), 3) F60 showed highest η_0* according to the tendency (Figure 2.5). The reason is unknown, but it might be due to a higher degree of polymerisation, longer sidechains, or/and heavy substitution by sidechains, which increase chain rigidity. The high temperature fractions showed slightly higher A/X ratio and, possibly, a higher degree of substitution. The differences between the composition of sidechains lead to different intermolecular association and rheological properties. Two hypotheses were proposed based on either chemical and structural properties or hierarchical molecular conformations. The first hypothesis

applies Haque et al. (1993a)'s model on low temperature fractions which support molecular association as reflected in amplitude sweep tests, TTS, and microstructures while 'physical gel' by Yu et al. (2019) might describe high temperature fractions. The second hypothesis is based on the hierarchical molecular conformations which can be influenced by sidechain compositions and spatial arrangements. The three step softening and melting might be due to changes in helical conformation and transition into coils or to softening and melting of tertiary and quaternary conformations.

However, there is no comprehensive evidence describing the molecular structure and conformation of PSY heteroxylan, and further investigations on sidechain composition and distribution and molecular conformation are necessary. Additionally, further investigation focusing on F60 and comparison between this fraction with alkaline extractable fractions would be intriguing. Investigations on long-term behaviours, e.g. aggregation and syneresis, would be also important for a deeper understanding and further application of this material.

Chapter 3.

Cellulose fibrillation and interaction with psyllium husk heteroxylan

Highlights:

- Flocculates of fibrillated cellulose are promoted by heating and centrifugation
- Unheated mixtures with psyllium husk can be described as binary phase dispersions
- Heated mixtures form interpenetrating composites with psyllium
- Psyllium husk heteroxylans weakly interact with (fibrillated) cellulose
- Increased fibrillation leads to a denser or clumped structure of the mixtures

Keywords:

Cellulose fibrillation, Turbiscan, psyllium husk, heteroxylan, rheological synergism, fluorescent microscopy

Abstract

Fibrillated cellulose (FC) and its mixture with psyllium seed husk powder (PSY) were investigated to broaden the applications of these two materials by a novel combination. Purified cellulose was processed by a colloid mill and relatively stable suspensions were obtained. An FC suspension shows localised concentrations appearing as flocculates, which can be promoted by heating or centrifugation.

The structures of unheated mixtures of FC and PSY appear to be a binary phase dispersion while, after heat treatment, FC fibres were incorporated into PSY gels and form composites. Fibrillation on the surface does not influence the structure and rheological property of the composite mixtures while fibre disintegration contributes to a denser structure and higher moduli. Fluorescent images show attachment of PSY heteroxylan aggregates on cellulose and fibrillated cellulose fibres. The interaction is weak and time-dependent because G' during cooling was higher than that during heating, and declined back to the same value as the start of heating during an isothermal test at 20 ºC. PSY was fractionated according to temperature and only F60 (fraction at 60 º C) clearly associates with the untreated cellulose fibres, possibly via long arabinan side chains similar to hairy pectin or/and conformational compatibility. The interaction was promoted by fibrillation, potentially trapping PSY heteroxylan aggregates within the cellulose dispersion. With further fibrillation, smaller FC fibres were generated and form interpenetrating particles with PSY gel or PSY fractions. Highly fibrillated cellulose has a higher surface area and smaller fibrils, which significantly increased the interaction resulting in a clumped structure.

3.1. Introduction

Cellulose exists in the cell wall of plants as a structuring material and it can also be secreted by algae and certain bacteria. There is a growing interest in cellulose treatment and application due to its abundance, biodegradability, and renewability. Cellulose is a β-(1→4)-D-glucan adopting a flat, 2-fold helical conformation with hydrophobic surfaces and hydrophilic sides of chains where every second glucose unit rotates 180° around the axis of the backbone (Huber et al., 2006; Wyman et al., 2005). The molecular structure of individual cellulose chain is stabilised by intramolecular hydrogen bonds between neighbouring glucose sugars. In native cellulose, the glucan molecules associate in parallel into crystalline sections stabilised by hydrogen bonds (cellulose I) and form elementary fibrils (protofibrils) with amorphous sections in between as dislocations (Habibi et al., 2010; Pääkkö et al., 2007; Wyman et al., 2005). The elementary fibrils then pack into larger units known as microfibrils with diameters ranging from 2 to 20 nm and amorphous dislocations lead to tilts and twists on the microfibrils. The microfibrils further form macrofibrils with lignin and hemicellulose with complex ultrastructure (Bledzki & Gassan, 1999). The cellulose crystalline regions can be in four forms i.e. I_α, I_β, II and III and cellulose I is the least stable form (Goldberg et al., 2015). Native cellulose is cellulose I, which can be in two forms, cellulose I_α and I_β. Cellulose I_α with a one-chain triclinic unit cell is secreted by bacteria and algae and cellulose I_β with monoclinic two-chain unit cell abundantly exist in the plant cell wall (Nishiyama et al., 2003; Sugiyama, Persson & Chanzy, 1991). Cellulose II can be produced by mercerization and regeneration from cellulose I, and cellulose III is generated by mercerizing cellulose I or II in ammonia (Atalla & Vanderhart, 1984; Hebert, 1985; Wada, Chanzy, Nishiyama & Langan, 2004).

Cellulose can be treated either chemically or mechanically to obtain desired functions. Microfibrillated cellulose (MFC) is firstly processed by high pressure and shearing which leads to physical unwinding of native cellulose fibres and generates highly entangled cellulose fibrils with high surface area, liquid retention, and reactivity (Herrick et al., 1983; Turbak et al., 1983a). MFC usually is in the form of aggregates of cellulose microfibrils (Svagan et al., 2007). Currently, the most widely applied mechanical fibrillation treatments are the application of high pressure homogeniser and microfluidiser (López-Rubio et al., 2007; Nakagaito & Yano, 2004; Pääkkö et al., 2007; Stenstad, Andresen, Tanem & Stenius, 2008; Zimmermann, Pöhler & Geiger, 2004). Refiners, cryocrushing, grinders, and extrusion were also used to produce MFC, which sometimes are combined with high pressure homogeniser and microfluidiser (Alemdar & Sain, 2008; Heiskanen et al., 2014; Iwamoto et al., 2005; Wang & Sain, 2007). The mechanical fibrillation process requires intensive energy input therefore pre-treatments are investigated to purify cellulose from hemicellulose and lignin, reduce hydrogen bonds, induce repulsive force by adding a repulsive charge, decrease degree of polymerisation, and/or break amorphous regions between individual MFC fibres (Lavoine et al., 2012; Siró & Plackett, 2010). Most MFC is produced based on cellulose I though MFC of cellulose II has been obtained by a cellulose regeneration process by electrospinning (Li & Xia, 2004; Walther et al., 2011). The MFC application can be across different industries such as foods, pharmacy, and cosmetics. In food productions, MFC can be used as a thickener, compound carriers, and suspension & emulsion stabilisers (Turbak, Snyder & Sandberg, 1982, 1983b).

Cellulose is one of the main components in the plant cell wall and it forms complexes with hemicellulose, pectin and/or lignin to compose the final structure of the cell wall.

The composition of non-cellulosic polysaccharides depends on the plant species. Apart from cellulose, the major polysaccharides in type I primary cell wall of most flowering plants are xyloglucan or pectin but that of the primary cell wall (type II) of poaceae are mixed linkage β-D-glucan and heteroxylan substituted with glucuronic acid or arabinose (Carpita & Gibeaut, 1993). The interaction between cellulose and these non-cellulosic materials has been studied to understand their roles in cell wall structuring and functioning as well as their further applications in other fields.

In addition, psyllium (*Plantago ovata* Forsk) seed husk is a natural source of dietary fibre, which triggers interests in food and pharmaceutical sciences as a functional ingredient. The main compound in the mucilage of the seed husk is β-(1 → 4)-D-heteroxylan substituted on O-3 and/or O-2 positions by arabinose and xylose with complex structures (Edwards et al., 2003; Fischer et al., 2004; Guo et al., 2008; Yu et al., 2017). For most substituted xylan, water solubility and extractability increase with higher A/X ratios since arabinose sidechains interfere the interactions between xylan backbones (Andrewartha et al., 1979; Izydorczyk et al., 1998; Mandalari et al., 2005; Zhang et al., 2014). However, psyllium husk heteroxylan has low solubility and water extractability because it is heavily substituted (Fischer et al., 2004; Guo et al., 2008; Yu et al., 2017). Psyllium husk polysaccharide shows a gel-like property when hydrated in water though there are differences between fractions extracted by either water or alkaline solutions (Farahnaky et al., 2010; Guo et al., 2009; Haque et al., 1993a; Yu et al., 2017). The influence on the gel properties by the ionic environment, concentration, temperature, and pH have also been investigated (Farahnaky et al., 2010; Guo et al., 2009). Additionally, the property and functionality of psyllium husk polysaccharides have been modified by the addition of other polysaccharides, phosphorylation and,

enzymatic treatment (Kale, Yadav & Hanah, 2016; Rao et al., 2016; Yu, DeVay, Lai, Simmons & Neilsen, 2001).

In this Chapter, cellulose was fibrillated using a colloid mill based on the rotor-stator principle, which disrupts particles by high speed shearing. Another focus was on the mixture of psyllium husk heteroxylan and fibrillated cellulose (FC) in order to understand a novel combination and broaden the applications of these two materials.

3.2. Materials and methods

3.2.1. Materials

Pure cellulose powder, Solka floc 900FCC, was supplied by International Fiber Corporation, US. Psyllium seed husk powder (Vitacel®) was kindly donated by the JRS (J. Rettenmaier & Söhne Group, Rosenberg, Germany). Fluorescein isothiocyanate (FITC) was purchased from Acros Organics (New Jersey, US). Methyl blue was purchased from Sigma–Aldrich (UK).

3.2.2. Cellulose fibrillation and influences of processing time

The cellulose was fibrillated using a colloid mill (Winkworth, Basingstoke, UK) at a rate of 2 min L^{-1}, 4 min L^{-1}, 10 min L^{-1}, 20 min L^{-1}, 40 min L^{-1}, and 60 min L^{-1} labelled as FC2, FC4, FC10, FC 20, FC40, and FC60. The unfibrillated sample was labelled as FC0. The colloid mill was adjusted to the smallest gap and 5 g of cellulose were dispersed in 500 mL of RO water as one batch.

The freshly fibrillated samples were tested by Turbiscan Lab (Formulation, L' Union, France) at 25 °C and imaged by light microscopy (Evos FL, Waltham, US) immediately after being processed. The stability of freshly fibrillated cellulose was calculated as Turbiscan stability index (TSI) by Turbisoft 2.2 using equation (3.1). $Scan_i(h)$ and $scan_{i-1}(h)$ are the average backscattering at the time i and i-1 respectively of measurement. H is the sample height.

$$TSI = \sum_i \frac{\sum_h |scan_i(h) - scan_{i-1}(h)|}{H} \qquad (3.1)$$

The freshly prepared FC were also stored at 20 °C and 80 °C and tested by Turbiscan. The samples were gently shaken by hand to redisperse the suspensions then the flocculation of fibrils can be solely tested excluding sedimentation.

Freshly prepared FC60 was centrifuged at 4000 g, 4 °C, for 15 min. The sediment was collected and recovered back to the original concentration, i.e. 0.77% (w/w). Part of the recovered suspension was re-homogenised using an Ultra-Turrax homogeniser (T25, Ika®-Werke, Germany). The freshly prepared, recovered, and re-homogenised FC60 was scanned by Turbiscan. In addition, rotational tests were performed at 20 °C using a MRC 301 rheometer (Anton Paar, Austria) with a shear rate increasing logarithmically from 0.04 to 4000 s^{-1}. The geometry used was the concentric cylinder with a measuring gap of 1 mm and the surface of the measuring cylinder was sandblasted (CC27/S-SN18049, Anton Paar).

To prepare stock suspensions of FC, the freshly processed FCs were centrifuged at 4000 g, 4 °C, for 15 min. The residues in supernatants, which were discarded, were checked

by drying at 105 °C and it was less than 0.01%. The concentration of sediment, which was collected, were verified by drying at 105 °C for each batch. The stock FC suspensions were kept at 4 °C. The stock suspensions were diluted to the required concentration and mixed via vortex for 2 min for further tests and sample preparations.

3.2.3. Time-domain NMR measurement

Proton relaxation measurements were performed with an R4 Benchtop NMR System (Advanced Magnetic Resonance Ltd, Abingdon, U.K.) equipped with a thermal controller (Advanced Magnetic Resonance Ltd). The transverse relaxation curves were obtained by the Carr-Purcell-Meiboom-Gill (CPMG) sequences (Meiboom & Gill, 1958), beginning with a 90° pulse followed by 32768 180°-pulses with 0.256 ms (TAU) between every two pulses. The 90° pulse for all sequences was approximately 2.6 µs and the signals were recorded 5 µs (dead time) after the pulse. Each CPMG sequence was repeated 64 times on each sample to obtain the average values. The samples were allowed to relax for 10 seconds between every two scans.

3.2.4. FC-PSY mixture preparation

Stock suspensions of FC10 and FC60 were diluted to 1.64% or 0.82% (w/w) by vortexing for 2 minutes and 1.64% and 0.82% FC0 were prepared by suspending pure Solka floc 900FC cellulose in RO water. Psyllium seed husk powder (PSY) was dispersed in RO water at a concentration of 1.64% or 0.82% and 1.64% PSY suspension was mixed with 1.64% FC suspensions immediately at a 1:1 ratio by weight. The mixtures were stirred slowly (less than 100 rpm) at room temperature for 1 hour. The heat treatment was performed by incubating samples in boiling water bath with slow

stirring (less than 100 rpm) for 20 minutes followed by cooling at room temperature for 1 hour.

3.2.5. Rheological properties

Oscillation tests were performed using a MRC 301 rheometer (Anton Paar, Austria), with parallel plate geometry including a sandblasted upper plate (PP50-SN11649, Anton Paar). The measuring gap was 1 mm. The temperature was controlled by a Peltier system with the assistant of a water bath (R1, Grant, Shepreth). Dynamic oscillatory shear tests were performed. Unheated samples and heated FC60 suspensions were loaded at 20 °C and held for 500 seconds before tests. The PSY containing samples which underwent heat treatment were loaded at 20°C then the temperature was increased to 60 °C and maintained for 5 min to melt the gel and release the energy stored due to normal stress by compression. Waiting time was also 500 seconds at 20 °C before tests. Frequency sweep tests were performed in the range of 100 to 0.1 rad s^{-1} with the angular frequency decreasing logarithmically. Temperature sweep tests were only performed on unheated PSY-containing samples where the temperature was increased from 20 °C to 98 °C, held for 10 minutes, and cooled back to 20 °C. The temperature ramps were conducted at 1 °C min^{-1}. Two cycles of heating and cooling were applied with 2 hours holding time at 20 °C in between. The strain used was in the LVE region and the angular frequency used in temperature sweep tests was 10 rad s^{-1}. The edge of samples was trimmed and covered by low viscosity mineral oil (Sigma, USA) to prevent drying of samples.

An index R was calculated by equation (3.2) describing rheological synergism behaviour of FC-PSY mixtures (Agoda-Tandjawa, Durand, Gaillard, Garnier &

Doublier, 2012). G' at angular frequencies of 0.1, 1, and 10 rad s^{-1} were adopted to calculate R individually.

$$R = \frac{G'_{FC+PSY} - (G'_{FC} + G'_{PSY})}{G'_{FC} + G'_{PSY}} \qquad (3.2)$$

3.2.6. Sample labelling and fluorescent microscopy

3.2.6.1. Covalent labelling

PSY was stained by FITC covalently either on the surface of the powder particles ($PSY_{toluene}$) or at the molecular level (PSY_{DMSO}). Additionally, PSY was fractionated by temperature and the procedure was described in Chapter 2. The obtained fractions (F20, F40, F60 and F80) were also labelled by FITC covalently ($F20_{DMSO}$, $F40_{DMSO}$, $F60_{DMSO}$, and $F80_{DMSO}$). More specifically, 0.05g of FITC was dissolved in 50 ml of toluene for surface staining or in DMSO for molecular level staining. Then PSY or PSY fractions (0.5g) were dispersed followed by adding 0.1 ml of pyridine and 0.047 ml of dibutyltin dilaurate with stirring. The reaction was executed with stirring at 100 ℃ in a closed system with nitrogen purge for the first 2 hours. After reacting for 24 hours, 200 ml of ethanol was poured into the DMSO mixture followed incubating at 4℃ overnight then the precipitate was washed by ethanol by multiple centrifugation steps at 2000 g, 4℃, for 10 minutes. As for the toluene reacting mixture, the stained PSY was directly washed by ethanol. The labelled samples were vacuum dried at 35℃.

3.2.6.2. Non-covalent labelling and image acquisition

A small amount of saturated methyl blue was added into 1.64% FC0, FC10, or F60 suspensions and left for 30 minutes. The unheated PSY-FC mixture was prepared with

$PSY_{toluene}$ via the procedure described in section 3.2.4 that 1.64% $PSY_{toluene}$ was mixed with 1.64% stained FCs by 1:1 ratio and incubated for 1 hour at room temperature with slow stirring. PSY and PSY fractions stained by FITC in DMSO were used to prepare heated samples. PSY_{DMSO}, $F20_{DMSO}$, $F40_{DMSO}$, $F60_{DMSO}$, and $F80_{DMSO}$ were dispersed in RO water by overnight stirring (1000 rpm) at room temperature. They were then mixed with methyl blue stained FC suspensions with same concentrations respectively by a 1:1 (w:w) ratio and incubated at room temperature with slow stirring for 1 hour. Heat treatment was described in section 3.2.4 that the mixtures were heated in a boiling water bath for 20 minutes and cold at room temperature for 1 hour. The samples were imaged by fluorescence microscopy (Evos FL, Waltham, US) equipped with a DAPI (357/44 - 447/60 nm) light cube and a GFP (470/22 - 525/50 nm) light cube.

3.3. Results and discussion

3.3.1. Cellulose fibrillation and process time

Pure cellulose powder was fibrillated using a colloid mill and the stabilities of freshly processed suspensions were evaluated by Turbiscan. The calculated TSI is shown in Figure 3.1a. Higher values of TSI indicate lower stability, which leads to faster sedimentation. FC processed for a longer time was more stable as TSI was lower and increased more slowly during storage. They occupied more volume after 4-days storage, as shown in Figure 3.1b. The less processed FCs settled faster and reached relative stability earlier than FCs processed for longer times, as shown in the insert of Figure 3.1a, which magnifies the first 1000 seconds. The microstructures of the FCs are shown in Figure 3.2. The untreated cellulose (FC0) has long fibres with a relatively smooth surface with kinks and bends. After processing even for a short time, fibrillation becomes evident (Figure 3.2 column b). The fibrillation causes significant effects on the

kinks and ends which are weaker points (Figure 3.2 column c). With the processing time increasing up to 10 minutes per litre (FC10), the fibrillation treatment mainly affected the surface of cellulose fibres. With further processing, most cellulose fibres lost their structure and were fully or partially transformed into cellulose microfibrils (FC40c and FC60c), where the FC suspension shows uneven and localised concentrations appearing as aggregates or flocculates (column a). FC40 and FC60 did not show a significant difference while there were some intact virgin cellulose fibres. The remaining large fibres and unfibrillated fibres were also observed by Herrick et al. (1983) and Andresen, Johansson, Tanem and Stenius (2006). Hence, cellulose was successfully fibrillated to a lower level by colloid mill but further fibrillation requires higher energy input by other equipment such as high-pressure homogeniser.

To evaluate the effects of processing on water mobility, FC0, FC10, and FC60 suspensions were evaluated by time domain ^{1}H NMR and the T2 spectra are shown in Figure 3.3. The T_2 spectra of FC0 show three peaks with values of 2477, 534, 132 ms. The peak at 2477 ms ranging up to 3000 ms is due to the bulk water, whereas the other two peaks indicate water mobility in the system with different constraint levels. Water in hydrated cellulose includes non-interacting water, interacting water, and proton exchangeable water (Ibbett, Wortmann, Varga & Schuster, 2014). The bound water has very short relaxation time, less than 10 ms, and water trapped by capillary forces in the lumen contribute to a peak at 110 ms (Felby, Thygesen, Kristensen, Jorgensen & Elder, 2008). However, in Figure 3.3, the bound water was not detected and water held by capillary forces only are seen, reflected by a small peak at 132 ms due to low concentration applied. The T_2 peak at 534 ms is assigned to water weakly interacting with cellulose surface. T_2 spectra of FC10 shown two peaks. One broad peak ranged

from 600 to 3000 ms indicating that more water molecules were interacting with cellulose surface as fibrillation significantly increased the total surface and exposure of hydroxyl groups. With an increase in processing time, FC60 shown one sharp peak at 614 ms which indicates that a large number of water molecules were interacting with cellulose, and a more uniform suspension was obtained.

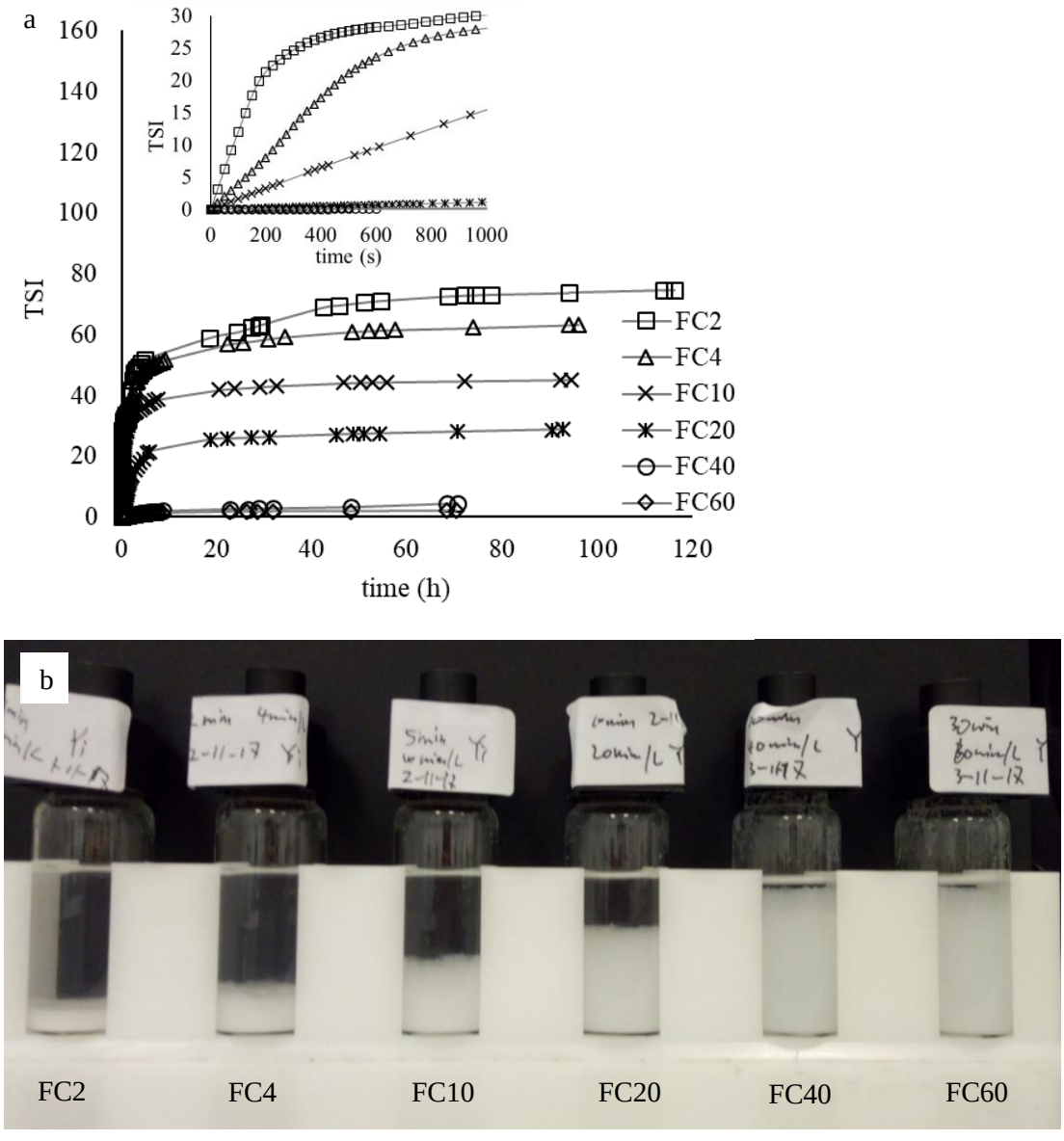

Figure 3.1. TSI of FC processed for different time (a) and the samples after 4-day storage (b). The insert shows the details of the first 1000s of Figure 3.1a.

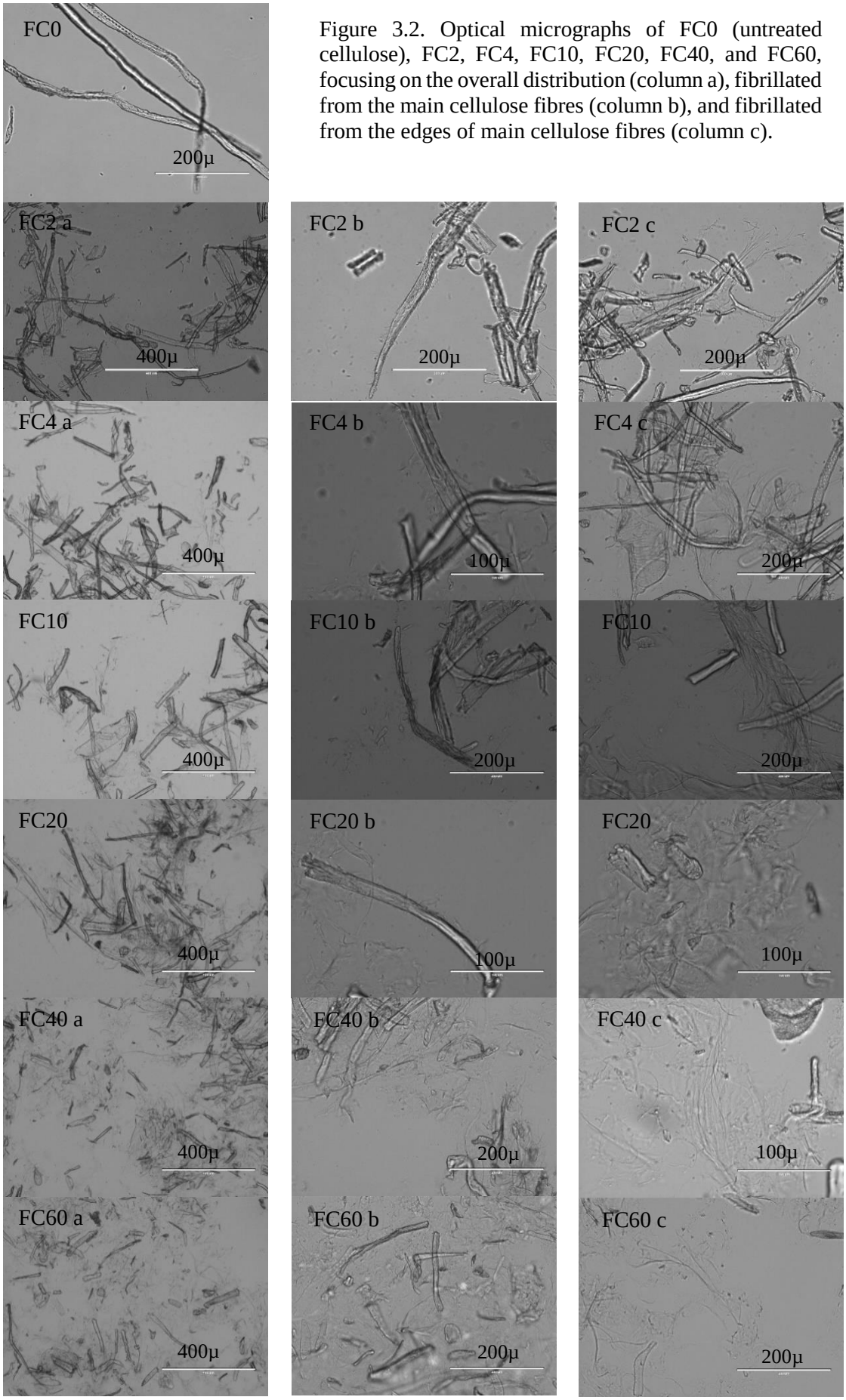

Figure 3.2. Optical micrographs of FC0 (untreated cellulose), FC2, FC4, FC10, FC20, FC40, and FC60, focusing on the overall distribution (column a), fibrillated from the main cellulose fibres (column b), and fibrillated from the edges of main cellulose fibres (column c).

Drying MFC leads to bundles and agglomerates of fibres due to decreased distances and increased contacts and hydrogen bonds between fibres and agglomerates (Quiévy et al., 2010). In conventional oven drying, there are two main factors, i.e. high temperature and reduced distances between fibres. These two factors were isolated as heat treatment in a sealed system and centrifugation respectively, and the influences on flocculation of FC were investigated by Turbiscan and rheometer. In the Turbiscan analysis, the sedimentation was eliminated by gently redispersing samples before each scan. The changes of backscattering (ΔBS) were calculated taking the first scan as reference shown as a straight line with a value of zero in Figure 3.4. The backscattering (BS) increases with the increase of particle size for small Rayleigh – Debye scatterers with the diameter smaller than approximately 0.3 μm (d*), while it decreases with particle size increase when the diameter is larger (Mengual, Meunier, Cayré, Puech & Snabre, 1999). It can be seen that the samples stored at 20 °C did not show significant ΔBS difference while ΔBS increased when they were stored at 80 °C and the increase was already significant during the second scan. It suggests that high temperature leads to flocculation or aggregation of FC fibres in a smaller size scale (< d*). The enhancement of fibre flocculation is due to the altered thermodynamic state of the dispersion.

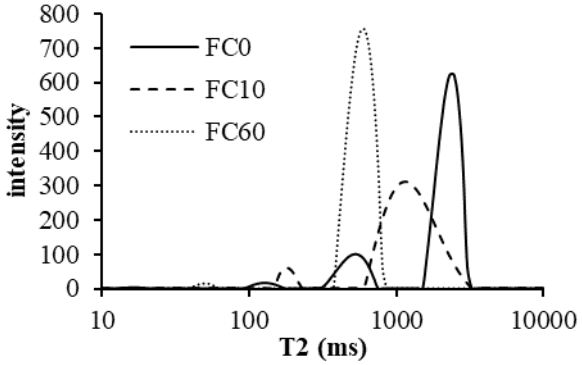

Figure 3.3. Distribution proton transverse relaxation times (T2) of 1.64% FC0, FC10, and FC60 measured with CPMG sequence.

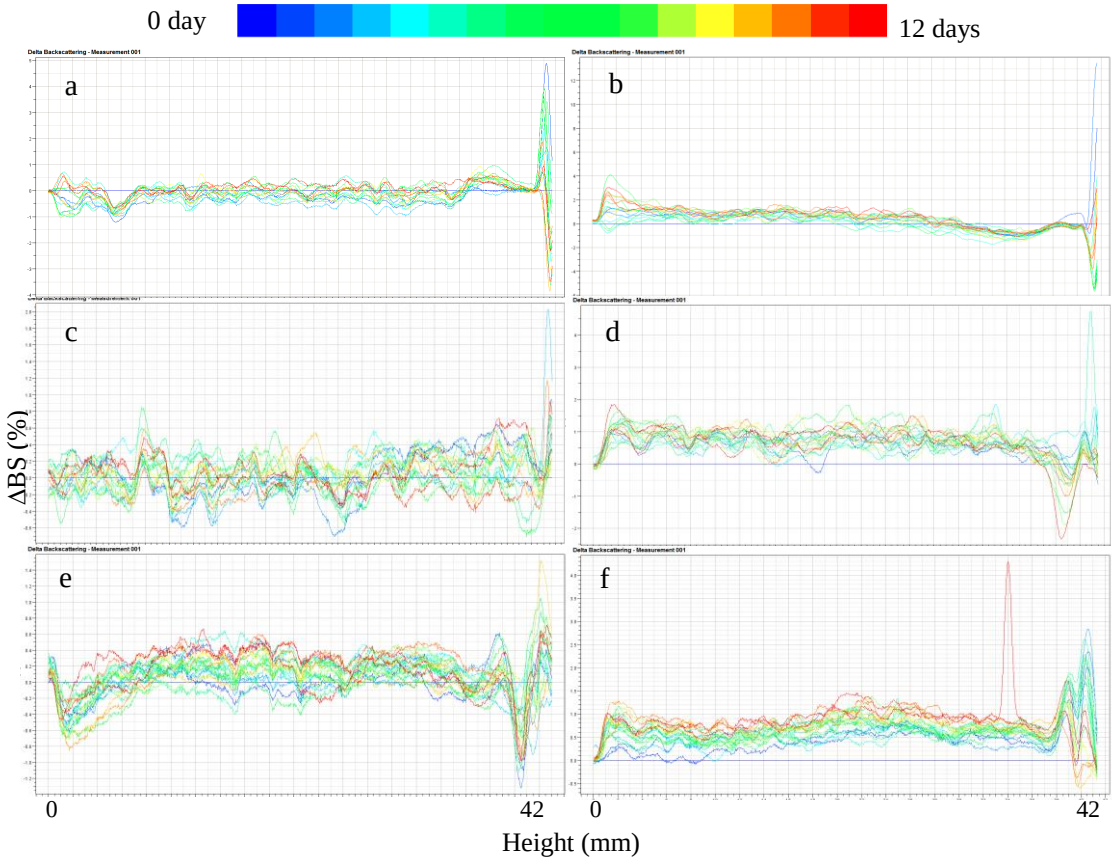

Figure 3.4. Delta backscattering of FC0 (a), FC10 (c), and FC60 (e) stored at 20 °C and FC0 (b), FC10 (d), and FC60 (f) stored at 80 °C.

In order to evaluate the influence of distances between fibres, freshly prepared FC60 was centrifuged and recovered in RO water to its original concentration (0.77%). Part of the recovered FC60 was re-homogenised using an Ultra-turrax. The backscattering and flow curves of freshly prepared, recovered, and re-homogenised FC60 are shown in Figure 3.5. As shown in Figure 3.5a, BS of recovered FC60 was lower than a freshly prepared suspension, which indicates the formation of flocculates or aggregates at a larger scale (> d*). Flocculation induced by centrifugation led to BS decrease while heat-induced flocculation showed BS increase, therefore, it can be deduced that the centrifuge (distance)-induced flocculates are larger than heat-induced flocculates.

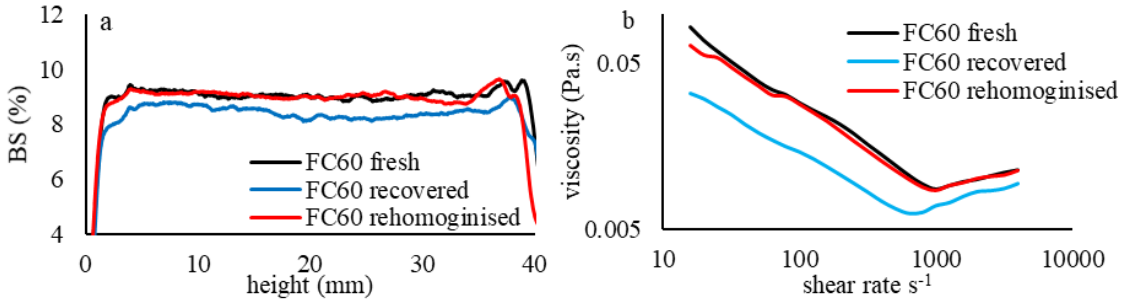

Figure 3.5. Backscattering (a) and flow curves (b) of freshly prepared, recovered, and rehomoginised FC60 measured by Turbiscan at 20 °C.

The flocculation can be fully or partially recovered by high-speed shearing as BS of re-homogenised FC60 increased close to the freshly prepared sample. These were also reflected by the shear viscosities shown in flow curves (Figure 3.5b). The recovered sample showed lower viscosity than the freshly prepared one, and it increased back after homogenisation. FC60 suspensions showed shear thinning behaviour while, interestingly, it was shear thickening at high shear rates (> 1000 s^{-1}) where the fresh, recovered, and re-homoginised FC60 were less different than at lower shear rates. The flow curves of MFC has been analysed showing two shear thinning regions at low and high shear rate and a plateau transition region with difference suspension structures (Jia et al., 2014; Karppinen et al., 2012). The viscosity and structure of MFC flocculates in shear flow are a result of the balance between 1) disentanglement and network breakage by shearing, and 2) collisions and contacts of fibres and flocculates (Karppinen et al., 2012). However, the results obtained in this study shown large variations and noise in the medium shear rate range (data not shown) corresponding to the transition region identified by Karppinen et al. (2012). It is possibly due to the existence of large unprocessed fibres. At higher shear rates, up to 1000 s^{-1}, the MFC flocculates show uniform structure where the size decreased with increasing shear rates and the

flocculates orientate in the directions of flow (Karppinen et al., 2012). However, the flow curves are rarely analysed in the shear rate range higher than 1000 s^{-1}, where in our case FC60 showed shear thickening behaviour. The shear thickening behaviour was first studied in detail by Hoffman (1972) who proposed an order-to-disorder transition as the reason. The hydrocluster mechanism where particles self-organise into stress bearing clusters under hydrodynamic lubrication forces was suggested later to explain the shear thickening behaviour (Bender & Wagner, 1996; Bossis & Brady, 1989; Maranzano & Wagner, 2001; Phung & Brady, 1992). MFC already form flocculates at high shear rates near 1000 s^{-1} (Karppinen et al., 2012). These flocculates might be further compressed in shear flow and behave like particle hydroclusters leading to shear thickening behaviour and the flocculates might be bigger than flocculates caused by centrifugation whose effects on viscosity are, therefore, masked. However, it is worth considering that the shear-thickening region is measured at high shear rates where turbulence flow might occur leading to overestimation of the viscosity (Matignon et al., 2014). Therefore, two Newtonian fluids, i.e. vegetable oil and heavy mineral oil, were measured by identical experiments which did not show increase in viscosity at high shear rates. It suggests that the observed shear thickening behaviour is originated from the FC suspensions themselves instead of the experimental condition. Deep investigation on the flow pattern would be useful to further verify this observation.

3.3.2. FC and psyllium heteroxylan interaction

3.3.2.1. Interactions between PSY and FCs

The mechanical spectra and temperature dependence of rheological parameters of heated and unheated PSY (1.64% or 0.82%) and FC-PSY mixtures (at a total concentration of 1.64%) are shown in Figure 3.6a and b. The storage moduli of all

samples were higher than loss moduli (G' > G'') suggesting gel-like behaviour. Before heat treatment, 0.82% FC and PSY mixtures show higher moduli and lower frequency dependence than 0.82% PSY, which is more pronounced when fibrillation processing time increases (FC60-PSY > FC10-PSY > FC0-PSY) (Figure 3.6a). FC60-PSY shows even higher moduli and less frequency dependence than 1.64% PSY. The slope of lgη* versus lgω became steeper, ranging from -0.62, -0.69, -0.78, -0.87, to -0.93 in the sequence of 0.82% PSY, FC0-PSY, FC10-PSY, FC60-PSY, and 1.64% PSY. Therefore, FC processed for a longer time is more dominant in the overall viscoelastic property of an unheated FC and PSY mixture. After heat treatment, there was no significant difference between FC0-PSY and FC10-PSY, while FC60-PSY showed higher moduli (Figure 3.6b). All spectra showed a similar frequency dependence with a similar lgη* versus lgω slope of -0.88. A similar value of -0.8 was reported by Whitney, Gothard, Mitchell and Gidley (1999) which is analogous across cellulose based cell wall materials from tomato and onion obtained by different extraction methods. Comparing unheated and heated FC-PSY mixtures (Figure 3.6a and b), when the FC was processed for a longer time, the difference between unheated and corresponding heated mixtures were reduced. This further evidence that FC processed for a longer time becomes more influential in determining the rheological behaviour of the mixtures as the heat treatment has less effect on FC than PSY.

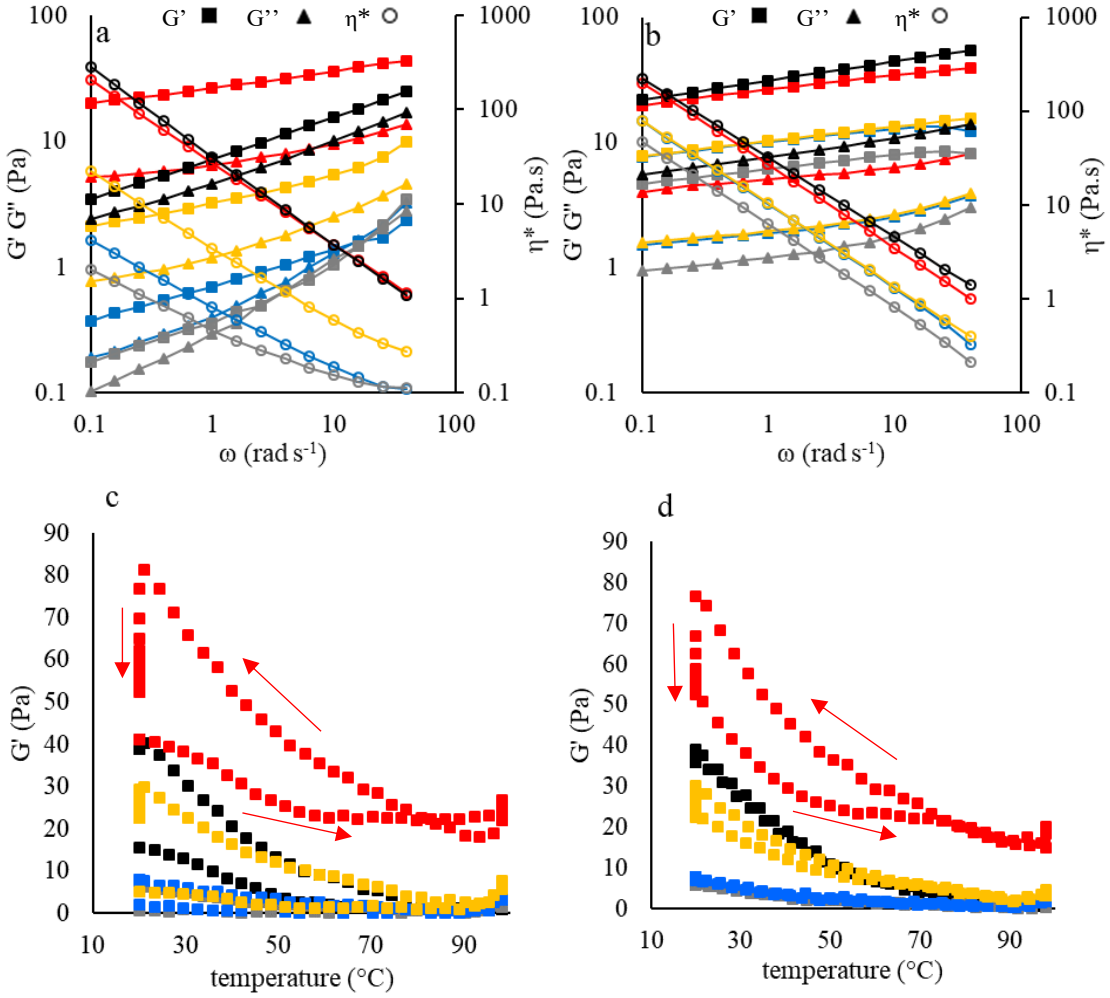

Figure 3.6. Mechanical spectra of 0.82% PSY (grey), 1.64% PSY (black), and mixtures (0.82%, 1:1 mixing ratio) of PSY and FCs: 0.82% FC0-PSY (blue), FC10-PSY (yellow), FC60-PSY (red), before (a) and after (b) heat treatment, and temperature dependence of G' during first heating and cooling cycle (c) and second heating and cooling cycle (d). G', square; G'', triangle; η*, circle. The red arrows indicate time flows. Strains used were in the LVE region and angular frequency was 10 rad s^{-1} in temperature sweep tests.

The temperature dependence of G' of 0.82% PSY, 1.64% PSY, and 0.82% FC and PSY mixtures are shown in Figure 3.6c and d. As reported in Chapter 2, PSY suspensions melt during heating and show stronger gel properties after cooling (Figure 3.6c). After mixing with FCs, the overall G' increased with the increase of FC processing time. At the end of cooling of the first cycle, a stronger gel was formed with increased processing

time, shown as much higher G' than the value before first heating. Figure 3.6d shows the G' profile during the second heating-cooling cycle. Similarly, G' increased when FC was processed for a longer time. It is noticed that PSY showed thermo-reversible behaviour, with G' traces overlapping during heating and cooling, as described in Chapter 2. However, PSY-FC mixtures tend to show that G' during cooling was higher than that during heating. Furthermore, G' declined gradually at 20 ℃ after both first and second heating cycles, shown as a vertical line at 20 °C on the graphs and, during an isothermal test after the second heating cycle G' decreased back to the same value as that before the start of second heating cycles which suggests time dependent reversible rheological behaviour. Therefore, it can be speculated that PSY heteroxylan interacts with FCs in the mixtures. It is likely that the interaction is weak and time dependent.

3.3.2.2. FC60 and PSY mixture and rheological synergism

In order to further understand the interactions between FC and PSY and the rheological synergistic behaviour, the mixture of FC60 and PSY were further investigated as FC60 at low concentration (0.82 or 1.64%) is stable for rheological measurements. The mechanical spectra of 0.82% FC60, PSY and their admixture at an individual concentration of 0.82% are shown in Figure 3.7a and b with and without heat treatment, respectively. The unheated 0.82% PSY (Figure 3.7a) presented very close G' and G'' though G'>G'', however, 0.82% FC60 displayed a much stronger gel-like property as G' was much higher than G'' and less dependent on angular frequency. G' of the FC60-PSY mixture is slightly more dependent on angular frequency than that of 0.82% FC60 alone, although it has higher moduli than either 0.82% FC60 or PSY. After heat treatment (Figure 3.7b), these three samples are similar in terms of the overall profiles of oscillatory tests parameters especially the G' dependence on angular frequency, even

though the FC60 containing samples displayed higher moduli. The slope of lgη* versus lgω was -0.925 for 0.82% FC60, which was similar to that of 1.64% FC60 regardless of heat treatment. Nevertheless, slopes were -0.88 for 0.82% PSY and 0.82% FC60-PSY (Figure 3.7 c, d), which were similar to the mixtures with FC0 and FC10 (Figure 3.6b). It is obvious that the heated PSY is dominant in determining the lgη* versus lgω slope of the mixtures with a characteristic value of -0.88.

The rheological parameters of dynamic oscillatory measurements of 1.64% FC60, 0.82% FC60-PSY, and 1.64% PSY are plotted in Figure 3.7c and d. The 50% replacement of unheated PSY by FC60 suspensions significantly increased the moduli and solid-like behaviour (less dependent G' on ω) although it is still lower than 1.64% FC60 which show more pronounced solid like property shown as the more significant difference between G' and G''. After being heated, G' of FC60, PSY and their admixture at the same total concentration of 1.64% were less diverse in values, although G'' of PSY was apparently higher than the other two which indicates that more energy was dissipated during small amplitude shear deformation, while the replacement by FC60 significantly reduced the energy loss. In addition, the reduced ω dependence of G' by FC60 addition (0.82% FC60-PSY) was also observed which falls between 1.64% FC60 and PSY. In conclusion, FC60 is more gel-like than PSY as it showed higher moduli and less dependent G' and it is dominant in the mixtures in terms of these two factors, while PSY governs the resistance in the viscoelastic flow of mixtures represented as complex viscosity.

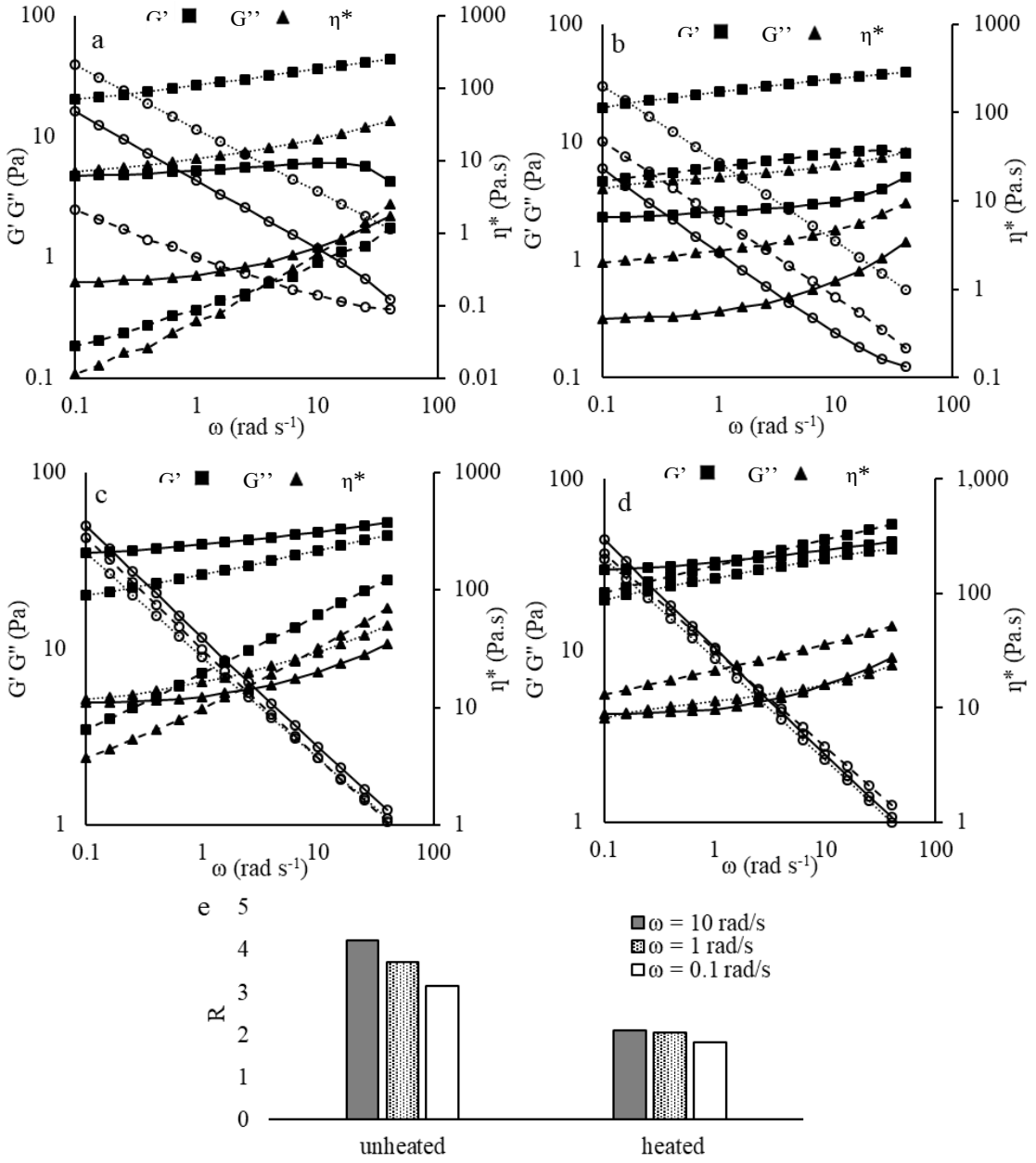

Figure 3.7. Mechanical spectra of 0.82% FC60 (solid line), 0.82% PSY (thin dashed line), and 0.82% FC60-PSY (dense dashed line), before (a) and after (b) heat treatment. Mechanical spectra of 1.64% FC60 (solid line), 1.64% PSY (thin dashed line), and 0.82% FC60-PSY (dense dashed line), before (c) and after (d) heat treatment. e: R value of unheated and heated 0.82% FC60-PSY calculated by G' values at 0.1, 1, and 10 rad s^{-1}.

In terms of rheological synergism, an index R was calculated and plotted in Figure 3.7e. G' at angular frequency of 0.1, 1, and 10 rad s^{-1} of either heated or unheated samples were fitted into equation (3.2) to calculated R. The positive R of unheated and heated

mixture suggested synergism that the addition of FC60 enhances the gel-like property of PSY. However, it is reduced by heat treatment shown as lower synergistic value R.

Table 3.1. Storage moduli (G') at different angular frequencies of 1.64% FC and PSY before and after heat treatment and upper and lower bounds calculated by equation 3.3 and 3.4 assuming no interaction between FC60 and PSY and the mixture is comparable to a binary mixed gel with the volume fraction of 0.5 for each

	Angular Frequency (rad s^{-1})	1.64% FC60	0.82% FC60-PSY	1.64% PSY	upper bound	lower bound
unheated	10	45.83±7.68	35.97±5.15	15.50±0.00	30.66	23.17
	1	38.87±6.77	26.23±4.23	7.22±0.00	23.05	12.18
	0.1	34.86±6.10	20.13±3.36	3.46±0.00	19.16	6.30
heated	10	38.52±11.64	34.42±3.99	44.20±4.46	41.36	41.17
	1	32.93±10.03	26.54±3.15	31.18±3.43	32.05	32.03
	0.1	29.43±8.90	19.55±2.49	21.70±2.54	25.57	24.98

To understand the structure of the mixture, an assumption was made temporarily that FC does not interact with PSY hence the mixture can be considered as a binary, phase separated gel and the volume fractions and concentrations of each phase were the same as that when they were originally mixed by a 1:1 ratio. The upper and lower bounds of the mechanical properties of the mixture were calculated by equation 3.3 and 3.4 (Clark, Richardson, Rossmurphy & Stubbs, 1983; Morris, 1990). The experimental value of G' of 1.64% FC60 and PSY at 0.1, 1, and 10 rad s^{-1} were fitted into the equations to calculate the upper and lower bounds which are shown in Table 3.1. The experimental G' of unheated 0.82% FC60-PSY was higher than the calculated upper bound especially at high angular frequencies. As for the heated mixtures, the measured G' was lower than the calculated lower bound. Therefore, the assumption is erroneous.

$$G_{upper} = \frac{G'_{FC60}}{2} + \frac{G'_{PSY}}{2} \qquad (3.3)$$

$$G_{lower} = \frac{2G'_{FC60} \cdot G'_{PSY}}{G'_{FC60} + G'_{PSY}} \qquad (3.4)$$

3.3.2.3. Fluorescence microscopy

The microstructure of the PSY and FC mixtures were explored using fluorescence microscopy images. Figure 3.8 shows the fluorescence images of unheated and heated mixtures of PSY and FCs with a total concentration of 1.64%, where PSY was covalently labelled by FITC shown in green in the images. In unheated mixtures with FC0 and FC10, as circled in red, unheated PSY presented as hydrated and swollen gel particles with an insoluble core (visible under polarised light, image not shown) and detailed in Chapter 2. FCs are not specified in colour but they were visible because of light diffraction. As shown in the images, the phase surrounding hydrated PSY particles were concentrated in FC0 or FC10 fibres. In Chapter 2, the freshly prepared PSY suspensions can be described as concentrated suspension of gel particles and its rheological properties can be ascribed to the viscoelastic property of and physical forces between these soft particles. In the case of FC0-PSY and FC10-PSY, they can be considered as gels consisting of two phases where one phase is hydrated PSY particles distributed in the other one; concentrated in FC fibres. Therefore, the overall rheological property of the mixture is highly dependent on the strength of FC fibres and the volume taken by them. FC60 was highly fibrillated and the FC fibres were not easily distinguished from PSY, therefore the transmitted light image of FC60-PSY was overlaid with the fluorescent images. Although FC60-PSY also consist of hydrated PSY particles and the surrounding mixture of FC60 and PSY gels, the structure is distinctly denser than FC0-PSY and FC10-PSY. This can be attributed to FC60 fibres occupying a larger volume than the unfibrillated and less fibrillated cellulose and they compete for

space with PSY. Although the structure of unheated FC60 and PSY mixtures can be roughly described as two phases, the measured G' was much higher than the calculated G' (Table 3.1). Hence, there might be water redistribution or reinforcement of FC60 fibres by PSY.

In heated samples, the intact swollen PSY parties were not observed (Chapter 2). Instead, FC fibres are incorporated into PSY gels and form a composite, where FC0-PSY b and FC10-PSY b displayed similar structure. The slight differences in fibre concentration and distribution and in the observation of PSY gels are due to variations of sampling. As shown in Figure 3.2, the majority of FC10 fibres maintained their integrity with smaller fibres peeled off the main cellulose fibres. This structural similarity is correlated with the similar rheological behaviour that mechanical spectra of heated FC0-PSY and FC10-PSY closely overlapped each other (Figure 3.6b). As for FC60-PSY, cellulose fibres were processed into smaller FC fibres by high degree fibrillation, therefore, they occupied much greater volume and contacted with PSY to a larger degree. The PSY gel, therefore, appears to be highly filled by F60 fibres with a much denser and clumped structure, which explains the distinct viscoelastic property of FC60-PSY (higher moduli). Similar effects on the strength of compressed MFC-resin composite was reported by Nakagaito and Yano (2004) that fibrillation treatment on cellulose surfaces is ineffective but fibre disintegration strengthens the composites.

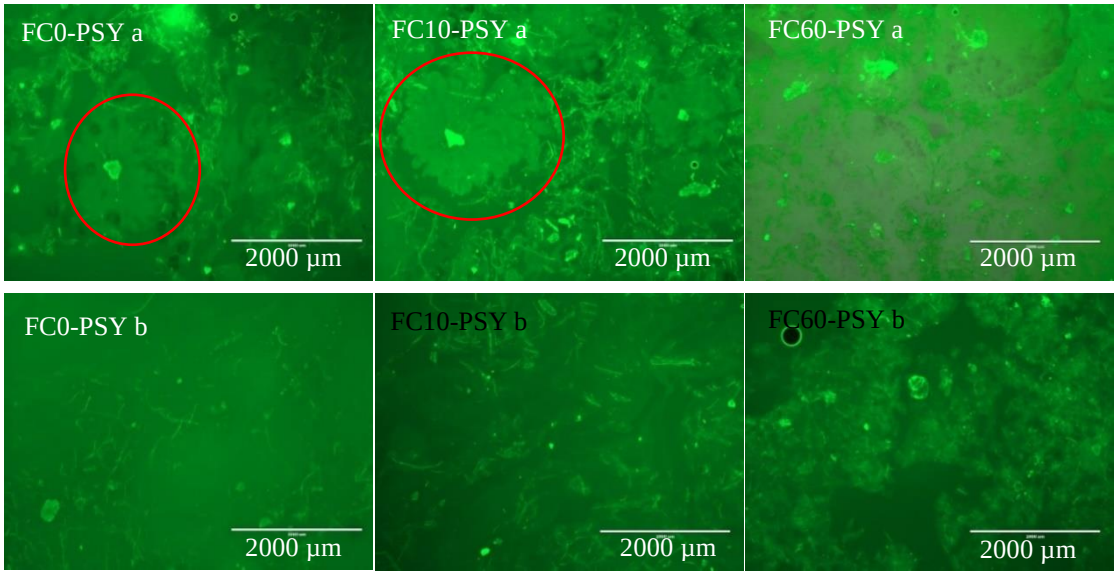

Figure 3.8. Fluorescence microscopy images of FC and PSY mixtures at concentration of 0.82% respectively before (a) and after (b) heat treatment. PSY was labelled with FITC shown in green in the images. FC was not specified in colour. The fluorescence image of FC60-PSY was overlapped with transmitted light microscopy image. A hydrated PSY particle is highlighted in red circle in FC0-PSY a and FC10-PSY a. The colour version has poor quality when printed. Please see the colour figure in electronic version or via https://uniofnottm-my.sharepoint.com/:b:/g/personal/yi_ren_nottingham_ac_uk/EWWHYPTJqGtMh4cY_BIp4zIB7PNtX91s5-Af7IHYgLtN3Q?e=ChKGx0

The concentrations of the mixtures were reduced to 0.25% for each component to further investigate the interactions between FC and PSY (Figure 3.9). The three images in the first row present the overall structure of diluted mixtures of FC and PSY with a scale bar of 2000 µm. FC0-PSY and FC10-PSY have similar structures appearing as a dispersion of fibres. Some larger pieces are also observed which might be the insoluble particles of psyllium husk, cellulose fibre clusters, or PSY polysaccharide aggregates. FC60-PSY is distinct from the other two where lumps with irregular shapes occupy a large volume fraction. The images in the second row represent details of FC-PSY mixtures with higher magnification. According to Chapter 2, it is known that PSY is not water soluble. It exists as gel aggregates, shown in Figure 3.9. Some of these aggregates (green) are attached and concentrated to the FC fibres which were stained by methyl blue, and shown in blue. A similar structure has been observed by Mikkelsen, Flanagan,

Wilson, Bacic and Gidley (2015) although, in their study, heteroxylan was incorporated into cellulose during bacteria fermentation and the scale was much smaller than what is shown in Figure 3.9. The absorption of heteroxylan aggregates rather than individual molecules to cellulose surface was also evidenced by Linder, Bergman, Bodin and Gatenholm (2003). In FC60-PSY, cellulose was highly fibrillated and occupy much larger volume with larger total surface; therefore, the interaction with PSY was more extensive than FC0 and FC10. FC60 dispersed as fibre clusters, as revealed under transmitted light microscopy (data not shown) and, when the fibre clusters interacted with PSY gel aggregates, they appear as lumps (Figure 3.9).

PSY polysaccharide is composed of a variety of heteroxylans varying in length, composition and distribution of sidechains, which lead to structural differences at the molecular level, different rheological properties and responses to temperature (Chapter 2). In this study, PSY was also fractionated at different temperatures and the difference in the interactions between PSY fractions and FC processed for different times, at the concentration of 0.25% are shown in Figure 3.9. F60 was the most prolifically attached to FC0 and FC10 fibres. Other PSY fractions barely interacted with FC0 and show slight interactions with FC10 fibres. There is no significant difference between the mixtures of FC60 and the four PSY fractions. Therefore, it can be concluded that 1) F60 is the main PSY fraction interacting cellulose fibres; 2) the interactions between PSY and cellulose is promoted by fibrillation. The interactions between cell wall materials i.e. hemicellulose and pectin with cellulose, have been widely studied while the interaction mechanisms are different. Pectin forms interpenetrating network with bacterial cellulose when it was added in bacteria culture (Chanliaud & Gidley, 1999; Mikkelsen et al., 2015). Xyloglucan and mannans bind to bacteria cellulose and form cross bridges

and the galactose content of xyloglucan has a significant effect on the cellulose composites (Mikkelsen et al., 2015; Whitney, Gothard, Mitchell & Gidley, 1999; Whitney et al., 2006). Arabinoxylan and mixed linkage glucan interact unspecifically with the more hydrophobic surface of cellulose via hydrophobic forces (Mikkelsen et al., 2015). The association of heteroxylan with cellulose decreases with increasing substitution (Kabel, van den Borne, Vincken, Voragen & Schols, 2007; Köhnke, Östlund & Brelid, 2011; Mikkelsen et al., 2015). Grantham et al. (2017) and Busse-Wicher, Grantham, Lyczakowski, Nikolovski and Dupree (2016) investigated the association patter between acetate and/or glucuronic acid decorated xylan with cellulose in native cell wall material extracted from plant stems. They found that xylan with both evenly or unevenly distributed decoration can interact with the hydrophobic surfaces of cellulose. Domains with even decoration, which adopts a twofold helical screw conformation, interacts with the hydrophilic surface of cellulose via hydrogen bonds but the unevenly substituted domains form loops, bridges between or within the microfibrils. It can be concluded that the xylan backbone can associate with both hydrophobic and hydrophilic surfaces of cellulose while the association to the hydrophilic surfaces is obstructed by substitution. However, as previously reported in Chapter 2, F60 is a highly substituted fraction, with high arabinose content, but only this fraction exhibited a significant association with FC0 (Figure 3.9). It has been reported that hairy pectin can interact with cellulose via its neutral sugar sidechains including arabinan (Iwai, Ishii & Satoh, 2001; Oechslin, Lutz & Amadò, 2003; Vignon, Heux, Malainine & Mahrouz, 2004). Arabinan adopts a conformation compatible with cellulose binding in terms of surface complementarity, therefore, it aligns with cellulose microfibrils which might be mediated by hydrogen bonds (Zykwinska, Ralet, Garnier & Thibault, 2005). Therefore, it is possible that F60 is branched by relatively long

sidechains of arabinan, which interact with cellulose in a similar way as the hairy pectin (Figure 3.10a).

In addition, the well-known synergistic interactions of xanthan and mannan based polysaccharides provide insights into polysaccharide interactions as a good example. The latest mechanism of interaction with konjac glucomannan has been proposed by Abbaszadeh, MacNaughtan, Sworn and Foster (2016) that two types of interactions are involved at different temperatures, where type A is interaction with ordered helical xanthan chains while type B is interaction with 2-fold disordered xanthan backbone. A polysaccharide with 2-fold helical conformation is compatible with cellulose allowing interactions between backbones (Busse-Wicher et al., 2016; Preston, 1979). PSY heteroxylans have been hypothesised to contain domains adopting helical conformation, which undergoes softening, helical conformational transition, and melting into coils upon heating which is similar to xanthan (Chapter 2). According to the similarities to xanthan, Abbaszadeh et al. (2016)'s model could be used and modified to explain the interactions between PSY and cellulose (Figure 3.10b). There is possibly interactions between helical domains of psyllium heteroxylan and cellulose. Additionally, a 2 fold helical (if existing in the conformational transition of PSY heteroxylan) or coil conformations might be able to associate, or adapt and associate respectively, to cellulose as a result of stereochemically compatibility (Berry, Davis & Gidley, 2001; Whitney, Brigham, Darke, Reid & Gidley, 1998). However, the softening and melting of PSY heteroxylans is thermal reversible (Chapter 2). In other words, based on the hypothesis, the heteroxylan molecules deviate from coil and 2 fold helical conformation and become unfavourable to the interaction with cellulose, which explains the isothermal G' decline shown in Figure 3.6c and d.

Another possible mechanism (Figure 3.10c) of the association with cellulose relies on the porous structure of microcrystalline cellulose where xyloglucan and heteroxylan can be trapped (Köhnke et al., 2011; Zykwinska et al., 2005). It is reasonable to consider that cellulose with rough surfaces or porous structure provides docking positions where PSY heteroxylan can be immobilised and accumulate. This behaviour is more obvious in FC10 whose surface roughness is increased by the fibrillation process as shown in the second column of images in Figure 3.9. The interaction between FC10 with all flour PSY fractions increased slightly compared to the association with FC0. However, at a higher concentration, this phenomenon does not significantly affect the structure and the rheological property of the gel composites composed by PSY and FC0 or FC10 (Figure 3.6b).

FC60 is heavily fibrillated and, as shown in Figure 3.9, the mixtures of FC60 with both whole PSY and PSY fractions appear to be interpenetrating gels or gel particles. Combining the fact that moduli of heated FC60-PSY were much higher than FC0-PSY and FC10-PSY, the influence of the trapping effect of cellulose on PSY increased and finally overcame the weak interaction between FC and PSY. The interpenetrating structure of FC60-PSY and dense volume occupation dominantly contributed to its overall rheological property. Another approach is considering the contribution to rheological properties of increased volume fractions of FC as reported by Hemar, Lebreton, Xu and Day (2011) that significant increase of volume fraction leads to the domination of the rheological responses.

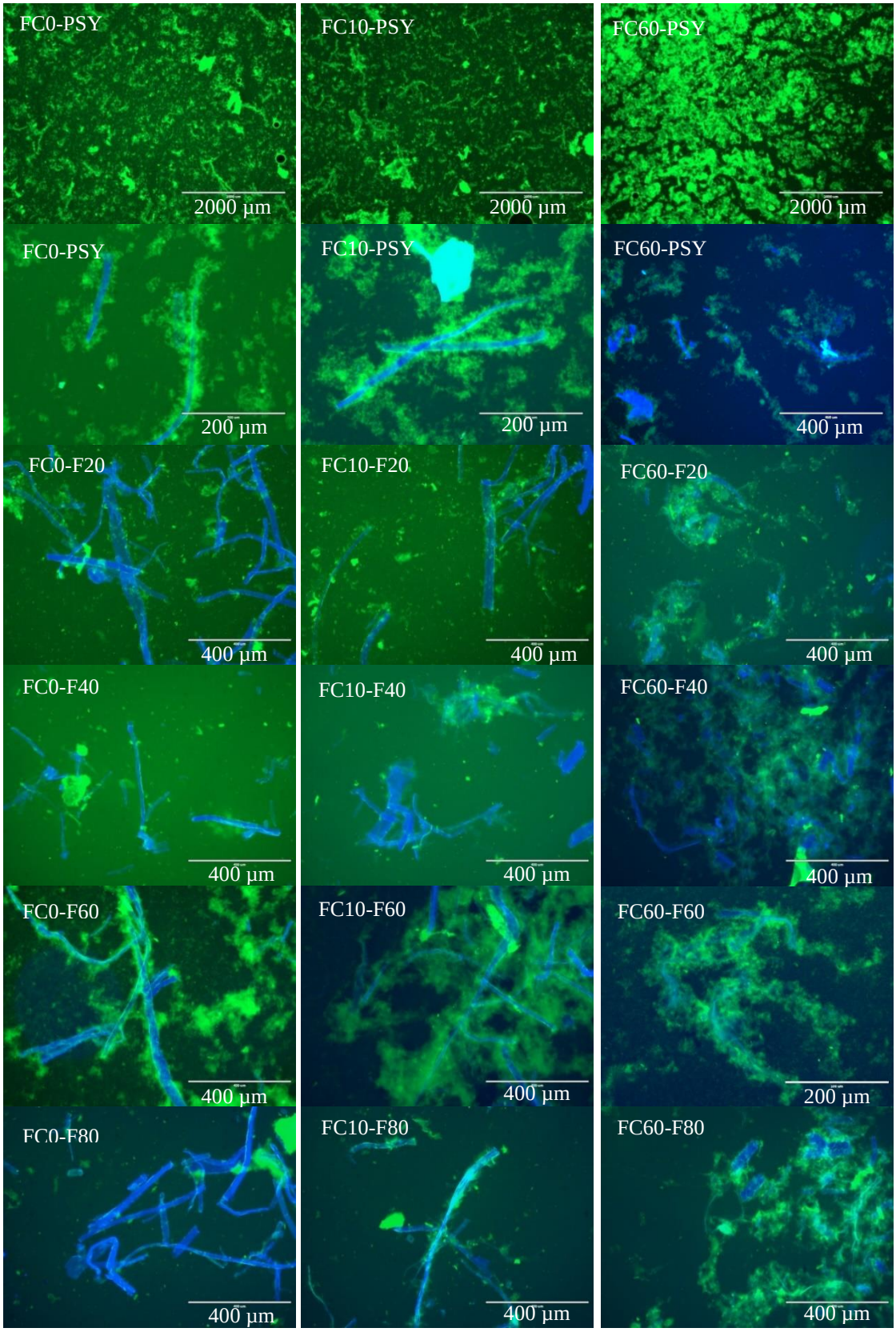

Figure 3.9. Fluorescence microscopy images of FC and PSY mixtures at concentration of 0.25% respectively PSY was labelled with FITC shown in green in the images. FC was not specified in colour in the three images in the first row and it was stained by methyl blue shown in blue in the remaining images. The colour version has poor quality when printed. Please see the colour figure in electronic version or via https://uniofnottm-my.sharepoint.com/:b:/g/personal/yi_ren_nottingham_ac_uk/EWWHYPTJqGtMh4cY_BIp4zIB7PNtX91s5-Af7IHYgLtN3Q?e=ChKGx0

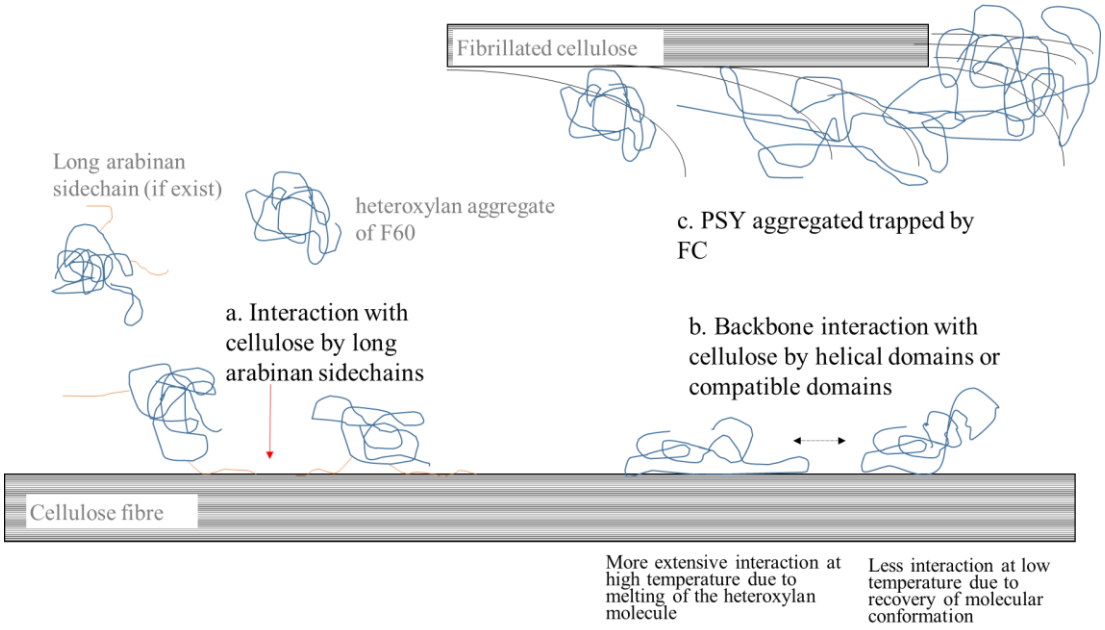

Figure 3.10. Schematic representation of possible mechanisms of the interaction between PSY/F60 and cellulose/FCs.

3.4. Conclusion

Fibrillation of cellulose starts from the surface, weak points, and tips of cellulose fibres. It significantly increases stability and water retention ability of cellulose suspensions. Distance-induced (by centrifugation, leading to reduced distance and increased contacts between fibres) FC flocculates are larger than heat-induced one. Unheated FC and PSY mixture can be considered as a binary phase separated mixture with one phase of hydrated PSY particles and the other one concentrated in FC. However, the mixtures are more similar to a composite gel after heat treatment. The rheological moduli of unheated mixtures increase with an increase in fibrillation time as the result that fibrillation increases the volume taken by FC fibres. Nevertheless, after heat treatment, there is no significant difference in structure and rheological property when the fibrillation only affects the surface of cellulose fibres while the loss of integrity of FC fibres contributes to higher moduli and distinct denser structure. The mixture of FC60

and PSY displays synergistic effects, which is more pronounced before heat treatment. PSY and its fractions form aggregates, which associate to FC fibres. The heavily substituted PSY heteroxylan (F60) is the only fraction which pronouncedly associates to unfibrillated cellulose via, possibly, interactions between arabinan sidechains and cellulose surface, or/and conformational (2-fold helix) compatibility. Additionally, the whole PSY and all fractions can be trapped by cellulose, which become more dominant with fibrillation. This study provides the possibility of applying the novel mixtures of FC and PSY in designing structured food, pharmaceutical, and cosmetic products.

Chapter 4.

Investigation of gluten free bread dough rheology, proving and baking performance and bread qualities by response surface design and principle component analysis

Highlights:

- Gluten free doughs and bread were comprehensively characterised and analysed by simultaneous application of response surface and principal component analysis.
- A generalised Maxwell model was applied to evaluated doughs.
- An additional peak was found on the pasting profiles of psyllium-flour blends.
- Extensibility is a sufficient predictor of gluten free bread quality.
- The dilution effect of water significantly affects proving performance and texture property
- Gluten free bread tends to have different types of voids in crumb structure.

Keywords:

Gluten free, dough rheology, dilution effect, response surface method, principal component analysis

Abstract

Contribution of methylcellulose (MC), psyllium seed husk powder (PSY), and water addition level to gluten free bread quality and correlations between dough rheological properties and bread qualities were investigated by response surface design and principal component analysis. The mechanical spectra of doughs were fitted by the generalised Maxwell model and relaxation frequency was calculated which is much higher than wheat bread doughs and higher than the deformation rates during proving. The addition of PSY has a complex influence on pasting viscosity at high temperature and an additional peak was observed, which possibly rely on a balance between formation and breakdown of PSY weak gel particles, PSY particle interactions, and interaction with amylose. The addition of MC and PSY reinforce dough rheological properties and increase dough stability while regulation of the water content was important for the hydrocolloids to be fully hydrated and functional and for soft, smooth and consistent doughs. The interacting effects of water and hydrocolloids, especially MC, significantly influenced dough extensibility and work of adhesion, which are good predictors of bread quality. However, the dilution effect of water can lead to problems such as low stability of doughs, overexpansion, and weak crumb structure. Other rheological responses are less significantly correlated to specific volume, but, sensitive to formulation variations and reflect dough structures and stability.

4.1. Introduction

Bread is mainly made from wheat flour, where gluten (the storage proteins) shows unique properties and functionalities. The function of gluten is maximised in bread due to the relatively high water content. Hydrated gluten develops into a viscoelastic network, which traps gas and allows expansion of gas cells during proving. It is denatured during baking and forms a bicontinuous phase with gelatinised starch, which together forms the breadcrumb. After baking, gluten participates in moisture control. However, many people around the world are intolerant to gluten, which leads to coeliac disease and other gluten-trigged health problems, which constrains a group of people from consuming wheat based products (Catassi et al., 2012; Czaja-Bulsa, 2015). On the other hand, 'free from' is a global trend of healthy lifestyle choices, which promotes the market of gluten free products. However, gluten free bread is generally inferior in flavour, sensory and nutritional qualities (Singh & Whelan, 2011; Thompson, 2009). For the purpose of dealing with gluten intolerance and meeting the "free from" trend, the production and quality improvement of gluten free bread are becoming a new favourite of both manufacturers and researchers. However, it is still a challenge to create products with acceptable sensory attributes.

Currently, several methodologies have been developed for gluten-free bread manufacturing, which can be categorised as the application of alternative flour blends, enzyme treatment and sourdough application, and other treatments, among which, the application of alternative flour blends is the most investigated. Alternative flour is mostly a blend of one or more types of starch and/or starch-based flours and, in most cases, hydrocolloids. A preferable alternative flour is rice flour, because of its bland taste, white colour, low sodium content, easily digestive carbohydrates and

hypoallergenic properties (Kadan et al., 2001). Hydrocolloids are the other type of ingredients in the alternative flour blends, usually with a small amount of addition, but, significant functionality. One of the early studies on rice bread was conducted by Nishita et al. (1976) who investigated the addition of different kinds of hydrocolloids, dough conditioners and lipids. They reported that hydroxypropyl methylcellulose (HPMC) and refined vegetable oils gave better loaves in the absence of dough conditioners and surfactants. Haque and Morris (1994) also investigated rice flour based bread and obtained higher aeration than most commercial wheat bread, with the addition of HPMC and psyllium seed husk powder at different water contents and proving temperatures.

Most research on gluten free bread includes hydrocolloid addition to enhance the structure building, improve mouthfeel, increase shelf-life, and increase the overall acceptability (Gallagher et al., 2004; Lazaridou, Duta, Papageorgiou, Belc & Biliaderis, 2007). The most commonly used hydrocolloid in a gluten-free bread formula is HPMC (Masure et al., 2016). Compared to HPMC, Methylcellulose (MC) is less studied and applied in gluten free bread. It forms thermoreversible gels at a lower temperature (50-55°C) than HPMC with a higher gel strength. The gelling property at high temperature is similar to gluten, which denatures and forms a stable network during heating and contributes to the final texture of bread crumb (Haque & Morris, 1994). On the other hand, a new star is recently rising in the field of gluten free products, i.e. the seed husk of psyllium (*Plantago ovata* Forsk), also known as ispaghula or isabgol. The mucilage of hydrated psyllium seed husk is mainly composed of heteroxylans, which are mainly substituted, by arabinose and xylose. As a natural fibre, it has been traditionally used in medical treatment in some countries and it is proven that psyllium has the ability to

lower cholesterol levels, be used as laxative and improve insulin sensitivity (Anderson et al., 2000; Rao, Warrier, Gaikwad & Shevate, 2016; Song et al., 2000). Though the mucilage of psyllium seed husk does not dissolve in water, its suspension shows a 'weak gel' property which is similar to xanthan (Haque et al., 1993a). In addition, water content is critical in bakery products which influences quality, texture, taste, smell, volume, flavours and mouth feel (Chieh, 2006) as its mobility and distribution influence dough rheology and baking performance (Leung, Magnuson & Bruinsma, 1979). It has been emphasised that an applicable water addition level is a critical factor in gluten free bread formulation (Haque & Morris, 1994; McCarthy, Gallagher, Gormley, Schober & Arendt, 2005).

Gluten free doughs and bread have been widely investigated (Mancebo et al., 2015; Mariotti et al., 2009; Martínez & Gómez, 2017; McCarthy et al., 2005; O'Shea, Rößle, Arendt & Gallagher, 2015; Ronda, Pérez-Quirce, Angioloni & Collar, 2013; Torbica et al., 2010). Dough rheology can be an indicator of the quality of end products (Lazaridou & Biliaderis, 2009). However, dough characterisation, crumb structure and dough-crumb transformation can be complicated as it involves dough stability, gas trapping ability and water distribution in doughs, which further influences starch gelatinisation, structure transformation, and crumb formation during baking. However, the information and properties investigated are limited in most studies.

This Chapter investigated the roles of MC and psyllium seed husk powder (PSY) at different water addition levels in gluten free dough and bread properties and qualities by response surface design (RSD). Effort has been made to generate a comprehensive characterisation, which leads to a large amount of data. Bratchell (1989) firstly applied principal components analysis (PCA) to RSD data which was later followed by Ribeiro,

Teofilo, Augusto and Ferreira (2010) and Das Purkayastha, Dutta, Barthakur and Mahanta (2015). A combination of PCA and RSD was applied in this Chapter to reduce the number of data dimensions and study the correlations between responses. To our best knowledge, this is the first attempt to combining PCA with RSD to investigate the addition of hydrocolloids in gluten free doughs and bread to generate a more comprehensive characterisation.

4.2. Materials and methods

4.2.1. Materials

Rice flour was purchased from Doves Farm online store. Allinson Easy Bake Yeast (Allinson Flour, Peterborough, UK), sugar (Sainsbury's, UK), sunflower oil (Sainsbury's, UK), and salt (Sainsbury's, UK) were purchased from local supermarkets. Methylcellulose (Methocel® A4M) was supplied by The Dow Chemical Company (Bomlitz, Germany). Vitacel® Psyllium husk powder was kindly donated by the JRS (J. Rettenmaier & Söhne Group, Rosenberg, Germany). Pure amylose from potato and amylopectin from corn were purchased from Sigma-Aldrich (Dorset, UK).

4.2.2. Biochemical analysis

The protein contents of rice flour and PSY were converted with the factor of 6.25 from nitrogen content analysis using a Nitrogen Analyser NA 2000 (Fisons Scientific Equipment, Loughborough, UK). Lipid contents were obtained by extraction with a chloroform-methanol mixture (2:1). Moisture contents were obtained by drying at 105 °C and ash contents were measured using a muffle furnace at 550°C for 6 hours.

AACC method (61-03) and the method from Kaufman, Wilson, Bean, Herald and Shi (2015) were modified to determine the amylose content of rice flour. Rice flour was defatted using 85% methanol. Defatted rice flour, potato amylose and corn amylopectin (100 mg) were dispersed in 1 ml of 95% ethanol and then dissolved in 9 ml of 1 M NaOH in a boiling water bath for 10 minutes. After standing at room temperature for 3 hours, the starch solutions were diluted to 100 ml. The standard curve was prepared using mixtures of potato amylose and corn amylopectin in a series of different ratios. Samples (5ml) were diluted by 20 times with additions of 1 ml of 1 M acetic acid and 2 ml of iodine solution (0.2% I_2 and 2% KI w/v) and were incubated at room temperature for 20 minutes. The absorbance at 720 nm was determined using a spectrophotometer. The amylose contents were calculated against the regression equation determined from the standard curve and verified by a standard starch sample with 66% amylose content.

4.2.3. Formulation and dough preparation

The basic formulation included 100 g of rice flour, 5 g of sugar, 2 g of salt, 1.5 g of yeast, and 5 g of sunflower oil. The addition levels of water, MC and PSY are shown in Table 4.1 according to IV-optimal design with the total hydrocolloid addition level lower than 3.5 g per 100 g of rice flour. Doughs were prepared based on 200 g of rice flour per batch by a stand mixer (Kenwood, UK) equipped with a CHEF flexible beater (AT501, Kenwood, Havant, UK). Dry ingredients were mixed thoroughly and then mixed with water and oil for 7 minutes at speed 1.

Table 4.1. Addition levels of water, MC and PSY per 100g of rice flour according to IV-optimal design

Run	water	MC	PSY
1	130	0.2	0
2	130	2	1
3	120	0	1
4	110	0	2
5	110	1	0.7
6	120	0	1
7	120	1	1
8	125	1.2	0.3
9	110	2	1.5
10	110	1	0.7
11	110	0	0
12	125	1.2	0.3
13	110	2	0.5
14	120	0.5	2
15	115	2	0
16	122	1.5	2
17	130	0	2
18	112	1.2	2
19	118	1.8	1
20	128	0.8	1.3

4.2.4. Dough evaluation

4.2.4.1. Fundamental rheological measurements

Dough sample preparation is described in section 4.2.3 excluding the addition of yeast. Samples were sealed in plastic containers and rested at room temperature for 1 hour before experiments. Controlled shear stress tests and small amplitude oscillatory tests were performed using a MRC 301 rheometer (Anton Paar, Austria) with serrated parallel plate geometry (PP25/P2-SN15766, Anton Paar), the measuring gap was 2 mm. The temperature was controlled by a Peltier system with the assistance of a water bath (R1, Grant, Shepreth). The excess sample was trimmed with a spatula and the edge of the samples were covered with low viscosity mineral oil (Sigma, USA) to prevent the drying of samples. Doughs were loaded at 20 °C and rested at 30 °C for 500 seconds before measurement. Controlled shear stress tests were performed to obtain the yield point with the stress increasing logarithmically from 0.03 to 30000 Pa over 18.5 minutes

at 30 °C. The yield point was determined by defining an upward bending point with 1% bandwidth using yield stress II in Rheoplus 3.4. Frequency sweep tests were performed in a logarithmic decrease with a strain of 0.02% which is in the LVE region. The frequency dependences of storage moduli G' and complex viscosity η* in the middle frequency range (0.881 to 40.9 rad s^{-1}) were represented by the slopes of lgG' versus lgω and lgη* versus lgω. Additionally, the obtained mechanical spectra were fitted to generalised Maxwell Model as shown in equation (4.1) with individual relaxation time (λ_i) and individual relaxation moduli (G_i) describing the discrete spectrum (i) of the sample.

$$G(t) = \sum_{i=1}^{N} G_i e^{-t/\lambda_i} \qquad (4.1)$$

The dynamic moduli G'(ω) and G''(ω) in small amplitude oscillatory experiments can be estimated and calculated from angular frequency (ω) by equation (4.2) and (4.3) (Baumgaertel & Winter, 1992; Ferry, 1980; Laun, 1986). The fitting was performed by varying individual relaxation moduli G_i minimising the sum of squared differences between calculated G'(ω), G''(ω) and experimentally obtained G', G'' with arbitrarily decided λ_i as shown in Table 4.2. G_e represents a pure elastic component in the model.

$$G'(\omega) = \sum_{i} G_i \frac{\omega^2 \lambda_i^2}{1 + \omega^2 \lambda_i^2} + G_e \qquad (4.2)$$

$$G''(\omega) = \sum_{i} G_i \frac{\omega \lambda_i}{1 + \omega^2 \lambda_i^2} \qquad (4.3)$$

4.2.4.2. Empirical rheological measurements

Doughs were also evaluated using a backward extrusion rig and SMS/Chen-Hoseney dough stickiness rig (Stable Micro Systems, UK) on a TA-XT plus texture analyser (Stable Micro systems, Surrey, UK) equipped with a 5 kg loading cell. In the backward extrusion test, doughs were loaded into a container (diameter of 42 mm) to a height of 36 mm avoiding big air pockets. A disc with a diameter of 30 mm and thickness of 5 mm centrally extruded into the dough by 22.5 mm and then returned to the height of 120 mm from the base at a speed of 1 mm s^{-1}. The start of data recording was trigged by a load of 5 g. The positive peak force and positive area during the downward stroke indicated firmness and consistency of doughs, respectively. The negative peak force and area during the upward stroke indicated cohesiveness and index of viscosity. The returning distance before the force reached a constant negative value indicated dough extensibility. For the stickiness test, doughs were loaded into a SMS/Chen-Hoseney Dough Stickiness Cell (A/DSC) and a uniform surface was generated (Chen & Hoseney, 1995). The surface was compressed at a speed of 0.5 mm s^{-1} by a 25 mm aluminium cylinder probe (P/25) with a target load of 40 g for 0.1 seconds, after which the probe withdrew at 10 mm s^{-1}. The maximum force, area, and travel distance during probe withdrawing indicated dough stickiness, work of adhesion, and dough strength individually. Data recording and analysis were performed using the equipped software Exponent 6.1.14.

Table 4.2. Individual relaxation time and relaxation moduli for Generalised Maxwell Model fitting

Individual relaxation time λi (s)	0.0001	0.001	0.01	0.1	1	10	100	1000	10000	100000	R^2
run 1	27081	0	0	31	205	587	0	0	0.008	0.001	0.725
run 2	0	9375	3944	1724	842	1403	1404	0.203	0.01	0.001	0.985
run 3	12853	0	2128	436	541	592	1760	0.203	0.01	0.001	0.888
run 4	0	9301	4038	3044	2201	1948	6658	0.213	0.012	0.001	0.994
run 5	0	4369	6429	1329	1521	2584	2857	0.204	0.01	0.001	0.895
run 6	0	2326	1472	491	451	604	1471	0.219	0.014	0.001	0.930
run 7	0	2203	4455	570	1032	0	2327	0.204	0.01	0.001	0.862
run 8	21548	0	2469	434	0	1288	0	0	0.01	0.001	0.881
run 9	180032	0	6957	4510	2281	5825	2733	0.202	0.01	0.001	0.998
run 10	0	5995	4750	1232	1237	1782	2503	0.205	0.01	0.001	0.928
run 11	0	0	1869	0	72	1100	0	0	0.009	0.033	0.629
run 12	0	3851	2660	363	458	0	997	0.202	0.01	0.001	0.889
run 13	0	15699	5603	3200	1362	3597	1188	0.202	0.01	0.001	0.997
run 14	125673	0	554	2252	1083	3477	1949	0.203	0.01	0.001	0.897
run 15	0	12560	4031	2204	903	3223	0	0.201	0.01	0.001	0.996
run 16	133958	0	3586	2635	1193	3709	1092	0.203	0.01	0.001	0.996
run 17	67997	0	0	1100	560	1726	1051	0.202	0.01	0.001	0.712
run 18	0	12918	6920	3305	2575	3437	4957	0.206	0.011	0.001	0.982
run 19	0	9833	5409	2011	1280	833	2569	0.206	0.01	0.001	0.974
run 20	0	4678	2722	695	736	860	1343	0.202	0.01	0.001	0.917

4.2.4.3. Pasting properties of flour blends

The flour blends were prepared by mixing rice flour with MC or/and PSY in the same ratio as shown in Table 4.1. Sugar, salt, yeast, and oil were excluded. The pasting properties of flour blends were characterised by Rapid Visco Analyser (RVA) (Newport Scientific Pty. Ltd., Warriewood, New South Wales, Australia) equipped with a water bath (Thermo scientific C10, Karlsruhe, Germany). The flour blends containing 2.5 g of rice flour and various amounts of MC and/or PSY were dispersed in 24 ml of RO water. After initial 60-second mixing at a high shear rate (960 rpm) and 60 seconds mixing at 160 rpm at 25 °C, the temperature increased to 95 °C over 350 seconds, was held at 95 °C for 150 seconds, and decrease to 25 °C in 350 seconds. Data were collected and peak 2, peak 3, though 1, trough 2, trough total, breakdown, final viscosity, setback, peak 2 time, peak 3 time, peak 2 temp, peak 3 temp, and pasting temp were analysed by the software, Thermalcline.

4.2.5. Baking tests

Gluten free doughs were prepared according to section 2.3 then 200 to 210 g of dough were loaded in a baking pan with a dimension of 7.5 x 7.5 x 10 cm. Two doughs were generated per batch of mixing. The baking pan was shaken to avoid big air pockets in doughs. The doughs were covered with cling film and proved in an incubator (Binder, Tuttlingen, Germany) at 30 °C for 85 minutes and baked in a deck oven (Tom Chandley, Manchester, UK) at 230 °C for 40 minutes. Then the loaves were cooled on a rack at ambient condition for 1 hour before further operations.

4.2.5.1. Basic analysis and calculations

Proving was monitored by loading approximately 10 ml of dough sample in a measuring cylinder and incubated at 30 °C for 85 minutes during which the volume was recorded. Maximum volume, final volume, maximum rate and maximum rate time were calculated. After cooling, the loaves were weighed and loaf volumes were measured by rapeseed displacement. The baking loss was calculated by equation (4.4). Specific volume was the ratio of loaf volume to loaf weight. A piece of crumb was cut from the centre of the loaves and the moisture content was measured.

$$baking\ loss = \frac{dough\ weight\ before\ proving\ -\ loaf\ weight\ after\ cooling}{dough\ weight\ before\ proving} \quad (4.4)$$

The loaves were cut into 1.25 cm thick slices and the surface of the middle slice was scanned by C-Cell (Calibre Control International LTD, Warrington, UK). Twenty-three parameters including slice area, area of cells, area of voids, cell diameter, wall thickness were obtained.

4.2.5.2. Bread textural evaluation

The texture property of gluten free bread was evaluated by texture profile analysis (TPA) on a TA-XT plus texture analyser (Stable Micro systems) equipped with 30 kg loading cell. A cylinder of bread crumb was cut from the centre of every loaf slice with a diameter of 3 cm and two pieces from the middle four slices (with the height of 1.25 cm) of each loaf were stacked together. Therefore, two specimens were obtained from the middle of each loaf with a cylinder shape with height and diameter of 2.5 cm and 3 cm. The samples were compressed 65% by a 100 mm plate at speed of 1 mm s^{-1} with 5 seconds between two compressions. Hardness, springiness, cohesiveness, gumminess, chewiness, and resilience were obtained from TPA profile.

4.2.6. Experiment design

The experiment was designed using IV-optimal design (RSD) by Design expert 9 based on three factors, addition levels of PSY, MC and water, this involved 20 runs (Table 4.1). The lack of fit of the models was evaluated by 6 runs, and 4 runs were repeated twice to evaluate error values. Both doughs and loaves were assessed and 74 responses were obtained to analyse the influence of the three factors and correlations between these responses.

4.2.7. Microstructure evaluation by confocal laser scanning microscopy

Three doughs were prepared in addition to the formula listed in table 4.1 without the addition of sugar, salt, yeast and oil. To prepare the doughs, 100 g of rice flour was mixed with 120 g of water containing 0.01 mg mL^{-1} FITC (Acros Organics, New Jersey, US). Rice flour (100 g) was also mixed with either 2 g of MC or PSY and then mixed with 120 g of water containing 0.01 mg mL^{-1} FITC and 0.01 mg mL^{-1} calcofluor white (Sigma-Aldrich, UK). The doughs were prepared as described in section 4.2.3. The three doughs were also prepared without the addition of Fluorescent dyes. After hydrated for 1 hour, the unstained doughs were cooked in sealed containers using an oven where the temperature was programmed to increase from 25 °C to 98 °C in 30 minutes and hold at 98 °C for 10 minutes mimicking the temperature profiles during bread making. After cooled at room temperature, the cooked gels were sliced into thin films and loaded onto glass slides coated with either FITC (for the rice flour only gel) or both FTIR and calcofluor white (for the samples containing either MC or PSY). Doughs and cooked gels were imaged using a Zeiss LSM880 confocal laser scanning

microscope. FITC and calcofluor white were excited at 488 nm and 405 nm respectively and the signals were collected at 510–540 nm and 440-475 nm respectively.

4.3. Results and discussion

4.3.1. Biochemical properties

The moisture content, protein content, ash content, and lipid content of rice flour were 11.1 %, 7.23 %, 0.42 %, and 2.8 % respectively. That of PSY was 7.23 %, 3.40 %, 2.89 %, and 3.30 % respectively (Chapter 2). The amylose content of rice flour was 28.79 %.

4.3.2. Effects on gluten free dough rheological properties

The gluten free doughs made based on rice flour were tested by either fundamental or empirical rheology tests. The fundamental tests included controlled shear stress tests and small amplitude oscillatory measurement, while empirical tests included backward extrusion and SMS/Chen-Hoseney Dough Stickiness measurements.

4.3.2.1. Fundamental rheological analysis of dough properties

The majority of the dough and porous crumb structure is developed during proving. The deformation rates during proving are at low magnitude in a range from 10^{-4} to 10^{-3} s^{-1} as reported by Babin et al. (2006) and Grenier, Lucas and Le Ray (2010). Therefore, it is beneficial to understand the rheological behaviour of doughs at a longer timescale including their relaxation time. Wyss et al. (2007) published Strain-Rate Frequency Superposition (SRFS) for metastable soft materials by shear rate controlled frequency sweep tests which, therefore, involve large amplitude oscillation when the shear rate is high and angular frequency is relatively low. However, this technique might generate

controversial results due to nonlinear contributions (Erwin, Rogers, Cloitre & Vlassopoulos, 2010). Additionally, most gluten free doughs in this study did not have a pronounced structural relaxation peak, possibly due to low stabilities and short linearity, which influence the generation of master curves. Therefore, it is problematic to apply SRFS to gluten free rice doughs.

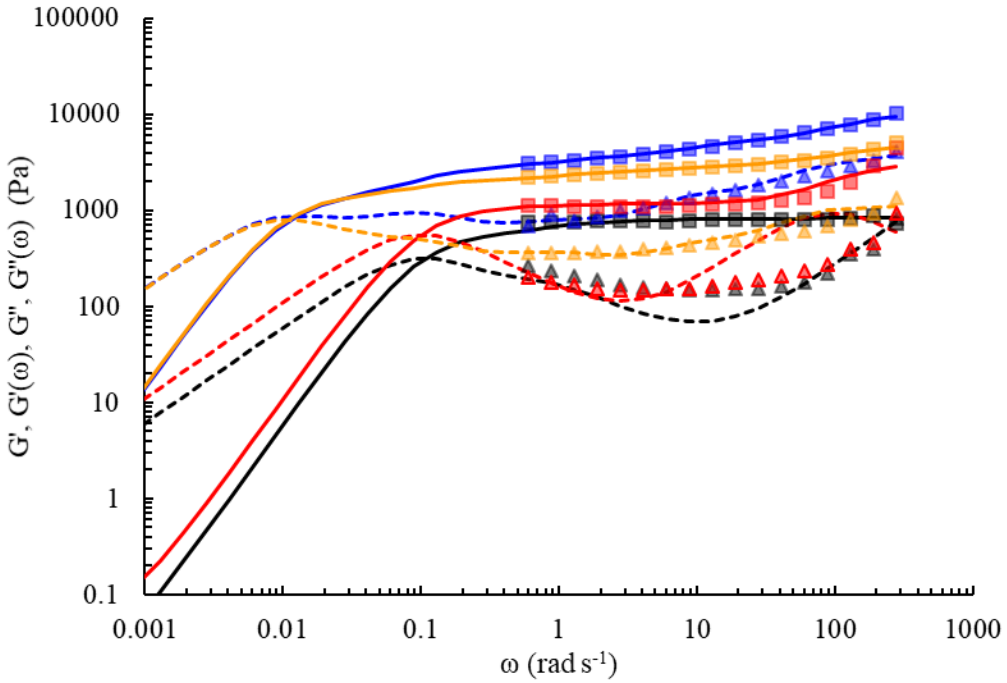

Figure 4.1. Mechanical spectra and curves calculated from generalised Maxwell model of run 1 (black), run 2 (blue), run 6 (yellow), and run 11 (red). The addition levels of water, MC and PSY of each run are shown in Table 4.1. Experimental storage moduli (G') and loss moduli (G'') are shown by square and triangle symbols respectively and Calculated G'(ω) and G''(ω) are presented by solid lines and dashed lines singly.

Another method is the generalised Maxwell model. A single Maxwell model is composed of a serially connected Newtonian dashpot characterised by viscous response η and a Hookean spring characterised by elastic response G, which produce an overall relaxation time λ. The generalised Maxwell model consists of several single Maxwell elements connected in parallel where each element is characterised by G_i and λ_i. A single spring can be included in the generalised Maxwell model characterised by G_e.

The model fitting led to 21 parameters including 10 predefined λ_i for each Maxwell element and 10 corresponding G_i as shown in Table 4.2, and G_e. G_e for all the samples was either zero or close to zero suggesting an insignificant contribution to the overall viscoelasticity and, therefore, was not listed in Table 4.2.

Four typical mechanical spectra and fittings to the generalised Maxwell model (run 1, run 2, run 6, and run 11) are given in Figure 4.1 showing the experimentally obtained storage (G') and loss moduli (G''), and calculated moduli (G'(ω) and G''(ω)). All four doughs are solid-like as G' is higher than G'' although they are different in the frequency dependence of moduli. The generalised Maxwell model fits the experimental data with a satisfactory R^2 (Table 4.2), however the fitting of G'' is not always accurate over the angular frequency range applied in the experiments as seen in Figure 4.1 (run 1, 6 and 11). The lack of fit mainly occurred at the higher angular frequency range (approx. 20 to 120 rad s^{-1}) as seen in run 6 in the same figure. There can be additional deviations from experimentally measured G'' at the lower frequency range at around 2.5 rad s^{-1} (run 11). Run 1 was the only one in all 20 runs showing lack of fit in the medium angular frequency range. Therefore, in RSD, for each run, the storage and loss moduli, complex viscosity, and tanδ at two angular frequencies (1.29 and 60 rad s^{-1}: $G'_{1.29}$, G'_{60}, $G''_{1.29}$, G''_{60}, $\eta^*_{1.29}$, η^*_{60}, $\tan\delta_{1.29}$, and $\tan\delta_{60}$), slopes of lgG' versus lgω and lgη* versus lgω, predicted relaxation frequency (ω_{rel}), with corresponding moduli (G'_{rel}) and complex viscosity (η^*_{rel}), and R square values of the generalised Maxwell model (R^2_M) are used in further analysis.

All three factors had significant effects on moduli and complex viscosity at both high and low angular frequency (1.29 and 60 rad s^{-1}) with $P < 0.0001$ (Table 4.3), where the

coefficients of each term in the regression models for G'_{60}, G''_{60}, $G'_{1.29}$, $G''_{1.29}$, lgG' vs lgω, and ω_{rel} are listed. The correlation coefficients (R^2) are higher than 0.9 for G'_{60}, G''_{60}, lgG' vs lgω, and R^2 is higher than 0.75 for generalised Maxwell model parameters (ω_{rel}). It can be seen that the addition of MC or PSY increased G'_{60}, G''_{60}, $G'_{1.29}$, $G''_{1.29}$, $\eta^*_{1.29}$, and η^*_{60} which suggest a reinforcement effect and they also had positive contributions to the slope of lgG' versus lgω, which indicates less frequency dependence and more solid-like property. This has been well documented as the results of the reinforcement effects of viscoelastic behaviour of hydrocolloids and dilution effect of water on both flour and hydrocolloids, respectively (Lazaridou et al., 2007; Mancebo et al., 2015; Ronda et al., 2013). Additionally, as shown in Figure 4.2, comparing the first column (a), flour particles are distributed more even with the addition of PSY or MC, although there is no significant difference between MC containing (DA) doughs and PSY containing (DP) doughs. The reason might be that higher viscosity increased the effectiveness of shearing during dough mixing. This more homogeneous packing pattern could also contribute to the reinforcement effect. At a low water addition level of 110 g/100g flour, the influence of PSY on G'_{60}, which increased by 6.5 times from 2200 Pa to 14700 Pa, is more significant than MC (G'_{60} increased by 3.3 times). This is also seen in the regression model of $G'_{1.29}$. However, MC is more influential on G''_{60} (increased by 10 to 20 times depending on water contents) while PSY is more influential on $G''_{1.29}$ (increased by 6 to 8 times). MC is known to significantly increase viscosity when dissolved in water and the mechanical spectrum show higher G' at high frequency and high G'' at low frequency (Haque et al., 1993b). On the other hand, PSY shows gel-like property (Farahnaky et al., 2010; Guo et al., 2009; Haque et al., 1993a; Yu et al., 2017). Therefore, MC and PSY show

different contributions to the elastic and viscous moduli of the doughs at different frequencies. Interestingly, MC*PSY had a negative coefficient in the model of lgG' vs lgω, which indicates a negative contribution. It might be similar to the depletion effects on G' between two types of HPMC due to, possibly, water competition (Ronda et al., 2013).

Water addition level is shown to had negative effects on G'_{60}, G''_{60}, $G'_{1.29}$, $G''_{1.29}$, $\eta^*_{1.29}$, and η^*_{60} (insignificant influence on the slope of lgG' versus lgω). Increased water addition level also counteracts the positive effect of PSY on G' as well as the positive effect of both PSY and MC on G''. It is due to the dilution effect of water on flour and hydrocolloids (Mancebo et al., 2015; Ronda et al., 2013). Similar counteraction between water and β-glucan on G' was reported by Ronda et al. (2013). The differences between MC and PSY in the counteracting effect with water is possibly also due to their different contributions to the storage component and loss component, and different water binding abilities.

Relaxation frequency (ω_{rel}) was predicted based on the generalised Maxwell model and, as seen in Table 4.3, PSY is the only term having significant ($p < 0.0001$) effect on ω_{rel} with satisfactory fitting ($R^2 = 0.777$) where ω_{rel} was significantly decreased when PSY addition increased to 1 g/100g flour but lessed influenced with further additions. The relaxation of gluten free doughs in this study is of the order of 0.01 to 0.1 rad s^{-1} which is much higher than wheat doughs which have a relaxation frequency of the order of 10^{-4} rad s^{-1} (Lefebvre, 2006; Meerts, Cardinaels, Oosterlinck, Courtin & Moldenaers, 2017). It suggests that gluten free doughs are more fluid like at the deformation rates during proving compared to wheat doughs. The relaxation frequency is also higher than the

strain rate during proving which indicates that the doughs behave like fluids during proving. However, the deformation rate can be influenced by the relaxation time, in addition to the stress caused by the generation of CO_2. It is worth to conduct further experiment to study the correlations between relaxation time and deformation rate during proving.

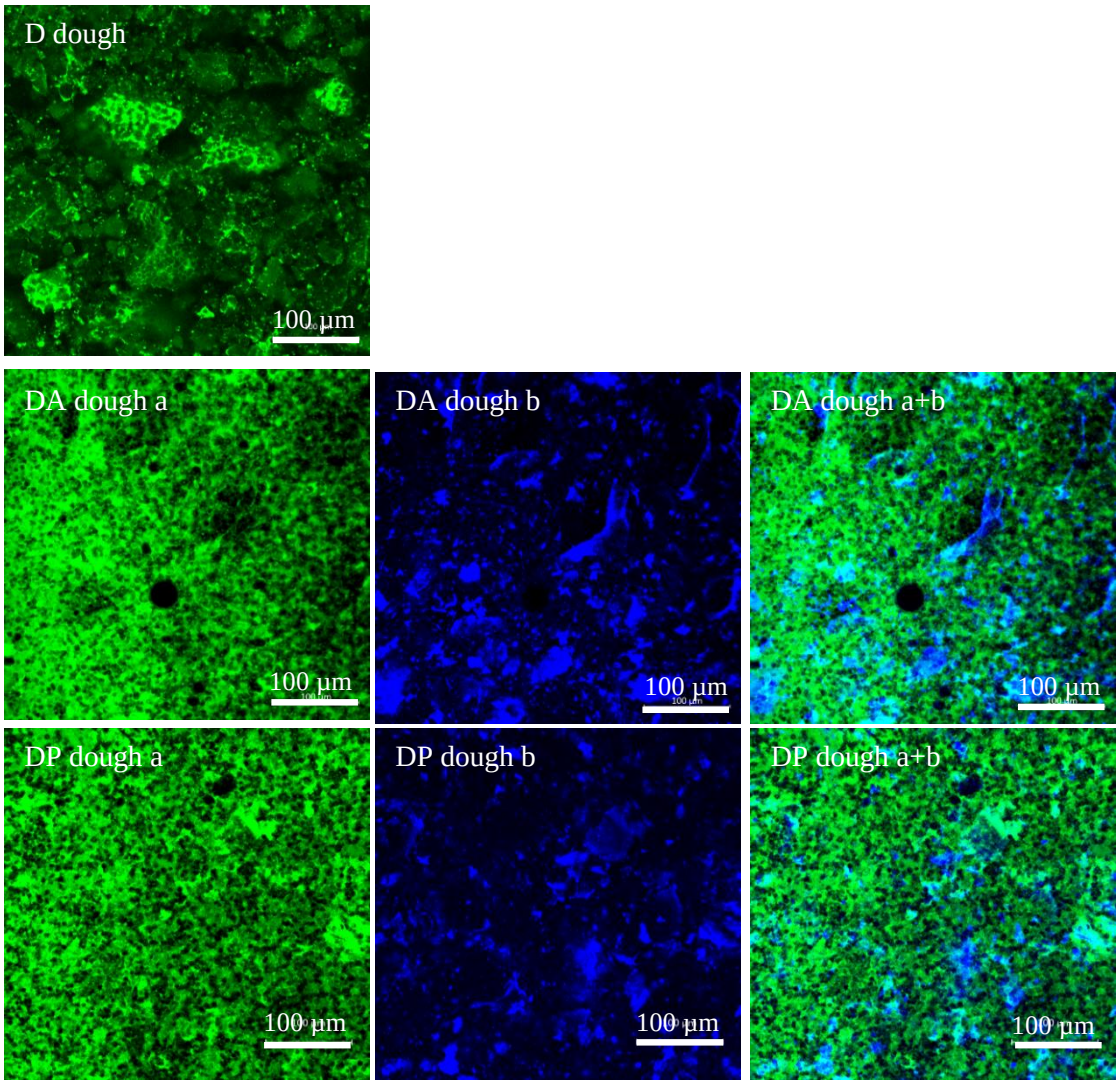

Figure 4.2. Gluten free doughs made by 100g rice flour + 120g water (D dough), 100g rice flour + 120g water + 2g MC (DA dough), or 100g rice flour + 120g water + 2g PSY (DP dough). Rice flour was stained by FITC and shown in green. MC and PSY were stained by calcofluor white and shown in blue. For the doughs with MC or psyllium, two channels (a and b) and overlaid images (a+b) are shown.

4.3.2.2. Empirical rheological analysis of dough properties

Large deformation rheological properties of gluten free doughs were tested by backward extrusion experiments and the dough stickiness was measured by a SMS/Chen-Hoseney Dough Stickiness rig. The coefficients in regression models for dough firmness, extensibility, and work of adhesion are listed in Table 4.3. The influences on dough firmness (Table 4.3) and consistency (data not shown) are generally consistent with the influences on the fundamental rheological parameters in that 1) water had negative effects while MC and PSY had positive effects, which can be counteracted by water addition at higher water addition levels, 2) the interaction MC*PSY had a negative contribution. As expected, water dilutes the dough system leading to softer doughs while hydrocolloid addition at low moisture content, which restrains their functionalities, increased dough rigidity. The contributions of different model terms on the different aspects of dough rheological properties (such as G', G'', and lgG' vs lgω) can be differentiated in the fundamental rheological measurements. However, all single, interacting, and quadratic model terms contribute to dough firmness and consistency by empirical measurements. The interacting effect by MC*PSY did not influence dough cohesiveness and index of viscosity (data not shown).

On the other hand, the term coefficients of all three individual factors and the interaction MC*PSY were negative in the model equation for dough extensibility which indicates that they have negative contributions to extensibility. The extensibility can only be increased by the interacting effects of water*MC or water*PSY, and water*MC was more influential than water*PSY seen as a higher term coefficient. The terms MC^2 and PSY^2 indicate the influence of MC and PSY is quadratic. Within the current range of water addition levels in this study, MC generally contribute to the increase of

extensibility and work of adhesion while the contribution of PSY is influenced by water addition levels. More specifically, when the water addition level was 110g, the extensibility increased from 35 mm to 60 mm with the increase of MC from 0 to 2 g while PSY had less influence on extensibility which decreased to 30 mm when 2 g PSY was added. At a higher water addition level (130 g), the influence of hydrocolloids became more significant. When the addition levels of MC or PSY increased from 0 to 2 g, extensibility increased from 12 mm to 60 mm or 29 mm, respectively. Extensibility was significantly decreased by water addition when neither MC nor PSY was added. These are similar to the parameters in the model for the work of adhesion. High extensibility and work of adhesion describe a homogeneous and smooth dough with high consistency which has good performance in extensional flow. It suggests that the high extensibility and work of adhesion are achieved by concurrently increased additions of water and hydrocolloids.

4.3.3. Pasting properties of flour blends

Pasting properties measured by RVA describe gelatinisation and retrogradation of starch and flour. A typical pasting curve of rice flour (run 11) is shown in Figure 4.3a. In addition, run 15, run 4, and run 16 containing different amount of MC and/or PSY showed lower pasting temperatures which appear as a shoulder or small peak (peak 1). Interestingly, an additional peak (peak 3) was observed on the viscosity profiles of PSY-containing samples. The viscosity profiles of run 15, run 13, run 2 and run 9 are shown in Figure 4.3b, which contain flour, MC, and different amount of PSY. As the PSY content increased, peak 3 became more pronounced which indicates that peak 3 is caused by PSY addition and it increases with the PSY addition level increase. Due to the existence of the extra peak compared to the classic analysis, extra parameters were

applied to describe the pasting properties of gluten free flour blends which are peak 2, peak 3, though 1, trough 2, though total, breakdown, final viscosity, setback, peak 2 time, peak 3 time, peak 2 temp, peak 3 temp, and pasting temp.

The model equation (Table 4.3) for pasting temperature indicates that both PSY and MC reduce pasting temperature of the hydrocolloid/flour blends in the tested range. The higher coefficient of MC indicates that the influence of MC is more significant than PSY. In the tested range, the pasting temperature was reduced by 20 °C or 10 °C from 90 °C when the addition level of MC or PSY increased from 0 to 2 g/100g flour, respectively. It has been concluded that the reduction of pasting temperature is common for most starch-hydrocolloid mixtures including the mixtures of MC and wheat flour and mixtures of MC and maize starch (BeMiller, 2011; Naruenartwongsakul, Chinnan, Bhumiratana & Yoovidhya, 2004; Sullo & Foster, 2010). The viscosity increasing effect of MC allows the detection of earlier granule swelling (Blanshard, 1987). Sullo and Foster (2010) suggest that the recording of lower pasting temperature might due to the viscosity increase caused by the thermal gelation of MC which occurs at a lower temperature than the significant swelling of starch granules, which enhance starch granule interactions by increasing starch concentration. Naruenartwongsakul et al. (2004) suggested that the concentration increase of starch is due to water competition with MC. Therefore, it can be concluded that the decreased pasting temperature is the result of water and volume competition between starch and hydrocolloid. This could also be the reason for the influence of PSY on the reduction of pasting temperature. It is worth to mention that pasting temperature is identified when the increasing rate of viscosity reaches a predefined value. A low value might lead to significantly different pasting temperatures. However, the interaction MC*PSY has a positive term coefficient

which indicates that the increase of addition level of one hydrocolloid negates the effect of the other hydrocolloid on pasting temperature. The reason might be the same as the negative contribution to lgG' vs lgω slope as mentioned in the previous section that water competition between MC and PSY lead to depletion between them.

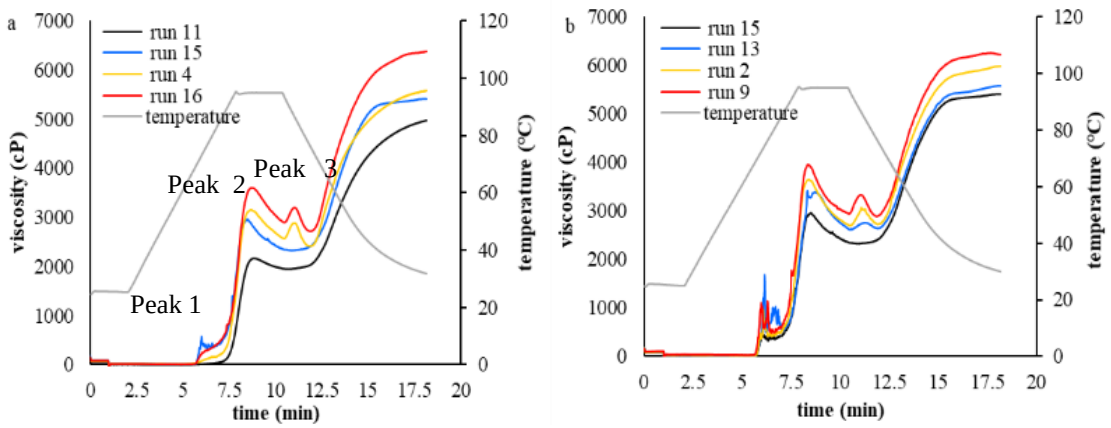

Figure 4.3. Pasting profiles of flour blends. The flour/hydrocolloids ratios are shown in Table 4.1 i.e. run 11 contains rice flour only; run 15 contains 2.5g flour and 0.05g MC; run 4 contains 2.5g flour and 0.05g PSY; run 16 contains 2.5g flour, 0.0375g MC and 0.05g PSY; run 13 contains 2.5g flour, 0.05g MC and 0.0125g PSY; run 2 contains 2.5 g flour, 0.05g MC and 0.025g PSY; run 9 contains 2.5g flour, 0.05g MC and 0.0375g PSY.

As for the main viscosity peak (peak 2), MC positively contributes to this response and increased it from 2200 cP to 2860 cP. The effect of PSY on peak 2 is more pronounced than MC. It shows a quadratic influence on peak 2 where peak 2 increased from 2200 cP to 3150 cP when PSY increased from 0 to 1.5g/100g flour while peak 2 was increased to a lesser extent by the further addition of PSY. Similar contributions of MC and psyllium to trough (data not shown) were also observed. There is no interacting effect of MC*PSY on the responses at high temperatures. MC gels at high temperature, which forms gel particles under the shearing conditions in RVA and significantly increase the viscosity (Sullo & Foster, 2010). PSY melts at high temperature (Chapter 2), hence it would be expected to be less influential on viscosity which is contrary to

what is observed. Norton, Foster and Brown (1998) and Norton, Jarvis and Foster (1999) illustrated the formation of fluid gels taking agar as the example which gels during cooling. The fluid gels are prepared by cooling agar with shearing which starts with the formation of gel nuclei, which grow in size and induce the increase of viscosity. Below a certain temperature, the amount of the particle forming nuclei ends and further molecular ordering occurs within the formed particles accompanied by reinforcement of the particles. The particles are hairy due to the disordered chains, which become smoother due to further molecular ordering which is accompanied by a decrease in viscosity. As PSY restructures during cooling and self-association has been observed as discussed in Chapter 3 and in (Yu, Yakubov, Martínez-Sanz, Gilbert & Stokes, 2018). It might undergo similar process as the formation of fluid gel with shearing in the RVA conditions. Being different from conventional gelling polysaccharides, the melting and restructuring of PSY is a continuous process as no peak is identified on DSC traces (Chapter 2) and (Guo et al., 2009). Haque et al. (1993a) showed that PSY gel does not fully melt up to 91 °C where weak interactions between molecules recover slowly (Chapter 2). Therefore, in the shearing field at the high temperature corresponding to the temperature range from peak 2 to trough, PSY associates and forms hairy weak gel particles, which interact with other particles or breakdown into smaller fragments. Therefore, PSY contributes more to viscosity than MC, which forms elastic, stable, and smooth particles. The quadratic contribution of PSY might due to more extensive self-association when the concentration increases which does not sufficiently contribute to the viscosity.

The unique peak 3 due to PSY occurs at approximately 85 °C in a similar temperature range to the trough. It is suggested that peak 3 is attributed to the formation of complex

with amylose as PSY becomes compatible with the interaction with amylose at this temperature (James M. Cowley, personal communication). It is also possibly due to the formation of hairy PSY gel particles, reinforcement of the these particles by interior structuring, and interactions between the hairy particles which contribute to the increase of viscosity, and superficial ordering of the hairy particles which causes decrease of viscosity. Hence, a balance between formation of weak PSY gel particles, PSY particle interactions, PSY particle breakdown, and interaction with amylose is critical deciding the pasting behaviour at this temperature range.

According to the model in Table 4.3, the addition of MC in the tested range (from 0 to 2 g) increased the breakdown, which describes the loss of integrity of starch granules, by 268 cP from 215cP, and PSY increased it by 535 cP. This phenomenon has been interpreted as a result of the viscosity increase by hydrocolloid addition which leads to an increase of shear force exerted on starch granules (Christianson, 1981; Naruenartwongsakul et al., 2004). However, it can also reflect the viscosity changes of hydrocolloids. As discussed above, in the temperature range from peak 2 to trough, PSY possibily undergoes changes from softer but hairy particles, which interact with each other, to rigid but and smooth particles with less interaction, as well as possible temporary interaction with amylose. These phenomena contribute to the more significant increase of breakdown value. High value of breakdown is observed when the PSY addition is higher than 1.5 g/100g flour which is correlated to its influence on peak 2.

4.3.4. Bread qualities

Specific volume is one of the most important parameters describing bread quality. As shown in Table 4.3, MC had the most significant ($p < 0.0001$) positive contribution to the specific volume. It doubled specific volume when its addition level increased from 0 to 2 g. As shown in Figure 4.4, column b, MC appears more continuous which is similar to gluten, at least in terms of microstructural distribution. The similarity in structure might suggest a similarity in functionalities between MC and gluten. A continuous phase apart from the starch matrix might be beneficial to a higher loaf volume. However, PSY is slightly detrimental to specific volume. The detrimental effect of PSY on specific volume was also confirmed by Mancebo et al. (2015). The interaction water*MC also has a negative contribution to the specific volume. This is contrary to what has been reported by others where a higher water addition level contributes to a higher specific volume (Gallagher, Gormley & Arendt, 2003; McCarthy et al., 2005). Hence, the influences of hydrocolloid and water on loaf volume can be complicated. The contrary observation in this study might due to different water absorbabilities of ingredients and, in a certain addition range, water might over dilute the doughs which lead to lower stability, poorer gas trapping ability, and lower loaf volume. Therefore, lower specific volume is observed. Baking loss could be correlated to specific volume, as the calculations of both responses include loaf weight. MC had the most significant ($p < 0.0001$) negative influence on baking loss (from 0.17 to 0.22) while PSY was less influential, which is because MC gels and has higher water binding ability than PSY which melts at baking temperature. The influence of PSY on baking loss is further reduced with high MC additions which is possibly due to their depletion effect.

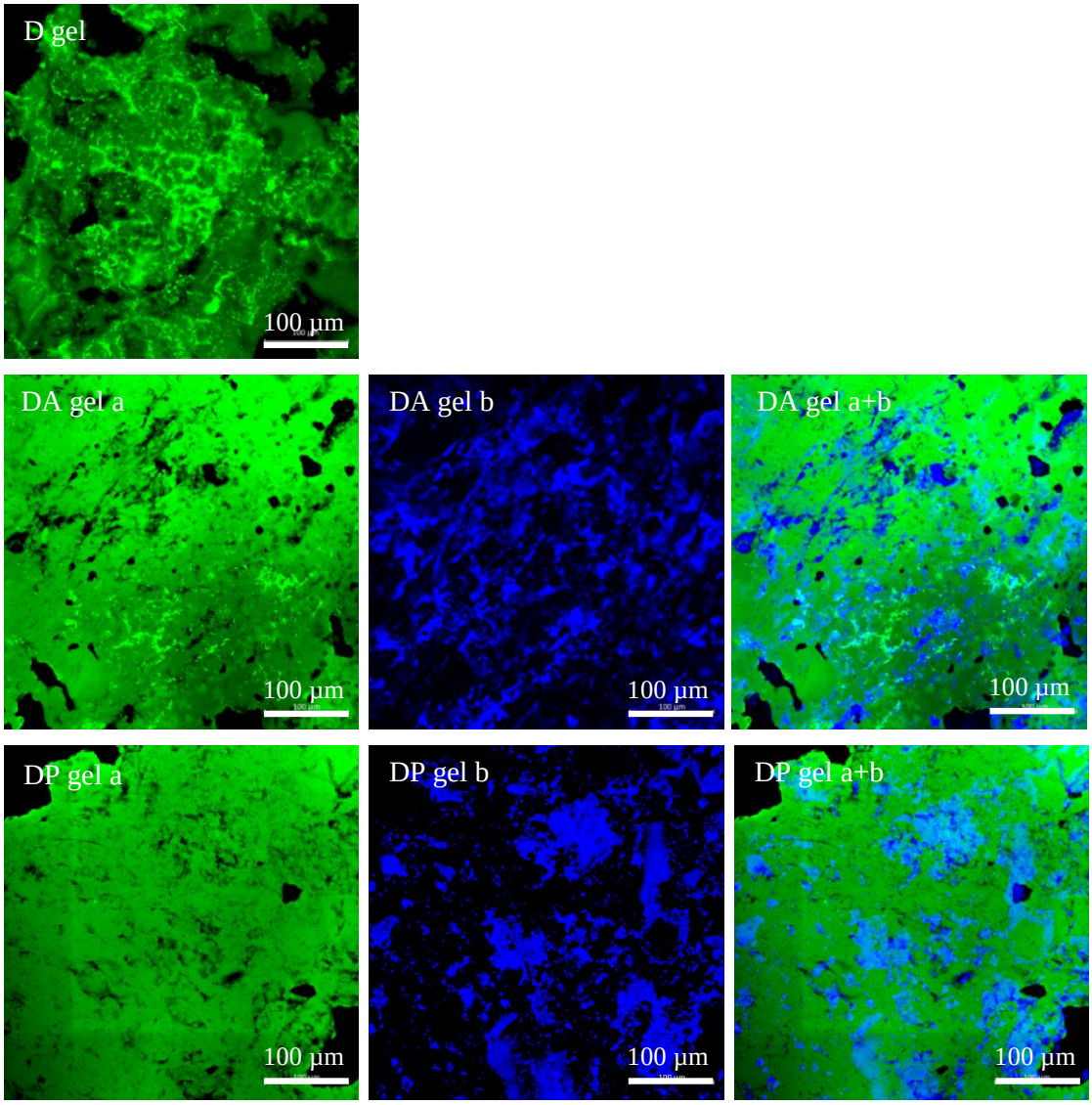

Figure 4.4. Cooked gluten free gels made by 100g rice flour + 120g water (D gel), 100g rice flour + 120g water + 2g MC (DA gel), or 100g rice flour + 120g water + 2g PSY (DP gel). Rice flour was stained by FITC and shown in green. MC and PSY were stained by calcofluor white and shown in blue. For the doughs with MC or psyllium, two channels (a and b) and overlaid images (a+b) are shown.

However, volume increase may also be accompanied by large voids in the crumb structure. It can be seen that MC and MC^2 have the most significant influence on the area of voids ($p < 0.0001$) and, according to the model equation, the minimum area of voids can be obtained when the addition level of MC is 0.6 g/100g flour. The area of voids significantly increased by 30 fold with the further increase of the MC addition up

to 2 g/100g flour. The existence of voids in gluten free bread has been also observed by Haque and Morris (1994), McCarthy et al. (2005) and Nishita et al. (1976). Nishita et al. (1976) suggested that this is due to excessive water addition which leads to overexpansion during baking. McCarthy et al. (2005) suggested that a soft consistent dough, with a relatively high amount of water and a limited amount of hydrocolloid, is preferable to promote volume increase while exceeding the limits leads to dough instability and voids in the crumb structure. However, the interacting influences of hydrocolloids and water on the area of voids can be complicated.

Overexpansion and dough instability might explain the formation of voids in the loaves made with high water and hydrocolloid contents. Water addition reduces dough viscosity and increases flowability, which allows expansion during proving and baking. When hydrocolloids are present, a homogeneous, smooth and viscous dough is generated with a stability, which promotes gas trapping. The combined effect allows the increase in loaf volume. However, a further higher water content decreases dough stability. High water content dilutes the flour or starch content which leads to weaker walls of gas cells and promotes coalescence especially during proving and early stage of baking. A similar statement has also been proposed by McCarthy et al. (2005). Starch gelatinisation is one of the dominant transitions in the formation of bread crumb structure (Zhou & Therdthai, 2007). Therefore, dilution of starch also leads to weaker crumb structure. In addition, the efficiency of MC stabilizing gas cells during baking might also be questioned. The thermal gel of MC at a higher temperature than 50 to 60 °C provides further stability and strengthens a system. Bousquières, Michon and Bonazzi (2017) reported an optimised gelation temperature of the mixture of HPMC and MC for a homogeneous structure of starch sponge cake. However, water content is

limited in the formulation of bread and significant water competition between flour, PSY and MC leads to a high concentration of MC. Therefore, the mobility of MC molecules might be reduced which restrains them from forming junction zones and inhibits the thermal gelation process.

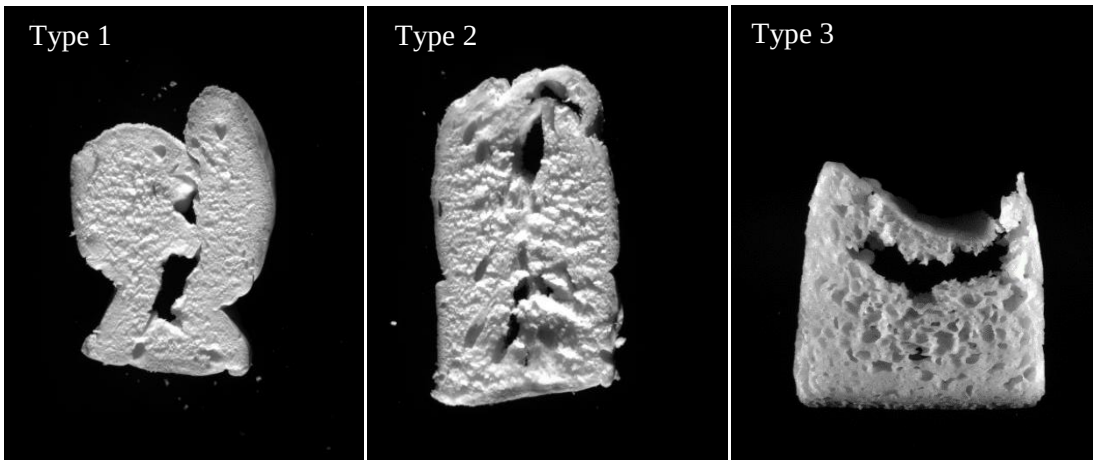

Figure 4.5. Three type of holes in the crumb of gluten free bread formulated with rice flour and hydrocolloids.

On the other hand, formulations with lower water content and higher hydrocolloid contents lead to high viscosity of doughs and air pockets can be trapped during dough mixing and loading into the pans. The size of voids might then be promoted by Ostwald ripening or further coalescence of small gas cells. Based on their appearance and formation reasons, the voids can be classified into three types (Figure 4.5). Two types of voids have smooth inner surfaces and the other has coarse surface. Type 1 with smooth surface might be caused by air trapped during mixing. Type 2 with a smooth surface was formed with excessive water addition. It is characterised by moving traces of gas cells which can, sometimes, form cluster of smooth tunnels. The formation of type 1 and type 2 can include Ostwald ripening and coalescence of gas cells during proving and early stage of baking before starch gelatinisation. Type 1 voids are

sometimes big and impermeable leading to shrinkage after baking which is also reported by Purna, Miller, Seib, Graybosch and Shi (2011). Type 3 voids have a coarse inner surface. The possible reason of this is high pressure during baking after starch gelatinisation is finished and sponge crumb structure is formed, which rips the porous structure.

Another parameter representing dough and crumb instability is top concavity, which is caused by collapse during proving or early stage of baking. MC, MC*PSY and MC^2 are the most significant terms with $p < 0.0001$, followed by water*PSY and PSY with $p < 0.01$. According to the model equation, the addition of hydrocolloids, especially MC, increase dough and crumb stability and reduce top concavity.

Textural properties of crumb structure are another type of descriptive parameter of bread quality. According to preliminary tests, the gas cells can occupy up to 60% of the loaf volume. Therefore, the loaves were compressed by 65% of their original height in TPA so the property of bulk crumb was also recorded in addition to the properties of the walls of gas cells. In addition, a higher strain mimics the oral process. As listed in Table 4.3, the single terms, water and MC, had negative effects on the crumb hardness but PSY had positive effects. The interaction terms: water*MC and MC*PSY, and their corresponding term coefficients indicate that the addition of MC reduces the dependence of hardness on water and PSY addition levels. According to the model, When MC was not added, PSY significantly increased the crumb hardness from 1500g to 3000g by a factor of 2 with 110g of water and from 750g to 2300g with 130g of water. This crumb hardening effect of PSY is in agreement with Mancebo et al. (2015). Hardness decreased from 1500 g to 700 g with the water addition increased from 110 g to 130 g. However, when 2g of MC was incorporated, the variation of water and PSY

only caused 500g difference in hardness. The reinforcement effects of PSY and dilution effect of water influence the strength of the crumb cell walls and, therefore, contribute to their positive and negative effect on hardness, respectively. Additionally, as shown in Figure 4.4, PSY exists as discrete particles in the cooked flour/hydrocolloid gels. Combining with the rheological property of PSY, i.e. weak gel (Haque & Morris, 1994), PSY can be expected to increase the strength of starch gels which compose the gas cell walls and, hence, increase the hardness of bread crumb. Their contributions to hardness are contrary to their contributions to specific volume, as a denser crumb is harder (McCarthy et al., 2005). The addition of MC significantly increases specific volume and reduced crumb density and hardness. Therefore, the influence of the strength of gas cell walls is diminished.

Table 4.3. Coefficients of model terms for response surfaces

	G'_{60}	G''_{60}	$G'_{1.29}$	$G''_{1.29}$	lgG' vs lgw	w_{rel}	dough firmness
constant	300654	41254	187922	32494	0.029	0.100	6638
water	-4897 [a]	-684 [a]	-3063 [a]	-542 [a]			-111 [a]
MC	2583 [a]	3996 [a]	993 [a]	2341 [a]	0.075 [a]		500 [a]
PSY	28826 [a]	5480 [a]	19574 [a]	3435 [a]	0.040 [e]	-0.144 [a]	1055 [a]
water * MC		-30.26 [a]		-16.54 [c]			-4.12 [a]
water * PSY	-205 [a]	-38.61 [a]	-141 [a]	-24.47 [a]			-7.78 [a]
MC * PSY					-0.030 [b]		-22.89 [c]
$Water^2$	19.85 [c]	2.83 [c]	12.45 [b]	2.25 [c]			0.460 [a]
MC^2		419 [a]					60.47 [a]
PSY^2						0.052	57.53 [a]
R^2	0.972	0.993	0.972	0.978	0.900	0.777	0.998

[a] $p < 0.0001$
[b] $p < 0.001$
[c] $p < 0.01$
[d] $p < 0.05$
[e] $p > 0.05$

Table 4.3. continued

	dough extensibility	work of adhesion	Pasting Temp	peak 2	Breakdown	specific volume	baking loss
constant	161	36.08	89.73	2133	215	0.754	0.137
water	-1.15 [e]	-0.247 [e]				0.010 [e]	0.001 [d]
MC	-44.68 [a]	-3.57 [a]	-20.80 [a]	167 [a]	134 [a]	3.211 [a]	-0.040 [a]
PSY	-48.64 [e]	-20.90 [e]	-9.13 [a]	1145 [a]	648 [a]	-0.152 [d]	-0.021 [c]
water * MC	0.650 [a]	0.087 [d]				-0.020 [d]	
water * PSY	0.527 [a]	0.196 [a]					
MC * PSY	-2.59 [d]		3.18 [a]				0.011 [c]
$Water^2$							
MC^2	-7.55 [a]	-2.12 [b]	5.35 [a]	97.85 [c]			0.023 [a]
PSY^2	-5.82 [b]	-1.40 [c]	1.89 [c]	-309 [a]	-195 [a]		
R^2	0.988	0.944	0.983	0.989	0.949	0.946	0.904

Table 4.3. continued

	Area of Voids	Top Concavity	hardness	Springiness	PC1	PC2	PC3
constant	2.33	28.64	8699	1.18	0.633	-0.248	15.62
water		-0.164 [e]	-62.07 [c]	-0.002 [c]	0.073 [a]	-0.034 [a]	-0.090 [b]
MC	-6.48 [a]	-10.55 [a]	-4229 [a]	-0.719 [a]	-10.02 [a]	0.028 [a]	-14.17 [e]
PSY		-19.53 [c]	805 [d]		-4.97 [a]	27.33 [a]	-1.68 [e]
water * MC			27.76 [d]	0.007 [b]	0.060 [c]		
water * PSY		0.134 [c]				-0.180 [b]	
MC * PSY		2.52 [a]	-571 [b]			-1.99 [b]	1.71 [a]
$Water^2$							
MC^2	5.34 [a]	2.75 [a]	395 [d]	-0.139 [a]	-1.94 [a]		6.05 [a]
PSY^2					0.963 [c]		
R^2	0.880	0.951	0.906	0.911	0.995	0.958	0.946

As for springiness, MC has a quadratic influence on springiness and the addition level for the maximum springiness increased from 0.34 to 0.87 g/100g flour with the increase of water addition in the tested range (110 to 130g/100g flour). Surprisingly, the influence of PSY is insignificant. Higher springiness with PSY addition was observed

in our preliminary experiments based on another type of rice flour with larger particle size and lower amylose content, which was also reported by Haque and Morris (1994). It is likely that the influence of PSY on the springiness of gluten free bread is less significant than other factors or it is dependent on the properties of the flour/starch.

4.3.5. Simultaneous application of principal component analysis and response surface method

Response surface methodology has been applied to investigate the effects of different factors on gluten free doughs and bread, to optimise formulation and process (Collar, Andreu, Martinez & Armero, 1999; Marco & Rosell, 2008; McCarthy et al., 2005; O'Shea, Rossle, Arendt & Gallagher, 2015; Ronda et al., 2013; Sanchez, Osella & de la Torre, 2002). However, the number of responses that can be analysed is limited as they are analysed individually but the gluten free bread and doughs cannot be fully described by the limited amount of responses. Therefore, principal component analysis (PCA) is applied to the full data set of 20 runs with 74 responses to reduce the response dimensions.

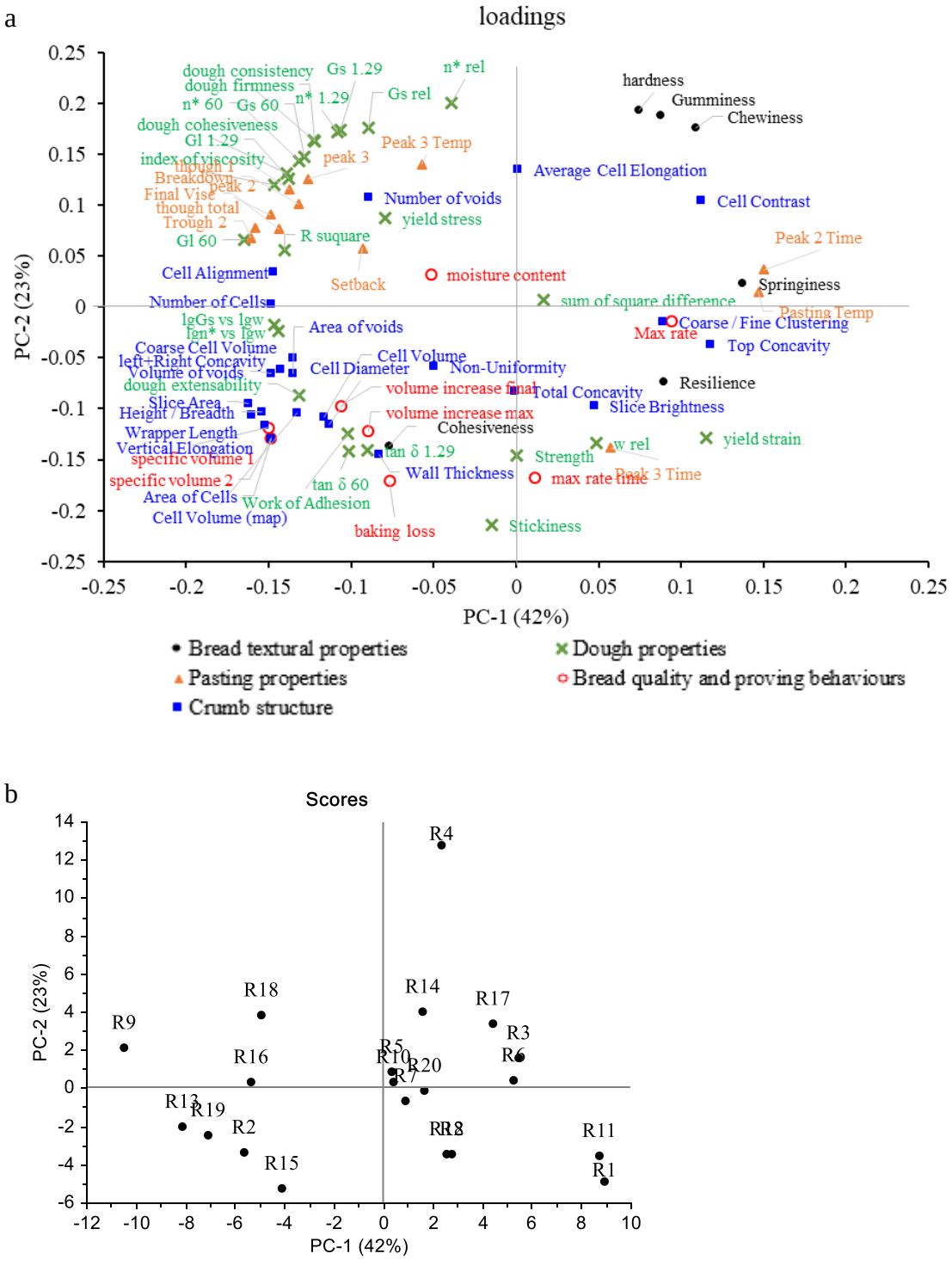

Figure 4.6 Loading plot (a) of the 74 responses (full data set) and the score plot (b) of the 20 runs

However, a large data dimension (74) versus a small sample size (20) is usually considered undesirable in PCA. To verify the validity of the full PCA (Figure 4.6), the data from each set of experiments were analysed by smaller prior PCA to identify the main driving responses in each data set (Figure 4.7) and then the main driving responses were chosen and analysed by a subsequent PCA (Figure 4.8) which was compared to the full PCA. The loading plot of the first data set of bread textural properties measured by TPA is shown in Figure 4.7a. It can be seen that the first principal component (PC1) explains 64% of the total variation. Cohesiveness is negatively correlated to PC1 but hardness, gumminess, and chewiness are positively correlated to PC1. PC2 explaining 31% of the total variation is mainly loaded by springiness, resilience and hardness. In addition, hardness, springiness, and cohesiveness are directly calculated from the raw data from the TPA curves, nevertheless, chewiness and gumminess are calculated based the other three parameters; hence, hardness, springiness, and cohesiveness are included in the subsequent PCA. Similarly, the prior PCAs were apply to data sets of dough properties, pasting properties, bread quality and proving behaviours, and crumb structure (Figure 4.7b, c, d, e). Yield strain, tanδ 60, η^*_{rel}, G'_{60}, dough firmness, dough extensibility, pasting temp, peak 3 time, peak 2, specific volume, moisture content, max rate, max rate time (proving), cell contrast, area of void, top concavity, and number of cells are used in the subsequent PCA and the loading plot and score plot are shown in figure 4.8.

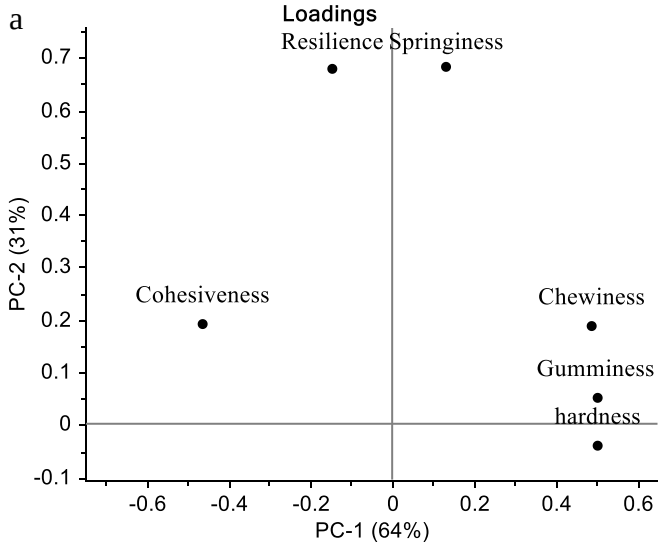
a
Loadings
Resilience Springiness
Cohesiveness
Chewiness
Gumminess
hardness
PC-2 (31%)
PC-1 (64%)

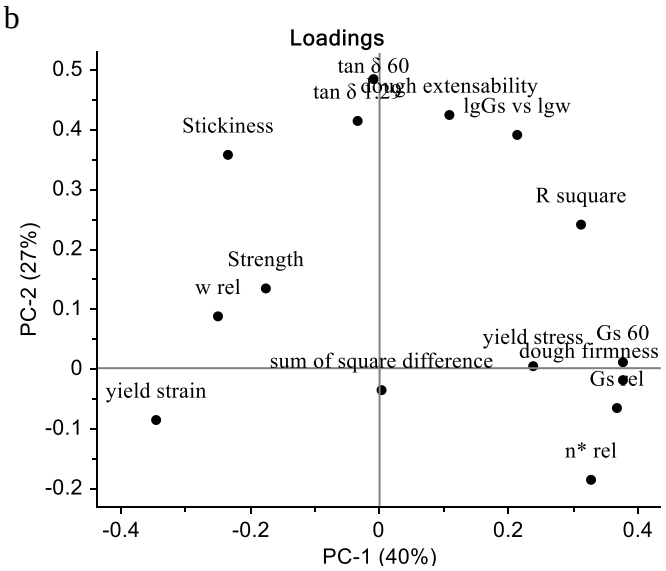
b
Loadings
tan δ 60
lgGs vs lgw
Stickiness
R suquare
Strength
w rel
yield stress
Gs 60
dough firmness
sum of square difference
Gs rel
yield strain
n* rel
PC-2 (27%)
PC-1 (40%)

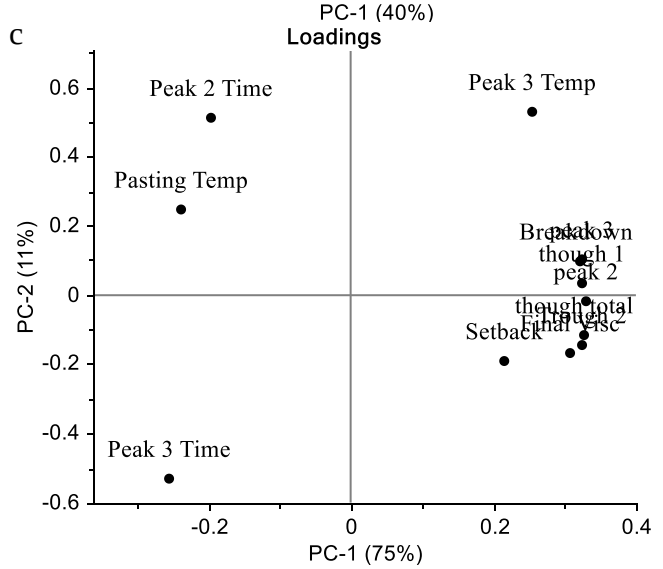
c
Loadings
Peak 2 Time
Peak 3 Temp
Pasting Temp
peak 2
Setback
Peak 3 Time
PC-2 (11%)
PC-1 (75%)

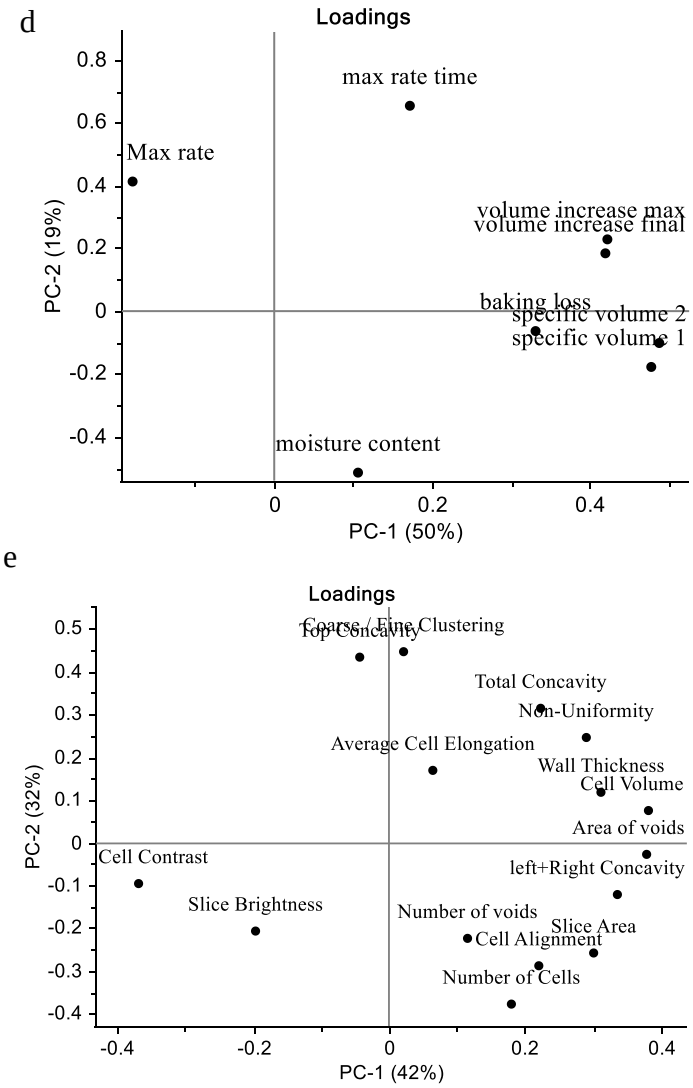

Figure 4.7. Loading plots of data sets of bread textural properties (a), dough properties (b), pasting properties (c), bread quality and proving behaviours (d), and crumb structure (e).

a

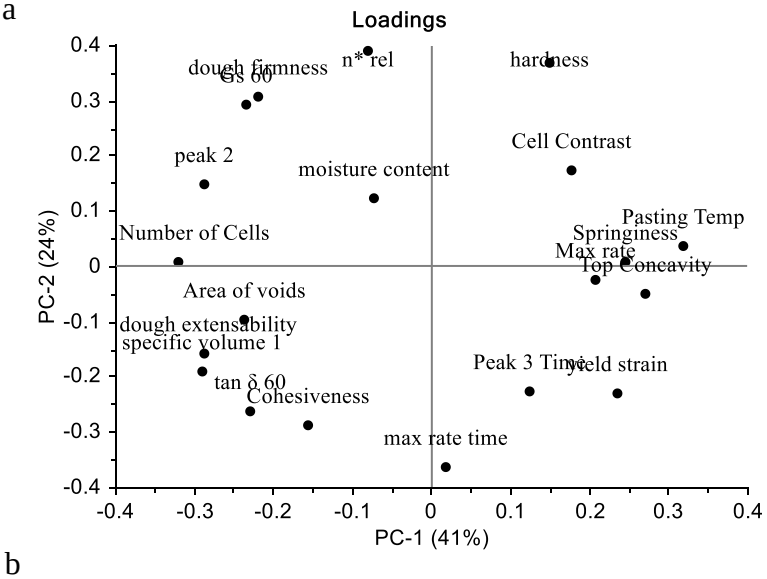

b

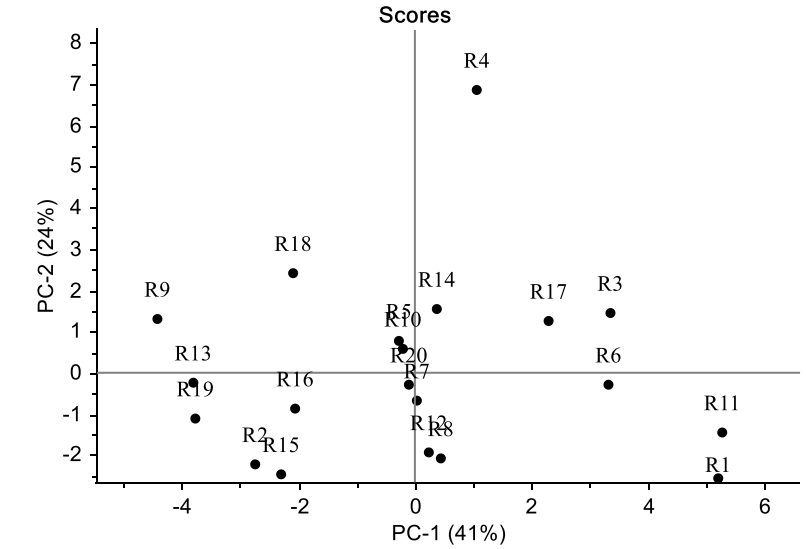

Figure 4.8. Loading plot (a) of the chosen responses selected based on Figure 4.7 and the score plot (b) of the 20 runs based on the chosen variables.

Comparing Figure 4.8 to figure 4.6, the positions of the 20 runs and the chosen variables in the mappings of the subsequent PCA and the total PCA are similar. Therefore, the reduction of the response dimensions is performed by the total PCA. Figure 4.6 shows the loadings of the original 74 responses and the scores of 20 runs. The first 3 components dominate with the eigenvalues of 31.53, 17.15, and 9.22 representing 41.5%, 22.6% and 12.1% of the variance in the data set.

As shown in Figure 4.6a, the specific volume is positively correlated with proofed loaf volume and it is closer to the final proving volume (volume increase final) instead of the maximum volume (volume increase max), which suggests that the final volume after proving is more critical in deciding the baked loaf volume. As listed in Table 4.3, the addition level of MC significantly influences the final volume increase. Therefore, the final volume increase and specific volume can be optimised by modifying proving conditions and formulation, especially MC addition level. As expected, loaf specific volume is clustered with parameters describing the size of bread slices measured by C Cell. It is also correlated to the volume of voids which is discussed in the analysis of individual responses in RSD. Specific volume is negatively related to springiness, hardness, chewiness, and gumminess. A similar relationship was also reported by Gallagher et al. (2003). Generally, a smaller loaf will have a hard crumb texture with a dense and tightly packed crumb structure (Scanlon & Zghal, 2001). This can also be explained by the dilution effect of water on flour/starch.

As for the relationship between specific volume and dough rheological properties, specific volume is closely and positively correlated with extensibility followed by work of adhesion, measured by empirical rheological tests, which are predominantly increased by hydrocolloid addition, especially MC, and water addition as discussed in 4.3.2.2. The dough with high extensibility and work of adhesion is expected to be homogeneous and smooth which has good performance in extensional flow. These two responses can describe the dough property in the development of the foam structure. The gas cell wall undergoes extensional flow during gas cell growing. Low extensibility and work of adhesion suggest that the doughs are rigid which prohibit the growth of gas cells. High extensibility and work of adhesion indicate that the gas cell walls allow the

expansion of gas cells and be able to trap gas to a certain degree, which increases specific volume. Loaves with high specific volume have less dense crumb and cell walls are further weakened due to dilution effect of water; therefore, they are softer and less springy as discussed above. However, the flowability of gas cell walls introduces instability and the failure of the walls is accompanied by coalescence of gas cells, which lead to voids in crumb as discussed in section 3.4. Therefore, these responses are good indicators of specific volume, crumb structure, and textural properties.

However, other empirical rheological parameters and moduli measured by fundamental rheological tests, especially storage moduli, are distributed more perpendicularly to specific volume in Figure 4.6a indicating less significant correlations. The angle between specific volume and loss moduli, especially G'', at the high frequency is smaller suggesting a closer positive correlation. Small amplitude oscillatory measurements can be viewed as being inappropriate in the evaluation of application and processing scenarios where the increase of loaf volume is important, as the deformation rate scales and experiment conditions do not simulate the conditions of dough making and baking (Mariotti et al., 2009). However, close negative correlation between viscoelastic parameters (G' and G'') and rice bread hardness was reported by Demirkesen, Mert, Sumnu and Sahin (2010a). Gluten is the 'structural' protein in bread which shows cohesive, elastic and viscous properties and grants extensibility and gas holding property (Gallagher et al., 2004). In wheat bread doughs, rheological properties are less influential than surface tension at the early stage of proving but they stabilise the foam structure of doughs by preventing rising of gas cells (Mills, Wilde, Salt & Skeggs, 2003). However, rheology is likely to play a different role in gluten free bread and doughs. High values of moduli and low tanδ (solid like property) indicate better

stability but inhibit loaf rising during proving while low moduli or a more fluid like property allow doughs to flow and expand during proving and early baking but might lack the ability to stabilise gas cells. In conclusion, although both empirical and fundamental dough rheological tests can provide certain information, the experiments characterising the flow behaviour is more descriptive and directly related to baking performance and quality of gluten free bread.

It can be seen in Figure 4.6a that most fundamental rheological parameters are close to dough firmness, cohesiveness, and consistency. Similar correlations were reported by Ronda et al. (2013) although the geometry for empirical measurement was different. Therefore, the firmness or strength of gluten free doughs can be described by both empirical large deformation tests or small deformation fundamental tests. These parameters are negatively correlated with top concavity. As described in section 4.3.3 and 4.3.5, the additions of MC and PSY increase moduli and dough firmness which suggest better dough stability and gas holding ability. Therefore, top concavity can be reduced and prevented by a firmer dough property. As expected, relaxation frequency predicted by the generalised Maxwell model is closely correlated with peak 3, because that both responses are singly influenced by PSY addition. Although relaxation frequency is neither correlated to specific volume nor springiness and hardness, it is related with dough strength/cohesiveness and max rate time during proving. It suggests that relaxation frequency has a significant effect on proving behaviour during which the porous structure is formed.

Generally, as shown in Figure 4.6a, some parameters characterising bread qualities and pasting profiles have high loadings on PC1 while most dough rheological parameters and few other bread quality parameters have high loadings on PC2. PC3 is mainly

loaded by some bread quality parameters, empirical (large deformation) dough rheological parameters, and volume increases during proving. These first three principal components were extracted as new responses and the scores of 20 runs are listed in Table 4.3 as new responses in RSD. All three factors (MC, PSY and water addition level) have significant effects on both PC1 and PC2 while only water significantly influenced PC3 ($p<0.0001$). The term water*MC in PC1 model suggests interaction effects of these two factors on gluten free bread. Hence, formula optimisation of gluten free bread requires deliberate and simultaneous consideration on the additions level of water and MC. The changes of water addition with different hydrocolloid addition can be achieved by experiences of the experimenter or a controlled viscosity or, say, consistency measured by different tests (Haque & Morris, 1994; Lazaridou et al., 2007; Nicolae, Radu & Belc, 2016). However, the dependence of water addition on hydrocolloid addition level can be influenced by water absorbability of the hydrocolloids. It is also noticed that MC and PSY have quadratic influences on PC1 but effects of water addition level are linear. As for PC2 which mainly represent dough rheological properties, it is more sensitive to single term PSY as seen by the high coefficient and sensitive to interaction effects of water*PSY and MC*PSY which indicates that the dough rheological properties are more sensitive to the incorporation of PSY and the variations of water and MC when PSY is added. In terms of PC3, water is the only factor having a significant contribution among three single terms (judged by 95% confidence) indicating that water is influential in determining the residual information on this component.

4.4. Conclusion

The study aimed at evaluating the influences of MC and PSY at different water addition levels on gluten free doughs and bread, and the correlations between dough rheological properties, baking behaviours and bread qualities. Simultaneous application of PCA and RSD was successful to reduce the size of response dimensions and evaluate the correlations between responses. Relaxation frequency of doughs, which was calculated by the generalised Maxwell model and is lower than wheat doughs, characterises proving behaviours and it suggests that gluten free doughs are fluid like at the deformation rate during proving. As expected, MC and PSY increase both moduli and firmness of doughs and overall viscosity of pasting profiles and PSY contribute more to storage moduli. The dilution effect of water leads to lower moduli and softer doughs. The additions of both MC and PSY decreased pasting temperature due to volume and water competition. The addition of PSY has more significant influence than MC on pasting viscosity at high temperature (from peak to trough) and leads to an extra peak on the pasting profiles, which might rely on a balance between formation and breakdown of PSY weak gel particles, PSY particle interactions, and interaction with amylose. MC and PSY tend to have depletion effects, which lead to counteracted contributions to frequency dependence of storage moduli, dough firmness, and pasting temperature. Dough extensibility and work of adhesion measured by empirical rheological measurements describe the flowability of doughs in extensional flow and they, especially extensibility, are evidenced to be sufficient predictors of bread qualities including specific volume, crumb structure, and texture. These two parameters can be increased by increasing water addition when hydrocolloids are added. Increasing MC and water additions contribute to dough extensibility more efficiently than PSY and

water. High extensibility allows doughs to easily increase in volume which is related to a high specific volume. A loaf with high specific volume is expected to have less dense crumb structure and softer texture. However, over addition of water dilutes hydrocolloids and flour, which leads to even higher flowability and reduced stability. Therefore, it could result in overexpansion during proving, coalescence of gas cells, and voids in crumb structure. Additionally, the dilution effect of water on starch in the crumb lead to thinner and weaker cell walls and, therefore, softer but weaker crumb. Other dough rheological parameters including small amplitude oscillatory tests, which are more sensitive to the formulation variations, provide indirect information such as dough stability and structure. Bread quality is significantly affected by the addition levels of MC and water while dough rheological properties can be sensitive to the addition of PSY. Combining PCA and RSD allows the analysis of a large amount of data which provides a relatively comprehensive characterisation of gluten free bread. Other parameters such as sensory evaluations could be involved in further investigations to provide a better understanding of gluten free bread.

Chapter 5.

Starch replacement in gluten free bread by cellulose and fibrillated cellulose

Highlights:

- Starch replacement by (fibrillated) cellulose in gluten free bread.
- The incorporation of (fibrillated) cellulose strengthened gluten free doughs.
- The generalised Maxwell model was applied to analyse dough rheology.
- The incorporation of (fibrillated) cellulose mainly influenced the later stage of proving.
- Volume and water competition dominates the thermal rheological behaviours.
- Loaves with (fibrillated) cellulose were smaller with a harder, denser but finer crumb.

Keywords:

Fibrillated cellulose, cellulose, gluten free bread, dough rheology, bread quality

Abstract

This study investigated starch reduction and replacement by purified cellulose (FC0) and fibrillated cellulose (FC60). The influences on the dough rheological and adhesive properties were evaluated by both fundamental and empirical measurements and the effects of heating and cooling were evaluated by Rapid Visco Analyser. Replacing flour with FC0 and FC60 was found to strength the doughs. The relaxation time calculated by the generalised Maxwell model was found to be shorter than the deformation rate during proving which suggests that the doughs behave like fluids during proving. The relaxation time was less influenced by the additions of FC0 and FC60. Although the initial stage of proving was less influenced, the later stage was significantly affected by the additions of FC0 and FC60 which increased dough rigidity and restrained the volume. The pasting properties were significantly influenced by competition for water between FC0/FC60 and flour. The bread qualities were characterised in terms of loaf volume and crumb properties. Loaves containing FC0 and FC60 had smaller specific volume, harder crumb, denser but finer crumb structures.

5.1. Introduction

Wheat flour is the main ingredient of bread, the staple food in many regions. However, many people around the world are intolerant or sensitive to gluten, which leads to coeliac disease and other gluten-trigged health problems (Catassi et al., 2012; Czaja-Bulsa, 2015; Sapone et al., 2012). In 2014, Aziz et al. (2014) conducted a survey in Sheffield, UK, and found that 13% of the population reported gluten sensitivity and the prevalence of diagnosed coeliac disease was 0.8%. An early study reported that the prevalence of coeliac disease in the world is approximately 1 in every 100 people (Zandonadi et al., 2009). Coeliac disease, the most widely studied gluten-triggered disease, is an autoimmune genetically determined chronic inflammatory intestinal disorder (Fasano & Catassi, 2001; Schuppan, 2000) which can be influenced by both genetic (intrinsic) and environmental (extrinsic) factors (Di Sabatino & Corazza, 2009; Schuppan, 2000; Wahab et al., 2002). On the other hand, 'free from' is becoming a global trend of a healthy lifestyle choice, which further promotes the market of gluten free products. The production and improvement of gluten free bread have been widely studied and the current methodologies can be categorised as the application of alternative flour blends, enzyme treatments and sourdough applications, and other treatments. The application of alternative flour blends is the most investigated which includes investigations on formulations (Haque & Morris, 1994; Lazaridou et al., 2007; Nishita et al., 1976; Ronda et al., 2013) and structured gel and colloids (van Riemsdijk, van der Goot, Hamer & Boom, 2011).

In addition, the proportion of overweight adults and children has increased around the world and obesity has become a global health challenge during the past three decades (Ng et al., 2014). The prevalence of obesity around the world is one of the main reasons for the increased morbidity rate of type-2 diabetes (Shaw et al., 2010). However, the removal of gluten from the diet easily lead to a significant decrease in carbohydrate oxidation rate, increase in body fat stores, and weight gain in coeliac patients (Capristo et al., 2000; Hager et al., 2012). Therefore, food containing low calories and/or glycaemic index is recommended and the production of gluten-free bread with low calorie content and glycaemic index will be beneficial to deal with gluten intolerance, obesity and type 2 diabetes simultaneously. The additions of dietary fibres or fibre enriched materials have been studied to improve the nutritional profiles of gluten free bread (Demirkesen, Mert, Sumnu & Sahin, 2010b; Djordjevic et al., 2019; Phimolsiripol, Mukprasirt & Schoenlechner, 2012). However, to our knowledge, the additions of pure cellulose and fibrillated cellulose have not been investigated.

Cellulose is one of the main components in the plant cell wall, which structures, with hemicellulose, pectin, and lignin, to maintain the mechanical property of cell walls. Microfibrillated cellulose (MFC) was firstly processed using high pressure and shearing by Herrick et al. (1983) and Turbak et al. (1983a), where the native cellulose fibres are physically unwound and highly entangled cellulose fibrils are generated with high surface area, liquid retention ability, and reactivity to chemical treatments. Currently, the applications of high pressure homogeniser and microfluidiser as mechanical cellulose fibrillation treatments

are widely investigated (López-Rubio et al., 2007; Nakagaito & Yano, 2004; Pääkkö et al., 2007; Stenstad et al., 2008; Zimmermann et al., 2004). In food productions, MFC can be used as a thickener, compound carriers, and suspension and emulsion stabilisers (Turbak et al., 1982, 1983b).

The aim of this Chapter was to investigate the starch/flour reduction of rice flour based gluten free bread by addition of cellulose and fibrillated cellulose. Both dough properties and bread qualities were of the interests of the current investigation.

5.2. Materials and methods

5.2.1. Materials

Materials for dough preparation are listed in section 4.2.1. Pure powdered cellulose (FC0), Solka floc 900FCC, was supplied by International Fiber Corporation, US (Chapter 3). Stock suspension of fibrillated cellulose (FC60) was prepared as described in section 3.2.2, which was then diluted to the required concentrations for dough preparations.

5.2.2. Dough formulation and preparation

The basic formulation (control) was decided according to preliminary tests and included 100 g of rice flour, 5 g of sugar, 2 g of salt, 1.5 g of yeast, 5 g of vegetable oil, 1 g of MC, 1 g of PSY, and 120 g of water. Rice flour was partially replaced with FC0 and/or FC60 as shown in Table 5.1. Apart from F(100) (control) and F(98)+FC60(2), all other FC0/FC60 incorporated formulas are expected to be claimed ‘high fibre’ according to Regulation (EC) No 1924/2006

based on a rough calculation that the fibre content is higher than 3 g per 100 kcal. Doughs preparation is the same as described in section 4.2.3. FC0 was directed mixed with other dry ingredients. FC60 was redispersed in water required in the formulation and added with oil into dry ingredients. Doughs prepared for rheological measurements did not contain yeast and were allowed for hydration at room temperature for 1 hour.

Table 5.1 Addition levels of rice flour, FC0, and FC60

Sample code	Rice flour	FC0	FC60
F(100) (control)	100	0	0
F(98)+FC60(2)	98	0	2
F(90)+FC0(10)	90	10	0
F(90)+FC0(8)+FC60(2)	90	8	2
F(80)+FC0(20)	80	20	0
F(80)+FC0(18)+FC60(2)	80	18	2
F(80)+FC0(16)+FC60(4)	80	16	4

5.2.3. Dough evaluation

5.2.3.1. Fundamental rheological measurements and thermal behaviour of doughs

The fundamental rheological measurements of doughs included controlled shear stress tests to obtain yield point or yield zone and frequency sweep tests where data were fitted into generalised Maxwell model. Details are described in section 4.2.4.1.

Additionally, temperature sweep tests were performed at a constant strain (0.02%) and frequency (10 rad s^{-1}) with the temperature increased from 20 °C to 98 °C with a heating rate of 2.6 °C min^{-1} mimicking the temperature profile during baking.

5.2.3.2. Empirical rheological measurements

Doughs were also characterised by backward extrusion tests and SMS/Chen-Hoseney Dough Stickiness tests as described in section 4.2.4.2.

5.2.4. Pasting properties of flour blends

The pasting properties of flour blends were measured by RVA. The solid levels of rice flour, MC, PSY, FC0, and FC60 are listed in Table 5.2, which were in the same ratio as in the dough formulation without sugar, salt, yeast, and oil. More specifically, flour, MC, PSY and FC0 were mixed thoroughly. Flour blends (2.55 g) prepared according to the formula which does not include FC60 were dispersed in 24 ml of RO water. As for FC60-containing formula, FC60 stock suspensions were diluted to 24.05 g or 24.1 g with FC60 concentration of 0.208% and 0.415% respectively for the formulations of 2% and 4% replacement by FC60. Flour blends (2.5 or 2.45 g respectively) were dispersed into diluted FC60 suspensions. The temperature profile is described in section 4.2.4.3.

Table 5.2. Addition levels of rice flour, MC, PSY, FC0, and FC60 in pasting property analysis.

Sample code	Rice flour	MC	PSY	FC0	total dry blends	FC60
F(100) (control)	2.5	0.025	0.025	0	2.55	0
F(98)+FC60(2)	2.45	0.025	0.025	0	2.5	0.05
F(90)+FC0(10)	2.25	0.025	0.025	0.25	2.55	0
F(90)+FC0(8)+FC60(2)	2.25	0.025	0.025	0.2	2.5	0.05
F(80)+FC0(20)	2	0.025	0.025	0.5	2.55	0
F(80)+FC0(18)+FC60(2)	2	0.025	0.025	0.45	2.5	0.05
F(80)+FC0(16)+FC60(4)	2	0.025	0.025	0.4	2.45	0.1

5.2.5. Baking tests

Bread baking is described in section 4.2.5.

5.2.5.1. Basic analysis and calculations

Proving behaviours, baking loss, specific volumes, and moisture contents of loaves, and slice properties (by C Cell) were evaluated as described in section 4.2.5.1.

5.2.5.2. Bread textural evaluation

The evaluations of the textural properties of gluten free bread are described in section 4.2.5.2.

5.3. Results and discussion

5.3.1. Dough rheological properties

The rheological properties of starch-reduced gluten free doughs were analysed by either fundamental or empirical measurements. The fundamental test included shear stress ramp tests and small amplitude oscillatory measurements while empirical tests included backward extrusion and SMS/Chen-Hoseney Dough Stickiness measurements.

5.3.1.1. Fundamental rheological analysis of dough properties

The stress ramp data are shown in Figure 5.1. It can be seen (Figure 5.1a) that the shear strain increased with shear stress with different rates in different stress ranges. The replacement of rice flour by FC0 and FC60 significantly decreases the shear strain caused by a certain applied shear stress in the higher stress range

(>10 Pa). The control dough (F100) shows a relatively short transition from the linear-elastic deformation behaviour (shear strain increases linearly with shear stress) to flow behaviour and a yield point can be defined by calculating the deviation from the linearity at low shear stress range. However, when FC0 or FC60 is added, it shows a long yield zone and yield point cannot be defined by this method. The viscosity from the same data sets is plotted versus shear stress in Figure 5.1b. All doughs follow the Newtonian-through-power-law-to-Newtonian model (Barnes, 1999) in that viscosity shows a plateau at low shear stress and decreases in high stress range. The addition of FC0 and FC60 significantly increased the viscosity plateau. The start of viscosity decrease also indicates yield stress (Walls, Caines, Sanchez & Khan, 2003), and although it is still difficult to define the yield point due to a long yield-flow transition, it can be seen that the replacement by FC0 and FC60 increased the stress at which doughs start to flow (significant decrease in viscosity). Similar enhancing effects on viscosity and yield stress by the addition of chestnut flour in gluten free rice bread has been reported by Demirkesen et al. (2010b), where chestnut flour has higher fibre content and, therefore, fibrous structure, and high water binding ability, which lead to reinforcement of the doughs.

The mechanical spectra of doughs and calculated moduli from the generalised Maxwell model are shown in Figure 5.2. In the mechanical spectra, it can be seen that all doughs show solid like property with G' higher than G''. The additions of FC0 or FC60 increased both moduli and decreased tanδ suggesting a more solid like property, which is in accordance with the strengthening effects of doughs evidenced by yield stress and viscosity as discussed above. Foods can

be described to be structured by strands constituted by weakly interacting flow units, and strongly interacting topological points, which is analogous to the classic 'true gel' with permanent cross-linked three dimensional network (Gabriele, de Cindio & D'Antona, 2001). In this model, the increase in both moduli and the decrease of tanδ suggests that the additions of FC0 or FC60 fibres increase the amounts of topologically interacting points or/and the strand strength. The slopes of lgG' versus lgω have a similar value of approximately 0.105 in all cases regardless of the addition of FC0 or FC60. This value is lower compared with most gluten free and wheat doughs which range from 0.11 to 0.37 (Georgopoulos, Larsson & Eliasson, 2004; Ronda et al., 2013; Tanner, Qi & Dai, 2008; Upadhyay, Ghosal & Mehra, 2012; Villanueva, Harasym, Muñoz & Ronda, 2019). Based on the model proposed by Gabriele et al. (2001), the low lgG' versus lgω slope suggests approaching a true gel at the angular frequency range studied. It might depend on the property of flour and hydrocolloids (Chapter 4) while less influenced by FC0 and FC60 at the addition levels studied.

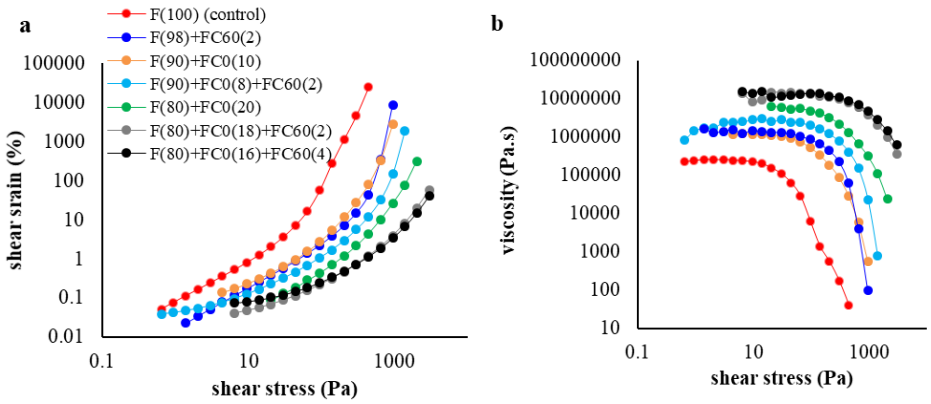

Figure 5.1. Shear stress ramp data (a) and viscosities plotted versus shear stress (b) of gluten free doughs.

FC60 has more pronounced influence than FC0 even with very low addition levels (2 or 4% replacement). This could be explained by its higher water holding ability as reported in Chapter 3 and in (Agarwal, Hewson & Foster, 2018a). In fact, the effect of 2% replacement by FC60 is similar to 10% replacement by FC0 shown as similar shear strains and viscosities plotted versus shear stress and similar mechanical spectra.

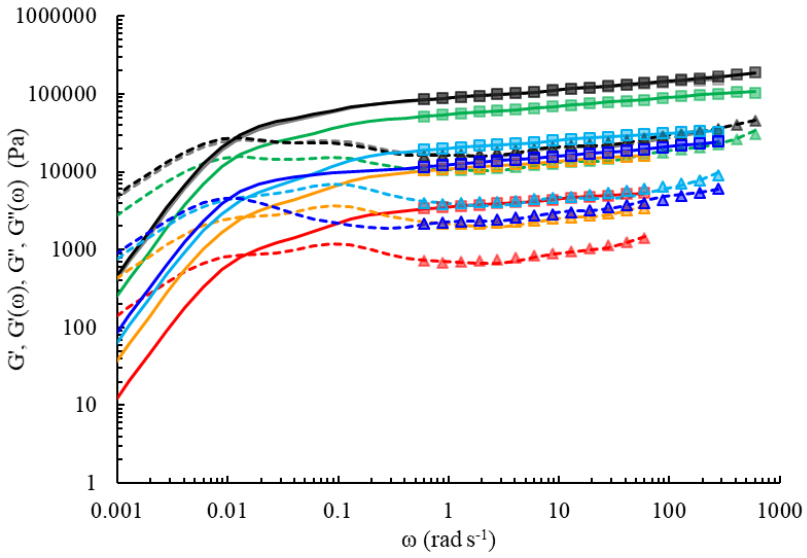

Figure 5.2. Mechanical spectra and curves calculated from generalised Maxwell model of F(100) (control) (red), F(80)+FC0(20) (green), F(80)+FC0(18)+FC60(2) (grey), F(80)+FC0(16)+FC60(4) (black), F(90)+FC0(10) (yellow), F(90)+FC0(8)+FC60(2) (light blue), and F(98)+FC60(2) (dark blue). Experimental storage moduli (G') and loss moduli (G'') are shown by squire and triangle symbols respectively and calculated G'(w) and G''(w) are presented by solid lines and dashed lines respectively.

A generalised Maxwell model was applied to estimate the dough rheological behaviours at longer time scale (slow deformation). The arbitrarily decided λ_i and calculated corresponding relaxation moduli G_i are listed in Table 5.3. Ten pairs of λ_i and G_i along with a G_e representing a single pure elastic component were used to calculate G'(ω) and G''(ω) by equation (4.2) and (4.3). The value

of G_e of each sample is either 0 or very low therefore it is not listed in Table 5.3. A zero value of G_e is typical for viscoelastic liquid of uncross-linked polymers (Ferry, 1980). Therefore, gluten free bread doughs are, structurally and rheologically analogous to viscoelastic fluid instead of a solid.

The generalised Maxwell model expands the evaluable mechanical spectra to a lower frequency range with R^2 higher than 0.98 (Table 5.3). It can be seen in Figure 5.2 that all doughs have a relaxation frequency of nearly 0.01 rad s^{-1}. The influences of FC0 and FC60 additions are insignificant. The porous structure of loaves mainly forms, develops, and sometimes collapses during proving with low strain rates (10^{-4} to 10^{-3} s^{-1} as reported by Babin et al. (2006) and Grenier et al. (2010)). The time scale is longer than the relaxation time (reciprocal of relaxation frequency) of gluten free doughs which is also observed in Chapter 4. In other words, doughs behave like fluids (G'' > G') in this low strain rate range as found during proving, which could be beneficial to the development of the loaf structure. However, this also implies that only strengthening doughs might not be able to provide efficient stability to maintain the porous structure. This could explain from, one aspect, why air pockets and big voids in crumb structure is a common and difficult issue in gluten free bread production which have been widely reported (Haque & Morris, 1994; McCarthy et al., 2005; Nishita et al., 1976; Paciulli, Rinaldi, Cirlini, Scazzina & Chiavaro, 2016; Schober, Bean & Boyle, 2007).

Table 5.3. Individual relaxation time and relaxation moduli for Generalised Maxwell Model fitting.

individual relaxation time λi (s)	0.0001	0.001	0.01	0.1	1	10	100	1000	10000	100000	R^2
F(100) (control)	123755	0	1201	1146	724	1934	1237	0	0.01	0.001	0.991
F(98)+FC60(2)	0	14804	6066	3950	3113	1925	8856	0	0.012	0.001	0.996
F(90)+FC0(10)	255156	0	3575	3270	2264	6034	3748	0	0.011	0.001	0.989
F(90)+FC0(8)+FC60(2)	279077	0	5451	6761	3917	11764	6455	0	0.013	0.002	0.98
F(80)+FC0(20)	354470	18597	23156	18045	12357	22615	25966	0	0.01	0.002	0.998
F(80)+FC0(18)+FC60(2)	904692	0	31077	29132	18275	37525	42383	0	0.01	0	0.994
F(80)+FC0(16)+FC60(4)	1271	88716	36796	29398	18524	32671	47364	0	0.01	0.017	0.998
F(90)+FC0(10)	255156	0	3575	3270	2264	6034	3748	0	0.011	0.001	0.989
F(90)+FC0(8)+FC60(2)	279077	0	5451	6761	3917	11764	6455	0	0.013	0.002	0.98

5.3.1.2. Empirical rheological analysis of dough properties

The influence of FC0 and FC60 addition on the behaviour of doughs under large deformation were analysed by backward extrusion experiments. Dough stickiness was measured using a SMS/Chen-Hoseney Dough Stickiness rig. As shown in Figure 5.3, the addition of FC0 and FC60 significantly increased dough firmness, cohesiveness, consistency, and index of viscosity, which is in agreement with the increasing effects on yield stress and dynamic moduli. Similar to what was observed in the fundamental rheological analysis, 2% replacement by FC60 and 10% replacement by FC0 show similar values for these four parameters which indicate that fibrillated cellulose is more efficient in strengthening doughs than untreated cellulose. The additions of FC0 and FC60 generally decreased dough extensibility by approximately 20 mm while the effects of FC0 fibres tend to be quadratic as 20% replacement doughs have higher extensibility than 10% replacement doughs by 6 mm. Extensibility describes the flowability of doughs in extensional flow. The negative effects of FC0 and FC60 is likely to be caused by their strengthening effect which lead to higher resistance to flow. However, the slight increase in extensibility by FC0 at higher addition level might because of its fibrous structure where the fibres are much longer (intact) than FC60 (fibrillated).

The addition of both FC0 and FC60 increased dough strength and work of adhesion while further increasing the addition levels decreased these two parameters. The stickiness was decreased by the addition of both FC0 and FC60. The reduction of dough stickiness is in agreement with the additions of fibres in wheat doughs (Collar, Santos & Rosell, 2007; Sangnark & Noomhorm, 2004).

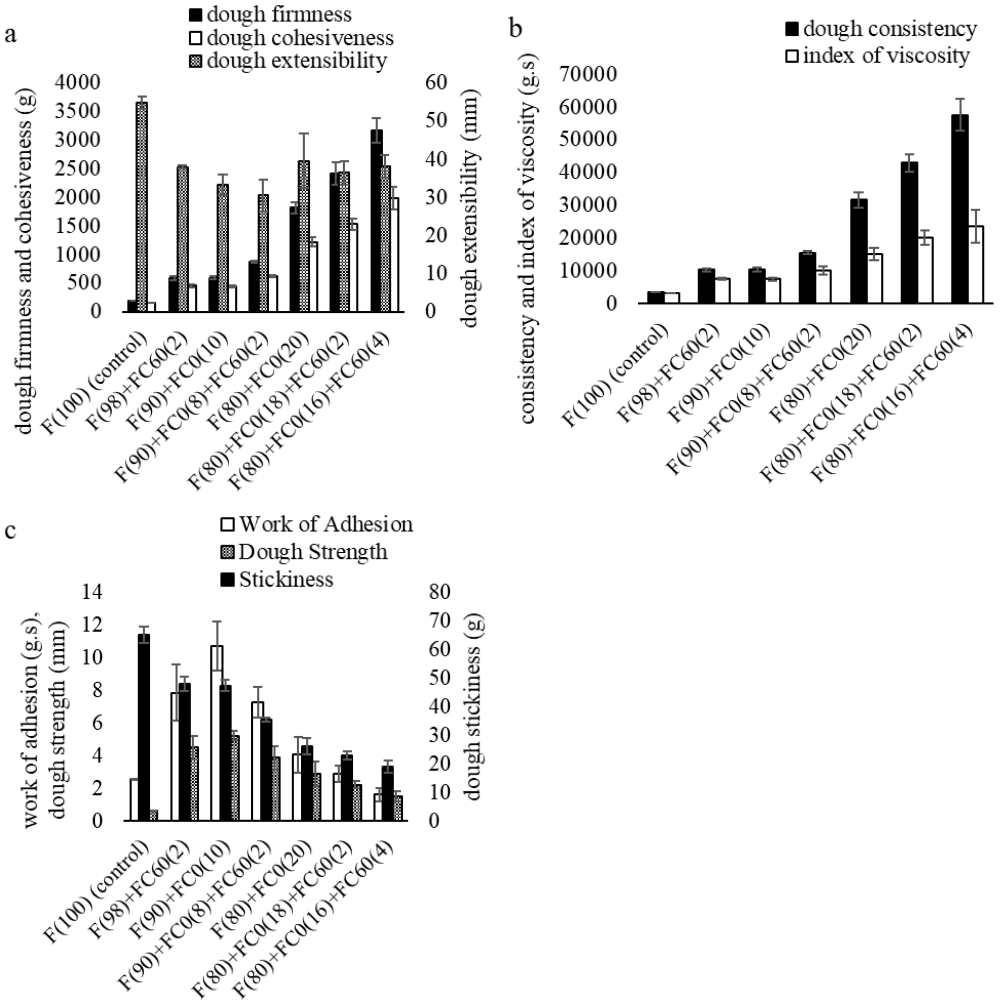

Figure 5.3. Effects of cellulose and FC fibres additions on dough firmness, Cohesiveness, extensibility (a), consistency, and index of viscosity (b) in backward extrusion measurements, and work of adhesion, dough strength, and dough stickiness (c) measured by SMS/Chen-Hoseney Dough Stickiness rig.

Minimised stickiness is a desirable dough textual property in the manufacture of wheat bread (Collar et al., 2007), where it is also beneficial to the handling property. Generally, stickiness of a material is affected by both adhesive force and cohesive (rheological) force which could oppose each other (Hoseney & Smewing, 1999). The SMS/Chen-Hoseney Dough Stickiness method minimises the interference from the bulk rheology (Chen & Hoseney, 1995). Therefore, it can be expected that the bulk rheology property has less influence on dough

stickiness measured in this experiment. Additionally, the adhesive force is influenced by water surface tension (Hoseney & Smewing, 1999). The influence of water absorption on the stickiness of wheat doughs has also been highlighted (Armero & Collar, 1997; Heddleson, Hamann, Lineback & Slade, 1994). The influence on dough stickiness is contrary to the influences on dough firmness and cohesiveness. In fact, they show close negative correlations when fitted by power equations with R^2 of 0.97 and 0.94 respectively. Therefore, the high water absorbability of FC0 and FC60 contribute both to the strengthening of doughs, in addition to the contributrion of the fibrous structure, and reduction of stickiness. However, dough strength and work of adhesion reflect both the adhesive force (stickness measured in this experiment) and cohesive force (bulk rheological, dough strengthening effect). Therefore, they increased with the replacemnets by FC0 and FC60 at lower addition levels but decreased coincidently with stickiness with furhter additions.

5.3.2. Proving behaviours

The proving behaviour of doughs are monitored by recording the volume increase of a piece of dough sample in a measuring cylinder and the proving profiles are shown in Figure 5.4. The differences in volume between gluten free doughs are less significant during the first 30 minutes. However, with increasing addition of FC0 or FC60, volume growth stopped earlier during proving which leads to lower final volume. Considering the correlations between low molecular weight sugars, yeast activity, and porosity kinetics (Romano, Toraldo, Cavella & Masi, 2007; Sahlström, Park & Shelton, 2004), sucrose in the formula might promote the volume increase during the early stage of proving but be less

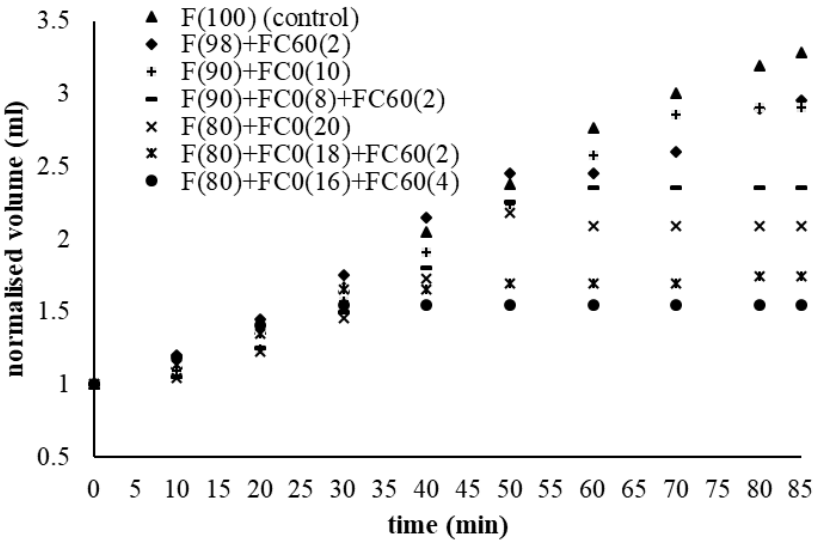

Figure 5.4. Proving profiles (normalised) of gluten free doughs.

influential after being consumed by yeasts during the later stage. The reduction of flour, instead, limits the further fermentation by yeast during the later stage of proving. However, the difference between F(100) (control), F(90)+FC0(10), and F(98)+FC60(2) are less pronounced although the flour was replaced by only 2% and 10% respectively. Hence, the answer could also lie in rheological properties. As shown by the generalised Maxwell model, doughs behave like fluids during proving and dough strengthening by FC0 and FC60 is less influential on the relaxation time. In addition, according to the model derived by Shah, Campbell, McKee and Rielly (1998), dough rheology is less influential during the early stage of proving while it becomes critical during the later stage (Mills et al., 2003). A rigid dough is highly resistant to deformation which limits the expansion of gas cells during proving (Lazaridou et al., 2007; Van Vliet, Janssen, Bloksma & Walstra, 1992). Therefore, the influences of FC0 and FC60 on proving behaviour during different stages can be also assigned to their strengthening effects on dough rheology. There is no difference between

maximum volume increase and final volume increase indicating that doughs did not collapse during the proving process even for F(80)+FC0(16)+FC60(4), whose volume did not change after 40 min of proving. This stabilising effect is atributed to the dough strengthening by FC0 and FC60 additions as seen by the rheological measurements.

5.3.3. Rheological properties during heating and cooling

Pasting profiles of flour blends are shown in Figure 5.5a. A secondary peak at 85 °C during cooling is observed at all curves due to the addition of PSY, as discussed in Chapter 4. The addition of FC0 and FC60 both significantly decreased the pasting temperature (the onset of viscosity increase) shown as a small shoulder before the main viscosity peak. The reduction of pasting temperature is widely observed for most starch/hydrocolloid mixtures (BeMiller, 2011; Naruenartwongsakul et al., 2004; Sullo & Foster, 2010). It is also observed for starch and bacterial cellulose mixtures (Díaz-Calderón et al., 2018). In the mixture of MC and starch, the thermal gelation of MC, which occurs at a lower temperature than the significant swelling of starch granules, leads to an increase in starch concentration and, therefore, enhanced starch granule interactions and increase in viscosity (Sullo & Foster, 2010). Naruenartwongsakul et al. (2004) suggested that the concentration increase of starch is due to water competition with MC. Therefore, the decreased pasting temperature of starch/hydrocolloid mixture is a result of both water and volume competition between starch and hydrocolloids (Chapter 4). Water and volume competition also explain the reduction of pasting temperature of FC0(FC60)/flour mixtures. When 20% of flour was replaced by FC0, the further

addition of FC60 lead to another smaller shoulder at a lower temperature, which suggests that FC60 is more powerful than FC0 in the competition with starch for volume and water due to its higher abilities to hold water and to occupy volume (Chapter 3) (Agarwal et al., 2018a).

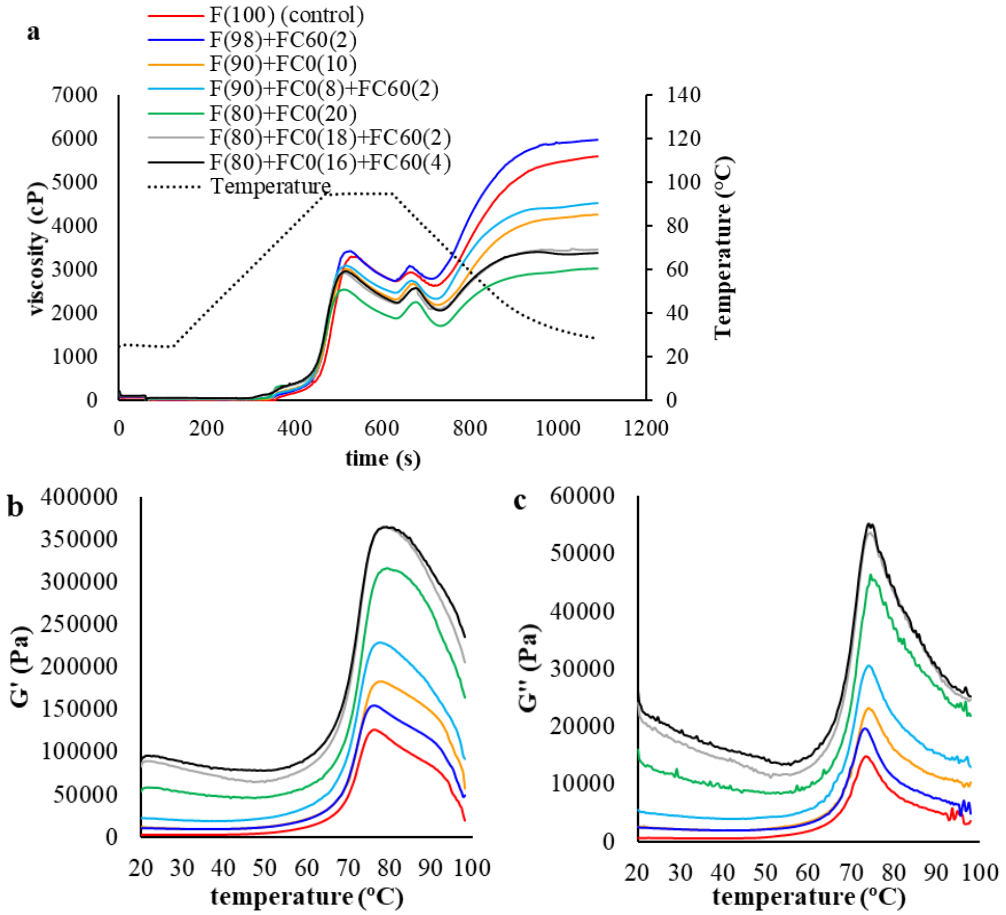

Figure 5.5. Pasting profiles (a), storage moduli G' (b), and loss moduli G'' (c) of flours blends. G' and G'' were recorded with a heating rate of 2.6 °C min^{-1}.

Replacement by FC0 decreased the overall viscosity, peak viscosity (the highest viscosity peak) time, and setback (difference between final viscosity and trough viscosity) while it increased breakdown (difference between peak viscosity and trough viscosity). The decrease of overall viscosity and setback is, due to the decrease in starch concentration, as it is replaced by FC0 which does not swell

as starch granules nor retrogradate as amylose. The reduction of swellable starch granules leads to a reduction of the ability to be closely packed which appears as early onset of breakdown. The increased breakdown is likely to be due to the enhancement of shear force exerted on starch granules by the fibrous structure of FC0. However, the substitution by FC60 result in an increase in the overall viscosity and decrease in breakdown. Fibrillated cellulose (FC60) appears as flocculates or aggregates (Chapter 3)(Agarwal, MacNaughtan & Foster, 2018b) which can be considered similar to swollen starch granules or granule fragments with freed fibrils similar to leaked amylose. The increase of viscosity indicates that FC60 is similar to or even more efficient than starch in increasing viscosity while it does not breakdown as starch granules. Therefore, the functionality of fibrillated cellulose has an effective enhancement of overall composite properties beyond the effects of the 'inert' unfibrillated filler.

The rheological property of doughs during cooking was monitored by temperature sweep tests (Figure 5.5b and c) with a temperature profile mimicking the temperature changes during baking. The increase of G' and G'' during heating can be attributed to swelling and volume filling of starch granules which are eventually close packed giving the peak in moduli. The reasons for G' and G'' decreasing after peaks might be the melting of remaining crystallites of starch, separation of amylose and amylopectin, amylopectin matrix breakdown, and disentanglement of amylopectin chains, which lead to granule softening (Keetels, vanVliet & Walstra, 1996). In contrast to pasting temperature, the onsets of G' and G'' increase shifted to a higher temperature when FC0 and/or FC60 were added. FC0/FC60 and flour are already closely packed with the

higher concentration in doughs compared to the experimental condition of RVA. When the starch content is reduced, the starch granules need to swell to a larger volume at a higher temperature to overcome the initial temperature-controlled softening (moduli decrease) and to contribute to the overall rigidity (G' increase). Being different from pasting properties, either the addition of FC0 or FC60 increased overall G' and G''. This could also be due to the closely packed structure where the swelling and rigidity changes of starch granules can be detected and, as demonstrated by the rheological properties in both fundamental and empirical experiments, the fibrous structure and high water binding ability of FC0 and FC60. FC0 and FC60 compete for water with starch, which restrains the swelling of the granules, increase their rigidity, and, hence, further increases moduli.

5.3.4. Bread qualities

The influence of the addition of FC0 and/or FC60 on specific volumes and baking loss of starch reduced gluten free bread are shown in Figure 5.6a. The influence on moisture content of the centre crumb is insignificant which is not shown. It has been reported that the water content of loaf core is the same or even higher than that before baking due to eveperation-condensation-diffusion behaviour of water during baking (Lucas et al., 2015; Wagner, Lucas, Le Ray & Trystram, 2007). However, the baking loss is significantly reduced upon the additions of FC0 and/or, especially, FC60, which could be attributed to their high water holding ability. The FC0/FC60 additions significantly reduced the specific volume, which is the same as their influences on final proving volume. The close correlation between loaf volume and final proving volume was also

documented in Chapter 4, which suggests that loaves are stable during both the later stage of proving and oven rising.

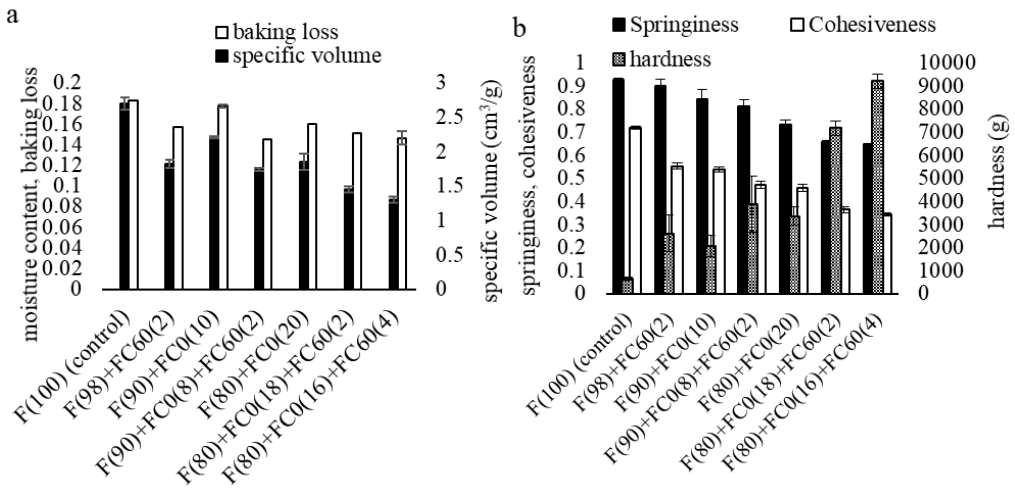

Figure 5.6. Baking lose, specific volume (a), and textural properties (b) of starch replaced gluten free breads.

The crumb was evaluated by C Cell and images are shown in Figure 5.7. Six C Cell parameters are chosen to describe the crumb structures (Table 5.4). The area of cells indicates the percentage of the cells of the total slice area and the number of cells is the number of discrete gas cells. The addition of FC0 and/or FC60 increased the number of cells but decreased the area of cells and wall thickness, and, consequently, reduced cell diameters. The detrimental effect on specific volume of fibre addition and generation of denser crumb structure have also been observed in studies on both fibre enriched wheat bread and gluten free bread (Demirkesen et al., 2010b; Gómez, Oliete, Caballero, Ronda & Blanco, 2008; Gomez, Ronda, Blanco, Caballero & Apesteguia, 2003). With the fact that the specific volume is decreased, which leads to a smaller slice area, a finer crumb structure is obtained. The finer structure might be attributed to

segmentation and framing of the fibres which build a fine skeleton where gelatinised starch and other ingredients can, attached. Area of holes and top concavity, which reflect the structural instability are not significant among all loaves.

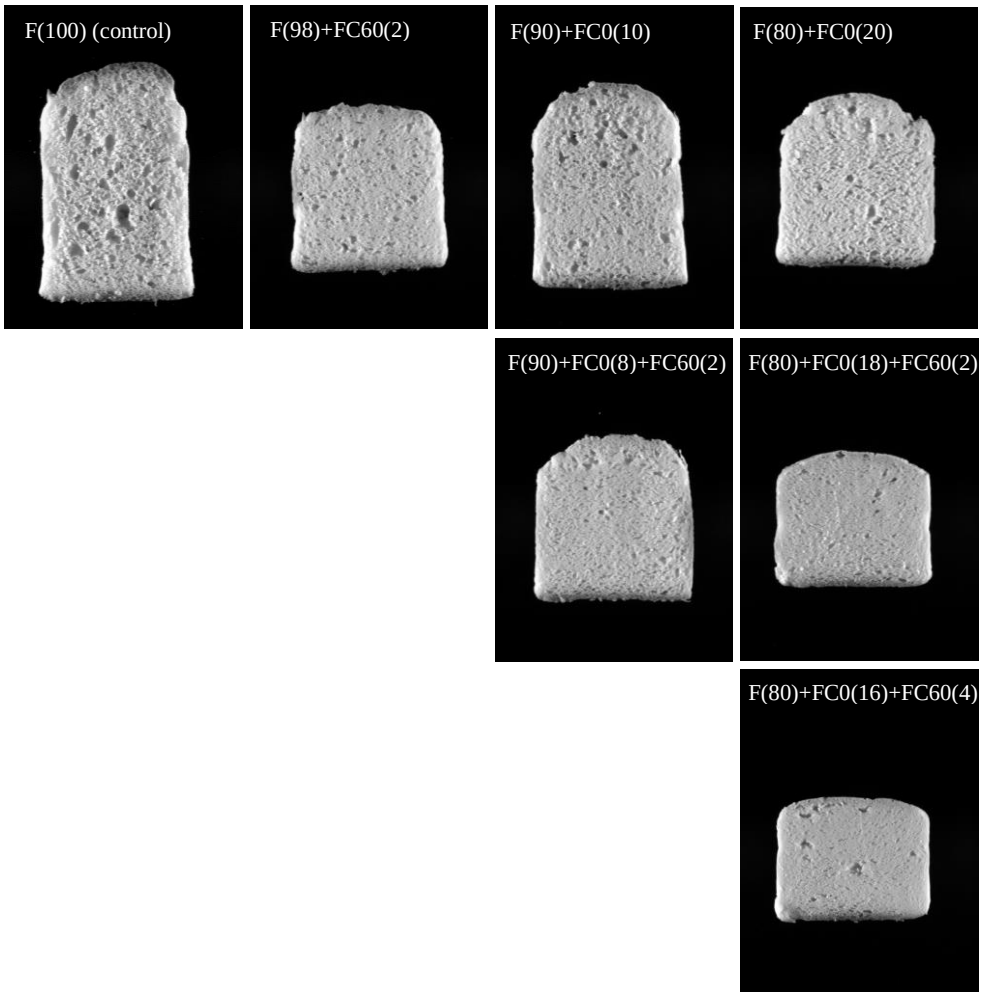

Figure 5.7. Images of starch replaced gluten free breads.

Table 5.4. C Cell parameters of starch replaced gluten free bread.

	Top Concavity (%)	Number of Cells	Area of Cells (%)	Area of Holes (%)	Wall Thickness (mm)	Cell Diameter (mm)
F(100) (control)	0.07±0.02	3523.25±27.90	50.83±0.96	2.41±0.39	0.50±0.01	2.61±0.07
F(98)+FC60(2)	0.78±0.38	3986.75±91.51	44.73±0.84	1.33±0.88	0.44±0.01	1.53±0.07
F(90)+FC0(10)	0.45±0.14	3781.50±84.82	48.20±0.57	1.43±0.81	0.46±0.01	1.88±0.09
F(90)+FC0(8)+FC60(2)	0.56±0.07	4033.50±69.00	45.00±0.43	0.85±0.48	0.43±0.00	1.44±0.02
F(80)+FC0(20)	0.47±0.07	3559.75±246.75	47.08±0.49	0.26±0.28	0.46±0.01	1.76±0.13
F(80)+FC0(18)+FC60(2)	0.27±0.04	4084.50±362.24	43.88±0.96	1.29±0.82	0.39±0.01	1.14±0.10
F(80)+FC0(16)+FC60(4)	0.21±0.04	4065.00±274.07	42.73±0.78	2.56±0.94	0.38±0.01	1.09±0.06

The texture properties of bread were evaluated by TPA. Hardness, springiness, and cohesiveness are shown in figure 5.6b. Specific volume is negatively

correlated with hardiness due to a denser crumb structure. As expected, loaves with FC0 and FC60, which have lower specific volume, have a harder crumb. They also show lower springiness and cohesiveness, which indicates that the crumb is less resistant to the applied large deformation. Good wheat bread is expected to have a thinner cell wall and uniform cells which, therefore, has softer but more elastic texture providing good mouth feel (Scanlon & Zghal, 2001). However, due to the absence of gluten and the more compact crumb structure, the starch reduced gluten free loaves show the opposite that they have smaller cells, thinner cell walls, but harder and less springy crumb. However, the springiness can also be influenced by the degree of compression during the experiment.

5.4. Conclusion

The conducted study aimed to evaluate the starch reduction of gluten free doughs and bread by FC0 and FC60 fibres. The addition of FC0 and/or FC60 significantly increased the dough strength shown as increased viscosity, yield zone, and storage and loss moduli measured by fundamental rheological measurements, and dough firmness, cohesiveness, consistency and index of viscosity measured by empirical measurements. Further analysis of the mechanical spectra by generalised Maxwell model suggests that gluten free doughs are structurally and rheologically analogous to a viscoelastic fluid instead of a solid. It also suggests that doughs are flowable at the time scales of structure developing during proving which is longer than their relaxation times. Generally, comprehensive design of experiments including both fundamental and empirical analysis would be necessary to maximise the characterisation of

doughs. Rheological properties of doughs influence the proving behaviour where the addition of FC0/FC60 mainly restrained the volume increase during the later stage of proving (after approximately 30 min). Fibrillation of cellulose increased its similarity of pasting properties to flour in a cellulose/flour blend. Volume and water competition of FC0 and FC60 restricted the hydration and swelling of starch granules significantly influencing the pasting and thermal mechanical behaviours of the blends. The additions of FC0 and FC60 decrease the specific volume of gluten free loaves, which is correlated with the decrease of final volume during proving. The additions of FC0 and FC60 generate denser and harder but finer crumb. The further improvement of cellulose enriched gluten free bread might rely on structuring of added hydrocolloids and fibrillated cellulose and optimisation of formulation including water addition levels to increase specific volume by obtaining desired rheological properties of doughs.

Chapter 6.

Conclusion and further work

6.1. Conclusions

The project was generally composed of two parts, i.e. gluten replacement and starch replacement in gluten free bread. Gluten replacement aimed to meet the requirement of gluten free diet due to gluten intolerance and the current "free from" trend as a healthy lifestyle. Starch replacement targeted a reduction in calorie content and glycaemic index of gluten free bread by addition of cellulose or fibrillated cellulose to deal with obesity and type 2 diabetes, especially the occurrences in the gluten intolerant population.

Psyllium seed husk powder (PSY) is one of the sources of hydrocolloids and dietary fibres commonly added in gluten free bread formula. However, it is less studied compared to other food hydrocolloids. The main polysaccharide of the PSY which is heavily substituted by xylose and arabinose. Small amounts of other sugars are also identified. This polysaccharide forms mucilage in water, which show 'weak gel' property (Haque et al., 1993a). When PSY is hydrated in water, the powder hydrated into gel particles and closely packed at the experiment concentration (1.64%). It melts during heating but forms a stronger gel during cooling where a fibrous structure with cloudy zones was observed. The PSY suspension was sequentially fractionated at 20 ºC , 40 ºC, 60 ºC, 80 ºC, and 100 ºC (F20, F40, F60, F80, F100 and residue respectively). From the work presented in this thesis it is now hypothesised that the low temperature fractions are the fibrous zone in the heated PSY gel while the high temperature fractions form the cloudy zones. The high temperature fractions show stronger gel properties with finer structures. All fractions show thermo-reversible rheological behaviour while F20 is the only fraction influenced by initial heat treatment. The reversible behaviour is shown as superimposable three-step G' changes during heating and cooling which involves heat-induced softening and conformational transition. An attempt was made to

perform time-temperature superposition (TTS) to further study the gelling properties. Less superimposability of F20 and F40 were observed when generating mater curves, which suggests structural changes at different temperatures. The TTS master curves show that F60 has longest relaxation time, which indicates that it is more resistant to flow. F60 might have the highest molecular weight as suggested by a higher zero shear viscosity. However, analysis by measuring monosaccharide content, FTIR, and ^{13}C – NMR, suggests differences in the substitution of sidechains. High temperature fractions have higher A/X which can also be estimated by 2^{nd}-derivative FTIR spectra and integration of C5 peaks on NMR spectra. It also suggests that high temperature fractions are more heavily substituted. Two hypotheses were proposed to interpret the distinct rheological behaviour from the view of chemical and structural of properties; and from a hierarchical molecular conformation perspective. In the first hypothesis, low temperature fractions perform molecular associations which than form tenuous linked weak gel while the structure of high temperature fractions are maintained by hydrogen bonds and described by 'physical gel' as. In this hypothesis, the three-step G' traces during heating are caused by heat-induced softening and conformational transitions from helices to coils. In the second hypothesis, the polymer is expected to form hierarchical molecular conformations However, the sidechain compositions and spatial arrangements are influential. The three-step G' changes against temperature can be assigned to softening and melting (recovery during cooling) of different levels of the hierarchical structure.

Four PSY fractions showing distinct rheological charactoristics were obtained and studied which broaden the application of PSY in different fields where materials with certain gel-like properties are required. The fractionation method is straightforward and

can be easily applied in industrial manufacture. Additionally, two hypothesis were proposed and provided insight into the molecular properties and rheological responces of this less understand material.

Cellulose fibrillation starts from the surface, weak points, and ends of cellulose fibres which significantly decreased fibre integrity and increased surface area, water retention ability, and stability against sedimentation, as fibres appear as flocculates in the suspension. Heating a sample in a sealed system or centrifuging show that the distance-induced flocculates are larger than heat-induced flocculates.

Unheated FC and PSY mixtures appear to be binary phase composites where one phase consists of hydrated PSY particles and the other one is concentrated in FC fibres. Increasing fibrillating time significantly increased the moduli of the mixtures as FC fibres processed for a longer time occupy larger volume with denser structure and become more dominant in the rheological property of the mixture. FC and PSY form interpenetrating composites after heat treatment where FC fibres are incorporated into the PSY gel. When fibrillating process time is short and only affects cellulose fibre surface, there is less difference between the structure and rheological properties of the mixtures. However, when fibrillating time increases and a large amount of cellulose fibres lose their integrity, the structure of the mixture appears to be denser and clumped and moduli significantly increases.

FC60, which is stable in suspension showed rheological synergism with PSY. FC60 dominates the rheological properties by a stronger gel like properties shown as higher moduli and less dependent storage moduli on frequency while PSY governs the

resistance in the viscoelastic flow. The mixture of FC60 and PSY show synergistic rheological behaviour, which is more pronounced before heat treatment.

PSY is shown to weakly interact with FC, as aggregates which associate on the FC fibres. F60 is the only fraction which associates with untreated cellulose fibres, possibly through the existence of arabinan sidechains on the heteroxylan molecules interacting with cellulose fibres. Another possibility is stereochemical compatibility between PSY and cellulose where the two fold helix (if exist) or coil can associate, or adapt and associate respectively, to cellulose which explains the higher storage moduli during cooling than that during heating; and the isothermal storage moduli decline observed in temperature sweep shear tests. The increased roughness and porosity of cellulose by fibrillation provides docking positions for PSY aggregates producing an interpenetrating structure and dense volume occupation, which dominantly contributed to its overall rheological property.

This part of the thesis investigated novel mixtures of FC and PSY. The gel-like mucilage materials of PSY can be reinforced by cellulose and the rheological properties of the obtained composites can be easily modified by increasing the time of fibrillating process. These novel mixtures can be applied in food, pharmaceutical, and cosmetic industries. This part of the thesis also provide insight into the interactions between PSY heteroxylan and cellulose where three possible mechanisms were hypothesised which are different from the interactions between cereal arabinoxylan and cellulose.

The addition of hydrocolloids to gluten-free doughs strengthen the doughs, which can be counteracted by high water addition. Water itself dilutes flour and hydrocolloids and lead to a negative contribution to dough rigidity. PSY contributes more to the storage

moduli as it shows ‘weak gel’ property while MC more efficiently increase loss moduli. Water competition between MC and PSY lead to depletion effect on dough strengthening. The relaxation frequency of gluten free doughs obtained using a generalised Maxwell model is correlated with proving behaviour and indicates that the doughs are flowable at the time scale. It, on the one hand, allows gas cells to expand, yet on the other hand, it suggests that the strengthening of doughs does not sufficiently increase stability to trap gas and prevent coalescence, which, from a rheological perspective, explains the formation of voids in crumb structure.

Fundamental rheological measurements with small deformation experimental condition are less efficient in the prediction of gluten free bread quality, however dough extensibility is, along with work of adhesion, an efficient predictor of specific volume. High extensibility can only be achieved by concurrent addition of water and hydrocolloids where a homogeneous and smooth dough is obtained. With the high addition of water, MC is more efficient than PSY in increasing extensibility and work of adhesion. High extensibility indicates high flowability of doughs which allow the gas cells to expend to achieve high volume. Therefore, MC addition with proper water addition level is beneficial to the increase of specific volume. However, PSY showed a slightly detrimental effect. The crumb of loaves with high specific volume is softer, less dense and less springy. The dilution effect of water further weakens the cell walls. Voids in crumb structure is a common issue in the production of gluten free bread and the reason could be dilution effect of water which lead to coalescence and weaker cell walls, or high consistency of doughs which trap gas during mixing. Although the fundamental rheological parameters and other empirical rheological parameters are less correlated

with specific volume, they are sensitive to the variation in formulation and provide other information such as dough stability which is negatively related to top concavity.

Pasting profiles of flour/hydrocolloid blends show that MC and PSY compete for water and volume with flour particles which decrease pasting temperature. They have significantly different effects at high temperature. MC gel at high temperature and believed to form gel particles under shearing. These gel particles significantly increased the overall viscosity. The behaviour of PSY at high temperature is more complicated, since after melting at high temperature, upon cooling self-association under shearing allows the formation of hairy and weak PSY particles which can interact with each other via the loose molecules. Another possible phenomenon is the formations of PSY/amylose complex. The balance between these different phenomena results in a more pronounced increase of viscosity than the MC containing blends.

The investigation on hydrocolloids and water addition levels in gluten free bread making provided a comprehensive characterisation of both doughs and bread. Correlations between different parameters were illustrated and bread quality can be predicted by measuring dough extensibility.

As the result of their fibrous structure and high water binding ability, FC0 and FC60 significantly strengthen the gluten free dough when replacing starch/flour and is shown as 1) a decrease of strain triggered by a certain shear stress; 2) an increase in the plateau viscosity; 3) shifting of the yield zone to a higher shear stress; 4) increases in both moduli and decrease of tanδ; and 5) increase in dough firmness, cohesiveness, consistency, and index of viscosity measured by backward extrusion tests. However, the quadratic influences of FC0 and FC60 on dough extensibility measured by backward

extrusion, and dough strength and work of adhesion measured by stickiness rig indicate that their influences on different factors (e.g. states of water, structure, and strength) participate in the determination of the dough behaviours. Stickiness is decreased upon the addition of FC0 and FC60 due to their high water binding ability, which is negatively correlated to dough firmness. The decrease in stickiness is beneficial to dough handling. The dough strengthening has less influence on the early stage of proving but it significantly inhibits expansion during the later stage.

The lower dependence of storage moduli on frequency suggests that, compared to other gluten free and wheat doughs in the literature, the doughs made by rice flour in this study are similar to a 'true gel' in the angular frequency range of 600 to 0.06 rad s^{-1} as measured, which is less influenced by the addition of FC0 or FC60. The However, FC0 and FC60 do not have significant influences on relaxation time.

FC0 and FC60 behave like most other hydrocolloids, which compete water and volume with starch and reduce the pasting temperature. Comparing FC0 and FC60, FC60 is more similar to, or more efficient than, starch in increasing viscosity during pasting. With low water content, the water competition with starch during heating also reduce granule swelling and, therefore, increase granule rigidity. Fibrillation effectively enhances the overall composite properties instead of being an 'inert' filler.

In terms of bread quality, the replacement by FC0 and FC60 lead to a decrease in specific volume, which is correlated to the restriction of volume rising during proving. The obtained loaves have denser, harder but finer crumb.

Gluten free bread with lower calorie content and glycaemic index can be obtained by replacing flour with cellulose and fibrillated cellulose and the obtained loaves have

harder but finer crumb structure though at the sacrifice of loaf volume. The application of cellulose in starch-riched food and the effects of fibrillation (more than ‘inert’ filler) were better understand.

6.2. Further work

Further investigations on the molecular structures, linkage analysis, and conformations would be required to fully understand the complex herteroxylan PSY and its distinct rheological behaviours. Different rheological properties of fractions of PSY can be further explored and extended to application in other areas. Investigations on long-term behaviours, e.g. aggregation and syneresis, would be also important for a deeper understanding of this material.

A more controlled fibrillating process with higher energy input by homogeniser or microfluidiser could be applied to produce microfibrillated cellulose and allow further study of the composites with PSY. Additionally, the application of the novel mixtures of FC and PSY can be extended to other areas such as foods, pharmaceutical, and cosmetic products.

As for bread making, the simultaneous application of RSD and PCA demonstrated the influences of three factors and correlations between dough properties and bread qualities. It provides a possibility to involve comprehensive characterisation and analysis, and other parameters such as sensory evaluation can be involved in further studies.

Starch replacement leads to inferior loaves. Therefore, further work needs to be done to improve loaf volume and textural properties. The strategy could rely on formula

optimisation especially water addition levels and elaborate screening and treatment of hydrocolloids and cellulose.

Reference

Abbaszadeh, A., Lad, M., Janin, M., Morris, G. A., MacNaughtan, W., Sworn, G. & Foster, T. J. (2015). A novel approach to the determination of the pyruvate and acetate distribution in xanthan. *Food Hydrocolloids,* 44, 162-171.

Abbaszadeh, A., MacNaughtan, W., Sworn, G. & Foster, T. J. (2016). New insights into xanthan synergistic interactions with konjac glucomannan: A novel interaction mechanism proposal. *Carbohydrate Polymers,* 144, 168-177.

Abdelaal, E. S. M., Hucl, P. & Sosulski, F. W. (1995). Compositional and nutritional characteristics of spring einkorn and spelt wheats. *Cereal Chemistry,* 72(6), 621-624.

Agarwal, D., Hewson, L. & Foster, T. J. (2018a). A comparison of the sensory and rheological properties of different cellulosic fibres for food. *Food & Function,* 9(2), 1144-1151.

Agarwal, D., MacNaughtan, W. & Foster, T. J. (2018b). Interactions between microfibrillar cellulose and carboxymethyl cellulose in an aqueous suspension. *Carbohydrate Polymers,* 185, 112-119.

Agoda-Tandjawa, G., Durand, S., Gaillard, C., Garnier, C. & Doublier, J. L. (2012). Rheological behaviour and microstructure of microfibrillated cellulose suspensions/low-methoxyl pectin mixed systems. Effect of calcium ions. *Carbohydrate Polymers,* 87(2), 1045-1057.

Aguedo, M., Fougnies, C., Dermience, M. & Richel, A. (2014). Extraction by three processes of arabinoxylans from wheat bran and characterization of the fractions obtained. *Carbohydrate Polymers,* 105, 317-324.

Alba, K., MacNaughtan, W., Laws, A. P., Foster, T. J., Campbell, G. M. & Kontogiorgos, V. (2018). Fractionation and characterisation of dietary fibre from blackcurrant pomace. *Food Hydrocolloids*, 81, 398-408.

Alemdar, A. & Sain, M. (2008). Isolation and characterization of nanofibers from agricultural residues – Wheat straw and soy hulls. *Bioresource Technology,* 99(6), 1664-1671.

Anderson, J. W., Allgood, L. D., Lawrence, A., Altringer, L. A., Jerdack, G. R., Hengehold, D. A. & Morel, J. G. (2000). Cholesterol-lowering effects of psyllium intake adjunctive to diet therapy in men and women with hypercholesterolemia: Meta-analysis of 8 controlled trials. *The American Journal of Clinical Nutrition,* 71(2), 472-479.

Andresen, M., Johansson, L.-S., Tanem, B. S. & Stenius, P. (2006). Properties and characterization of hydrophobized microfibrillated cellulose. *Cellulose,* 13(6), 665-677.

Andrewartha, K. A., Phillips, D. R. & Stone, B. A. (1979). Solution properties of wheat-flour arabinoxylans and enzymically modified arabinoxylans. *Carbohydrate Research,* 77, 191-204.

Arendt, E. K., Renzetti, S. & Bello, F. D. (2009). Dough microstructure and textural aspects of gluten-free yeast bread and biscuits. In E. Gallagher (Ed.), *Gluten-free food science and technology* (pp. 107-129). Chichester: Wiley-Blackwell.

Armero, E. & Collar, C. (1997). Texture properties of formulated wheat doughsRelationships with dough and bread technological quality. *Zeitschrift für Lebensmitteluntersuchung und -Forschung A,* 204(2), 136-145.

Atalla, R. H. & Vanderhart, D. L. (1984). Native cellulose: A composite of two distinct crystalline forms. *Science,* 223(4633), 283-285.

Aziz, I., Lewis, N. R., Hadjivassiliou, M., Winfield, S. N., Rugg, N., Kelsall, A., Newrick, L. & Sanders, D. S. (2014). A UK study assessing the population prevalence of self-reported gluten sensitivity and referral characteristics to secondary care. *European Journal of Gastroenterology & Hepatology,* 26(1), 33-39.

Babin, P., Della Valle, G., Chiron, H., Cloetens, P., Hoszowska, J., Pernot, P., Réguerre, A. L., Salvo, L. & Dendievel, R. (2006). Fast X-ray tomography analysis of bubble growth and foam setting during breadmaking. *Journal of Cereal Science,* 43(3), 393-397.

Bache, I. C. & Donald, A. M. (1998). The structure of the gluten network in dough: A study using environmental scanning electron microscopy. *Journal of Cereal Science,* 28(2), 127-133.

Bao, F., Yu, L., Babu, S., Wang, T., Hoffenberg, E. J., Rewers, M. & Eisenbarth, G. S. (1999). One third of HLA DQ2 homozygous patients with type 1 diabetes express celiac disease-associated transglutaminase autoantibodies. *Journal of Autoimmunity,* 13(1), 143-148.

Barnes, H. A. (1999). The yield stress—a review or ‘παντα ρει’—everything flows? *Journal of Non-Newtonian Fluid Mechanics,* 81(1), 133-178.

Baumgaertel, M. & Winter, H. H. (1992). Interrelation between continuous and discrete relaxation time spectra. *Journal of Non-Newtonian Fluid Mechanics,* 44, 15-36.

Belitz, H.-D., Grosch, Werner, Schieberle, Peter. (2009). *Food Chemistry*. Berlin: Springer-Verlag

BeMiller, J. N. (2011). Pasting, paste, and gel properties of starch–hydrocolloid combinations. *Carbohydrate Polymers,* 86(2), 386-423.

Bender, J. & Wagner, N. J. (1996). Reversible shear thickening in monodisperse and bidisperse colloidal dispersions. *Journal of Rheology,* 40(5), 899-916.

Berry, M. J., Davis, P. J. & Gidley, M. J. (2001). Conjugated polysaccharide fabric detergent and conditioning products. US6225462B1.

Biesiekierski, J. R. (2017). What is gluten? *Journal of Gastroenterology and Hepatology,* 32(S1), 78-81.

Blanshard, J. (1987). Starch granule structure and function: A physicochemical approach. In T. Galliard (Ed.), *Starch: Properties and Potential* (pp. 16-54). Chichester : Wiley for Society of Chemical Industry.

Bledzki, A. K. & Gassan, J. (1999). Composites reinforced with cellulose based fibres. *Progress in Polymer Science,* 24(2), 221-274.

Bossis, G. & Brady, J. F. (1989). The rheology of brownian suspensions. *The Journal of Chemical Physics*, 91(3), 1866-1874.

Bousquières, J., Michon, C. & Bonazzi, C. (2017). Functional properties of cellulose derivatives to tailor a model sponge cake using rheology and cellular structure analysis. *Food Hydrocolloids,* 70, 304-312.

Bratchell, N. (1989). Multivariate response surface modelling by principal components analysis. *Journal of Chemometrics,* 3(4), 579-588.

Brown, R. M. (1996). The biosynthesis of cellulose. *Journal of Macromolecular Science, Part A,* 33(10), 1345-1373.

Buléon, A., Colonna, P., Planchot, V. & Ball, S. (1998). Starch granules: Structure and biosynthesis. *International Journal of Biological Macromolecules,* 23(2), 85-112.

Burchard, W. (2003). Solubility and solution structure of cellulose derivatives. *Cellulose,* 10(3), 213-225.

Busse-Wicher, M., Grantham, Nicholas J., Lyczakowski, Jan J., Nikolovski, N. & Dupree, P. (2016). Xylan decoration patterns and the plant secondary cell wall molecular architecture. *Biochemical Society Transactions,* 44(1), 74-78.

Cappa, C., Lucisano, M. & Mariotti, M. (2013). Influence of psyllium, sugar beet fibre and water on gluten-free dough properties and bread quality. *Carbohydrate Polymers,* 98(2), 1657-1666.

Capristo, E., Addolorato, G., Mingrone, G., De Gaetano, A., Greco, A. V., Tataranni, P. A. & Gasbarrini, G. (2000). Changes in body composition, substrate oxidation, and resting metabolic rate in adult celiac disease patients after a 1-y gluten-free diet treatment. *The American Journal of Clinical Nutrition,* 72(1), 76-81.

Carpita, N. C. & Gibeaut, D. M. (1993). Structural models of primary cell walls in flowering plants: Consistency of molecular structure with the physical properties of the walls during growth. *The Plant Journal*, 3(1), 1-30.

Catassi, C., Anderson, R. P., Hill, I. D., Koletzko, S., Lionetti, E., Mouane, N., Schumann, M. & Yachha, S. K. (2012). World perspective on celiac disease. *Journal of Pediatric Gastroenterology and Nutrition,* 55(5), 494-499.

Cauvain, S. (2015). *Technology of breadmaking* (3rd ed.). London: Springer International Publishing.

Chanliaud, E. & Gidley, M. J. (1999). In vitro synthesis and properties of pectin/Acetobacter xylinus cellulose composites. *The Plant Journal,* 20(1), 25-35.

Chavanpatil, M. D., Jain, P., Chaudhari, S., Shear, R. & Vavia, P. R. (2006). Novel sustained release, swellable and bioadhesive gastroretentive drug delivery system for ofloxacin. *International Journal of Pharmaceutics,* 316(1), 86-92.

Chen, W. Z. & Hoseney, R. C. (1995). Development of an objective method for dough stickiness. *LWT - Food Science and Technology,* 28(5), 467-473.

Cheng, Z., Blackford, J., Wang, Q. & Yu, L. (2009). Acid treatment to improve psyllium functionality. *Journal of Functional Foods,* 1(1), 44-49.

Chieh, C. (2006). Water. In Y. H. Hui (Ed.), *Bakery products science and technology* (pp. 211-232). Oxford: Blackwell Publishing.

Christianson, D. D. (1981). Gelatinization of wheat starch as modified by xanthan gum, guar gum, and cellulose gum. *Cereal Chemistry,* 58(6), 513-517.

Clark, A. H., Richardson, R. K., Rossmurphy, S. B. & Stubbs, J. M. (1983). Structural and mechanical-properties of agar gelatin co-gels - small-deformation studies. *Macromolecules,* 16(8), 1367-1374.

Cleemput, G., Roels, S., Van Oort, M., Grobet, P. & Delcour, J. (1993). Heterogeneity in the structure of water-soluble arabinoxylans in European wheat flours of variable bread-making quality. *Cereal Chemistry,* 70, 324-324.

Collar, C., Andreu, P., Martinez, J. C. & Armero, E. (1999). Optimization of hydrocolloid addition to improve wheat bread dough functionality: A response surface methodology study. *Food Hydrocolloids,* 13(6), 467-475.

Collar, C., Santos, E. & Rosell, C. M. (2007). Assessment of the rheological profile of fibre-enriched bread doughs by response surface methodology. *Journal of Food Engineering,* 78(3), 820-826.

Cuq, B., Boutrot, F., Redl, A. & Lullien-Pellerin, V. (2000). Study of the temperature effect on the formation of wheat gluten network: Influence on mechanical properties and protein solubility. *Journal of Agricultural and Food Chemistry,* 48(7), 2954-2959.

Czaja-Bulsa, G. (2015). Non coeliac gluten sensitivity - A new disease with gluten intolerance. *Clinical Nutrition,* 34(2), 189-194.

Das Purkayastha, M., Dutta, G., Barthakur, A. & Mahanta, C. L. (2015). Tackling correlated responses during process optimisation of rapeseed meal protein extraction. *Food Chemistry,* 170, 62-73.

Davidson, T. C., Newman, R. H. & Ryan, M. J. (2004). Variations in the fibre repeat between samples of cellulose I from different sources. *Carbohydrate Research,* 339(18), 2889-2893.

Day, L., Augustin, M. A., Batey, I. L. & Wrigley, C. W. (2006). Wheat-gluten uses and industry needs. *Trends in Food Science & Technology,* 17(2), 82-90.

Delcour, J., Vanhamel, S. & De Geest, C. (1989). Physico-chemical and functional properties of rye nonstarch polysaccharides. I. Colorimetric analysis of pentosans and their relative monosaccharide compositions in fractionated (milled) rye products. *Cereal Chemistry,* 66(2), 107-111.

Demirkesen, I., Mert, B., Sumnu, G. & Sahin, S. (2010a). Rheological properties of gluten-free bread formulations. *Journal of Food Engineering,* 96(2), 295-303.

Demirkesen, I., Mert, B., Sumnu, G. & Sahin, S. (2010b). Utilization of chestnut flour in gluten-free bread formulations. *Journal of Food Engineering,* 101(3), 329-336.

Dervilly-Pinel, G., Thibault, J.-F. & Saulnier, L. (2001). Experimental evidence for a semi-flexible conformation for arabinoxylans. *Carbohydrate Research,* 330(3), 365-372.

Dhital, S., Shrestha, A. K. & Gidley, M. J. (2010). Effect of cryo-milling on starches: Functionality and digestibility. *Food Hydrocolloids,* 24(2), 152-163.

Di Sabatino, A. & Corazza, G. R. (2009). Coeliac disease. *The Lancet,* 373(9673), 1480-1493.

Díaz-Calderón, P., MacNaughtan, B., Hill, S., Foster, T., Enrione, J. & Mitchell, J. (2018). Changes in gelatinisation and pasting properties of various starches (wheat, maize and waxy maize) by the addition of bacterial cellulose fibrils. *Food Hydrocolloids,* 80, 274-280.

Diener, M., Adamcik, J., Sánchez-Ferrer, A., Jaedig, F., Schefer, L. & Mezzenga, R. (2019). Primary, secondary, tertiary and quaternary structure levels in linear polysaccharides: From random coil, to single helix to supramolecular assembly. *Biomacromolecules,* 20(4), 1731-1739.

Djordjevic, M., Soronja-Simovic, D., Nikolic, I., Djordjevic, M., Seres, Z. & Milasinovic-Seremesic, M. (2019). Sugar beet and apple fibres coupled with hydroxypropylmethylcellulose as functional ingredients in gluten-free

formulations: Rheological, technological and sensory aspects. *Food Chemistry,* 295, 189-197.

Donovan, J. W. (1979). Phase transitions of the starch–water system. *Biopolymers,* 18(2), 263-275.

Edwards, S., Chaplin, M. F., Blackwood, A. D. & Dettmar, P. W. (2003). Primary structure of arabinoxylans of ispaghula husk and wheat bran. *Proceedings of the Nutrition Society*, 62(1), 217-222.

Engleson, J. A., Lendon, C. A. & Atwell, W. A. (2012). System for gluten replacement in food products. US8088427B2.

Erwin, B. M., Rogers, S. A., Cloitre, M. & Vlassopoulos, D. (2010). Examining the validity of strain-rate frequency superposition when measuring the linear viscoelastic properties of soft materials. *Journal of Rheology,* 54(2), 187-195.

Farahnaky, A., Askari, H., Majzoobi, M. & Mesbahi, G. (2010). The impact of concentration, temperature and pH on dynamic rheology of psyllium gels. *Journal of Food Engineering,* 100(2), 294-301.

Fasano, A. & Catassi, C. (2001). Current approaches to diagnosis and treatment of celiac disease: An evolving spectrum. *Gastroenterology,* 120(3), 636-651.

Felby, C., Thygesen, L. G., Kristensen, J. B., Jorgensen, H. & Elder, T. (2008). Cellulose-water interactions during enzymatic hydrolysis as studied by time domain NMR. *Cellulose,* 15(5), 703-710.

Fellstone, D. S. (2011). *Gluten properties, modifications and dietary intolerance*. New York: Nova Science Publishers.

Ferry, J. D. (1980). *Viscoelastic properties of polymers* (3rd ed.). New York: John Wiley & Sons.

Fischer, M. H., Yu, N. X., Gray, G. R., Ralph, J., Anderson, L. & Marlett, J. A. (2004). The gel-forming polysaccharide of psyllium husk (*Plantago ovata* Forsk). *Carbohydrate Research,* 339(11), 2009-2017.

Foster, T. J. (1992). *Conformation and properties of xanthan variants.* PhD thesis, Cranfield Institute of Technology, Silsoe College, Bedfordshire, UK.

Foster, T. J. (2010). Technofunctionality of hydrocolloids and their impact on food structure. *Gums and Stabilisers for the Food Industry 15*, 103-112.

Foster, T. J., Ablett, S., McCann, M. C. & Gidley, M. J. (1996). Mobility-resolved ^{13}C-NMR spectroscopy of primary plant cell walls. *Biopolymers,* 39(1), 51-66.

Franz, G. & Blaschek, W. (1990). Cellulose. In P. M. Dey (Ed.), *Methods in Plant Biochemistry* (Vol. 2, pp. 291-322). London: Academic Press.

French, D. (1972). Fine structure of starch and its relationship to the organization of starch granules. *Journal of the Japanese Society of Starch Science,* 19(1), 8-25.

Funami, T., Kataoka, Y., Hiroe, M., Asai, I., Takahashi, R. & Nishinari, K. (2007). Thermal aggregation of methylcellulose with different molecular weights. *Food Hydrocolloids,* 21(1), 46-58.

Gabriele, D., de Cindio, B. & D'Antona, P. (2001). A weak gel model for foods. *Rheologica Acta,* 40(2), 120-127.

Gallagher, E., Gormley, T. R. & Arendt, E. K. (2003). Crust and crumb characteristics of gluten free breads. *Journal of Food Engineering*, 56(2–3), 153-161.

Gallagher, E., Gormley, T. R. & Arendt, E. K. (2004). Recent advances in the formulation of gluten-free cereal-based products. *Trends in Food Science & Technology,* 15(3–4), 143-152.

Gallant, D. J., Bouchet, B. & Baldwin, P. M. (1997). Microscopy of starch: Evidence of a new level of granule organization. *Carbohydrate Polymers,* 32(3), 177-191.

Georgopoulos, T., Larsson, H. & Eliasson, A.-C. (2004). A comparison of the rheological properties of wheat flour dough and its gluten prepared by ultracentrifugation. *Food Hydrocolloids*, 18(1), 143-151.

Gidley, M. J. (1989). Molecular mechanisms underlying amylose aggregation and gelation. *Macromolecules*, 22(1), 351-358.

Gidley, M. J. & Bociek, S. M. (1985). Molecular organization in starches: A carbon 13 CP/MAS NMR study. *Journal of the American Chemical Society,* 107(24), 7040-7044.

Goldberg, R. N., Schliesser, J., Mittal, A., Decker, S. R., Santos, A. F. L. O. M., Freitas, V. L. S., Urbas, A., Lang, B. E., Heiss, C., Ribeiro da Silva, M. D. M. C., Woodfield, B. F., Katahira, R., Wang, W. & Johnson, D. K. (2015). A thermodynamic investigation of the cellulose allomorphs: Cellulose(am), cellulose Iβ(cr), cellulose II(cr), and cellulose III(cr). *The Journal of Chemical Thermodynamics*, 81, 184-226.

Gómez, M., Oliete, B., Caballero, P. A., Ronda, F. & Blanco, C. A. (2008). Effect of nut paste enrichment on wheat dough rheology and bread volume. *Food Science and Technology International,* 14(1), 57-65.

Gomez, M., Ronda, F., Blanco, C. A., Caballero, P. A. & Apesteguia, A. (2003). Effect of dietary fibre on dough rheology and bread quality. *European Food Research and Technology*, 216(1), 51-56.

Grantham, N. J., Wurman-Rodrich, J., Terrett, O. M., Lyczakowski, J. J., Stott, K., Iuga, D., Simmons, T. J., Durand-Tardif, M., Brown, S. P., Dupree, R., Busse-Wicher, M. & Dupree, P. (2017). An even pattern of xylan substitution is critical for interaction with cellulose in plant cell walls. *Nature Plants*, 3(11), 859-865.

Grenier, D., Lucas, T. & Le Ray, D. (2010). Measurement of local pressure during proving of bread dough sticks: Contribution of surface tension and dough viscosity to gas pressure in bubbles. *Journal of Cereal Science*, 52(3), 373-377.

Grover, J. A. (1993). Methylcellulose and its derivatives. In W. J. N. Roy L, Bemiller (Ed.), *Industrial Gums, Polysaccharides and Their Derivatives* (3rd ed.). London: Academic Press.

Guo, Q., Cui, S. W., Wang, Q., Goff, H. D. & Smith, A. (2009). Microstructure and rheological properties of psyllium polysaccharide gel. *Food Hydrocolloids*, 23(6), 1542-1547.

Guo, Q., Cui, S. W., Wangb, Q. & Young, J. C. (2008). Fractionation and physicochemical characterization of psyllium gum. *Carbohydrate Polymers*, 73(1), 35-43.

Habibi, Y., Lucia, L. A. & Rojas, O. J. (2010). Cellulose nanocrystals: Chemistry, self-assembly, and applications. *Chemical Reviews*, 110(6), 3479-3500.

Hager, A. S., Wolter, A., Czerny, M., Bez, J., Zannini, E., Arendt, E. K. & Czerny, M. (2012). Investigation of product quality, sensory profile and ultrastructure of breads made from a range of commercial gluten-free flours compared to their wheat counterparts. *European Food Research and Technology*, 235(2), 333-344.

Hamaker, B. R. & Bugusu, B. A. (2003). Overview: Sorghum proteins and food quality. In *Workshop on the proteins of sorghum and millets: Enhancing nutritional and functional properties for Africa*. Pretoria, South Africa.

Han, X. Z., Campanella, O. H., Mix, N. C. & Hamaker, B. R. (2002). Consequence of starch damage on rheological properties of maize starch pastes. *Cereal Chemistry*, 79(6), 897-901.

Haque, A. & Morris, E. R. (1993). Thermogelation of methylcellulose. Part I: Molecular structures and processes. *Carbohydrate Polymers*, 22(3), 161-173.

Haque, A. & Morris, E. R. (1994). Combined use of ispaghula and HPMC to replace or augment gluten in breadmaking. *Food Research International*, 27(4), 379-393.

Haque, A., Richardson, R. K., Morris, E. R. & Dea, I. C. M. (1993a). Xanthan-like weak gel rheology from dispersions of ispaghula seed husk. *Carbohydrate Polymers*, 22(4), 223-232.

Haque, A., Richardson, R. K., Morris, E. R., Gidley, M. J. & Caswell, D. C. (1993b). Thermogelation of methylcellulose .2. Effect of hydroxypropyl substituents. *Carbohydrate Polymers,* 22(3), 175-186.

Haslam, D. W. & James, W. P. T. (2005). Obesity. *The Lancet,* 366(9492), 1197-1209.

Hatcher, D. W., Anderson, M. J., Desjardins, R. G., Edwards, N. M. & Dexter, J. E. (2002). Effects of flour particle size and starch damage on processing and quality of white salted noodles. *Cereal Chemistry,* 79(1), 64-71.

Hayashi, A., Kinoshita, K. & Miyake, Y. (1981). The conformation of amylose in solution. I. *Polymer Journal,* 13(6), 537-541.

Hebert, J. J. (1985). Crystalline form of native celluloses. *Science,* 227(4682), 79-79.

Heddleson, S. S., Hamann, D. D., Lineback, D. R. & Slade, L. (1994). Pressure-sensitive adhesive properties of wheat-flour dough and the influence of temperature, separation rate, and moisture-content. *Cereal Chemistry,* 71(6), 564-570.

Heiskanen, I., Harlin, A., Backfolk, K. & Laitinen, R. (2014). Process for the production of microfibrillated cellulose in an extruder and microfibrillated cellulose produced according to the process. WO2011051882A1.

Hemar, Y., Lebreton, S., Xu, M. & Day, L. (2011). Small-deformation rheology investigation of rehydrated cell wall particles–xanthan mixtures. *Food Hydrocolloids,* 25(4), 668-676.

Herrick, F. W., Casebier, R. L., Hamilton, J. K. & Sandberg, K. R. (1983). Microfibrillated cellulose: morphology and accessibility. In *Journal of Applied Polymer Science: Applied Polymer Symposium;(United States),* 37, 797–813.

Heymann, E. (1935). Studies on sol-gel transformations. I. The inverse sol-gel transformation of methylcellulose in water. *Transactions of the Faraday Society,* 31(1), 0846-0863.

Hisseine, O. A., Omran, A. F. & Tagnit-Hamou, A. (2018). Influence of cellulose filaments on cement paste and concrete. *Journal of Materials in Civil Engineering,* 30(6), 04018109.

Hodge, A. M., English, D. R., O'Dea, K. & Giles, G. G. (2004). Glycemic index and dietary fiber and the risk of type 2 diabetes. *Diabetes Care,* 27(11), 2701-2706.

Hoffman, R. L. (1972). Discontinuous and dilatant viscosity behavior in concentrated suspensions. I. Observation of a flow instability. *Transactions of the Society of Rheology,* 16(1), 155-173.

Holmes, G., Catassi, C. & Fasano, A. (2009). *Fast facts: Celiac disease 2e*. Oxford: Health Press.

Hoover, R. (2001). Composition, molecular structure, and physicochemical properties of tuber and root starches: A review. *Carbohydrate Polymers,* 45(3), 253-267.

Hopman, E. G. D., le Cessie, S., von Blomberg, B. M. E. & Mearin, M. L. (2006). Nutritional management of the gluten-free diet in young people with celiac disease in the netherlands. *Journal of Pediatric Gastroenterology and Nutrition,* 43(1), 102-108.

Hoseney, R. C. & Smewing, J. (1999). Instrumental measurement of stickiness of doughs and other foods. *Journal of Texture Studies,* 30(2), 123-136.

Huber, G. W., Iborra, S. & Corma, A. (2006). Synthesis of transportation fuels from biomass: Chemistry, catalysts, and engineering. *Chemical Reviews,* 106(9), 4044-4098.

Hug-Iten, S., Handschin, S., Conde-Petit, B. & Escher, F. (1999). Changes in starch microstructure on baking and staling of wheat bread. *Food Science and Technology-Lebensmittel-Wissenschaft & Technologie,* 32(5), 255-260.

Ibbett, R., Wortmann, F., Varga, K. & Schuster, K. C. (2014). A morphological interpretation of water chemical exchange and mobility in cellulose materials derived from proton NMR T-2 relaxation. *Cellulose,* 21(1), 139-152.

Imberty, A., Buléon, A., Tran, V. & Péerez, S. (1991). Recent advances in knowledge of starch structure. *Starch - Stärke,* 43(10), 375-384.

Iwai, H., Ishii, T. & Satoh, S. (2001). Absence of arabinan in the side chains of the pectic polysaccharides strongly associated with cell walls of Nicotiana plumbaginifolia non-organogenic callus with loosely attached constituent cells. *Planta,* 213(6), 907-915.

Iwamoto, S., Nakagaito, A. N., Yano, H. & Nogi, M. (2005). Optically transparent composites reinforced with plant fiber-based nanofibers. *Applied Physics A,* 81(6), 1109-1112.

Izydorczyk, M., Biliaderis, C. & Bushuk, W. (1991). Comparison of the structure and composition of water-soluble pentosans from different wheat varieties. *Cereal Chemistry,* 68(2), 139-144.

Izydorczyk, M. S., Macri, L. J. & MacGregor, A. W. (1998). Structure and physicochemical properties of barley non-starch polysaccharides—II. Alkaliextractable β-glucans and arabinoxylans. *Carbohydrate Polymers,* 35(3), 259-269.

Jackson, D. S. (2003). Starch structure, properties, and determination. In B. Caballero (Ed.), *Encyclopedia of Food Sciences and Nutrition* (2nd ed., pp. 5561-5567). Oxford: Academic Press.

Jane, J., Chen, Y. Y., Lee, L. F., McPherson, A. E., Wong, K. S., Radosavljevic, M. & Kasemsuwan, T. (1999). Effects of amylopectin branch chain length and amylose content on the gelatinization and pasting properties of starch. *Cereal Chemistry,* 76(5), 629-637.

Jane, J. & Robyt, J. F. (1984). Structure studies of amylose-V complexes and retrograded amylose by action of alpha amylases, and a new method for preparing amylodextrins. *Carbohydrate Research,* 132(1), 105-118.

Jia, X., Chen, Y., Shi, C., Ye, Y., Abid, M., Jabbar, S., Wang, P., Zeng, X. & Wu, T. (2014). Rheological properties of an amorphous cellulose suspension. *Food Hydrocolloids,* 39, 27-33.

Kabel, M. A., van den Borne, H., Vincken, J. P., Voragen, A. G. J. & Schols, H. A. (2007). Structural differences of xylans affect their interaction with cellulose. *Carbohydrate Polymers,* 69(1), 94-105.

Kacurakova, M., Capek, P., Sasinkova, V., Wellner, N. & Ebringerova, A. (2000). FT-IR study of plant cell wall model compounds: Pectic polysaccharides and hemicelluloses. *Carbohydrate Polymers,* 43(2), 195-203.

Kadan, R. S., Robinson, M. G., Thibodeaux, D. P. & Pepperman, A. B. (2001). Texture and other physicochemical properties of whole rice bread. *Journal of Food Science,* 66(7), 940-944.

Kale, M. S., Yadav, M. P. & Hanah, K. A. (2016). Suppression of psyllium husk suspension viscosity by addition of water soluble polysaccharides. *Journal of Food Science,* 81(10), E2476-E2483.

Karppinen, A., Saarinen, T., Salmela, J., Laukkanen, A., Nuopponen, M. & Seppälä, J. (2012). Flocculation of microfibrillated cellulose in shear flow. *Cellulose,* 19(6), 1807-1819.

Kaufman, R. C., Wilson, J. D., Bean, S. R., Herald, T. J. & Shi, Y. C. (2015). Development of a 96-well plate iodine binding assay for amylose content determination. *Carbohydrate Polymers,* 115, 444-447.

Keetels, C. J. A. M., vanVliet, T. & Walstra, P. (1996). Gelation and retrogradation of concentrated starch systems .1. Gelation. *Food Hydrocolloids,* 10(3), 343-353.

Kennedy, J. F., Sandhu, J. S. & Southgate, D. A. T. (1979). Structural data for the carbohydrate of Ispaghula Husk ex *Plantago ovata* Forsk. *Carbohydrate Research,* 75, 265-274.

Köhnke, T., Östlund, Å. & Brelid, H. (2011). Adsorption of arabinoxylan on cellulosic surfaces: Influence of degree of substitution and substitution pattern on adsorption characteristics. *Biomacromolecules,* 12(7), 2633-2641.

Kokelaar, J. J., van Vliet, T. & Prins, A. (1996). Strain hardening properties and extensibility of flour and gluten doughs in relation to breadmaking performance. *Journal of Cereal Science,* 24(3), 199-214.

Kono, H., Yunoki, S., Shikano, T., Fujiwara, M., Erata, T. & Takai, M. (2002). CP/MAS ^{13}C NMR study of cellulose and cellulose derivatives. 1. Complete assignment of the CP/MAS ^{13}C NMR spectrum of the native cellulose. *Journal of the American Chemical Society,* 124(25), 7506-7511.

Kontogiorgos, V. (2011). Microstructure of hydrated gluten network. *Food Research International,* 44(9), 2582-2586.

Lai, V. M. F., Lu, S., He, W. H. & Chen, H. H. (2007). Non-starch polysaccharide compositions of rice grains with respect to rice variety and degree of milling. *Food Chemistry*, 101(3), 1205-1210.

Laidlaw, R. A. & Percival, E. G. V. (1949). Studies on seed mucilages. Part III. Examination of a polysaccharide extracted from the seeds of *Plantago ovata* Forsk. *Journal of the Chemical Society*, 1600-1607.

Laun, H. M. (1986). Prediction of elastic strains of polymer melts in shear and elongation. *Journal of Rheology,* 30(3), 459-501.

Lavoine, N., Desloges, I., Dufresne, A. & Bras, J. (2012). Microfibrillated cellulose – Its barrier properties and applications in cellulosic materials: A review. *Carbohydrate Polymers,* 90(2), 735-764.

Lazaridou, A. & Biliaderis, C. G. (2009). Gluten-free doughs: Rheological properties, testing procedures – methods and potential problems. In E. Gallagher (Ed.), *Gluten‐Free Food Science and Technology*. Chichester: Wiley-Blackwell.

Lazaridou, A., Duta, D., Papageorgiou, M., Belc, N. & Biliaderis, C. G. (2007). Effects of hydrocolloids on dough rheology and bread quality parameters in gluten-free formulations. *Journal of Food Engineering,* 79(3), 1033-1047.

Lefebvre, J. (2006). An outline of the non-linear viscoelastic behaviour of wheat flour dough in shear. *Rheologica Acta*, 45(4), 525-538.

Leung, H. K., Magnuson, J. A. & Bruinsma, B. L. (1979). Pulsed nuclear magnetic-resonance study of water mobility in flour doughs. *Journal of Food Science,* 44(5), 1408-1411.

Li, D. & Xia, Y. (2004). Electrospinning of nanofibers: Reinventing the wheel? *Advanced Materials,* 16(14), 1151-1170.

Li, L., Shan, H., Yue, C. Y., Lam, Y. C., Tam, K. C. & Hu, X. (2002). Thermally induced association and dissociation of methylcellulose in aqueous solutions. *Langmuir,* 18(20), 7291-7298.

Linder, Å., Bergman, R., Bodin, A. & Gatenholm, P. (2003). Mechanism of assembly of xylan onto cellulose surfaces. *Langmuir*, 19(12), 5072-5077.

López-Rubio, A., Lagaron, J. M., Ankerfors, M., Lindström, T., Nordqvist, D., Mattozzi, A. & Hedenqvist, M. S. (2007). Enhanced film forming and film properties of amylopectin using micro-fibrillated cellulose. *Carbohydrate Polymers*, 68(4), 718-727.

Lorini, R., Scotta, M. S., Cortona, L., Avanzini, M. A., Vitali, L., De Giacomo, C., Scaramuzza, A. & Severi, F. (1996). Celiac disease and type I (insulin-dependent) diabetes mellitus in childhood: Follow-up study. *Journal of Diabetes and its Complications*, 10(3), 154-159.

Lucas, T., Doursat, C., Grenier, D., Wagner, M., Trystram, G. & Flick, D. (2015). Modeling of bread baking with a new, multi-scale formulation of evaporation–condensation–diffusion and evidence of compression in the outskirts of the crumb. *Journal of Food Engineering*, 149, 24-37.

Ludwig, D. S. (2002). The glycemic index: Physiological mechanisms relating to obesity, diabetes, and cardiovascular disease. *JAMA*, 287(18), 2414-2423.

Lundin, L. & Hermansson, A. M. (1995). Supermolecular aspects of xanthan-locust bean gum gels based on rheology and electron microscopy. *Carbohydrate Polymers*, 26(2), 129-140.

Luppino, F. S., de Wit, L. M., Bouvy, P. F., Stijnen, T., Cuijpers, P., Penninx, B. W. J. H. & Zitman, F. G. (2010). Overweight, obesity, and depression: A systematic review and meta-analysis of longitudinal studies. *JAMA Psychiatry*, 67(3), 220-229.

Madgulkar, A. R., Rao, M. R. P. & Warrier, D. (2015). Characterization of psyllium (*Plantago ovata*) polysaccharide and its uses. In K. G. Ramawat & J. M. Mérillon (Eds.), *Polysaccharides: Bioactivity and Biotechnology* (pp. 1-17). New York: Springer International Publishing.

Maki, M., Hallstrom, O., Huupponen, T., Vesikari, T. & Visakorpi, J. K. (1984). Increased prevalence of coeliac disease in diabetes. *Archives Disease Child*, 59(8), 739-742.

Mancebo, C. M., San Miguel, M. Á., Martínez, M. M. & Gómez, M. (2015). Optimisation of rheological properties of gluten-free doughs with HPMC, psyllium and different levels of water. *Journal of Cereal Science*, 61, 8-15.

Mandalari, G., Faulds, C. B., Sancho, A. I., Saija, A., Bisignano, G., LoCurto, R. & Waldron, K. W. (2005). Fractionation and characterisation of arabinoxylans from brewers' spent grain and wheat bran. *Journal of Cereal Science*, 42(2), 205-212.

Maranzano, B. J. & Wagner, N. J. (2001). The effects of particle size on reversible shear thickening of concentrated colloidal dispersions. *The Journal of Chemical Physics,* 114(23), 10514-10527.

Marasco, G., Di Biase, A. R., Schiumerini, R., Eusebi, L. H., Iughetti, L., Ravaioli, F., Scaioli, E., Colecchia, A. & Festi, D. (2016). Gut microbiota and celiac disease. *Digestive Diseases and Sciences*, 61(6), 1461-1472.

Marchessault, R. H. & Liang, C. Y. (1962). The infrared spectra of crystalline polysaccharides. VIII. Xylans. *Journal of Polymer Science*, 59(168), 357-378.

Marco, C. & Rosell, C. M. (2008). Functional and rheological properties of protein enriched gluten free composite flours. *Journal of Food Engineering,* 88(1), 94-103.

Mariani, P., Viti, M. G., Montuori, M., La Vecchia, A., Cipolletta, E., Calvani, L. & Bonamico, M. (1998). The gluten-free diet: A nutritional risk factor for adolescents with celiac disease? *Journal of Pediatric Gastroenterology and Nutrition,* 27(5), 519-523.

Mariotti, M., Lucisano, M., Pagani, M. A. & Ng, P. K. W. (2009). The role of corn starch, amaranth flour, pea isolate, and psyllium flour on the rheological properties and the ultrastructure of gluten-free doughs. *Food Research International,* 42(8), 963-975.

Marlett, J. & Fischer, M. (2005). Gel-forming polysaccharide from psyllium seed husks. WO2005116087A1.

Martínez, M. M. & Gómez, M. (2017). Rheological and microstructural evolution of the most common gluten-free flours and starches during bread fermentation and baking. *Journal of Food Engineering,* 197, 78-86.

Mason, W. R. (2009). Starch use in foods. In J. BeMiller & R. Whistler (Eds.), *Starch* (3rd ed., pp. 745-795). San Diego: Academic Press.

Masure, H. G., Fierens, E. & Delcour, J. A. (2016). Current and forward looking experimental approaches in gluten-free bread making research. *Journal of Cereal Science,* 67, 92-111.

Mathlouthi, M. & Koenig, J. L. (1987). Vibrational spectra of carbohydrates. In R. S. Tipson & D. Horton (Eds.), *Advances in Carbohydrate Chemistry and Biochemistry* (Vol. 44, pp. 7-89). London: Academic Press.

Matignon, A., Ducept, F., Sieffermann, J.-M., Barey, P., Desprairies, M., Mauduit, S. & Michon, C. (2014). Rheological properties of starch suspensions using a rotational rheometer fitted with a starch stirrer cell. *Rheologica Acta,* 53(3), 255-267.

McCarthy, D. F., Gallagher, E., Gormley, T. R., Schober, T. J. & Arendt, E. K. (2005). Application of response surface methodology in the development of gluten-free bread. *Cereal Chemistry*, 82(5), 609-615.

Meerts, M., Cardinaels, R., Oosterlinck, F., Courtin, C. M. & Moldenaers, P. (2017). The interplay between the main flour constituents in the rheological behaviour of wheat flour dough. *Food and Bioprocess Technology*, 10(2), 249-265.

Miguel, Â., Martins-Meyer, T., Figueiredo, É., Lobo, B. & Dellamora-Ortiz, G. (2013). Enzymes in Bakery: Current and Future Trends. In I. Muzzalupo (Ed.), *Food industry* (pp. 287-321). Rijeka: Intech.

Meiboom, S. & Gill, D. (1958). Modified Spin‐Echo method for measuring nuclear relaxation times. *Review of Scientific Instruments*, 29(8), 688-691.

Mengual, O., Meunier, G., Cayré, I., Puech, K. & Snabre, P. (1999). TURBISCAN MA 2000: Multiple light scattering measurement for concentrated emulsion and suspension instability analysis. *Talanta*, 50(2), 445-456.

Mikkelsen, D., Flanagan, B. M., Wilson, S. M., Bacic, A. & Gidley, M. J. (2015). Interactions of arabinoxylan and (1,3)(1,4)-β-glucan with cellulose networks. *Biomacromolecules*, 16(4), 1232-1239.

Miles, M. J., Morris, V. J., Orford, P. D. & Ring, S. G. (1985). The roles of amylose and amylopectin in the gelation and retrogradation of starch. *Carbohydrate Research*, 135(2), 271-281.

Mills, E. N. C., Wilde, P. J., Salt, L. J. & Skeggs, P. (2003). Bubble formation and stabilization in bread dough. *Food and Bioproducts Processing*, 81(3), 189-193.

Morris, E. R. (1990). Mixed polymer gels. In P. Harris (Ed.), *Food Gels* (pp. 291-359). London : Elsevier Applied Science.

Morrison, W. R., Tester, R. F. & Gidley, M. J. (1994). Properties of damaged starch granules. II. Crystallinity, molecular order and gelatinisation of ball-milled starches. *Journal of Cereal Science*, 19(3), 209-217.

Morrison, W. R., Tester, R. F., Snape, C. E., Law, R. & Gidley, M. (1993). Swelling and gelatinization of cereal starches. IV. Some effects of lipid-complexed amylose and free amylose in waxy and normal barley starches. *Cereal Chemistry*, 70, 385-385.

Nakagaito, A. N. & Yano, H. (2004). The effect of morphological changes from pulp fiber towards nano-scale fibrillated cellulose on the mechanical properties of high-strength plant fiber based composites. *Applied Physics a-Materials Science & Processing*, 78(4), 547-552.

Naruenartwongsakul, S., Chinnan, M. S., Bhumiratana, S. & Yoovidhya, T. (2004). Pasting characteristics of wheat flour-based batters containing cellulose ethers. *LWT - Food Science and Technology,* 37(4), 489-495.

Ng, M., Fleming, T., Robinson, M., Thomson, B., Graetz, N., Margono, C., Mullany, E. C., Biryukov, S., Abbafati, C., Abera, S. F., Abraham, J. P., Abu-Rmeileh, N. M. E., Achoki, T., AlBuhairan, F. S., Alemu, Z. A., Alfonso, R., Ali, M. K., Ali, R., Guzman, N. A., Ammar, W., Anwari, P., Banerjee, A., Barquera, S., Basu, S., Bennett, D. A., Bhutta, Z., Blore, J., Cabral, N., Nonato, I. C., Chang, J.-C., Chowdhury, R., Courville, K. J., Criqui, M. H., Cundiff, D. K., Dabhadkar, K. C., Dandona, L., Davis, A., Dayama, A., Dharmaratne, S. D., Ding, E. L., Durrani, A. M., Esteghamati, A., Farzadfar, F., Fay, D. F. J., Feigin, V. L., Flaxman, A., Forouzanfar, M. H., Goto, A., Green, M. A., Gupta, R., Hafezi-Nejad, N., Hankey, G. J., Harewood, H. C., Havmoeller, R., Hay, S., Hernandez, L., Husseini, A., Idrisov, B. T., Ikeda, N., Islami, F., Jahangir, E., Jassal, S. K., Jee, S. H., Jeffreys, M., Jonas, J. B., Kabagambe, E. K., Khalifa, S. E. A. H., Kengne, A. P., Khader, Y. S., Khang, Y.-H., Kim, D., Kimokoti, R. W., Kinge, J. M., Kokubo, Y., Kosen, S., Kwan, G., Lai, T., Leinsalu, M., Li, Y., Liang, X., Liu, S., Logroscino, G., Lotufo, P. A., Lu, Y., Ma, J., Mainoo, N. K., Mensah, G. A., Merriman, T. R., Mokdad, A. H., Moschandreas, J., Naghavi, M., Naheed, A., Nand, D., Narayan, K. M. V., Nelson, E. L., Neuhouser, M. L., Nisar, M. I., Ohkubo, T., Oti, S. O., Pedroza, A., Prabhakaran, D., Roy, N., Sampson, U., Seo, H., Sepanlou, S. G., Shibuya, K., Shiri, R., Shiue, I., Singh, G. M., Singh, J. A., Skirbekk, V., Stapelberg, N. J. C., Sturua, L., Sykes, B. L., Tobias, M., Tran, B. X., Trasande, L., Toyoshima, H., van de Vijver, S., Vasankari, T. J., Veerman, J. L., Velasquez-Melendez, G., Vlassov, V. V., Vollset, S. E., Vos, T., Wang, C., Wang, X., Weiderpass, E., Werdecker, A., Wright, J. L., Yang, Y. C., Yatsuya, H., Yoon, J., Yoon, S.-J., Zhao, Y., Zhou, M., Zhu, S., Lopez, A. D., Murray, C. J. L. & Gakidou, E. (2014). Global, regional, and national prevalence of overweight and obesity in children and adults during 1980–2013: A systematic analysis for the Global Burden of Disease Study 2013. *The Lancet,* 384(9945), 766-781.

Nickerson, M. T., Paulson, A. T. & Speers, R. A. (2004). Time–temperature studies of gellan polysaccharide gelation in the presence of low, intermediate and high levels of co-solutes. *Food Hydrocolloids,* 18(5), 783-794.

Nicolae, A., Radu, G. L. & Belc, N. (2016). Effect of sodium carboxymethyl cellulose on gluten-free dough rheology. *Journal of Food Engineering,* 168, 16-19.

Nieduszynski, I. A. & Marchessault, R. H. (1972). Structure of β,D(1->4')-xylan hydrate. *Biopolymers,* 11(7), 1335-1344.

Nishita, K. D., Roberts, R. L., Bean, M. M. & Kennedy, B. M. (1976). Development of a yeast-leavened rice-bread formula. *Cereal Chemistry,* 53(5), 626-635.

Nishiyama, Y., Sugiyama, J., Chanzy, H. & Langan, P. (2003). Crystal structure and hydrogen bonding system in cellulose Iα from synchrotron X-ray and neutron

fiber diffraction. *Journal of the American Chemical Society,* 125(47), 14300-14306.

Norton, I. T., Foster, T. J. & Brown, C. R. T. (1998). The science and technology of fluid gels. In P. A. Williams & G. O. Phillips (Eds.), *Gums and stabilisers for the food industry* (Vol. 9, pp. 259–268). Cambridge: Royal Society of Chemistry.

Norton, I. T., Goodall, D. M., Frangou, S. A., Morris, E. R. & Rees, D. A. (1984). Mechanism and dynamics of conformational ordering in xanthan polysaccharide. *Journal of Molecular Biology,* 175(3), 371-394.

Norton, I. T., Jarvis, D. A. & Foster, T. J. (1999). A molecular model for the formation and properties of fluid gels. *International Journal of Biological Macromolecules,* 26(4), 255-261.

O'Shea, N., Rossle, C., Arendt, E. & Gallagher, E. (2015). Modelling the effects of orange pomace using response surface design for gluten-free bread baking. *Food Chemistry,* 166, 223-230.

O'Shea, N., Rößle, C., Arendt, E. & Gallagher, E. (2015). Modelling the effects of orange pomace using response surface design for gluten-free bread baking. *Food Chemistry,* 166, 223-230.

Oechslin, R., Lutz, M. V. & Amadò, R. (2003). Pectic substances isolated from apple cellulosic residue: Structural characterisation of a new type of rhamnogalacturonan I. *Carbohydrate Polymers,* 51(3), 301-310.

Öhlund, K., Olsson, C., Hernell, O. & Öhlund, I. (2010). Dietary shortcomings in children on a gluten-free diet. *Journal of Human Nutrition and Dietetics,* 23(3), 294-300.

Onyango, C., Unbehend, G. & Lindhauer, M. G. (2009). Effect of cellulose-derivatives and emulsifiers on creep-recovery and crumb properties of gluten-free bread prepared from sorghum and gelatinised cassava starch. *Food Research International,* 42(8), 949-955.

Oostergetel, G. T. & van Bruggen, E. F. J. (1993). The crystalline domains in potato starch granules are arranged in a helical fashion. *Carbohydrate Polymers,* 21(1), 7-12.

Pääkkö, M., Ankerfors, M., Kosonen, H., Nykänen, A., Ahola, S., Österberg, M., Ruokolainen, J., Laine, J., Larsson, P. T., Ikkala, O. & Lindström, T. (2007). Enzymatic hydrolysis combined with mechanical shearing and high-pressure homogenization for nanoscale cellulose fibrils and strong gels. *Biomacromolecules,* 8(6), 1934-1941.

Paciulli, M., Rinaldi, M., Cirlini, M., Scazzina, F. & Chiavaro, E. (2016). Chestnut flour addition in commercial gluten-free bread: A shelf-life study. *LWT - Food Science and Technology,* 70, 88-95.

Palaniappan, A., Yuvaraj, S. S., Sonaimuthu, S. & Antony, U. (2017). Characterization of xylan from rice bran and finger millet seed coat for functional food applications. *Journal of Cereal Science,* 75, 296-305.

Payen, A. (1838). Mémoire sur la composition du tissu propre des plantes et du ligneux. *Comptes rendus,* 7, 1052-1056.

Peat, S., Whelan, W. J. & Thomas, G. J. (1952). Evidence of multiple branching in waxy maize starch. *Journal of the Chemical Society (Resumed),* 4536-4538.

Pérez, S. & Bertoft, E. (2010). The molecular structures of starch components and their contribution to the architecture of starch granules: A comprehensive review. *Starch - Stärke,* 62(8), 389-420.

Phimolsiripol, Y., Mukprasirt, A. & Schoenlechner, R. (2012). Quality improvement of rice-based gluten-free bread using different dietary fibre fractions of rice bran. *Journal of Cereal Science,* 56(2), 389-395.

Phung, T. & Brady, J. F. (1992). Microstructured fluids: Structure, diffusion and rheology of colloidal dispersions. *AIP Conference Proceedings*, 256(1), 391-400.

Preston, R. D. (1979). Polysaccharide conformation and cell wall function. *Annual Review of Plant Physiology,* 30(1), 55-78.

Purna, S. K. G., Miller, R. A., Seib, P. A., Graybosch, R. A. & Shi, Y. C. (2011). Volume, texture, and molecular mechanism behind the collapse of bread made with different levels of hard waxy wheat flours. *Journal of Cereal Science,* 54(1), 37-43.

Quiévy, N., Jacquet, N., Sclavons, M., Deroanne, C., Paquot, M. & Devaux, J. (2010). Influence of homogenization and drying on the thermal stability of microfibrillated cellulose. *Polymer Degradation and Stability,* 95(3), 306-314.

Rao, M. R. P., Warrier, D. U., Gaikwad, S. R. & Shevate, P. M. (2016). Phosphorylation of psyllium seed polysaccharide and its characterization. *International Journal of Biological Macromolecules*, 85, 317-326.

Resnick, H. E., Valsania, P., Halter, J. B. & Lin, X. (2000). Relation of weight gain and weight loss on subsequent diabetes risk in overweight adults. *Journal of Epidemiology and Community Health,* 54(8), 596-602.

Ribeiro, J. S., Teofilo, R. F., Augusto, F. & Ferreira, M. M. C. (2010). Simultaneous optimization of the microextraction of coffee volatiles using response surface methodology and principal component analysis. *Chemometrics and Intelligent Laboratory Systems*, 102(1), 45-52.

Richardson, P. H., Clark, A. H., Russell, A. L., Aymard, P. & Norton, I. T. (1999). Galactomannan gelation: A thermal and rheological investigation analyzed using the cascade model. *Macromolecules,* 32(5), 1519-1527.

Ring, S. G., Colonna, P., I'Anson, K. J., Kalichevsky, M. T., Miles, M. J., Morris, V. J. & Orford, P. D. (1987). The gelation and crystallisation of amylopectin. *Carbohydrate Research,* 162(2), 277-293.

Robert, P., Marquis, M., Barron, C., Guillon, F. & Saulnier, L. (2005). FT-IR investigation of cell wall polysaccharides from cereal grains. Arabinoxylan infrared assignment. *Journal of Agricultural and Food Chemistry,* 53(18), 7014-7018.

Robin, J. P., Mercier, C., Charbonniere, R. & Guilbot, A. (1974). Lintnerized starches gel-filtration and enzymatic studies of insoluble residues from prolonged acid treatment of potato starch. *Cereal Chemistry,* 51(3), 389-406.

Romano, A., Toraldo, G., Cavella, S. & Masi, P. (2007). Description of leavening of bread dough with mathematical modelling. *Journal of Food Engineering,* 83(2), 142-148.

Ronda, F., Pérez-Quirce, S., Angioloni, A. & Collar, C. (2013). Impact of viscous dietary fibres on the viscoelastic behaviour of gluten-free formulated rice doughs: A fundamental and empirical rheological approach. *Food Hydrocolloids,* 32(2), 252-262.

Rondeau-Mouro, C., Ying, R., Ruellet, J. & Saulnier, L. (2011). Structure and organization within films of arabinoxylans extracted from wheat flour as revealed by various NMR spectroscopic methods. *Magnetic Resonance in Chemistry,* 49(S1), S85-S92.

Rose, D. J. & Inglett, G. E. (2010). Production of feruloylated arabinoxylo-oligosaccharides from maize (*Zea mays*) bran by microwave-assisted autohydrolysis. *Food Chemistry,* 119(4), 1613-1618.

Sahlström, S., Park, W. & Shelton, D. R. (2004). Factors influencing yeast fermentation and the effect of LMW sugars and yeast fermentation on hearth bread quality. *Cereal Chemistry,* 81(3), 328-335.

Sanchez, H. D., Osella, C. A. & de la Torre, M. A. (2002). Optimization of gluten-free bread prepared from cornstarch, rice flour, and cassava starch. *Journal of Food Science,* 67(1), 416-419.

Sandhu, J. S., Hudson, G. J. & Kennedy, J. F. (1981). The gel nature and structure of the carbohydrate of ispaghula husk ex *Plantago ovata* Forsk. *Carbohydrate Research,* 93(2), 247-259.

Sangnark, A. & Noomhorm, A. (2004). Effect of dietary fiber from sugarcane bagasse and sucrose ester on dough and bread properties. *LWT - Food Science and Technology,* 37(7), 697-704.

Sapone, A., Bai, J. C., Ciacci, C., Dolinsek, J., Green, P. H., Hadjivassiliou, M., Kaukinen, K., Rostami, K., Sanders, D. S., Schumann, M., Ullrich, R., Villalta, D., Volta, U., Catassi, C. & Fasano, A. (2012). Spectrum of gluten-related disorders: Consensus on new nomenclature and classification. *BMC Medicine,* 10(1), 1-12.

Sasaki, T., Yasui, T. & Matsuki, J. (2000). Effect of amylose content on gelatinization, retrogradation, and pasting properties of starches from waxy and nonwaxy wheat and their F1 seeds. *Cereal Chemistry,* 77(1), 58-63.

Scanlon, M. G. & Zghal, M. C. (2001). Bread properties and crumb structure. *Food Research International,* 34(10), 841-864.

Schirmer, M., Jekle, M. & Becker, T. (2015). Starch gelatinization and its complexity for analysis. *Starch - Stärke,* 67(1-2), 30-41.

Schober, T. J. (2009). Manufacture of gluten-free specialty breads and confectionery products. In E. Gallagher (Ed.), *Gluten-free food science and technology* (pp. 130-180). Chichester: Wiley-Blackwell.

Schober, T. J., Bean, S. R. & Boyle, D. L. (2007). Gluten-free sorghum bread improved by sourdough fermentation: Biochemical, rheological, and microstructural background. *Journal of Agricultural and Food Chemistry,* 55(13), 5137-5146.

Schuppan, D. (2000). Current concepts of celiac disease pathogenesis. *Gastroenterology,* 119(1), 234-242.

Shah, P., Campbell, G. M., McKee, S. L. & Rielly, C. D. (1998). Proving of bread dough: Modelling the growth of individual bubbles. *Food and Bioproducts Processing,* 76(2), 73-79.

Shaw, J. E., Sicree, R. A. & Zimmet, P. Z. (2010). Global estimates of the prevalence of diabetes for 2010 and 2030. *Diabetes Research and Clinical Practice,* 87(1), 4-14.

Shepherd, S. J. & Gibson, P. R. (2013). Nutritional inadequacies of the gluten-free diet in both recently-diagnosed and long-term patients with coeliac disease. *Journal of Human Nutrition and Dietetics,* 26(4), 349-358.

Shewry, P. R., Halford, N. G., Belton, P. S. & Tatham, A. S. (2002). The structure and properties of gluten: An elastic protein from wheat grain. *Philosophical Transactions of the Royal Society B: Biological Sciences,* 357(1418), 133-142.

Singh, B. (2007). Psyllium as therapeutic and drug delivery agent. *International Journal of Pharmaceutics,* 334(1), 1-14.

Singh, J. & Whelan, K. (2011). Limited availability and higher cost of gluten-free foods. *Journal of Human Nutrition and Dietetics,* 24(5), 479-486.

Siqueira, G., Bras, J. & Dufresne, A. (2010). Cellulosic bionanocomposites: A review of preparation, properties and applications. *Polymers,* 2(4), 728-765.

Siró, I. & Plackett, D. (2010). Microfibrillated cellulose and new nanocomposite materials: A review. *Cellulose,* 17(3), 459-494.

Skypala, I. J. & McKenzie, R. (2019). Nutritional issues in food allergy. *Clinical Reviews in Allergy & Immunology,* 57(2), 166-178.

Song, Y. J., Sawamura, M., Ikeda, K., Igawa, S. & Yamori, Y. (2000). Soluble dietary fibre improves insulin sensitivity by increasing muscle glut-4 content in stroke-prone spontaneously hypertensive rats. *Clinical and Experimental Pharmacology and Physiology,* 27(1-2), 41-45.

Stenstad, P., Andresen, M., Tanem, B. S. & Stenius, P. (2008). Chemical surface modifications of microfibrillated cellulose. *Cellulose,* 15(1), 35-45.

Ström, A., Ribelles, P., Lundin, L., Norton, I., Morris, E. R. & Williams, M. A. K. (2007). Influence of pectin fine structure on the mechanical properties of calcium−pectin and acid−pectin gels. *Biomacromolecules,* 8(9), 2668-2674.

Sugiyama, J., Persson, J. & Chanzy, H. (1991). Combined infrared and electron diffraction study of the polymorphism of native celluloses. *Macromolecules,* 24(9), 2461-2466.

Sullo, A. & Foster, T. J. (2010). Characterisation of starch/cellulose blends. *Annual Transactions of the Nordic Rheology,* 18, 1-7.

Sullo, A., Wang, Y., Koschella, A., Heinze, T. & Foster, T. J. (2013). Self-association of novel mixed 3-mono-O-alkyl cellulose: Effect of the hydrophobic moieties ratio. *Carbohydrate Polymers,* 93(2), 574-581.

Svagan, A. J., Azizi Samir, M. A. S. & Berglund, L. A. (2007). Biomimetic polysaccharide nanocomposites of high cellulose content and high toughness. *Biomacromolecules,* 8(8), 2556-2563.

Tanner, R. I., Qi, F. & Dai, S. C. (2008). Bread dough rheology and recoil: I. Rheology. *Journal of Non-Newtonian Fluid Mechanics,* 148(1), 33-40.

Tester, R. F. & Morrison, W. R. (1990). Swelling and gelatinization of cereal starches .2. Waxy rice starches. *Cereal Chemistry,* 67(6), 558-563.

The DOW Chemical Company. (2002). *Methocel cellulose ethers technical handbook.* USA: The DOW Chemical Company.

Thompson, T. (2009). The nutritional quality of gluten ‐ free foods. In E. Gallagher (Ed.), *Gluten-free food science and technology*. Chichester: Wiley-Blackwell.

Torbica, A., Hadnadev, M. & Dapcevic, T. (2010). Rheological, textural and sensory properties of gluten-free bread formulations based on rice and buckwheat flour. *Food Hydrocolloids,* 24(6-7), 626-632.

Tran, T. T. B., Shelat, K. J., Tang, D., Li, E., Gilbert, R. G. & Hasjim, J. (2011). Milling of rice grains. The degradation on three structural levels of starch in rice flour can be independently controlled during grinding. *Journal of Agricultural and Food Chemistry,* 59(8), 3964-3973.

Turbak, A. F., Snyder, F. W. & Sandberg, K. R. (1982). Food products containing microfibrillated cellulose. US4341807.

Turbak, A. F., Snyder, F. W. & Sandberg, K. R. (1983a). Microfibrillated cellulose. US4374702A.

Turbak, A. F., Snyder, F. W. & Sandberg, K. R. (1983b). Suspensions containing microfibrillated cellulose. US4378381A.

Unsworth, D. J. & Brown, D. L. (1994). Serological screening suggests that adult coeliac disease is underdiagnosed in the UK and increases the incidence by up to 12%. *Gut,* 35(1), 61-64.

Upadhyay, R., Ghosal, D. & Mehra, A. (2012). Characterization of bread dough: Rheological properties and microstructure. *Journal of Food Engineering,* 109(1), 104-113.

Van Craeyveld, V., Delcour, J. A. & Courtin, C. M. (2009). Extractability and chemical and enzymic degradation of psyllium (*Plantago ovata* Forsk) seed husk arabinoxylans. *Food Chemistry,* 112(4), 812-819.

van Riemsdijk, L. E., van der Goot, A. J., Hamer, R. J. & Boom, R. M. (2011). Preparation of gluten-free bread using a meso-structured whey protein particle system. *Journal of Cereal Science,* 53(3), 355-361.

Van Vliet, T., Janssen, A. M., Bloksma, A. H. & Walstra, P. (1992). Strain hardening of dough as a requirement for gas retention. *Journal of Texture Studies,* 23(4), 439-460.

Vignon, M. R., Heux, L., Malainine, M. E. & Mahrouz, M. (2004). Arabinan–cellulose composite in *Opuntia ficus-indica* prickly pear spines. *Carbohydrate Research,* 339(1), 123-131.

Villanueva, M., Harasym, J., Muñoz, J. M. & Ronda, F. (2019). Rice flour physically modified by microwave radiation improves viscoelastic behavior of doughs and its bread-making performance. *Food Hydrocolloids,* 90, 472-481.

Wada, M., Chanzy, H., Nishiyama, Y. & Langan, P. (2004). Cellulose IIII crystal structure and hydrogen bonding by synchrotron X-ray and neutron fiber diffraction. *Macromolecules,* 37(23), 8548-8555.

Wagner, M. J., Lucas, T., Le Ray, D. & Trystram, G. (2007). Water transport in bread during baking. *Journal of Food Engineering,* 78(4), 1167-1173.

Wahab, P. J., Meijer, J. W., Goerres, M. S. & Mulder, C. J. (2002). Coeliac disease: Changing views on gluten-sensitive enteropathy. *Scandinavian Journal of Gastroenterology*, (236), 60-65.

Walls, H. J., Caines, S. B., Sanchez, A. M. & Khan, S. A. (2003). Yield stress and wall slip phenomena in colloidal silica gels. *Journal of Rheology*, 47(4), 847-868.

Walther, A., Timonen, J. V. I., Díez, I., Laukkanen, A. & Ikkala, O. (2011). Multifunctional high-performance biofibers based on wet-extrusion of renewable native cellulose nanofibrils. *Advanced Materials,* 23(26), 2924-2928.

Wang, B. & Sain, M. (2007). Dispersion of soybean stock-based nanofiber in a plastic matrix. *Polymer International,* 56(4), 538-546.

Whitney, S. E., Gothard, M. G., Mitchell, J. T. & Gidley, M. J. (1999). Roles of cellulose and xyloglucan in determining the mechanical properties of primary plant cell walls. *Plant Physiology,* 121(2), 657-664.

Whitney, S. E. C., Brigham, J. E., Darke, A. H., Reid, J. S. G. & Gidley, M. J. (1998). Structural aspects of the interaction of mannan-based polysaccharides with bacterial cellulose. *Carbohydrate Research,* 307(3), 299-309.

Whitney, S. E. C., Wilson, E., Webster, J., Bacic, A., Reid, J. S. G. & Gidley, M. J. (2006). Effects of structural variation in xyloglucan polymers on interactions with bacterial cellulose. *American Journal of Botany,* 93(10), 1402-1414.

Wickholm, K., Larsson, P. T. & Iversen, T. (1998). Assignment of non-crystalline forms in cellulose I by CP/MAS ^{13}C NMR spectroscopy. *Carbohydrate Research,* 312(3), 123-129.

Wieser, H. (2007). Chemistry of gluten proteins. *Food Microbiology,* 24(2), 115-119.

Willhoft, E. M. A. (1971). Bread staling II. *Journal of the Science of Food and Agriculture,* 22(4), 180-183.

World Health Organization. (2018). Obesity and overweight fact sheet. Retrieved from https://www.who.int/en/news-room/fact-sheets/detail/obesity-and-overweight. Accessed on 30 July 2019

Wyman, C. E., Decker, S. R., Himmel, M. E., Brady, J. W., Skopec, C. E. & Viikari, L. (2005). hydrolysis of cellulose and hemicellulose. In S. Dumitriu (Ed.),

Polysaccharides: Structural Diversity and Functional Versatility (2nd ed., pp. 995 - 1034). New York: Marcel Dekker.

Wyss, H. M., Miyazaki, K., Mattsson, J., Hu, Z. B., Reichman, D. R. & Weitz, D. A. (2007). Strain-rate frequency superposition: A rheological probe of structural relaxation in soft materials. *Physical Review Letters,* 98(23).

Yu, L., DeVay, G. E., Lai, G. H., Simmons, C. T. & Neilsen, S. R. (2001). Enzymatic modification of psyllium. US6248373B1.

Yu, L., Yakubov, G. E., Gilbert, E. P., Sewell, K., van de Meene, A. M. L. & Stokes, J. R. (2019). Multi-scale assembly of hydrogels formed by highly branched arabinoxylans from *Plantago ovata* seed mucilage studied by USANS/SANS and rheology. *Carbohydrate Polymers,* 207, 333-342.

Yu, L., Yakubov, G. E., Martínez-Sanz, M., Gilbert, E. P. & Stokes, J. R. (2018). Rheological and structural properties of complex arabinoxylans from *Plantago ovata* seed mucilage under non-gelled conditions. *Carbohydrate Polymers,* 193, 179-188.

Yu, L., Yakubov, G. E., Zeng, W., Xing, X., Stenson, J., Bulone, V. & Stokes, J. R. (2017). Multi-layer mucilage of *Plantago ovata* seeds: Rheological differences arise from variations in arabinoxylan side chains. *Carbohydrate Polymers,* 165, 132-141.

Yui, T., Imada, K., Shibuya, N. & Ogawa, K. (1995). Conformation of an arabinoxylan isolated from the rice endosperm cell wall by X-ray diffraction and a conformational analysis. *Bioscience, Biotechnology, and Biochemistry,* 59(6), 965-968.

Zandonadi, R. P., Botelho, R. B. A. & Araujo, W. M. C. (2009). Psyllium as a substitute for gluten in bread. *Journal of the American Dietetic Association,* 109(10), 1781-1784.

Zannini, E., Jones, J. M., Renzetti, S. & Arendt, E. K. (2012). Functional Replacements for Gluten. *Annual Review of Food Science and Technology,* 3(1), 227-245.

Zhang, Z. X., Smith, C. & Li, W. L. (2014). Extraction and modification technology of arabinoxylans from cereal by-products: A critical review. *Food Research International,* 65, 423-436.

Zhbankov, R. G., Andrianov, V. M. & Marchewka, M. K. (1997). Fourier transform IR and Raman spectroscopy and structure of carbohydrates. *Journal of Molecular Structure,* 437, 637-654.

Zhou, S. M., Liu, X. Z., Guo, Y., Wang, Q. A., Peng, D. Y. & Cao, L. (2010). Comparison of the immunological activities of arabinoxylans from wheat bran with alkali and xylanase-aided extraction. *Carbohydrate Polymers,* 81(4), 784-789.

Zhou, W. & Therdthai, N. (2007). Three-dimensional CFD modeling of a continuous industrial baking process. In D. Sun (Ed.), *Computational fluid dynamics in food processing* (pp. 306-331). Boca Raton: CRC Press.

Zimmermann, T., Pöhler, E. & Geiger, T. (2004). Cellulose fibrils for polymer reinforcement. *Advanced Engineering Materials,* 6(9), 754-761.

Zykwinska, A. W., Ralet, M.-C. J., Garnier, C. D. & Thibault, J. F. J. (2005). Evidence for in vitro binding of pectin side chains to cellulose. *Plant Physiology,* 139(1), 397-407.